Mechanisms of Mechanotransduction by Dorsal Root Ganglia Neurons

Liam J. Drew

A thesis submitted for the degree of Doctor of Philosophy
to University of London

Department of Biology
University College London
2004

ProQuest LLC
789 East Eisenhower Parkway
P.O. Box 1346
Ann Arbor, MI 48106-1346

Abstract

The molecular mechanisms that mediate mammalian sensory mechanotransduction are poorly understood. Detection of mechanical events by sensory neurons of the dorsal root ganglia (DRG) is the primary event in the senses of touch, pressure-induced pain and proprioception. Recent work has demonstrated that the somatic membrane of cultured DRG neurons is a suitable system for studying physical transduction. In this thesis the responses of cultured DRG neurons to focal mechanical stimulation were investigated. It was shown that mechanical stimulation activated non-selective cation channels in these cells. The response properties of different subclasses of sensory neurons were characterised and were consistent with the presumed *in vivo* phenotypes of these cells. A number of antagonists of mechanically activated currents, with affinity in the low micromolar range, were identified; these included the pore blocking compounds gadolinium and ruthenium red and FM1-43 acted as a permeant blocker of mechano-sensitive channels. Modulation of mechanically activated currents by extracellular calcium was observed and it was shown that currents were regulated by the actin cytoskeleton and the extracellular matrix protein laminin. Investigation of null mutant mice revealed that the acid sensing ion channels 2 and 3, which are widely hypothesised to function in mammalian mechanosensation, did not contribute to mechanically activated currents. Venom of the marine snail *Conus ventricosus* was found to block mechanically activated currents although the active component of this venom is yet to be identified. Overall, this work has shown that cultured DRG neurons are a useful system for studying mechanotransduction and has revealed a number of functional and pharmacological properties of the ion channels that underlie this process.

Declaration

I, Liam Drew, did all the work presented in this thesis unless indicated otherwise.

Contents

List of Figures

Chapter 1

Chapter 2

Chapter 3

Chapter 4

Chapter 5

List of Tables

Chapter 1

Chapter 4

Acknowledgements

Thank you to my teachers John Wood, Paolo Cesare and Mark Baker. I am deeply indebted to all of them for the patience and guidance they have given me throughout my PhD and for sharing their appetite for discovery with me. I thank John for his supervision throughout; his direction, support and enthusiasm are extremely appreciated and it has been a pleasure to work in his lab. I am exceptionally grateful to Paolo for teaching me so much and for remaining a great colleague and friend. Many thanks go to Mark for being a remarkably generous and invaluable source of knowledge and guidance throughout this work.

I thank James for his help and advice whilst enduring the conopeptide project with me. Special thanks to Karen, and also to Sarah and Louise, for all the long hours spent genotyping. I'd like to thank all other members of the lab, past and present, for being fantastic colleagues and teachers; special thanks go to Kenji for constantly sharing his immense knowledge, and also special mentions go to Anastasia, Caroline, Louisa, Manue, Mohammed and Sam for all their help. I would also like to thank all the other people at UCL who I have worked with or who have given me their time and advice during the last four years.

Thank you to Dan Rohrer and Debbie Cockayne for provision of ASIC1 and ASIC3 null mutants and to Margaret Price and Michael Welsh for ASIC2 knockouts.

I thank the many people at UCL who have been great colleagues and made it a tremendous environment in which to work. Special thanks go to Rob, Damian, Simon and all the other people who have become true friends over the course of this thesis. I also thank the members of the Zoology football set-up for providing the most welcome of distractions.

My sincerest gratitude goes to Jethro and Steph for friendships that constantly mean so much to me. And to my friends from Nottingham, especially Rache, my friends from home and all the wonderful people I've met in the last 4 years, I thank you all for supporting me and making London a great place to live. Also, my gratitude goes to Sarah for everything she gave me during the first 3 years of this thesis.

Finally, I dedicate this thesis to my mum, dad, brother and nan. The extent of their love, kindness and support never ceases to astonish and inspire me. Thank you so much.

Abbreviations

ANOVA	Analysis of variance
AP	Action potential
ASIC	Acid sensing ion channel
ATP	Adenosine triphosphate
BDNF	Brain derived neurotrophic factor
Caps	Capsaicin
cDNA	Complimentary deoxyribonucleic acid
CGRP	Calcitonin gene related protein
C-MH	Mechanoheat sensitive C-fibres
D-hair	Down hair
DEG	Degenerin
DKO	Double knockout
DMSO	Dimethyl Sulphoxide
DRG	Dorsal root ganglia
EGTA	Ethylene glycol-*bis*(β-aminoethyl ether)-N,N,N',N'-tetraacetic acid
ENaC	Epithelial sodium channel
ERD	Extracellular regulatory domain
EST	Expressed sequence tags
FM1-43	*N*-(3-triethylammoniumpropyl)-4- (4-(dibutylamino)styryl)pyridinium dibromide
G-hair	Guard Hair
GDNF	Glial (cell line) derived neurotrophic factor
GFP	Green fluorescent protein
GPCR	G-protein coupled receptor
HEPES	N-[2-hydroxyethyl]piperazine-N'-[2-ethanesulphonic acid]
HT	High threshold
HTMR	high threshold mechanoreceptor
IA	intermediately adapting
IB4	*Griffonia simplicifolia* I isolectin B4
IC_{50}	Concentration inhibiting by 50%
IV	Current-voltage
KO	Knockout
K_D	Dissociation constant
K_V	Voltage-gated potassium channel
LT	Low threshold
LTMR	low threshold mechanoreceptor

MA	Mechanically activated
MEC	Mechanosensory abnormal
mmHg	Millimetres of mercury
mRNA	Messenger ribonucleic acid
nA	Nanoampere
Na_V	Voltage-gated sodium channel
NF200	200-kDa neurofilament
NMG	*N*-methyl-*D*-glucamine
NGF	Nerve growth factor
NOMP	No mechanoreceptor potential
P1	Postnatal day 1
pA	Picoampere
PBS	Phosphate buffered saline
PC	Pacinian corpuscle
PCR	Polymerase chain reaction
RA	Rapidly adapting
RT	Reverse transcriptase
SA	Slowly adapting
SCG	Superior cervical ganglia
TrkA	Tyrosine kinase receptor A
TRP	Transient receptor potential
TRPC/M/V	TRP-classical/melastatin/vanilloid
TTX	Tetrodotoxin
TTX-r/s	Tetrodotoxin resistant/sensitive
unc	Uncoordinated phenotype
YFP	Yellow fluorescent protein

Ion Channel Nomenclature

The key families of ion channels discussed in this thesis are the acid sensing ion channels (ASICs) and the transient receptor potential (TRP) channels. Also there is some description of the distribution and function of voltage-gated sodium (Na_V) channels. The molecular identification of members of these groups of ion channels has been achieved by a large number of groups leading to a disparate nomenclature. Recently, attempts have been made to standardise the classification of all three families; the nomenclatures proposed by Montell *et al* (2002) for TRP channels and Goldin *et al* (2000) for voltage-gated sodium channels are now widely accepted and are used herein. Also, in this thesis I use the nomenclature proposed for ASIC channels by Waldmann and Lazdunski (1998). The most commonly discussed channels and their former names are summarised below.

Ion Channel	Former Names
ASIC1a	ASICα, BNaC2α
ASIC1b	ASICβ, BNaC2β
ASIC2a	BNaC1α, MDEG1, BNC1
ASIC2b	BNaC1β, MDEG2, BNC1β
ASIC3	DRASIC, TNaC
ASIC4	SPASIC
TRPV1	VR1, OTRPC1
TRPV2	VRL-1, OTRPC2, GRC
TRPV3	
TRPV4	VR-OAC, OTRPC4, VRL-2, TRP 12
TRPV5	ECaC1, CaT2
TRPM8	TRP-p2
ANKTM1	
$Na_V1.8$	SNS
$Na_V1.9$	NaN, SNS2

1 Introduction

1.1 Dorsal Root Ganglion Neurons: Structure and Function

The receptor cells of the somatosensory system for the limbs and trunk are the primary sensory neurons of the dorsal root ganglia (DRG) and for cranial structures it is the equivalent neurons of the trigeminal ganglia[1]. Sensory neurons can be divided into three functional domains: 1) The peripheral terminal, where sensory transduction occurs. This region mediates the conversion of physical or chemical energy into an electrochemical signal. 2) The axon, or primary afferent fibre; responsible for conveying action potentials generated by sensory transduction from the periphery to the central nervous system (CNS). 3) The central terminal, which forms synapses with second order sensory neurons of the dorsal horn of the spinal cord for DRG neurons and of the spinal trigeminal nucleus caudalis (Vc) for neurons of the trigeminal ganglia.

The DRG contain multiple subtypes of sensory neurons, each of which is specialised to detect a distinct stimulus modality. Broadly, the three forms of stimuli that can excite somatic receptors are mechanical force, thermal stimuli and specific chemical activators. Neurons can broadly be classified as those that signal information about innocuous stimuli acting upon the body and those with nociceptive functions, in that they respond to noxious stimuli, i.e. stimuli of sufficient intensity to cause, or potentially cause, tissue damage (Section 1.1.1.1). Most innocuous receptors are mechanoreceptors associated with auxiliary end organs whereas the peripheral terminals of nociceptors exist as bare nerve endings (Section 1.1.2.1). The activity of nociceptors is not only determined by the intensity of an externally applied stimulus but is also modulated by the physiological state of the body. When tissue damage has occurred (or during illness) inflammatory responses lead to the release of chemical mediators that can significantly alter the

[1] The following description of neuronal physiology and anatomy will focus on the DRG but the same basic principles are likely to apply to the functionally and morphologically homologous neurons of the trigeminal ganglia.

sensitivity of nociceptors to exogenous stimuli or generate ongoing activity in these neurons (see Wood, 2000).

Table 1.1 summarises the primary types of sensory neurons found in the DRG indicating the modality of these neurons, their association with end organs and the fibre type possessed by each class. Below general physiological and anatomical properties of different neuronal populations are outlined and then the ways in which these neurons respond to mechanical stimuli is discussed.

Receptor Type	*Modality*	*Fibre Group*
Cutaneous and Subcutaneous Mechanoreceptors	**Touch**	
Meissner's corpuscle	Stroking, Fluttering	Aβ (Aα)
Merkel cell	Pressure, Texture	Aβ (Aα)
Pacinian corpuscle	Vibration	Aβ (Aα)
Ruffini ending	Skin Stretch	Aβ (Aα)
Guard-hair	Stroking, Fluttering	Aβ (Aα)
Down-hair	Light Stroking	Aδ
Thermal Receptors	**Temperature**	
Cool receptors	Skin cooling (< 25°C)	Aδ
Warm receptors	Skin warming (> 41°C)	C
Heat nociceptors	Hot temperatures (>45°C)	Aδ
Cold nociceptors	Cold temperatures (< 5°C)	C
Nociceptors	**Noxious Stimuli / Pain**	
Mechanical	Sharp, pricking pain	Aδ
Thermal-mechanical	Burning pain	Aδ
Thermal-mechanical	Freezing pain	C
Polymodal	Slow, burning pain	C
Muscle and Skeletal Mechanoreceptors	**Limb Proprioception**	
Muscle spindle primary	Muscle length and speed	Aα
Muscle spindle secondary	Muscle stretch	Aβ
Golgi tendon organ	Muscle contraction	Aα
Joint capsule mechanoreceptors	Joint angle	Aβ
Stretch-sensitive free endings	Excess stretch or force	Aδ

Table 1.1 Receptor classes of the DRG. The table indicates the types receptors present in the DRG and the typical natural stimulus that each receptor type responds to and the fibre type (classified by conduction velocity) associated with each class. (Table adapted from Gardner *et al*, 2000.)

1.1.1 General Properties of DRG Neurons

It is hypothesised that each functional category of DRG neurons is homogenous in terms of anatomy, physiology and gene expression. Although a stage has not been reached where the detailed phenotype of each neuronal subtype can be described, numerous properties characteristic of broader categories of neurons are well documented. Thus, neuronal populations can be distinguished by a number of attributes including cell size and axon diameter, degree of axonal myelination, conduction velocity, termination of peripheral and central projections, neurotrophic dependence, neurotransmitter content and the expression of specific signalling molecules and transcription factors (see below and Wood, 2000 and reviews therein).

1.1.1.1 Modality, Fibre Type and Electrical Properties of Sensory Neurons

Afferent nerve fibres have traditionally been divided into categories according to their axonal conduction velocity (Perl, 1992), there are four conduction categories: Aα; >30 m/sec, Aβ; 10-30 m/sec, Aδ; 1.2-10 m/sec and C; < 1.2 m/sec[2]. Aα- and Aβ-fibre categories mainly contain neurons that respond to innocuous mechanical stimuli either derived from cutaneous stimulation or associated with muscle, joint or tendon activity. Aδ-fibres tend to be associated with cutaneous heat or mechanical nociceptors, cooling receptors and low threshold Down-hair (D-hair) mechanoreceptors and also some muscle nociceptors and visceral afferents. C-fibres are predominately nociceptive in function, be they thermal, mechanical, chemical or polymodal in their receptive properties, although some low threshold C-fibre mechanoreceptors have been reported.

Conduction velocity is largely determined by axonal diameter and the degree of axonal myelination; the larger the axon and the greater the amount of myelination the faster it conducts. Aα and Aβ fibres are large and heavily myelinated, Aδ-fibres are relatively small and sparsely myelinated and C-fibres are unmyelinated and thin. Axonal diameter

[2] The conduction velocities are approximations for rat/mouse nerve fibres. There is considerable inter-species variation; typically the larger the mammal the greater the conduction velocity.

and conduction velocity generally correlate with the size of the neuronal cell body; C-fibre neurons have small cell bodies whereas A-fibre neurons have medium to large cell bodies although some fall within the small range (Harper and Lawson, 1985a; Lee *et al*, 1986). Histologically, cell types can be distinguished by staining with Nissl substance; neurons associated with A-fibres appear as "large, light" neurons and C-fibre neurons stain as "small, dark" cells (Lawson, 1979). These two cell types can also be discriminated immunocytochemically by staining with RT97 or N52, monoclonal antibodies against 200-kDa neurofilament subunit (NF200, RT97 recognises phosphorylated NF200), which is present at high levels in "light" neurons and is either absent or present at low levels in "dark" neurons (Lawson *et al*, 1984). In accordance, Lawson and Waddell (1991) using *in vivo* intracellular recordings with immuno-cytochemistry showed that NF200-positive neurons had A-fibres and that nearly all negative neurons had C-fibres. Conversely, peripherin, an intermediate neurofilament, immunoreactivity is often used as a marker of small, nociceptive neurons in the DRG (Goldstein *et al*, 1991).

Action potentials also vary across classes of DRG receptors; sensory neurons exhibit two primary classes of action potentials; those that are narrow and sensitive to TTX and those that are broad and resistant (or partially sensitive) to TTX. In narrow action potentials the upswing is mediated solely by TTX-sensitive voltage-gated Na^+ channels, whereas, the shape of broad action potentials, typically characterised by an inflection on the downswing, is due to an interplay between TTX-resistant and TTX-sensitive Na^+ channels and high threshold voltage-gated Ca^{2+} channels (see Koerber and Mendell, 1992 and references therein; Blair and Bean, 2002).

Using DRG explants, Yoshida and Matsuda (1979) noted a correlation between neurons' action potential shapes and their conduction velocities and their size; narrow, TTX-sensitive action potentials were generated by large cells with rapid conduction velocities whereas small neurons with slowly conducting axons displayed broad action potentials that were TTX-resistant. They also found, however, that a subpopulation of medium sized neurons with relatively rapid conduction also generated broad action potentials.

Investigations utilising intracellular recordings from DRG neurons in the intact animal found a more robust correlation between action potential shape and the receptor type of a neuron than the conduction velocity *per se*. It was found that although all C-fibres display broad action potentials regardless of their modality, amongst Aβ- and Aδ-fibres action potentials were associated with receptive properties; low threshold mechano-receptors had narrow spikes and high threshold mechanoreceptors displayed broad, inflected action potentials (Rose *et al*, 1986; Koerber *et al*, 1988 (both cat); Ritter and Mendell, 1992 (rat); Table 1.2). Whilst this relationship is well established it is unclear what its functional significance is (see Koerber and Mendell, 1992). The duration of afterhyperpolarisations (AHP) following action potentials also correlates with receptive properties; short AHPs are associated with non-nociceptive A-fibres displaying narrow action potentials and also non-nociceptive C-fibres that have inflected action potentials. This is in contrast to nociceptive fibres, in all categories, that have long AHPs (Djouhri *et al*, 1998).

Axon Classification	Receptor Threshold	Inflected Action Potential
Aβ	Low (SA, RA, G-hair)	No
Aβ	High (HTMR)	Yes
Aδ	Low (D-hair)	No
Aδ	High (HTMR)	Yes
C	Low (LTMR)	Yes
C	High (polymodal, mechanoheat, HTMR)	Yes

Table 1.2 This table shows the association between the presence or absence of an inflection on the falling phase of the action potential and the receptive properties of sensory neurons. (Table adapted from Koerber and Mendell, 1992.)

1.1.1.2 Differential Ion Channel Expression by DRG Neurons

Different classes of DRG neurons display distinct patterns of gene expression consistent with their designated function. Different receptor types vary according to their expression of transcription factors (Akopian *et al*, 1996a), neurotrophic receptors and associated signalling molecules (Davies, 2000; Silos-Santiago, 2000), ion channels and GPCRs (Akopian *et al*, 2000a), enzymes (Lawson, 1992) and neurotransmitters and

neuropeptides (Lawson, 1992). In this section I will briefly outline how certain key ion channels are differentially distributed amongst sensory neurons.

The ion channel that mediates the predominant TTX-resistant sodium current in nociceptors is the Na^+ channel $Na_V1.8$ (Akopian *et al*, 1996b). $Na_V1.8$ is expressed exclusively in sensory ganglia where its distribution is limited to small diameter neurons (Akopian *et al*, 1996b). Immunocytochemical investigation of functionally defined sensory neurons showed that $Na_V1.8$ expression is strongly associated with a nociceptive phenotype; the channel was expressed highly in approximately 90% of nociceptors and in 60% of Aβ-fibre HTMRs whereas only weak immunoreactivity was found in D-hair receptors and in a minor fraction of LTMRs (Djouhri *et al*, 2003a). Nociceptors also selectively exhibit another TTX-resistant voltage-activated Na^+ current (Cummins *et al*, 1999), which has very slow activation and inactivation kinetics and is likely mediated by $Na_V1.9$. Of the TTX-sensitive Na^+ channels, $Na_V1.6$ and 1.7 are abundant in DRG and $Na_V1.1$ and 1.2 are also present (see Wood and Baker, 2001) whereas $Na_V1.3$ is expressed only after nerve injury (Boucher *et al*, 2000). Djouhri *et al* (2003b) have shown $Na_V1.7$ immunoreactivity in all DRG cell types, although it is most prevalent in C- and Aδ-fibres. $Na_V1.6$ is thought to be the major Na^+ channel subtype in myelinated neurons (Caldwell *et al*, 2000). Rasband *et al* (2001) have also found a differential distribution of voltage-gated K^+ channels in sensory neurons; $K_V1.4$ was the only α-subunit found immunohistochemically in small neurons whereas it was absent from large cells that expressed a mixture of $K_V1.1$ and $K_V1.2$.

C-fibre nociceptors can be divided into two major classes based upon their neurotrophic requirements; one of these populations selectively (amongst DRG neurons) binds the isolectin IB4 (Silverman and Kruger, 1990). Briefly, in early stages of development, small nociceptive neurons express TrkA and require NGF for their survival (Davies, 2000). Postnatally, in the IB4 binding population TrkA expression is downregulated and, concurrent with an upregulation of C-Ret receptor complexes, these neurons become dependent on GDNF (Molliver *et al*, 1997). Neurons that express TrkA into adulthood are nearly all peptidergic, containing the neuropeptides substance P and CGRP, whereas

IB4-positive neurons are non-peptidergic (Molliver *et al*, 1997). Although these two populations of neurons have clearly different central termination patterns, the functional distinction between them remains unclear; there is no clear difference in their gross physiology, including their modalities. Stucky and Lewin (1999) have shown differences between IB4 positive and negative groups in action potential properties, TTX-resistant Na^+ currents and heat-evoked currents but all disparities were quantitative rather than qualitative. Dirajlal *et al* (2002) showed, in mice, a quantitative difference in capsaicin sensitivity but more clearly demonstrated that IB4-negative neurons displayed transient proton-gated current (indicative of functional ASIC expression, Section 1.2.2.3) that were absent in IB4-positive neurons. Additionally, $P2X_3$ receptors are expressed almost exclusively in IB4 positive neurons in adults (Burgard *et al*, 1999).

Key differences in ion channel expression between receptor types is expected amongst those channels that transduce physical stimuli, that is the complement of channels activated by physical stimuli expressed by a neuron will determine its modality. Thus, low threshold mechanoreceptors would be expected to selectively express mechanically activated ion channels that are gated by small fluctuations in pressure. Likewise, a polymodal C-fibre will express ion channels allowing it to respond to intense mechanical stimuli, noxious levels of heat and chemical mediators of inflammation (Caterina and Julius, 1999; Julius and Basbaum, 2001). Recently, a number of ion channels that are modulated by temperature have been identified and a molecular description of distinct thermoreceptors is beginning to emerge (Section 1.3.2). Presently however the identities the molecules mediating sensory mechanotransduction remain unknown (Section 1.2).

The most extensively characterised ionotropic receptor activated by a physical stimulus is TRPV1, which is activated and/or modulated by heat (> 43°C), capsaicin, protons, various lipids including endocannabinoids and ethanol (Caterina and Julius, 2001; Section 1.3.2). Prior to the cloning of this receptor, capsaicin was known to have excitatory and toxic actions on neurons with nociceptive phenotypes (see Szolcsanyi, 1993). For example, Szolcsanyi *et al* (1988) found only heat sensitive nociceptive fibres responded to capsaicin. The identification of TRPV1 demonstrated that it was the

receptor, rather than the nerve ending, that was sensitive to both capsaicin and heat. TRPV1 is present predominantly in small, NF-200-negative neurons colocalising with both substance P immunoreactivity and IB4 staining (Caterina *et al*, 1997; Michael and Priestley, 1999). In the rat, TRPV1 mRNA was in around 83% of the N52-negative population (Michael and Priestley, 1999).

The P2X and ASIC families of ion channels are highly expressed in sensory ganglia and each is selectively expressed in subsets of neurons. Six P2X ion channels ($P2X_{1-6}$) are expressed in DRG (Collo *et al*, 1996), although the physiological role of these channels is poorly understood. P2X receptors may function presynaptically, as these receptors can modulate glutamate release from sensory neurons (Gu and MacDermott, 1997), and may also function in peripheral activation of afferent fibres; ATP and P2X agonists can induce pain related behaviours (Hamilton *et al*, 1999) and electrical activity in C-fibres (Hamilton *et al*, 2001). $P2X_3$ is of particular interest as it is expressed selectively in sensory ganglia, predominantly in small-medium, IB4-positive neurons (Chen *et al*, 1995). A function for this channel in sensing mechanically evoked ATP release has been proposed (see Section 1.2.4). ASICs are highly expressed in sensory neurons. Currently the only known activator of ASICs is protons but there is speculation, due to their homology to putative *C. elegans* mechanosensitive channels, that they may function as DRG mechanosensors. The distribution and function of these channels is discussed in Section 1.2.2.3.

1.1.2 Mechanosensation by DRG Neurons

In the 1920s when Adrian and co-workers recorded mechanically evoked electrical impulses in single frog afferent fibres it was the first demonstration of a natural stimulus inducing action potentials (Adrian, 1928). Mechanical stimuli activate the majority of DRG fibre classes and different types of sensory neurons detect distinct forms of movement. Each class has a specific termination pattern in the periphery and is distinguished by the intensity of mechanical deformation required for activation and by the firing pattern evoked by a mechanical stimulus (Figs. 1.1 and 1.2). Amongst

cutaneous low threshold mechanoreceptors there are also differences in the spatial and temporal profiles of mechanical stimuli that maximally activate particular fibre types.

1.1.2.1 Mechanoreceptor Types and End Organs[3]

Low threshold mechanoreceptors all have peripheral terminals that are closely associated with specialised end organs whereas nociceptive units, with high mechanical thresholds, terminate in peripheral tissues as bare nerve endings. Afferents conveying sensory information from muscles and joints innervate muscle spindles, Golgi tendon organs and joint capsules and typically conduct in the Aβ or Aα range (see Table 1.1). Cutaneous Aβ-fibre low threshold mechanoreceptors are of four types in glabrous skin (see Fig. 1.1): slowly adapting types 1 and 2 (SA1/2), rapidly adapting afferents (RA) and rapidly adapting Pacinian corpuscle afferents (PC) (see Tables 1.1 and 1.3). In hairy skin there are guard hair (G-hair) receptors that fire with rapid adaptation.

Receptor type	End organ	Preferred stimulus	Receptive field (diameter; human)
SA1	Merkel cells	Skin indentation	2-3 mm
RA	Meissner corpuscles	Dynamic skin deformation (low frequency)	3-5 mm
PC	Pacinian corpuscles	Vibration (high frequency)	Large (e.g. up to an entire hand)
SA2	Ruffini corpuscles	Skin stretch	10-15 mm
RA (G-hair)	Lanceolate endings on hair follicle	Hair displacement	Hair movement

Table 1.3 The five classes cutaneous, low threshold Aβ-fibre mechanoreceptors. Table shows each receptor types' association with end organs, preferred stimuli and its typical receptive field size in humans.

[3] This section covers general properties of mechanoreceptors and their association with end organs the section is thinly referenced; for full reviews see Catton, 1970; Sinclair, 1981; Zelena, 1994; Fain, 2003.

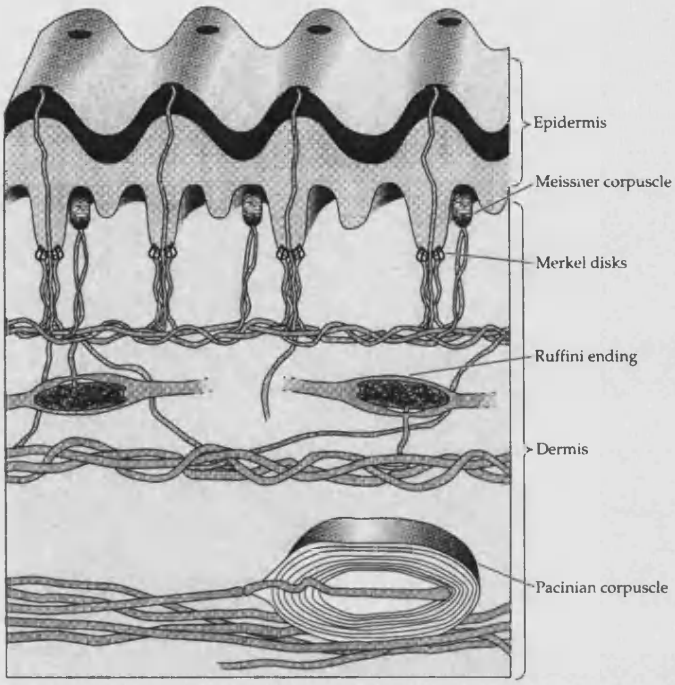

Fig. 1.1 End organs innervated by low threshold mechanoreceptors in glabrous skin. (From Fain, 2003.)

In response to mechanical stimuli rapidly adapting receptors generate action potentials during both the application and withdrawal of a stimulus but cease to fire during the static phase. In contrast, slowly adapting mechanoreceptors fire most rapidly during the application of a mechanical stimulus but continue to generate action potentials throughout the stimulus and do not generate an "off" responses (Fig. 1.2).

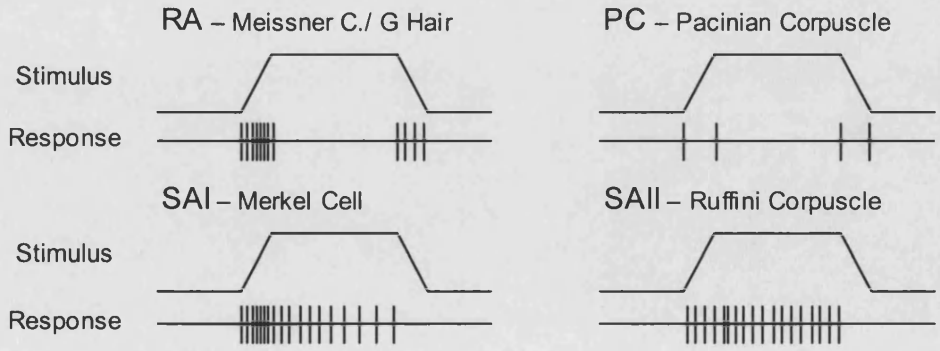

Fig. 1.2 Response properties of low threshold cutaneous mechanoreceptors. The stimulus trace represents a mechanical displacement. The response trace shows the pattern of action potentials (*vertical lines*) evoked by such a stimulus. (Adapted from Zelena, 1994.)

SA1 fibres terminate in the basal layer of the epidermis at Merkel cells. Merkel cells are discoid shaped cells (diameter; 9-16 μm) anchored in the epidermis by spiny projections; they are clustered in touch domes (in hairy skin) or touch spots (in glabrous skin). A single afferent fibre innervates each touch spot/dome and divides so that each branch terminates at a single Merkel cell; nerve endings have cap-like structures that appose the Merkel cell. SA2 mechanoreceptors terminate in Ruffini corpuscles that are situated in the dermis of the skin. Each corpuscle is innervated by a single afferent fibre, which loses it myelin sheath and then branches extensively within a proturbence of collagen. SA2 fibres are more sensitive to skin stretch than to indentation *per se* and adapt more slowly than Merkel cells to a sustained stimulus.

Pacinian corpuscles are the largest of the end organs (typically 0.5 x 1.0 mm) and are found in the dermal layer of skin. A single afferent fibre innervates each corpuscle and each afferent innervates one corpuscle. These receptors adapt very rapidly to skin movements and are specialised to respond to high frequency vibratory stimuli. Pacinian corpuscle afferents are remarkably sensitive, capable of responding to a 10 nm displacement of the skin surface (Johnson *et al*, 2000). The receptive fields of these receptors are therefore very large, often apparently encompassing an entire hand or arm. The structure of these corpuscles is often likened to an onion as it contains many (up to 70) concentric lamellae; the structure is thought to act as a mechanical filter that transmits dynamic forces to the nerve ending but prevents responses to sustained displacements (Section 1.1.2.2). RA fibres terminate more superficially in Meissner's corpuscles. Each RA afferent innervates between 30-80 Meissner's corpuscle with each end organ receiving 2-9 axons; within the corpuscle the unmyelinated nerve ending is entwined with the lamellae of Schwann cells and collagen fibres. RA fibres have much smaller receptive fields than Pacinian corpuscle afferents and are less sensitive to displacement.

In hairy skin, the same receptor types are present although there is a much lower density of Meissner's corpuscles; instead there is a dense innervation of hair follicles by RA Aβ-mechanoreceptors, termed guard-hair (G-hair) receptors. The axons of these neurons lose their myelin and branch to form around fifty comb-like lanceolate (or palisade) endings

that surround the hair with individual branches running parallel to the hair. Some endings wrap around the hair and are termed circumferential endings. All such receptors are excited by deflections of hairs and their discharge frequency is correlated with the velocity of hair movement.

Amongst Aδ-fibres mechanosensitive receptors can be classified as mechanonociceptors and Down-hair (D-hair) receptors. The former category are characterised by high thresholds of activation and their endings exist as bare nerve endings. D-hair receptors are amongst the most sensitive of all mechanoreceptors and have very high dynamic sensitivity. They are activated by the deflection of hairs, although little detailed information is known of the structure of their endings. Mechanosensitive C-fibres all terminate peripherally as bare nerve endings.

1.1.2.2 Mechanosensory Physiology

The vast majority of research in this field supports the notion that the sensory apparatus responsible for the transduction of mechanical forces into a change in membrane conductance is intrinsic to the peripheral terminal of the DRG nerve fibre (Lewin and Stucky, 2000). This is supported by a number of observations; firstly the rapidity of sensory transduction, in particular the ability of Pacinian corpuscle afferents to encode high frequency vibratory stimuli, precludes the contribution of a slow process such as communication between the nerve ending and an auxiliary mechanotransducing cell. Secondly, the peripheral termination of mechanosensitive nociceptive neurons as bare, unspecialised sensory endings indicates that transduction occurs in cells in the absence of complex end organs. Thirdly, despite the association of low threshold mechanoreceptors with end organs, detailed studies have demonstrated that in the absence of such specialisations transduction still proceeds (albeit adaptation may be affected by these structures, see below). Fourthly, when afferent nerves are ligated or cut the resultant neuroma acquires mechanosensitivity indicative of the insertion of the mechanotransduction apparatus into the cell membrane at this point (Welk *et al*, 1990)

and finally, a number of studies (discussed in Section 1.3.2.4) have demonstrated that mechanical stimuli are transduced by cultured sensory neurons.

Merkel cells have a number of attributes of a neurosecretory cell; saliently, they contain dense core vesicles close to the region apposing the nerve terminal. This morphology led to speculation that Merkel cells respond to mechanical stimulation and chemically communicate sensory information to the nerve terminal. However, the majority of research now suggests that they do not contribute to mechanotransduction (Zelena, 1994). Toxic ablation of these cells had given conflicting data, probably due to incomplete eradication of Merkel cells and secondary damage to the sensory nerves, however when Mills and Diamond (1995) used this approach and carefully mapped touch domes they showed that normally functioning SA1 fibres were present in the absence of Merkel cells. Moreover, Kinkelin *et al* (1999) have shown that Merkel cells are almost entirely eliminated postnatally in p75 null mutant mice with apparent no change in the physiology of SA mechanoreceptors.

Pacinian corpuscles are believed to act as a mechanical filter, converting the way mechanical forces are transmitted to the mechanosensory ending at their cores. Using Pacinian corpuscles isolated from the cat mesentery, Loewenstein and colleagues (see Loewenstein and Skalak, 1966) showed that when an intact corpuscle was stimulated the application and withdrawal of the stimulus evoked a receptor potential in the nerve fibre but that when the corpuscle was removed and the bare nerve ending was stimulated the receptor potential was monophasic lasting the duration of the stimulus.

Loewenstein's investigations formed part of a body of work in the 1950s and 1960s that attempted to use extracellular recordings from nerve endings to study transduction events directly. Such investigations are technically demanding due to the small size and inaccessibility of most mechanoreceptor nerve endings, thus, only a small number of preparations have been used for such studies. The most commonly used systems are Pacinian corpuscles from the cat mesentery, frog muscle spindles and crayfish mechano-receptors. In all such studies it was found that mechanical stimuli induce depolarising

receptor potentials of the sensory membrane proportional to the intensity of the stimulus (Catton, 1970 and references therein). A number of studies sought to investigate the ionic basis of the receptor potential, however diffusion barriers created by the structures that encapsulate the sensory terminals often hampered such work making results difficult to interpret. Overall, the data suggest that the receptor potential is mediated via sodium channels with poor selectivity including calcium permeability. Receptor potentials were proportional to external sodium concentrations, although, indicative of a non-selective cationic conductance complete removal of sodium did not ablate responses (see Catton, 1970; Akoev *et al*, 1988). Calcium has a regulatory effect on receptor potentials; increasing external calcium levels led to a reduction in receptor potential amplitude in Pacinian corpuscles, frog muscle spindles and crustacean mechanoreceptors whilst in Pacinian corpuscles removal of extracellular calcium induced a potentiation of the receptor potential (Akoev, 1982; and see Akoev *et al*, 1988 and references therein). Little is known of the pharmacology of receptor potentials, local anaesthetics and tetrodotoxin block the initiation of action potentials in mechanoreceptors but have little effect on the receptor potential itself. Again pharmacological investigation may be complicated by poor drug penetration to the sites of transduction.

The extracellular environments in which the sensory terminals of mechanoreceptors reside may be expected to alter with different end organs. However, in most of these structures extensive clusters of collagen fibres have been noted; for example within Meissner's corpuscle there are thick collagen fibres continuous with epidermal collagen and in Ruffini endings there is a dense collagen network. There is also much collagen in the subcapsular space of Pacinian corpuscles (Zelena, 1994; Fain, 2003). Laminin is found throughout Ruffini corpuscles (Maeda *et al*, 1991) and is found adjacent to the unmyelinated nerve terminals in Pacinian corpuscles (Chouchkov *et al*, 2003). Whether collagen and/or laminin play a role in the transmission of mechanical forces to the sensory transduction apparatus or if they simply have supportive/structural functions remains to be determined.

The majority of Aβ-fibres' sensory terminals innervating end organs contain a dense array of mitochondria and often contain 50-80 nm diameter vesicles. Neurofilaments and microtubules are detectable in the axons also (see Zelena, 1994). The actual site of transduction on the nerve terminal is unclear; transduction elements may be dispersed uniformly across the membrane or may be localised to specific areas. The latter hypothesis is supported for Pacinian corpuscle afferents where lateral axonal spines extending into the radial clefts of the corpuscle are apparent. These spines contain no organelles but are full of dense actin network. Lateral spines have also been observed on Meissner corpuscles' afferents (see Sinclair, 1981; Zelena, 1994).

Extracellular recordings from sensory nerve endings are currently technically unfeasible in rodents; instead a popular technique for assessing mechanosensitivity is the skin-nerve preparation developed by Peter Reeh and co-workers (Reeh, 1988). In this technique an afferent nerve (for example the sural or saphenous nerve) is dissected from the animal with the area of skin that it innervates still attached. This preparation is then maintained in an organ bath for a number of hours whilst single axons are teased from the nerve and placed over an extracellular recording electrode. Natural or electrical stimuli can then be applied to the receptive field of the nerve fibre and its action potential discharge can be recorded. This technique was originally developed in rats but recently, given the importance of genetically manipulated mice in the study of physiology, the response properties of murine sensory fibres have been extensively classified. Koltzenburg *et al* (1997) analysed fibre types in hairy skin; amongst Aβ-fibres, 54% were rapidly adapting and 46% were slowly adapting mechanoreceptors. 34% of Aδ-fibres were D-hair receptors and the remaining 66% were high-threshold mechanonociceptors. All C-fibres had high mechanical thresholds. Later, Cain *et al* (2001) assessed the response properties of fibres innervating mouse glabrous skin; they found that 71% of Aβ-fibres displayed rapidly adapting firing and that the remainder were slowly adapting, the vast majority of these fibres had low mechanical thresholds although some were significantly higher. Amongst Aδ-fibres, 71% had properties of nociceptors whereas 29% had lower mechanical thresholds and did not respond to heat. 77% of C-fibres had high mechanical

thresholds and were polymodal whereas 23% had low thresholds and were, all bar one, purely mechanosensitive. (It should be noted that a mechanical search probe was used in these studies so mechanically insensitive fibres were excluded.)

This technique gives useful data regarding the modality, conduction velocity, thermal/mechanical thresholds and firing rates of fibres. As the output of the system (i.e. action potential firing) is downstream of transduction events, it can, however, be affected by alterations not only in transduction efficiency but also in the initiation and propagation of action potentials.

Little is known of endogenous factors that modulate mechanosensitivity; the majority of data from studies of hyperalgesia and/or allodynia suggest that reductions in mechanical thresholds for pain behaviour occur due to central changes (Woolf and Costigan, 1999). However, developmentally, BDNF has been shown to modulate the mechanosensitivity of slowly adapting mechanoreceptors. In juvenile animals lacking the BDNF gene and in adults heterozygous at this gene locus, slowly adapting mechanoreceptors exhibited higher mechanical thresholds of activation and flattened stimulus-response relationships when assessed using the skin nerve preparation. This deficit was reversed by treatment with recombinant BDNF and all other fibre types assessed were normal (Carroll *et al*, 1998).

1.2 Sensory Mechanotransduction

Mechanotransduction is the primary event in numerous sensory pathways, most obviously in the senses of touch and hearing, but beyond these two modalities, the sensation of acceleration (linear and angular), muscle stretch and tension, joint position, vascular pressure and pain in response to noxious pressure are likewise based on responses to mechanical stimuli.

Rapid sensation of mechanical events external to the cell, as distinct from slower signalling induced by mechanical forces in, say, cell growth, involves the induction of changes in membrane excitability in specialised receptor cells. Despite the ubiquity of mechanosensory transduction, our understanding of it at the molecular level lags behind that of all other sensory modalities (Gillespie and Walker, 2001). It remains to be determined if there is a basic mechanism of mechanotransduction, or a single class of mechanosensitive ion channels, that is conserved across classes of animals. Likewise, it is unknown if different mechanosensory systems, as diverse as the elaborate cochlear hair cell and the bare nerve ending of the nociceptor, are dependent on essentially the same fundamental mechanism (Kernan and Zuker, 1995)? This section will focus on the mechanisms underlying sensory mechanotransduction with a particular focus on mechanosensitive ion channels that in most cases appear central to transduction.

1.2.1 Mechanosensitive Ion Channels: General Considerations

Mechanosensitive ion channels are directly modulated by changes in pressure. Channels may either be intrinsically sensitive to the application of pressure in the plane of the plasma membrane or can be mechanosensitive due to their interactions with auxiliary proteins that allow mechanical forces to be transmitted to the gating mechanism of the channel. The former mechanism has been demonstrated for a number of bacterial channels (see below) whereas the latter mechanism is the favoured hypothesis for metazoan sensory transduction.

Mechanically activated currents have been observed in numerous systems both at the single-channel and whole-cell levels, with the most commonly observed being stretch-activated cation currents (see Hamill and Martinac, 2001; Sackin, 1995). In terms of pharmacology, antagonists of stretch-activated currents have been identified from three chemical classes; amiloride and its analogues, gentamicin and related aminoglycoside antibiotics and gadolinium and other lanthanides. None of these compounds however, act with high affinity or specificity, and the range of effective blocking concentrations varies widely across preparations (see Hamill and McBride, 1996). Consequently, although they allow for some pharmacological characterisation of mechanosensitive channels no antagonist so far identified is able to act as a biochemical "tag".

In only a few cases have the molecular identities of the channels underlying mechanically activated currents been identified and to date no eukaryotic ion channel has unequivocally been shown to be both mechanically gated and crucial to mechano-sensation at the cellular level. Numerous ion channels have been shown to be mechanosensitive where there is no clear connection between this property and the established physiological function of the channel. For instance, the potassium channels TREK-1 (Patel *et al*, 1998), TRAAK (Maingret *et al*, 1999), and *Shaker* (Gu *et* al, 2001) are mechanically gated whereas NMDA receptor activity is also modulated by membrane stretch (Paoletti and Ascher, 1994). In such cases it is unclear if mechanical force represents a relevant physiological stimulus or if it is an artefact of multi-conformational gating, i.e. as membrane tension is altered different channel conformations may be favoured. Therefore, mechanosensitivity is insufficient evidence to ascribe a sensory function to an ion channel (Goodman and Schwarz, 2002; Gu *et al*, 2001; Hamill and Martinac, 2001). Moreover, mechanical gating of ion channels has often been recorded at the single-channel level, when mechanically activated whole-cell currents have been absent (Morris and Horn, 1991; Zhang and Hamill, 2000). This has led some investigators to suggest that mechanical gating may not always be of physiological relevance (Morris and Horn, 1991). Such discrepancies may be due (at least in part) to pathological effects on membrane morphology caused during or after seal formation, in particular the flattening of the membrane across the pipette tip and the decoupling of the

membrane from the underlying cytoskeleton (Hamill and McBride, 1997; Zhang and Hamill, 2000).

Conversely, a number of ion channels (described below) have been identified using genetic approaches as proteins essential for the normal functioning of mechanosensory systems but none have been demonstrated to be directly gated by pressure. The use of classical genetics in invertebrates has been essential in the study of mechanosensation for a number of reasons. Firstly, the absence of high affinity ligands for mechanically gated channels, analogous to TTX for Na^+ channels or α-bungarotoxin for nicotinic receptors, prevents screening of cDNA libraries using this technique. Secondly, harvesting extensive amounts of concentrated channel protein is not technically feasible: For example, vertebrate cochleae contain only several thousand hair cells and each is thought to only express around 100 transduction channels (which probably also means transcript levels are in low abundance) and similarly mechanoreceptors of the somatosensory system are diffusely distributed throughout the body. In contrast, the human retina contains around 10^9 rods that each contains 10^7 molecules of the phototransducer rhodopsin. (Ernstrom and Chalfie, 2003 and references therein). Finally, work on mechanotransduction in hair cells, and subsequent work in *C. elegans*, suggests that the functioning of the transduction channel is dependent on it binding to both extracellular and cytoskeletal proteins (Strassmaier and Gillespie, 2002; Section 1.2.2.1). If a channel were functionally dependent on interactions with auxiliary proteins then the use of an expression cloning approach would be precluded (unless the interacting proteins were present in the host cell).

The only examples of ion channels gated by mechanical tension in the plane of the membrane are the bacterial channels MscL, MscS and MscK, of which the former two are extensively characterised (see Blount and Moe, 1999; Hamill and Martinac, 2001; Sukharev and Corey, 2004 for reviews). MscL and MscS both form active mechano-sensitive ion channels when purified and reconstituted in liposomes. Both channels have large central pores that form non-selective cation channels and both are thought to act as osmotic "safety valves" in bacteria. However, no animal homologues of these channels

have been identified and it is uncertain if channels that function in this way exist higher organisms.

1.2.2 Genetic Screening of Mechanosensory Mutants in C. elegans *and the DEG/ENaC Superfamily of Ion Channels*

C. elegans display a variety of mechanically induced behaviours (Tavernarakis and Driscoll, 1997) but the best characterised is the response to gentle body touch (typically delivered with an eye lash hair) (Chalfie and Sulston, 1981). Touch induces movement away from the stimulus, i.e. stimulation of the posterior field causes forward locomotion and *vice versa*, so mutant screening can be achieved using a simple behavioural assay. Chalfie *et al* (1985) used laser ablation techniques to demonstrate that this behaviour requires 6 touch receptors (Fig. 1.3a), 5 interneurons and 69 motor neurons. Posterior touch sensitivity is dependent on two touch receptors; the posterior lateral microtubule cell (PLM L/R) pair whilst the remaining 4, the anterior lateral microtubule cell pair (ALM L/R) and the anterior ventral microtubule pair (AVM L/R), mediate touch sensation in the anterior field (Fig. 1.3a, Chalfie *et al*, 1985). The defining features of these neurons are their processes, which run along the cuticle of the worm surrounded by the mantle, a specialized extracellular matrix, and selectively express bundles of 15-proto-filament (pf) microtubules (Fig. 1.3b). These specialised microtubules are essential for the mechanosensory functioning of these neurons (Chalfie and Thomson, 1982).

Chalfie and co-workers have for the last 20 years deployed this system to investigate the molecular basis of mechanosensation. The starting point for this work was a screen for mutant nematodes that retained normal locomotion but did not move when stroked with an eyelash hair (Chalfie and Sulston, 1981). This screen resulted in the isolation of 450 touch insensitive worm strains, accounted for by mutations in 18 different genes. All but one gene (*mec*-17, which was weakly insensitive) were found multiple times suggesting that the screen was saturated (Chalfie and Sulston, 1981; Ernstrom and Chalfie, 2003)

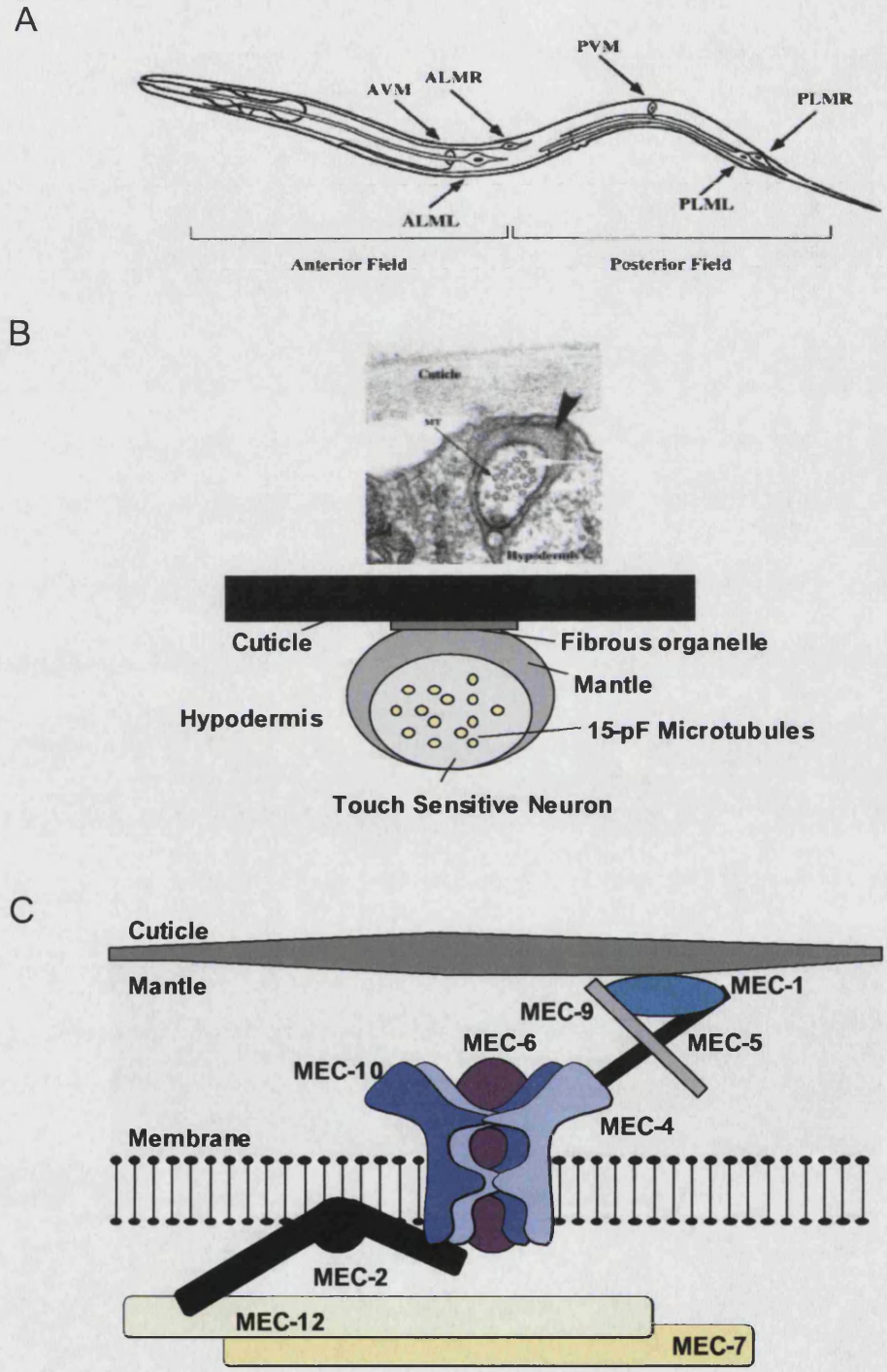

Fig. 1.3 Mechanotransduction in *C. elegans*. *A*, Schematic diagram of a nematode indicating the 6 body touch receptor neurons. *B*, Electron micrograph and schematic diagram of a cross section through the touch process. The specialised 15 pF microtubules are clearly visible in the electron micrograph. *C*, The proposed model of how different MEC proteins interact to form a mechanotransduction complex. (Figure adapted from Tavernarakis and Driscoll, 1997).

although genes that cause death or locomotive defects when mutated could also have a role in mechanosensation.

1.2.2.1 Degenerin Ion Channels and other *Mec* genes identified in *C. elegans*.

The genes identified by Chalfie and Sulston (1981) were termed *mec* genes for mechanosensory abnormal. *unc*-86 and *mec*-3 are two transcription factors required for the differentiation and development of the touch receptors. *mec*-3 is required for the specification of touch receptor cell fate; in its absence the receptors develop as neurons but do not exhibit touch receptor specific features such as the mantle and 15-pf microtubules (see Tavernarakis and Driscoll, 1997; Ernstrom and Chalfie, 2003). Consistent with these morphological abnormalities it was shown that *mec*-3 regulates the expression of *mec*-7 and *mec*-4, and later analysis of *mec*-3 mutants using microarrays revealed around 70 genes regulated by this transcription factor (Zhang *et al*, 2002).

The remaining genes are proposed to encode the structural elements of a multi-protein complex that mediates mechanotransduction by these neurons. This complex is thought to contain an ion channel tethered, via a specific linker protein, to specialised cytoskeletal structures and to specific elements of the extracellular matrix. Tension generated by the relative movements of molecules bound to the channel's internal and external domains are hypothesised to gate the channel (Fig. 1.3c; Gu *et al*, 1996; Tavernarakis and Driscoll, 1997; Ernstrom and Chalfie, 2003; Goodman and Schwarz, 2002). Loss-of-function mutations in any of the 12 *mec* genes independently causes touch insensitivity suggesting each gene is required for normal touch cell physiology and each gene functions non-redundantly. Of the cloned genes, all but one are expressed in touch receptors (*mec*-5 is expressed by hypodermal cells) and *mec*-4 and *mec*-18 are selectively expressed by these cells. Only *mec*-6 is broadly expressed whilst most genes are expressed in touch receptors and a limited number of other cells.

Current evidence suggests that the ion channel within this complex is a heteromeric channel composed of MEC-4, MEC-10 and MEC-6 subunits. The phenotype of *mec*-4

and *mec*-10 mutant nematodes immediately suggested that these genes encoded ion channel subunits although it was not until 2002 that Goodman *et al* managed to reconstitute channel activity in a heterologous system (see below). Originally two classes of mutations were identified in *mec*-4 and *mec*-10 that induced touch insensitivity. One class was loss-of-function mutations in which touch receptors appeared morphologically normal but were insensitive to mechanical stimulation, suggestive of neurons that lacked a functional transduction channel. The second class was gain-of-function mutations that caused cells to become vacuolated, swell and degenerate consistent with ionic dysregulation caused by constitutively active channels (hence the term degenerin). The latter mutations were substitutions of long chain amino acids for a conserved alanine near the second transmembrane domain (MEC-4: aa 713, MEC-10; aa 673); which generate steric interference causing the channel to remain in an open configuration (Lai *et al*, 1996; Tavernarakis and Driscoll, 1997). Genetic interactions between loss- and gain-of-function mutants of *mec-4* and *mec-10* predict a channel complex that includes at least two MEC-4 and two MEC-10 subunits (Hong and Driscoll, 1994) and *mec-10* (Huang and Chalfie, 1994).

García-Añoveros *et al* (1995) uncovered another mutant *mec*-4 allele that induced neurotoxicity; they found that disruption of an extracellular regulatory domain (ERD), either by a point mutation (A404T) or a 9 aa deletion (Δ399-407), was sufficient to promote constitutive activity in this channel. This suggested that the ERD normally keeps the channel in a closed state and the authors proposed that this domain might act as an external gating mechanism necessary for mechanical activation of this channel.

Reconstitution of channel activity through expression of MEC-4 and MEC-10 subunits in *Xenopus* oocytes was achieved by Goodman *et al* (2002). Coexpression of MEC-4 (A713T) and MEC-10 (A673T) (i.e. the mutant,'d', open forms) produced an amiloride sensitive, constitutively active sodium current. This current was essentially K^+ impermeant but more permeable to Li^+ than Na^+ and the IC_{50} for amiloride blockade was 0.12 ± 0.03 μM. They also showed coimmunoprecipitation of MEC-4d and MEC-10d indicating a physical interaction between these proteins. Furthermore, the development

of a successful expression system allowed the modulation of MEC-4 and MEC-10 channel activity by the interacting proteins MEC-2 and MEC-6 to be investigated (Goodman *et al*, 2002; Chelur *et al*, 2002).

Genetic studies suggested that MEC-2 interacted with the transducing ion channel to regulate its function, potentially linking it to the cytoskeleton (Huang *et al*, 1995; Tavernarakis and Driscoll, 1997). *mec-2* encodes a 481 aa protein with three apparent functional domains that include one that is homologous to human red blood cell stomatin (Huang *et al*, 1995). Goodman *et al* (2002) provided direct evidence of MEC-2 interaction with MEC-4 and MEC-10. They showed that MEC-2 co-immunoprecipitates independently with both MEC-4d and MEC-10d and that co-expression of MEC-2 with MEC-4d and MEC-10d in oocytes increased currents by about 40-fold. Increases in current amplitude were achieved without changes in the current's IV relationship or kinetics and independent of recruitment of more channels to the cell membrane. Expression of MEC-2 with wild-type MEC-4 alone or together with wild-type MEC-10 showed these channels could also generate constitutively active, amiloride sensitive currents, albeit of much smaller amplitude than the mutant. These currents were unaffected by low pH (suggesting a distinct gating mechanism to ASICs) or hypoosmolarity (suggesting membrane stretch does not affect channel gating).

MEC-6 was likewise proposed to regulate channel activity in touch receptors based upon genetic studies showing *mec-6* mutants suppressed neurodegeneration in *mec-4* and *mec-10* gain-of-function mutants. (Huang and Chalfie, 1994). Chelur *et al* (2002) cloned *mec-6* and showed it to be a novel type of ion channel subunit. *mec-6* encodes a single membrane pass protein, with a low homology to human paraoxonases, which is expressed in many neurons, including all six touch receptors, and in muscle cells. Co-expression of MEC-6 with MEC-4d and MEC-10d greatly potentiated (by around 24 times) the observed amiloride sensitive, sodium current. Also, MEC-6 expressed with MEC-4d alone, but not MEC-10d, produced significant currents. Interestingly, the effects of MEC-2 and MEC-6 on current amplitude were synergistic; MEC-4d and MEC-4d/MEC-10d mediated currents were increased approximately 400- and 200-fold, respectively.

This observation suggests that these proteins increase conduction by distinct mechanisms. Given that neither protein increases the surface expression of the degenerins, the possible means by which they act include increasing single channel conductance, mean open time or open probability; single channel analysis should allow the testing of these hypotheses. Physical interactions between MEC-6 and MEC-2, MEC-4 and MEC-10 were demonstrated using coimmunoprecipitation. Tagged MEC-6 and MEC-4 proteins colocalised in distinct puncta along the sensory process of touch receptors and the punctate distribution of MEC-4-YFP was shown to be disrupted in mutant *mec*-6 animals.

One long standing objection to the model proposed by Chalfie and colleagues is that the ion channel encoded for by *mec*-4 and *mec*-10 may simply be necessary for the normal functioning of touch receptors and not be mechanically gated (see for example, Kernan and Zuker 1995). Without a direct demonstration of channel gating by mechanical stimulation this claim cannot be refuted, however, two groups have recently used *in situ* techniques to investigate touch receptor function in mutant animals.

Suzuki *et al* (2003a) used transgenic nematodes expressing cameleon Ca^{2+} indicator proteins to observe changes in intracellular Ca^{2+} evoked by mechanical stimulation; worms were immobilised and mechanical stimuli delivered to the receptive field of the ALM touch receptor by a glass probe. Displacements of 10 μm, corresponding to light touch, were applied with different temporal profiles (i.e. brief pokes, longer presses or buzzes where the probe moves against the cuticle) and changes in intracellular Ca^{2+} in the soma of ALM were recorded. The authors reported that all types of stimuli caused ratiometric changes in fluorescence proportional to stimulus duration. Presses induced elevations in Ca^{2+} at the onset and removal of the stimulus; in contrast buzzes generated much larger transients that increased throughout the stimulus likely due to persistent movement preventing adaptation to constant pressure. This method was then used to investigate responses of *mec-4*, *mec-6* and *mec-2* loss-of-function mutants to touch. Consistent with behavioural data, in each of these mutants, low levels of mechanical stimulation failed to evoke Ca^{2+} transients. To determine if this effect was specifically caused by mechanotransduction deficits Suzuki and colleagues cultured touch receptors

and demonstrated that Ca^{2+} transients evoked by high external K^+ were normal in *mec*-2 and *mec*-4 mutants and that voltage-activated currents were indistinguishable in wild-type and *mec*-4 mutant neurons. Hence, the basic physiology of these neurons seems normal. Finally, it was shown that harsh touch, a rapid, 30 μm displacement, also evoked Ca^{2+} transients in touch cells and this effect was present in the absence of functional MEC-4 and MEC-2 proteins.

Miriam Goodman and Martin Chalfie's group have begun to investigate the physiology of touch receptor neurons using *in situ* patch clamp electrophysiology (see Goodman *et al*, 1998). Recording from a touch receptor neuron and stimulating the adjacent cuticle with a glass probe, these investigators have shown that these neurons respond to a "square wave" of pressure with a rapidly activating and inactivating inward current at the application and the withdrawal of the stimulus (MB Goodman and M Chalfie, personal communication). Such a response is consistent with the conclusion reached by Suzuki *et al* (2003a) that touch receptors are more sensitive to movement than sustained pressure. Mechanically activated currents were absent in nematodes with loss-of-function mutations in *mec-2*, *mec-4* and *mec-6* and *mec-7* mutants displayed currents significantly smaller than those in wild-type animals. These results do not directly demonstrate that a MEC-4, MEC-2, and MEC-6 containing channel complex is gated by mechanical displacement, i.e. gating could be a consequence of a separate mechanosensitive process, but it does indicate that this channel mediates the mechanically activated receptor current of these neurons. Direct demonstration of channel gating by mechanical displacement will doubtlessly prove to be technically difficult. Ernstrom and Chalfie (2003) have suggested using the attachment of antibody coated magnetic beads to the channel or adapting laser tweezers. That Goodman *et al* (2002) demonstrated that channels were not modulated by hypotonicity-induced membrane stretch suggests that if the channels are directly gated by pressure the effects of binding proteins will have to be recapitulated.

The other components of the putative mechanotransduction complex are MEC-12 and MEC-7, which are α- and β-tubulins, respectively, and the three extracellular proteins MEC-1, MEC-5 and MEC-9 (see Tavernarakis and Driscoll, 1997 and references

therein). Both MEC-7 and MEC-12 are necessary for touch sensitivity and are required for the formation of the 15-pf microtubules that are unique to touch receptors. The distal ends of these microtubules are positioned outside of the microtubule bundle in close proximity to the cell membrane where they could interact with the channel complex. Microtubules are required for the normal distribution of MEC-2 (Huang *et al*, 1995), although this may only be due to a role in protein trafficking; electron microscopy data showing the relative positioning of the ion channel complex and microtubules would be instructive (Ernstrom and Chalfie, 2003). At present, the available data are equivocal as to whether microtubules play a direct role in channel gating or are only structurally supportive.

The identified extracellular proteins are proposed to act as external-gating springs for the transduction channel through interactions with the channel's large extracellular domains, although to date no biochemical interactions between these proteins and channel subunits has been demonstrated nor have they been shown to modulate functional channels. MEC-5 is a unique collagen made by hypodermal cells; the phenotype of *mec*-5 mutants is restricted to touch insensitivity suggesting that it functions solely in this sensory pathway (Du *et al*, 1996). *mec-1* and *mec-9* both encode proteins containing multiple EGF/Kunitz domains (Du *et al*, 1996; Ernstrom and Chalfie, 2003) that are likely to underlie protein-protein interactions. Although genetic interactions have been observed between genes encoding extracellular proteins and channel complex components (Du *et al*, 1996; Gu *et al*, 1996) it again remains to be determined if their functions are directly related to channel gating or are of a more structural/supportive nature.

1.2.2.2 Epithelial Sodium Channels (ENaC).

ENaCs are heteromeric channels composed of α, β and γ subunits and are found predominately in the apical membranes of epithelial cells where they form constitutively open sodium channels (Canessa *et al*, 1994). The homology between the ENaC subunits and MEC-4 and 10 led to the hypothesis that ENaCs are mechanosensitive.

Awayda *et al* (1995) found evidence that increasing hydrostatic pressure increased the open probability of α-ENaC subunits reconstituted in planar lipid bilayers; interestingly the permeability of the channel changed from being relatively selective for Li^+ and Na^+ over K^+ (Na^+/K^+ selectivity ratio: 7.1) to being a non-selective monovalent cation channel and the IC_{50} for amiloride increased from approximately 150 nM to over 25 μM. Using the same experimental system this group provided evidence that relief of Ca^{2+} blockade underlies mechanical gating of ENaC (Ismailov *et al*, 1997).

A number of doubts about the validity of these studies have however arisen. It has been suggested that the use of an *in vitro* translation system may have caused novel channel behaviour due to incorrect folding and/or oligomultimerisation of the channel or that contaminant proteins were present in the preparation (Hamill and Martinac, 2001). In support of this interpretation the sodium selectivity of the channel is much lower and the single channel conductance much larger than that reported for ENaC in most other preparations (see Kellenberger and Schild, 2002). When αβγ ENaC channels were expressed in *Xenopus* oocytes, a system that generated constitutively active currents essentially identical to those seen in the native epithelium, channels were not gated by membrane stretch (Awayda and Subramanyam, 1998). Studies of ENaC expressed in other heterologous systems have given conflicting results. Kizer *et al* (1997) reported that when the α-subunit was stably transfected in LM (TK^-) cells these channels displayed stretch-evoked activity, the observed channels were however non-specific cation channels with low amiloride sensitivity. Moreover, endogenous stretch activated currents have also been observed in this cell line (Wan *et al*, 1999). When recording native ENaC channel activity in rat cortical collecting tubules Palmer and Frindt (1996) found mechanically gated activity in 6 of 22 patches. This could have been due to differential separation of the channel from cytoskeleton when pulling patches. Ma *et al* (2002) have suggested that ATP tonically inhibits stretch-induced activity in native ENaCs; recording in cell-attached patches from A6 distal nephron cells these investigators found that sequestering ATP or blocking P2 receptors increased the incidence of a stretch-induced increase in P_O from a third to all patches. Overall, the mechanosensitivity of ENaCs in their native environment remains contentious and it has

not been reported that a mechanical stimulus can generate an ENaC-mediated whole cell current.

The detection of ENaC subunit expression in a number of mechanosensory cell types has however led several groups to propose that these channels function in mechanotransduction. That amiloride blocks the hair cell's transduction channel had suggested a role for ENaCs in hearing (see Strassmaier and Gillespie, 2002) and Hackney *et al* (1992) found that an antibody raised against an α-ENaC epitope labelled discrete sites on hair bundles, suggesting this may be the transduction channel. However, amiloride blockade of the hair cell transduction channel is by binding to two sites outside of the electrical field, whereas blockade of ENaCs is due to a single amiloride molecule occluding the channel pore within the electric field and the Ca^{2+} permeability of the two channels is drastically different (see Strassmaier and Gillespie, 2002). Moreover, hair cells of neonatal mice lacking the gene for α-ENaC display normal mechanotransduction (Rusch and Hummler, 1999).

Drummond *et al* (1998) found γ-ENaC immunoreactivity on the peripheral terminals of baroreceptors innervating the aortic arch and carotid sinus and using RT-PCR found transcripts for the β- and γ- but not α-ENaC subunits in nodose ganglia. Functionally, cultured baroreceptor neurons (labelled by an injection of Di-I into the aorta) responded to a "puff" of external buffer with an increase in intracellular Ca^{2+} and this response was blocked by 100 nM amiloride. In a carotid sinus preparation the amiloride analogue benzamil inhibited pressure-induced baroreceptor discharge and the resultant reflex mediated fall in blood pressure. Subsequently, transcripts for β- and γ- ENaC but not α-ENaC subunits were found in the DRG using RT-PCR and β- and γ- ENaC immuno-reactivity was found in medium-large cells (largely colocalised with NF200) and in a number of mechanosensory nerve endings in the footpad (Drummond *et al*, 2000). Fricke *et al* (2000) using RT-PCR and immunocytochemistry investigated the expression of ENaC subunits in the trigeminal ganglia and found transcripts for all three channels and immunoreactivity for each in every neuron of this ganglion (although satellite and

Schwann cells were negative). In the periphery immunoreactivity for α-, β- and γ- ENaC was detected in lanceolate endings in the rat vibrissal follicle-sinus complex.

Although the evidence is indirect, these data together suggest a role for ENaC subunits in somatosensory mechanotransduction. Physiological investigation of mice lacking the appropriate genes has been precluded by the neonatal lethality of all three knockouts (Hummler *et al*, 1996; Barker *et al*, 1998; McDonald *et al*, 1999) although now tissue specific knockouts could be generated. The observation of immunoreactivity for all three ENaC subunits in trigeminal ganglia by Fricke *et al* (2000) is at odds with the absence of a report of constitutively active, amiloride sensitive sodium currents in these cells. β- and γ-ENaC subunits do not form an active ion channel when expressed without the α-subunit and no interactions with ASIC subunits have been reported. Drummond *et al* (1998; 2000) have suggested that this may reflect the formation of a channel that remains in the closed state unless activated by mechanical force. In a previous study by the same group using isolated baroreceptor neurons it was shown that mechanically-evoked increases in intracellular Ca^{2+} were unlikely to be mediated by secondary activation of voltage-gated Ca^{2+} channels (Sullivan *et al*, 1997), hence the underlying mechanosensitive channel must be Ca^{2+} permeable, a feature not associated with ENaC channels. Furthermore, the specificity of amiloride for ENaCs is unclear, as much previous work has shown that this compound blocks multiple types of mechanosensitive ion channels (Hamill and McBride, 1996).

Although benzamil blocks mechanically evoked activity in baroreceptor nerves (Drummond *et al*, 1998), it does so (as may be expected in a whole organ preparation) at a concentration (>50 μM) significantly higher than at which it inhibits ENaC activity. Carr *et al* (2001) found that amiloride and benzamil (100 μM) inhibited mechanically-evoked activity in vagal mechanoreceptors of the trachea but then went onto to discover that these and related compounds also inhibited electrically-evoked activity in these nerve fibres. Moreover, the orders of potency of amiloride analogues for inhibiting nerve fibre activity and for blocking ENaC currents were found to be different and 100 μM benzamil was shown to significantly reduce voltage-activated sodium currents in isolated neurons.

These data therefore suggest that amiloride analogues do not inhibit vagal mechanosensory signalling via an action on mechanotransducing ENaCs and such a study of the carotid sinus system (as used by Drummond *et al*, 1998) would be informative.

1.2.2.3 Acid Sensing Ion Channels (ASIC)[4]

ASICs form a distinct branch of the DEG/ENaC phylogenetic tree (Fig. 1.4a). Currently there are four identified genes encoding ASIC subunits, ASIC1-4, with two alternative splice variants of ASIC1 and 2 taking the number of known subunits to six. Although, protons are the only confirmed activator of ASICs, the homology between ASICs and MEC channels, coupled to high levels of expression of ASICs in sensory neurons, has led to the hypothesis that these channels function in sensory mechanotransduction (Lewin and Stucky, 2000; Welsh *et al*, 2001). Similar to other members of the DEG/ENaC family, ASICs have two transmembrane domains with intracellular C- and N-termini and a large extracellular domain (Fig. 1.4b).

The first ASIC to be cloned was discovered simultaneously by the groups of Michael Welsh (Price *et al*, 1996) and Michel Lazdunski (Waldmann *et al*, 1996). Both groups identified ASIC2a by searching EST databases for sequences homologous to the degenerins. The following year ASIC1a was identified by Waldmann *et al* (1997a) and was found to be activated by extracellular acidification (pH < 6.9). Shortly afterwards, Lingueglia *et al* (1997) demonstrated that protons (pH < 4.5) also gate ASIC2a and identified a splice variant of ASIC2, ASIC2b, that differs in the first 236 amino acids. Although, ASIC2b is not gated by low pH it heteromultimerised with ASIC2a and ASIC3 and altered the inactivation kinetics, pH sensitivities and ionic permeabilities of these channels. ASIC3 was cloned by Waldmann *et al* (1997b) and shown to encode a proton-gated ion channel with a biphasic response to external acidification; below pH 6.5 ASIC3 generates a transient current whereas below pH 4.0 it also gives rise to a sustained current. In 1998, a splice variant of ASIC1a was discovered with a distinct 172 amino acids at the N terminus (Chen *et al*, 1998). This subunit, termed ASIC1b, also forms a

[4] See Ion Channel Nomenclature for alternative names applied to ASICs.

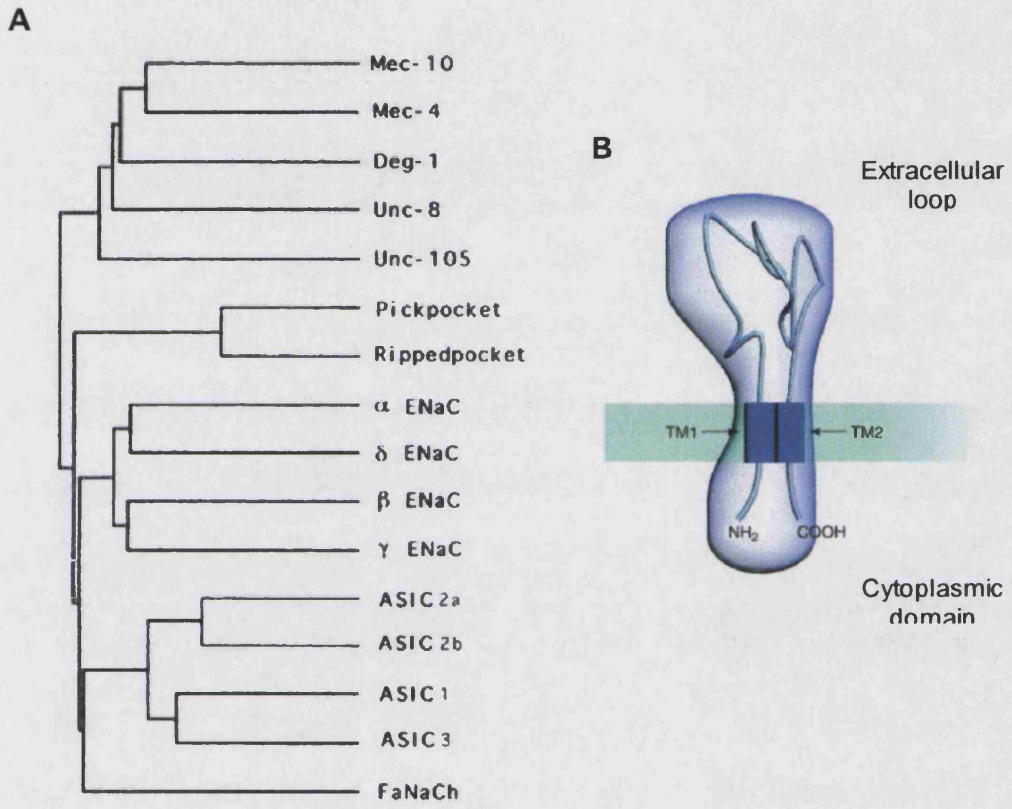

Fig 1.4 *A*, Phylogenetic relationship of characterised members of the DEG/ENaC family of ion channels. ASICs form a distinct branch of the family and are most closely related to FaNaCh, a mollusc channel gated by neuropeptides (Perry *et al*, 2001). *B*, Schematic diagram of postulated ASIC structure; each subunit has two transmembrane domains with a large extracellular domain and intracellular amino and carboxy termini. (*A* from Alvarez de la Rosa *et al*, 2000; *B* adapted from Krishtal, 2003.)

functional homomeric ion channel gated by protons (pH ≤ 6.5). The final member of this channel family, ASIC4 was cloned by Akopian *et al* (2000b); ASIC4 does not form a proton-gated channel when expressed in COS-7 cells and heteromultimerisation of ASIC4 with other ASIC subunits has not been reported.

Original studies of heterologously expressed ASIC subunits showed that the majority of proton-gated currents mediated by ASIC homomers and two subunit heteromers are transient, sodium currents (see Waldmann and Lazdunski, 1998 and references therein). A few key differences are apparent though, most notable is the late, sustained component displayed by channels containing ASIC3, interestingly this component is Na^+ selective in ASIC3 homomers (Waldmann *et al*, 1997b) but is transformed into a non-selective cation conductance when ASIC2b is present (Lingueglia *et al*, 1997).

ASICs are distributed throughout the nervous system suggesting they have a physiological function in multiple systems. Consistent with this observation are multiple studies showing that numerous types of central and peripheral neurons exhibit proton-activated currents that are likely to be mediated by these channels (see Waldmann and Lazdunski, 1998 and references therein). Overall it appears that transcripts for all ASIC subunits are expressed to greater or lesser degrees in DRG neurons and ASIC1b (Chen *et al*, 1998) and ASIC3 (Waldmann *et al*, 1997b) are exclusively expressed in sensory ganglia. Primary sensory neurons of the trigeminal ganglia (Krishtal and Pidoplichko, 1980; 1981) and DRG (Bevan and Yeats, 1991) both display transient, ASIC-like, proton-gated currents.

It has long been known that an acidification of the extracellular environment is a component of inflammation and low pH can activate and/or sensitise nociceptors (Steen *et al*, 1992; 1995). Therefore, it was hypothesised that ASICs may have a nociceptive function in the response of DRG neurons to inflammation (Krishtal and Pidoplichko, 1981; Waldmann *et al*, 1997a, Reeh and Kress, 2001). However, ASICs are not the only ion channels gated by low pH in the DRG; TRPV1, expressed in nociceptors, is also activated when the external pH falls below 5.5 (Caterina *et al*, 1997). Other workers in

the field, noting the homology between ASICs and MEC-4 and –10 proposed that ASICs might function as the elusive mammalian mechanotransducers.

A number of groups have investigated the distribution of ASIC channels across the cell types of the DRG. Waldmann *et al* (1997a), using *in situ* hybridisation, found ASIC1a to be most highly expressed in small DRG neurons. Olson *et al* (1998) reported that an antibody directed against a 15 amino acid sequence in the C-terminus of ASIC1 stained predominately substance P and CGRP-positive small neurons, although in the data shown a number of non-peptidergic, larger cells also display ASIC staining. Alvarez de la Rosa *et al* (2002), using a polyclonal antibody against a region of the C-terminus of ASIC1 (i.e. a region common to 1a and 1b), found expression of this protein in subsets of both peripherin-positive, small and NF200-positive, large DRG neurons. The results from Chen *et al* (1998) suggest that immunoreactivity in larger neurons may represent the expression of ASIC1b; using *in situ* hybridisation ASIC1b transcripts were found predominantly (70% of positive cells) in peripherin-negative neurons, whereas transcripts for ASIC1a were found in peripherin positive, small neurons.

Current data largely suggest ASIC2a is expressed predominately in medium to large DRG neurons; both García-Añoveros *et* al (2001), using a splice variant specific N-terminus directed antibody, and Alvarez de la Rosa *et* al (2002), using an antibody against the shared ASIC2 C-terminus, detected immunoreactivity in NF200-positive, peripherin-negative neurons. Price *et al* (2000), using *in situ* hybridisation and immuno-cytochemistry (pan-ASIC2 C-terminus antibody), found the most intense staining for ASIC2 in large neurons although staining was also present in small cells. The *in situ* hybridisation data of Lingueglia *et al* (1997) showed the most intense staining for ASIC2b in small neurons.

With regards to ASIC3, Lazdunski's group again reported that transcripts are found most abundantly in small DRG neurons (Waldmann *et al*, 1997b). Alvarez de la Rosa *et al* (2002) in contrast found immunoreactivity most abundantly in large neurons, mainly colocalised with ASIC2, whilst in Price *et al* (2001) the authors report ASIC3 staining in

most small and large DRG neurons and that almost all substance P positive cells are immunoreactive for ASIC3.

Functionally, a number of groups have investigated the distribution of ASIC-like currents in sensory neurons. In their original descriptions of transient, proton-gated currents in trigeminal sensory neurons Krishtal and Pidoplichko (1980, 1981) found these currents predominately in small diameter neurons and thus they suggested a nociceptive function for the underlying channels. They also reported three classes of inactivation kinetics, the predominant class (25/32 responsive neurons) was inactivation within 0.5-1.0 sec and the two other classes were slower. This may indicate different subunit compositions of underlying channels or, in the slowest class, a contribution from TRPV1.

Petruska *et al* (2000; 2002) subclassified, acutely dissociated rat DRG neurons into a number of groups (see Section 1.3.1) and found transient low pH-activated currents mainly in small and medium neurons, that on the basis of their long afterhyper-polarisations, were putatively considered silent Aδ- and C-fibre nociceptors. These currents were sensitive to amiloride blockade and again different kinetic profiles were observed suggesting differential ASIC subunit oligomerisation (or distinct posttranslational modifications). One further population of presumptive non-nociceptive small neurons (narrow action potentials, CGRP, substance P and IB4 negative) also displayed ASIC-like currents (properties of large DRG neurons are yet to be reported). Cheryl Stucky's group (Dirajlal *et al*, 2003) has looked at proton-gated currents in small diameter cultured mouse neurons and dividing cells according to IB4 staining, they reported that only IB4- nociceptors (35% of them) express desensitising responses to low pH.

Other groups have compared channel activity observed in sensory neurons with that of heterologously expressed ASICs. Alvarez de la Rosa *et al* (2002) made outside-out patch recordings from rat DRG neurons and contrasted the currents with currents generated by heterologous expression of either ASIC1a alone or ASIC2a and 3 together in *Xenopus* oocytes. Their findings were that most (58/66) large (30-50 μm) neurons were proton

sensitive and that 35 of 58 cells responded with ASIC1a like currents whereas the remaining 23 had ASIC2a/3 like currents, this arrangement however would not have been predicted by their, or others, immunocytochemistry data (see above). In small neurons about half (20/39) displayed transient proton-gated currents and 17 of these cells had ASIC1 like activity, which is consistent with their localisation data. These analyses are compromised by the incomplete analysis of subunits in oocytes suggesting that their classification of DRG currents may be oversimplified. For example it seems that ASIC1b is the abundant ASIC1 transcript in larger DRG neurons whereas most reports suggest ASIC2b is more abundant than ASIC2a in DRG and they did not coexpress all 3 subunits. Ed McCleskey's group have shown that cardiac afferent neurons, labelled using the retrograde tracer Di-I, display low pH-evoked currents that closely resemble those mediated by ASIC3 expressed in COS-7 cells (Sutherland *et al*, 2001). The large proton-gated currents displayed by cardiac afferents coupled to the high sensitivity of ASIC3 to small drops in pH led these authors to suggest that this ion channel is important in sensing myocardial acidity. Subsequent work demonstrating that lactate can potentiate, via Ca^{2+} chelation, cardiac afferent and ASIC3 responses to protons further supports this hypothesis (Immke and McCleskey, 2001).

Generation of ASIC1, 2 and 3 null mutant mice allowed the effect of specific subunit removal on proton-gated currents to be investigated. In "large" DRG neurons lacking the ASIC3 gene there were substantial alterations to proton-evoked currents (Xie *et al*, 2002)[5]. Transient currents were present in similar proportions of cells (44% +/+ versus 34% -/-) tested but in ASIC3 null neurons currents were larger, had slower desensitisation kinetics and were much less sensitive to pH drops between 6.5-6.9. There were also changes in the rundown of currents and the mutant animals had responses more sensitive to amiloride blockade and less sensitive to FMRFamide-induced potentiation. The authors concluded that ASIC3 is likely to heteromultimerise with one or more ASIC subunits to mediate "large" neurons' responses to acidification. Benson *et al* (2002) systematically studied the responses of DRG neurons derived from ASIC1, 2 and 3 null

[5] It should be noted that the neurons classified as large in this study had a mean diameter of 32-33 μm, which in most classifications would be considered medium and likely to be nociceptive in function.

mutants and compared them to coexpression of ASIC1a, ASIC2a and ASIC3 in COS-7 cells. The properties of the currents compared were: pH sensitivity, τ desensitisation and τ recovery. Coexpression of all three subunits generated currents similar to transient currents seen in wild-type neurons; significantly, desensitisation of wild-type responses was faster than that of any individual subunit, which negates the possibility that they are the average of concurrently activated homomeric channels. Moreover, the responses of single knock out neurons (e.g. ASIC3 KO) were very similar to those generated by the coexpression of the two other subunits (e.g. ASIC1a and 2a). These data are strong evidence that all three subunits coassemble in heteromeric channels in DRG neurons. Again, it is likely that this situation is oversimplified due to the omission of ASIC1b and ASIC2b from the analysis and the expression studies, outlined above, tend to suggest that the three subunits are not entirely colocalised. Moreover, some investigators (e.g. Petruska *et al*, 2000; 2002) observe significant heterogeneity amongst transient pH-gated currents that is not reported in the work of Xie *et al* (2002) and Benson *et al* (2002). It therefore remains to be determined if some subpopulations express different complements of ASIC subunits (perhaps coexpression of all 3 is the most common arrangement in medium-large neurons), if the subunits can undergo functionally significant posttranslational modification or if the contribution of other pH sensitive channels is important (possibly ASIC4, TRPV1 or others).

Overall much has been learnt of the biophysical properties of ASICs and their distribution in the nervous system, however definitive evidence regarding their physiological function remains elusive. A major issue regards the physiological relevance of the rapid drops in pH used to activate these channels, i.e. do physiological increases in acidity occur quickly enough to generate significant currents through these rapidly desensitising channels? Furthermore, given homeostatic acid-base buffering *in vivo* it is unclear what values of pH the receptors are exposed to *in situ*. Other questions include whether there are undiscovered physiological ligands for these channels and the outstanding question of whether these channels can be mechanically gated.

Besides the unresolved role of inflammatory acidosis in modulating ASIC activity, it has been suggested that the release of synaptic vesicles may cause a rapid acidification of the synaptic cleft capable of activating ASICs. ASIC1 is distributed in regions of high synaptic density in the brain (Wemmie *et al*, 2003) and this hypothesis has been supported by deficits seen in hippocampal synaptic plasticity in ASIC1 null mutants, specifically in changes induced by high frequency stimulation (Wemmie *et al*, 2002). Currently no ligands bar protons are known to activate ASICs, although the related molluscan channel FaNaC is gated by FMRFamide (see Perry *et al*, 2001). In mammals, FMRFamide and related compounds slow the desensitisation rates of ASIC1a/b and 3. However these peptides do not directly gate the channel and regulatory effects are only seen at high concentrations (≈ 50-100 μM) (Askwith *et al*, 2000). Nonetheless, modulation of endogenous DRG proton-gated currents by related peptides has enabled Deval *et al* (2003) to show that potentiation of the sustained component of ASIC-mediated currents can significantly increase sensory neuron excitability.

If ASICs function in mechanotransduction they must be expressed in the sensory terminals of mechanoreceptor neurons García-Añoveros *et al* (2001) studied ASIC2a distribution in DRG neurons. At the cell body ASIC2a immunoreactivity was found in the cytoplasm predominantly near the axon hillock and it was shown that this subunit is selectively transported to the periphery by sensory neurons. When nerve endings were stained for ASIC2a, immunoreactivity was largely colocalised with NF200 staining and was seen in nerve endings associated with Meissner corpuscles, Merkel cells, hair follicle afferents (circumferential and lanceolate), vibrissal afferents and the subpopulation of bare intraepidermal terminals that expressed NF200. In agreement with this work, Price *et al* (2000) reported staining of lanceolate nerve endings surrounding hair follicles, although staining in other peripheral structures was not reported.

ASIC3 immunoreactivity was also detected in the sensory terminals of DRG neurons by Price *et al* (2001). They reported staining of nerve fibres associated with Meissner's corpuscles, hair follicles, Merkel cell complexes and in fine epidermal nerve endings.

Olson *et al* (1998) presented data suggesting ASIC1 is also located in nerve endings of the skin and claimed that it is often colocalised with substance P staining.

Expression in sensory terminals would be necessary for a role in the transduction of either acidic or mechanical stimuli. That the majority of Aβ-fibres' sensory terminals are immunoreactive for ASICs is at odds with the observation that low threshold mechano-receptors are not activated by low pH (see Lewin and Stucky, 2000). Thus, Welsh *et al* (2001) have proposed that ASICs may exist, analogous to MEC-4 and MEC-10, in a multiprotein transduction complex that through an unknown mechanism masks the proton sensitivity of these channels. Other possibilities include that encapsulation of Aβ-fibre endings by end organs creates a diffusion barrier preventing experimental acidification reaching the nerve membrane or that ASICs are restricted to intracellular compartments at the terminal.

To investigate the role of ASIC2 (Price *et al*, 2000) and ASIC3 (Price *et al*, 2001; Chen *et al*, 2002) in somatosensory physiology null mutants for each of these genes were assayed electrophysiologically and behaviourally for sensory responses to a range of stimuli. For both mutants, Gary Lewin's group used the skin nerve preparation (see Section 1.1.2.2) to study the response properties of DRG fibres to mechanical, thermal and chemical stimulation. In ASIC2 knockouts Aβ-fibre mechanoreceptors displayed decreased firing rates in response to suprathreshold mechanical stimulation, whilst all other fibres types had normal responses (Fig.1.5a). In rapidly adapting mechanoreceptors firing rates were approximately 50% of those seen in wild-types. Slowly adapting fibres had a significant reduction in firing but this was only approximately 20% below control values at the highest stimulus intensity. Acid sensitivity of C-fibres was unchanged in ASIC2 nulls. These data suggest that ASIC2 selectively plays a role in modulating the sensitivity of low threshold mechanoreceptors; it is however notable that the threshold of activation is normal in all fibre types. The authors show with whole-cell patch clamp recordings that there is no difference in action potential thresholds between nulls and controls suggesting electrical excitability *per se* is not disrupted, however it would be informative to determine if the firing rates of all fibre types are normal in response to

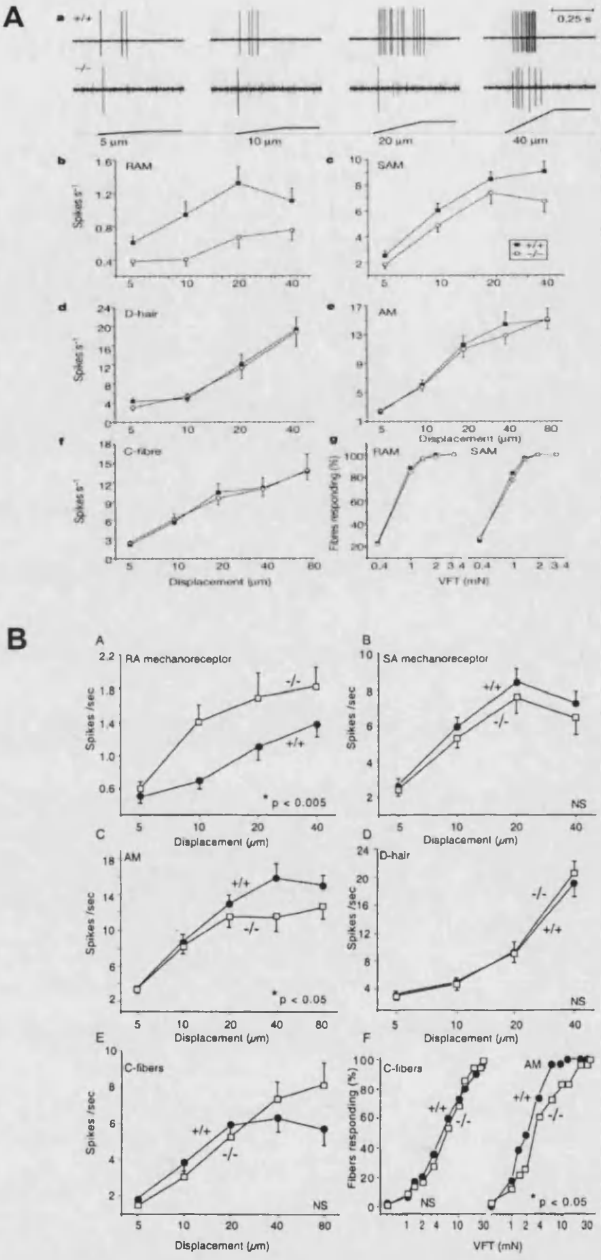

Fig. 1.5 Mechanoreceptor sensitivity assessed in ASIC2 (***A***) and ASIC3 (***B***) null mutants using the skin-nerve preparation. ***A***, ASIC2 nulls. *a*, Examples of rapidly adapting mechanoreceptor responses from wild-type (+/+) and ASIC2 null (-/-) mice. *b-f*, Stimulus-response functions for fibre types indicated. (*RAM;* rapidly adapting Aβ-fibre mechanoreceptor, *SAM;* slowly adapting Aβ-fibre mechanoreceptor, *D-hair*; down-hair Aδ-fibre mechanoreceptor, *AM*; Aδ-fibre mechanonociceptor). *b* and c, Firing frequencies of RAM and SAM fibres were significantly lower in ASIC2 nulls. *g*, Median force required to activate low threshold mechanoreceptors. VFT is von Frey threshold. ***B***, ASIC3 nulls. *A-E*, Stimulus-response functions for fibre types indicated. *A*, RAM fibres fire at higher frequencies in knockouts and, *C*, AM fibre responses are reduced in the knockouts. *F*, Activation thresholds are unchanged for C-fibres and are slightly increased for AM fibres. (Figures taken from *A*, Price *et al* (2000) and *B*, Price *et al* (2001). X axes should read 50-800 μm (*Errata* published).

electrical stimulation of their receptive fields. It may be the case that although action potential thresholds are normal, ASICs somehow contribute to the ability of neurons to fire trains of action potentials; in the raw data presented the first mechanically evoked action potential occurs as normal but subsequent firing is reduced.

In mice lacking the gene for ASIC3 Price *et al* (2001) found deficits in the responses of nerve fibres to activation by heat, protons and mechanical stimuli. In response to mechanical stimulation rapidly adapting mechanoreceptors showed *enhanced* firing to suprathreshold stimuli, the maximal difference being an approximate doubling of the firing rate. Conversely, at high stimulus intensities, Aδ-mechano-nociceptors showed reduced responses and also a minor increase in mechanical thresholds (Fig. 1.5b). No other fibre type was different from wild-type fibres. To determine if ASIC3 contributes to acid-induced firing in C-fibre mechanoheat (C-MH) receptors two strengths of acidic solutions were injected into the receptive field. Following the application of a pH 5 solution C-MH fibres in null mutants fired at a lower rate than in wild-types, by contrast no difference was detectable at pH 4 owing to an increase in firing in the nulls and little change in evoked activity in wild-types. This may represent a differential contribution of TRPV1 at the two pHs, suggesting ASIC3 functions in the detection of smaller drops in pH. Finally, quite unexpectedly, a shortening of the response to heating the receptive field to 52°C was observed in ASIC3 knockouts.

At the behavioural level both Price *et al* (2001) and Chen *et al* (2002) have assayed ASIC3 nulls' responses to painful stimuli. Despite the outlined deficits in Aδ-afferent fibres' responses to mechanical stimulation, neither group found changes in acute behavioural responses to mechanical stimuli (i.e. von Frey withdrawal thresholds). Price *et al* (2001) also found no effect of ASIC3 gene ablation on paw withdrawal latencies to radiant heat (temperature not given) in carageenin inflamed or non-inflamed mice. Neither did they find differences in response to 0.6% acetic acid injection. However, differences were found in two tests of hyperalgesia; mechanical withdrawal thresholds following carageenin administration were interestingly lower in ASIC3 nulls than in controls and conversely, following hyperalgesia induced by intramuscular acid (pH 4)

injection ASIC3 nulls were much less responsive than wild-types. The overall conclusion of Chen *et al*'s (2002) analysis of ASIC3 nulls was that this protein has a modulatory role in responses to high intensity pain. This group, in slight disagreement with Price *et al* (2001), found no difference in responses to acute thermal or mechanical stimuli between groups following carageenin-induced hyperalgesia. However, differences emerged between nulls and controls when high intensity noxious stimuli were applied to non-inflamed animals. For instance, although there was no significant difference in the tail flick test at 50°C, when the temperature was increased to 52.5°C or 55°C nulls had shorter withdrawal latencies. Likewise when 0.1-0.5% acetic acid was injected intraperitoneally no significant strain differences were apparent but (in contrast to Price *et al*, 2001) at 0.6% writhing behaviour was more frequent and onset latency shorter in nulls. Finally, in the tail pressure assay the pain threshold was reduced by approximately 40% in the absence of ASIC3.

In contrast to the ASIC2 knockouts, where abnormalities were limited to one modality, the picture that emerges from studying ASIC3 nulls is that this channel contributes to sensation in multiple modalities. The skin-nerve preparation data shows certain fibres have altered sensitivity to heat, protons and pressure. Although the behavioural data is confusing, with a mixture of hypo- and hyperalgesic changes, it is consistent with ASIC3 functioning in various modalities. It remains to be determined if the type of acid injection given in these studies is functionally relevant, in terms of the rate and magnitude of pH change, to acidosis that occurs during inflammation.

Studies of the knockout animals are the most significant indication that ASICs play a role in mammalian mechanosensation. Yet, no studies have reported mechanically activated currents, either at the whole-cell or single-channel level, that are attributable to ASICs. Moreover, the observation that amiloride and its analogues block a number of mechano-sensitive ion channels does not strongly implicate ASICs as this compound does not have specific affinity for a single class of channels. The skin-nerve preparation is a powerful approach for studying the response properties of DRG fibres but in recording action potential discharge it gathers data a number of steps down stream of transduction. Hence,

ablation of ASICs could affect firing by decreasing the efficiency of transduction or dysregulation of action potential generation, possibly specifically, during high frequency firing. If the latter scenario were true the modality specificity in ASIC2 could be due the predominant expression of ASIC2 in large neurons, likely to be low-threshold mechanoreceptors, whereas, consistent with the broader consequences of its ablation, ASIC3 appears to be more widely distributed across different cell types.

The demonstration that ASICs contribute to the mechanical sensitivity of DRG neurons, in combination with work in *C. elegans*, has led to the hypothesis that these channels are part of the mammalian mechanotransduction apparatus. It is argued that ASIC2, ASIC3 and, given the evidence of heteromultimerisation, ASIC1 exist in a mechanotransduction complex analogous to that seen in nematodes (Welsh *et al*, 2001; Lewin and Stucky, 2000). At present little is known of the other putative components of such a complex although Gary Lewin's group have cloned a number of neuron specific stomatin-like proteins (homologous in part to MEC-2) and shown that one of them, Nstom-1, binds to ASIC2 (Eilers *et al*, 2002 and GR Lewin, personal communication). Conversely, a number of other groups have used the yeast 2-hybrid system to look for ASIC binding proteins but at present no other interacting molecules are similar to MEC proteins (see Section 1.3.3). A further key difference is that in the 6 body touch receptors of *C. elegans* microtubules are the key cytoskeletal specialisation required for mechanotransduction, putatively anchoring the transduction complex but most studies of mammalian sensory terminals suggest that at the likely site of transduction the axoplasm is rich in actin rather than tubulin (see Section 1.1.2.2).

If such a complex does exist, how would the channel within it be gated? Current data suggest that acid-gating of ASICs is achieved when protons displace Ca^{2+} from a binding site on the external face of the channel pore (Immke and McCleskey, 2003). It is thought that when Ca^{2+} is bound to this site it occludes the channel pore but that proton binding allows the passage of cations through the channel. This model suggests that ASIC gating is independent of a conformational change. Perhaps mechanically induced changes in the protein could unblock the channel by reducing the binding affinity for Ca^{2+} or

alternatively an extracellular binding protein could interact directly with the Ca^{2+} binding site. When cerebellar Purkinje neurons were swelled by exposure to 25% hypotonic solution ASIC-mediated responses to pH 6 were potentiated by around 20% (Allen and Attwell, 2002). The authors conclude that this supports the notion that ASICs are modulated by membrane stretch although the mechanism by which this occurs is unclear (it is also uncertain if this phenomenon is specific to ASICs as no data is presented on the behaviour of other channels during hypotonicity). Although this effect is modest, it could indicate that membrane stretch shifts pH-sensitivity of ASICs to more neutral values. Interestingly, the extracellular regulatory domain identified in MEC channels by García-Añoveros *et al* (1995) and postulated to be important in mechanical gating, has since been shown to be present only in MEC-4, MEC-10 and seven other closely related nematode degenerins (Goodman and Schwarz, 2002); some of which are associated with mechanosensory cells (see Section1.2.2.4). Thus, this region is absent from ASICs and all other branches of this ion channel superfamily; many of which have functions distinct from mechanosensation.

1.2.2.4 Other DEG/ENaC Channels Implicated in Mechanosensation

Beyond the ion channels described above many members of the DEG/ENaC superfamily remain uncharacterised or only partially analysed. In a recent survey of genome databases Goodman and Schwarz (2002) found 28 sequences encoding related proteins in *C. elegans* and 25 in *Drosophila*. Interestingly, many fewer subunits were present in vertebrate genomes; 9, 8 and 7 in humans, mice and *Fugu rubripes*, respectively. Goodman and Schwarz's analysis classified DEG/ENaC channels into 6 subgroups; 3 were specific to *C. elegans*, the majority of *Drosophila* channels were in a large single subgroup and ASICs were contained in a group also containing nematode, *Fugu* and other mammalian channels.

Mechanosensory functions have been proposed for two nematode DEG channels other than MEC-4 and MEC-10; both of which are in the same subgroup as the MEC channels and have the conserved extracellular regulatory domain (Goodman and Schwarz, 2002).

One of these channels is UNC-105 (Liu *et al*, 1996), which is expressed in muscle cells and *unc-105* mutants show hypercontracted musculature and paralysis (Park and Horvitz, 1986). The effects of semi-dominant alleles of *unc-105* can be suppressed by mutations in a type IV collagen (*let-2*), which by analogy to the MEC complex, suggests UNC-105 is regulated by an interaction with the extracellular matrix (Liu *et al*, 1996). UNC-8 was characterised by Tavernarakis *et al* (1997) and is expressed in sensory neurons, motor neurons and interneurons. The phenotype of *unc-8* mutants is a relatively subtle one affecting locomotion. *C. elegans* typically move in sinusoidal body waves; although mutants still display this behaviour, they exhibit waves of reduced amplitude and wavelength, suggesting that the primary functions of motor neurons are intact but that their modulation (perhaps by mechanosensory feedback) is aberrant.

In *Drosophila* Adams *et al* (1998) first identified DEG/ENaC homologues of degenerins when, by homology screening, they cloned ripped pocket (RPK) and Pickpocket (PPK, now PPK1). PPK1 is of interest as it is expressed in the sensory dendrites of Type II sensory receptors in late stage embryos and larvae. When Ainsley *et al* (2003) ablated the gene for PPK1 they found that mutants had normal larval touch sensitivity but showed locomotor abnormalities. Specifically, in an environment devoid of food, animals did not display typical searching behaviour, characterised by short movements punctuated with exploratory head movements, but displayed long straight movements with low frequency stops and turns. Such a phenotype might be due to a reduction in mechanosensory feedback during movement.

1.2.3 Transient Receptor Potential (TRP) Channels

The TRP ion channel family contains an array of channels with remarkably diverse functions (Harteneck *et al*, 2000; Clapham *et al*, 2001; Clapham, 2003). Mammalian TRP channels can be divided into three phylogenetic groups; TRPC1-7 (Classical/short), TRPV1-6 (Vanilloid receptor-like), and TRPM1-8 (Melastatin/long) (see Clapham *et al*, 2001, Montell *et al*, 2002; Clapham, 2003; Fig. 1.6a). TRP channels are characterised by 6 transmembrane domains (with a highly conserved pore forming region between the 5th

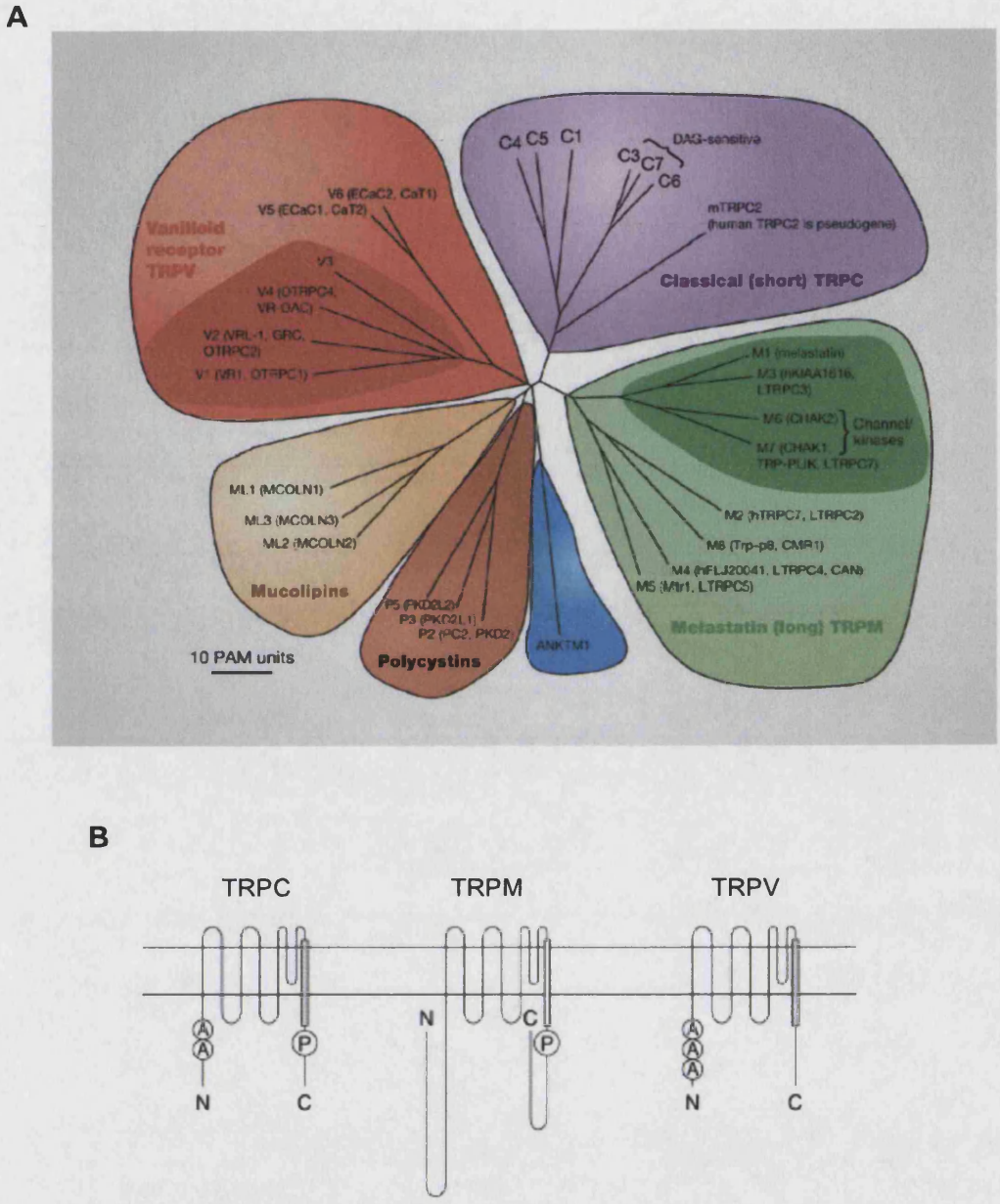

Fig. 1.6 The mammalian TRP family of ion channels. *A*, Phylogenetic tree of TRP channel groups. Shown are the TRPV, TRPC and TRPM families and the related polycystins, mucolipins and ANKTM1. *B*, Schematic diagrams showing the proposed structures of TRPC, TRPM and TRPV ion channels. TRP have six transmembrane domains with intracellular amino (N) and carboxy (C) termini and often contain ankyrin domains (A) and proline rich regions (P) as indicated. (*A*, from Clapham, 2003; *B*, adapted from Harteneck *et al*, 2000)

and 6th domains), cationic conductance (typically including permeability to Ca^{2+}) and intracellular C- and N-termini, the latter often containing ankyrin domains (Fig.1.6b). A number of TRP related channels are believed to function in thermal transduction by sensory neurons (see Section 1.3.2), however, following work performed in *C. elegans* and *Drosophila*, recent attention has focussed on the idea that certain TRP channels may act as mechanosensors.

1.2.3.1 TRP Channels Participate in Invertebrate Mechanosensation

The first TRP related channel implicated in mechanosensation was OSM-9 (Colbert *et al*, 1997). Nematodes with mutant forms of this channel have severe defects in avoidance behaviours evoked by olfactory stimuli, nose touch and hyperosmolarity. Nose touch avoidance is mediated primarily by ASH neurons and also FLP and OLQ neurons all of which are ciliated; consistent with a role in sensory transduction heterologously expressed *osm-9::GFP* fusion proteins were heavily localised to the sensory cilia. It remains to be determined if OSM-9 is directly activated by sensory stimuli or if it acts downstream of the transduction process. In osmosensation, ASH directed behaviours also require functional expression of *ocr-2* (another TRP-related ion channel, Tobin *et al*, 2002), *odr-3* (a Gα-protein, Roayaie *et al*, 1998) and *osm-10* (a cytoplasmic protein, Hart *et al*, 1999) but in mechanosensation only *ocr-2* and *odr-3* are required. The dependence of osmotic but not nose touch responses on OSM-10 expression suggests that distinct transduction mechanisms operate in each modality, potentially converging on OSM-9 activation, although the data do not preclude direct mechanical activation of OSM-9. It appears that OSM-9 heteromultimerises with OCR-2 and that these channels mutually regulate subcellular channel distribution (Tobin *et al*, 2002).

The *Drosophila* TRP-like channel NOMPC was also identified via genetic screening (Walker *et al*, 2000) from a survey of mutants insensitive to touch as larvae or displaying uncoordinated movement as adults (Kernan *et al*, 1994). Recordings made from Type I sensory bristle neurons (Fig. 1.7a) revealed that a number of these mutants generated no mechanoreceptor potentials (NOMP) suggestive of deficits in transduction. So far

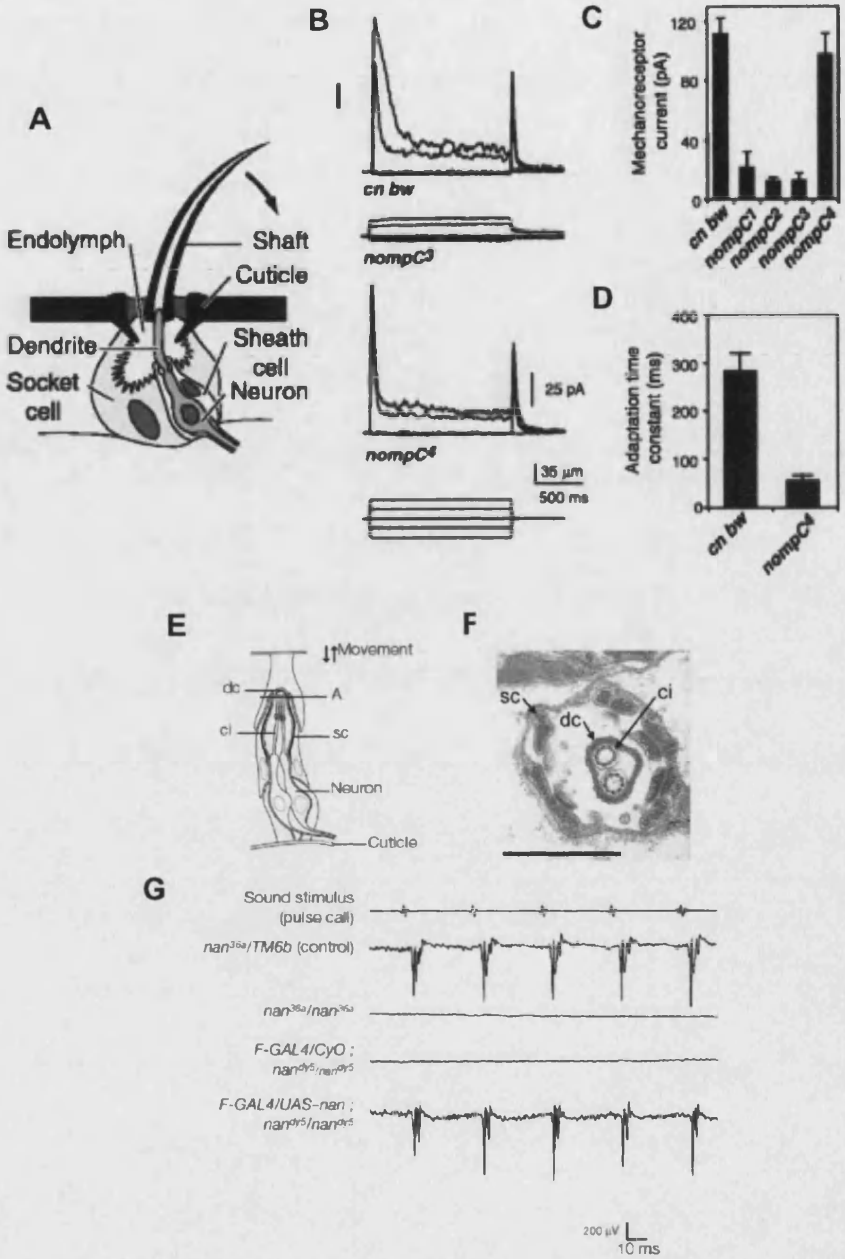

Fig. 1.7 *Drosophila* Mechanoreceptors. *A*, Bristle mechanoreceptors are composed of socket and sheath cells, a mechanosensory neuron and a hollow hair shaft. Hair shaft movement compresses the dendritic tip and activates neuronal transduction channels. Electrophysiological recordings are made by clipping the hair shaft and placing an electrode over its tip. *B*, Transduction currents in response to four displacements (*bottom trace*). *Top*, wild-type response, *upper middle*, *nompC3* mutants lose the transient mechano-receptive current, *lower middle*, *nompC4* mutants had near normal peak current amplitude but currents adapted much more rapidly. *C*, Peak current amplitudes in 4 mutant strains versus control. *D*, Adaptation rates in controls and *nompC4* mutants. *E*, Antennal chordotonal organs contain 2 sensory neurons with sensory cilia (*ci*) positioned within the scolopales (*sc*) and anchored via their dendritic caps (*dc*). *F*, Electron micrograph (along line A in *E*) through *nan* mutant antenna. *G*, Sound stimuli (*top trace*) evoked extracellular potentials (each trace is an average of 10 trials). Potentials are normal in heterozygous control flies but are absent in homozygous *nan* mutants (*nan36a* or *nandy5*). Potentials were restored by *UAS-nan* driven by *F-GAL4*. (*A-D* adapted from Walker *et al*, 2000; *E-G* adapted from Kim *et al*, 2003).

NOMPA and NOMPC have been characterised molecularly; NOMPA is an extracellular ZP-domain containing protein that is a candidate to tether the neuronal transduction machinery to the moving bristle (Chung *et al*, 2001). Mutants with truncated forms of *nompC* lose the rapidly adapting component of mechanically evoked receptor currents (Fig.1.7b, c) whereas a substitution of a cysteine by a tyrosine at position 1400 (between the 3rd and 4th transmembrane domains) produces a mutant in which transduction currents adapt much more rapidly than wild-type responses (Fig. 1.7b, d). NOMPC has a predicted membrane topology similar to known TRP channels and shows homology in the conserved pore-forming domain, additionally it has 29 ankyrin repeats in its N-terminal. The subcellular distribution of NOMPC is yet to be characterised and again it remains conceivable that it acts downstream of transduction events although the rapidity of transduction in these cell types argues against this possibility. It is also notable that a small non-adapting receptor potential remains in *nompC* mutants; this may mean another transduction channel operates independently in these cells.

In *Drosophila* responses to auditory stimuli are detected by structures analogous to bristle receptors in Johnston's organ, within the antennae of the fly. This organ consists of a number of chordotonal neurons suspended between two cuticular structures in such a way that the neurons detect the relative movement of these structures generated by vibration of the antennal capsule (Fig. 1.7e, f, Eberl *et al*, 2000). It appears likely that similar mechanisms operate in bristle receptors and chordotonal neurons; several mutations that ablated or severely reduced receptor potentials in somatic bristle receptors also had similar effects on compound potentials recorded from the afferent nerve of Johnston's organ (Eberl *et al*, 2000). Notably, *nompC* mutants were reported to have only moderate deficits in auditory responses. This appears to be due to the expression of an alternative transduction channel in Johnston's organ; Kim *et al* (2003) identified Nanchung (Nan), as a TRP-like channel required for responses of chordotonal neurons to sound waves. Nan is related to OSM-9 and the mammalian TRPV channels and is selectively expressed in chordotonal neurons. In flies lacking functional Nan channels sound-evoked activity in antennal afferent nerves was absent suggestive of a key role in transduction (Fig. 1.7g). When *Nan* was expressed in CHO cells it generated Ca^{2+} permeant, cationic currents in

response to hypotonic solutions, although these currents developed slowly and it is uncertain if such gating is via the same mechanism that would operate during hearing.

Despite the minor role played by NOMPC in *Drosophila* audition, Sidi *et al* (2003) found that the zebrafish homologue of this channel is fundamental to hair cell physiology in larvae of this species. *nompC* mRNA was selectively detected in the larval and embryonic zebrafish hair cells of the inner ear. Knockdown of *nompC* expression using antisense oligonucleotides produced larvae that, although touch responsive, failed to respond to acoustic stimuli and showed vestibular defects. Also, in treated larvae extra-cellular recordings from hair cell afferents revealed an ablation of movement-evoked activity. This study suggests that there is a conservation of NOMPC function across phyla; cluster analysis performed by this group suggests that *nompC* exists in its own class of TRP-related channels, distantly but most closely related to TRPV/OSM-9 channels. Walker *et al* (2000) also identified a *C. elegans* homologue of *nompC* and showed that NOMPC::GFP fusion proteins are expressed in the sensory cilia of nematode mechanosensory neurons (and some interneurons) but functional studies of this channel in worms are yet to be reported.

Finally, in *Drosophila* a third TRP related ion channel, *painless*, has been implicated in noxious mechanosensation by Tracey *et al* (2003). This group developed a genetic screen for studying nocifensive behaviour in *Drosophila* larvae and showed that animals lacking functional *painless* expression showed defective behavioural responses to noxious temperatures and noxious pressure. Painless is expressed in a discrete punctate fashion on the dendrites of putative nociceptors and the sensory deficits of mutants led to the idea that painless functions as a transducer of noxious stimuli in multiple modalities. Again, although the data are consistent with such a hypothesis direct channel activation by physical stimuli was not demonstrated, thus it is possible that the protein acts up- or downstream of transduction.

1.2.3.2 Are there Mechanically Gated TRP Channels Expressed by Mammals?

The studies outlined above have naturally led to much speculation on the role of TRP channels in mammalian mechanosensation. To date no channels with close homology to either NOMPC or Nan have been reported in mammals but TRPV4 (Liedtke *et* al, 2000; Strotmann *et* al, 2000) shows moderate homology to OSM-9 (26% amino acid identity, 44% identity or conservative change; Liedtke *et al*, 2003). TRPV4 is widely expressed in rodents with the highest expression levels in the kidney and significant expression in liver, heart, testes, and brain. Interestingly, expression is also seen in cochlea, trigeminal ganglia and Merkel cells, all of which are associated with mechanosensation (Liedtke *et al*, 2000; Strotmann *et al*, 2000). Heterologously expressed TRPV4 is gated by hypotonicity and also by phorbol esters, lipids and moderate temperatures, giving rise to a non-selective cation conductance that is blocked by La^{3+}, Gd^{3+} and ruthenium red (Liedtke *et al*, 2000; Strotmann *et al*, 2000; Section 1.3.2). It is currently uncertain which of these stimuli that activate this channel *in vitro* are physiologically relevant.

Gating by hypotonicity has fuelled conjecture that TRPV4 is mechanically gated. When recording from cell-attached patches Strotmann *et al* (2000) found that reducing external osmolarity increased channel activity but application of negative or positive pressure through the pipette did not alter gating. Moreover, activation of TRPV4 by hypotonicity occurs slowly, after a lag of "a few seconds to 2 minutes" (Liedtke *et al*, 2000; Strotmann *et al*, 2000), and work by Xu *et al* (2003) suggests that such gating maybe indirect rather than a direct consequence of membrane stretch. In this study it was shown that hypotonicity rapidly induces tyrosine phosphorylation of TRPV4 that increased with stimulus duration. Inhibitors of Src family kinases blocked phosphorylation of TRPV4 and it was demonstrated that one such kinase, Lyn, coimmunoprecipitates with TRPV4, is activated by hypotonicity and can phosphorylate TRPV4 at tyrosine-253. Blockade of osmotically induced TRPV4 activity by Src kinase inhibitors was not reported but, consistent with indirect gating by osmolarity, when tyrosine-253 was mutated to a phenylalanine hypotonic gating of TRPV4 was abolished.

In a study of TRPV4 null mutants Suzuki *et al* (2003b) reported impaired pressure sensation in these animals. In the tail pressure behavioural assay it was found that TRPV4 nulls had thresholds around twice those of controls, however von Frey hair withdrawal thresholds were unchanged. In a crude electrophysiological analysis of these mice the authors found that activation thresholds of "rapid response" and "slow response" A-fibres were approximately trebled and doubled, respectively. The authors report that mechanically sensitive C-fibres are absent in mutants but only report 6 such fibres out of 300 recordings in wild-type mice. It would be of interest to analyse the response properties of DRG fibre types in these animals using the skin-nerve preparation

Alessandrei-Haber *et al* (2003) reported that the expression of TRPV4, assayed by single cell RT-PCR, correlated with the expression of hypotonicity-induced changes in the excitability of cultured DRG neurons. The frequency of such neurons was approximately one in three and around 90% of responsive cells had wide action potentials indicative of nociceptors. TRPV4 immunoreactivity was undetectable in the DRG but western blots from saphenous nerve suggested that this protein was transported to the periphery in sensory nerves. Behaviourally, pain responses to water injection after PGE2 sensitisation were reduced by treatment with TRPV4 antisense oligonucleotides but downregulation of TRPV4 did not alter mechanical hyperalgesia or acute mechanical withdrawal thresholds.

A novel approach to the study of ion channel function was employed by Liedtke *et al* (2003) to study TRPV4. Given its homology to OSM-9, TRPV4 was expressed in *C. elegans* on an *osm-9* mutant background to assess if this channel could phenotypically rescue these animals. TRPV4 restored responses of mutants to mechanical stimulation of the nose and to hypertonic stimuli but not to repellent odorants. However, just as it is unclear if OSM-9 acts as a primary transducer of sensory stimuli, it remains ambiguous if TRPV4 is being activated directly or is acting downstream of other transduction events. TRPV4 did not rescue OSM-9 mutants that also lacked functional OCR-2, ODR-3 or OSM-10 and TRPV4 is gated by *hypo*tonicity in mammalian cells whereas here it is mediating responses to *hyper*tonicity, which suggests different mechanisms are in operation. One possible route to resolving these issues would be to express the T253F

mutant form of TRPV4 (see above) in *osm-9* mutants to determine if this channel rescued either osmotic or touch sensitivity, i.e. do both of these stimuli converge upon tyrosine-253 phosphorylation or do they gate the channel via independent mechanisms.

Overall, it remains unclear if TRPV4 can be mechanically activated directly or if it participates in the detection of mechanical stimuli *in situ*. The striking phenotype reported by Suzuki *et al* (2003b) using electrophysiology is at odds with the relatively sparse expression of TRPV4 in DRG neurons; Suzuki *et al* (2003b) reported immunoreactivity for this channel in only 11% of DRG neurons. Moreover, only limited behavioural changes were observed by Alessandrei-Haber *et al* (2003) and Suzuki *et al* (2003b). It also remains to be determined if hypotonicity is a relevant stimuli, and thus a physiological activator of TRPV4, in pain pathways. It may be the case that osmosensitivity is important for this channel's function in other systems such as hypothalamic osmosensation (see Liedtke and Friedman, 2003).

TRPV1 has also been postulated to function in bladder mechanosensation. Birder *et al* (2002) demonstrated that, despite having morphologically normal bladders, TRPV1 knockout mice had deficits in voiding reflexes and spinal signalling of bladder volume. Distension of the bladder is known to evoke ATP release (Section 1.2.4) and the absence of TRPV1 caused a reduction in the amount of ATP released from both stretched whole bladders and hypotonically swelled urothelial cells. Moreover, stimulation of cultured urothelial cells with capsaicin evoked ATP suggesting that TRPV1 activation is both necessary and sufficient to evoke ATP release. No group has reported mechanical gating of TRPV1 and cutaneous mechanosensation is normal in TRPV1 nulls (Caterina *et al*, 2000). Hence, the role of TRPV1 in this pathway remains to be determined; mechanical stimuli could gate TRPV1 via a chemical (perhaps a lipid) mediator. Electro-physiological analysis of mechanically stimulated urothelial cells may be informative.

The polycystins are distantly related to TRP channels. Polycystin 1 (PC1) has been described as an "untraditional G-protein-coupled receptor" that regulates Ca^{2+} and K^{+} channels via modulation of G-protein signalling pathways (Delmas *et al*, 2002) whereas

PC2 is a Ca^{2+} permeable cation channel (Vassilev *et al*, 2001). Both have similar membrane topology to TRP channels. Mutations in either gene can cause polycystic kidney disease. Nauli *et al* (2003) showed that the normal function of these proteins is pivotal to mechanosensation by the cilia of kidney epithelial cells. In animals lacking functional PC1 the normal increase in intracellular Ca^{2+} levels evoked by fluid stress of the cilium was either greatly reduced or absent. In wild-type cells removal of external Ca^{2+} inhibited such responses and the use of antibodies against the external domain of PC2 suggested that Ca^{2+} entry is via these channels. The authors postulate that PC1 may act as a mechanosensor that subsequently activates the tightly associated PC2 channel.

Finally, it is of interest that in their survey of the known physiological and pharmacological properties of the hair cell transduction channel Strassmaier and Gillespie (2002) noted a number of similarities with those of TRP channels. Notably, like the transduction channel, TRP channels have high single-channel conductances, non-selective cationic permeability (typically with high Ca^{2+} permeability) and are regulated by external Ca^{2+}. They also noted some shared antagonists.

1.2.4 Chemically Mediated Mechanosensation

In addition to direct activation of mechanosensitive ion channels, organisms can also sense changes in mechanical forces via the release of chemical mediators. This hypothesis purports that mechanical force induces chemical release from cells in close proximity to sensory endings and that these mediators act in a paracrine fashion to activate sensory neurons via ligand-gated ion channels or GPCRs.

It has long been known that endothelial cells release a number of factors, including nitric oxide, ATP and substance P, in response to changes in blood flow (see Burnstock, 1999). It was also suggested that purinergic signalling might be important in nociception due to activation of damage sensing neurons by endothelial cells in the microcirculation and that the sensing of mechanical distension of tubes (e.g. gut, vagina, urethra) or sacs (e.g. bladder, lung) may be via mechanically induced ATP release from epithelial cells

(Burnstock, 1999). Empirical support for this idea came from studies of $P2X_3$ null mutants; Cockayne *et al* (2000) showed that such mice displayed a marked bladder hyporeflexia, demonstrating reduced micturition frequency and increased bladder volume. $P2X_3$ receptor immunoreactivity was present on sensory nerves innervating the bladder and it was shown that bladder distension evoked a graded ATP release and that the response of sensory fibres to bladder distension was attenuated in $P2X_3$ knockouts. In wild-type mice, ATP activated sensory fibres and distension-evoked activity was inhibited by purinergic antagonists (Vlaskovska *et al*, 2001).

How far this mechanism generalises is unclear. Cook *et al* (2002) showed that when keratinocytes or fibroblasts were mechanically lysed in the vicinity of sensory neurons, neurons were depolarised by ATP acting at P2X receptors. Noxious mechanical stimuli may activate nociceptors via damage to nearby cells and consequent ATP release; the viability of this mechanism *in vivo* would be dependent on the actions of diffusion barriers to ATP and the presence of ectonucleotidases. Nakamura and Strittmatter (1996) had previously proposed that $P2Y_1$ purinergic receptors might contribute to touch-induced impulse generation. They identified this GPCR from an expression cloning screen of *Xenopus* oocytes expressing DRG cRNAs; eggs expressing $P2Y_1$ responded, via mechanically evoked ATP release, to a puff of external buffer with an inward current. Transcripts for $P2Y_1$ receptors were shown to be expressed in large diameter rat DRG neurons and in a frog teased nerve fibre preparation ATP excited and sensitised mechanically sensitive fibres and touch-induced activity was attenuated by the purinergic receptor antagonist suramin and the nucleotidase apyrase. It is unlikely though that increases in membrane excitability via activation of a GPCR would be rapid enough to act as a primary transduction mechanism. Similar findings have not been reported for mammalian mechanoreceptors although nociceptors are activated by ATP (Hamilton *et al*, 2001; Molliver *et al*, 2002) and the expression of $P2Y_1$ in large nerve fibres suggests that it could modulate the excitability of these cells.

1.2.5 Conclusion

The extensive research discussed in this section highlights both the recent progress made in understanding the molecular basis of mechanosensation and also how far there is to go. Although, a number of invertebrate channels have been implicated in this sensory modality by forward and backward genetic techniques, no metazoan ion channel has been shown to be unequivocally mechanically gated *and* central to sensory mechanotransduction. Genetic and behavioural studies, and even electrophysiological investigation, are always open to the caveat that the identified channel is activated downstream of the primary transduction event. Heterologous expression of mechanically evoked channel activity (as discussed in Section 1.3.3) is likely to prove technically demanding due to the elaborate sensory cells in which such channels are expressed and their likely inclusion in multiprotein mechanosensory complexes.

Strong evidence implicates MEC-4 and MEC-10 in *C. elegans* body touch sensation and NOMPC and Nan, in mechanosensation by *Drosophila*. Consequently, at present the primary candidates for the role of mammalian mechanotransducers are in the TRP and DEG/ENaC ion channels families, both of which are remarkably functionally diverse. However, in no case is the available evidence supporting a function for a mammalian channel in mechanotransduction as strong as it is in fruit flies or nematodes.

The findings in invertebrates suggest that there is not simply one family of mechanosensitive ion channels underlying metazoan mechanotransduction. The extensiveness of genetic screens in *C. elegans* and *Drosophila* suggest that other ion channels are unlikely to function in these species (although extensive studies of other submodalities, such as harsh body touch, have not been undertaken). However, if mechanosensitivity has evolved in two markedly distinct families of proteins it is possible that it has also done so in further ion channel types. It is of interest to note the diversity in DEG/ENaC channels in *C. elegans* and *Drosophila* (28 and 25 homologues, respectively) when compared to the number of related channels in vertebrates (8, for example, in mice).

Related to the diversity of putative mechanosensory ion channels is the issue of diversity in cellular systems that mediate mechanosensation. Despite superficial similarities, that are often emphasised, the phylogenetic relationship between mammalian hair cells and primary somatosensory neurons and the analogous cells types in invertebrates is poorly established. It is notable that in *C. elegans* body touch neurons, mechanosensation is critically dependent on microtubules and that the cilia of *Drosophila* neurons innervating Type I sensory organs contain typical microtubule arrangements. In contrast, at the site of transduction in mammalian hair cells and in somatosensory neurons the cytoplasm is dominated by actin microfilaments. Finally, the extent to which various systems rely on chemically mediated mechanosensation remains to be determined. In some systems it may have a modulatory role in association with faster mechanisms and in others, such as bladder stretch and potentially nociception, it may be the primary mechanism. Thus, much remains to be determined regarding the molecular basis of mechanotransduction and when this is achieved, it should be possible to determine the evolutionary relationships of multiple mechanosensory systems.

1.3 Investigation of Physical Transduction Mechanisms Using Cultured DRG Neurons

Major obstacles in studying sensory neuron transduction mechanisms include the inaccessibility and diffuse distribution of these neurons' peripheral terminals where the process occurs. Sensory endings are both small and embedded in complex peripheral tissues. Consequently, it is difficult, if not impossible, to make *in situ* intracellular recordings from these structures. Moreover, the dispersed distribution of the nerve endings prevents the harvesting of protein fractions enriched in proteins expressed at the transduction sites.

Some investigators have made extracellular recordings from peripheral nerve endings (Section 1.1.2.2) and recently the guinea pig cornea has been use to make extracellular recordings (Brock *et al*, 1998) and to image Ca^{2+} transients (Gover *et* al, 2003) in sensory terminals. However, such recordings are difficult (particularly in response to a mechanical stimulus) and have only been made in a handful of preparations. An alternative approach is to study ion channels in cultured sensory neurons.

1.3.1 Cultured DRG Neurons as a System for Studying Ion Channel Function

The principle advantage of using isolated neurons is that, freed from surrounding tissue, these cells are easily accessible for investigation using imaging and electrophysiological techniques. Moreover, such neurons may be readily genetically manipulated and drugs may be applied locally and rapidly, uncomplicated by issues of slow or incomplete penetration through the extracellular environment. Another major advantage, particularly relevant to the study of sensory neurons, is that the direct effects of inflammatory mediators on neuronal excitability can be isolated uncomplicated by inflammatory cascades activated by such compounds in intact tissues.

When using this approach to study DRG physiology, the two most salient considerations are the heterogeneity of the DRG neuronal population and the more general issue of how

well the phenotype of cultured neurons recapitulates that of neurons *in situ*. As was summarised in Section 1.1 primary sensory neurons can be functionally and morphologically distinguished by a number of factors including their modality, cell size, degree of axonal myelination, conduction velocity, properties of their action potentials and anatomically by their central and peripheral projections. Of these properties, neurons in culture can be discriminated (although by no means completely) by their somatic size, action potential properties (and expression of distinct voltage-activated currents) and their sensitivity to chemical and physical stimuli.

Many studies of isolated DRG neurons have used simple binary systems to classify cells into nociceptive and non-nociceptive subtypes. The most commonly used selection criteria are cell size (e.g. Baker *et al*, 2003) and action potential properties (e.g. Dirajlal *et al*, 2003). With regards to somatic size, the assumption is often made that neurons with diameters of less than 25-30 μm are nociceptive (Harper and Lawson, 1985a; Perl, 1992). However, a small population of C-fibres (likely to have small cell bodies) respond to innocuous mechanical stimulation, whereas amongst the Aβ-fibre population (likely to have large cell bodies) there are some high threshold mechanoreceptors (Koerber *et al*, 1988; Djouhri *et al*, 1998; Lawson, 2002). There are a number of strong correlates between action potential properties and the receptive properties of different fibre types (Koerber *et al*, 1988; Ritter and Mendell, 1992; Djouhri *et al*, 1998; Lawson, 2002, Section 1.1.1.1). Low threshold mechanoreceptors have narrow, uninflected action potentials with small, short afterhyperpolarisations and nociceptive neurons have wide, inflected spikes with large, long after-hyperpolarisations (Koerber *et al*, 1988; Ritter and Mendell, 1992; Djouhri *et al*, 1998; Lawson, 2002). These properties, particularly afterhyperpolarisation, are highly predictive of neuronal phenotype although C-fibre low threshold mechanoreceptors have wide action potentials.

In DRG cultures nociceptive neurons retain sensitivity to capsaicin (Section 1.1.1.2). Winter (1987), using staining for cobalt uptake, showed that capsaicin sensitivity in cultured neurons was limited to small dark neurons. Wood *et al* (1988) conversely showed that less than 10% of capsaicin sensitive cells contain NF200 immunoreactivity.

Hence capsaicin sensitivity in cultures is a good predictor of a nociceptive phenotype. Capsaicin insensitive cells are likely to include heat insensitive nociceptors as the robust excitatory and neurotoxic effects of capsaicin on nerve fibres *in vivo* has been shown to be largely confined to heat sensitive nociceptive fibre types (Szolcsanyi *et al*, 1988; see Szolcsanyi, 1993). In agreement with *in vitro* studies, *in situ* over 80% of rat NF200-negative neurons express TRPV1 mRNA (Michael and Priestley, 1999) although NGF can upregulate TRPV1 expression *in vitro* (Story *et al*, 2003 and references therein; see below). Another important variable is interspecies variation in the expression pattern of this receptor, for example, in rats capsaicin excites the majority of unmyelinated nociceptive fibres (Kenins, 1982; Szolcsanyi *et al*, 1988) but in mice only around half of C-fibres are activated by capsaicin (Caterina *et al*, 2000).

Overall, DRG neurons can be broadly divided into nociceptive and non-nociceptive classifications according to the above systems with a fair degree of confidence. With regards to cell diameter, it is likely that although the smallest neurons *are* nociceptive and the largest non-nociceptive, the phenotype of medium sized neurons is more ambiguous. Using capsaicin means that most cells will correctly be classified although some heat insensitive nociceptors will be mistakenly categorised as non-nociceptive.

Beyond binary classifications, nociceptors can be distinguished by the use of IB4 as a vital stain in culture (Section 1.1.1.2). $P2X_3$ receptor expression is largely confined to IB4 positive neurons (Burgard *et al*, 1999) whereas Stucky and Lewin (1999) have shown that IB4 positive and negative small neurons differ with respect to action potential duration and threshold and the magnitude of TTX-r sodium currents and heat-evoked currents. Likewise Dirajlal *et al* (2003) showed clear differences between IB4 positive and negative murine neurons in terms of their responses to low pH and capsaicin. In this study they also extended their classification by characterising the neurons immunocyto-chemically after recording from them; distinguishing myelinated and unmyelinated cell types according to N52 staining.

An alternative approach that has been developed by Cooper's group, building on work done in the Scroggs lab, is to classify DRG cell types according to their current signatures in response to 3 families of voltage-steps. Scroggs and Cardenas (Cardenas *et al*, 1995) divided cells according to capsaicin sensitivity, magnitude of hyperpolarisation-evoked currents and expression of various voltage-activated Ca^{2+} currents and showed that within groups there was internal homogeneity with regards to cell size, action potential duration and sensitivity to serotonin. Petruska *et al* (2000; 2002) used 3 voltage step protocols to describe 9 subtypes of neurons defined by their hyperpolarisation-activated currents, transient outward K^+ currents and inward Na^+ currents. Within groups cells were fairly homogeneous with regards to diameter, responses to capsaicin, pH 5 and ATP, action potential and afterhyperpolarisation duration, IB4 binding and substance P and CGRP immunoreactivity.

A final consideration is how well the largest DRG neurons survive the isolation and culture processes. Baker and Bostock (1997) (and MD Baker, personal communication) suggest that to obtain very large (50-75 μm) rat DRG neurons in culture it is necessary to rapidly remove ganglia from anaesthetised rodents. Usually rodents are killed prior to ganglia extraction which suggests that Aβ/α fibre neurons are significantly under represented *in vitro*.

The issue of how well cultured neurons recapitulate their *in vivo* phenotype is less easily resolved. Neurons are ubiquitously isolated using techniques that involve enzymatic digestion of the tissue and then a mechanical separation that unavoidably removes axons and dendrites from the cell body. Neurons are then grown in culture medium that typically contains serum; a supplement that contains a mixture of growth factors that are necessary for cell survival but that are not characterised either in terms of what compounds are actually present or at what concentrations. Consequently the culturing procedure results in a redistribution of membrane components and a change in neuronal morphology and the isolation process and culture medium are both likely to induce changes in gene expression.

Changes in gene expression can be minimised by conducting experiments on isolated neurons as soon after their extraction as is possible. For example, Scott and Edwards (1980) showed that with time in culture action potential duration increased significantly in DRG neurons. More recently, investigation of voltage-gated sodium channel expression has shown that DRG neurons after 24 hours in culture express a complement of channels comparable in distribution and intensity to neurons *in situ* (Black *et al*, 1996). However, work by the same group has shown that with time in culture there are changes in sodium channel expression that appear to mirror the pathological changes that occur *in vivo* following nerve transection. Black *et al* (1997) showed that over 7 days in culture the level of transcripts for $Na_V1.8$ decreased and that there was *de novo* synthesis of $Na_V1.3$ mRNA; this is similar to the observations of Boucher *et al* (2000) who axotomised sensory neurons *in vivo*. In the former study it was showed that NGF partly attenuated changes in gene expression (Black *et al*, 1997). Much evidence has been produced that NGF alters the expression of a number of genes in cultured DRG neurons. Saliently, NGF increases the proportion of neurons that respond to capsaicin (Winter *et al*, 1988) and Story *et al* (2003) showed that NGF induces *de novo* synthesis of TRPV1 mRNA in a distinct population cells. The implications of this are twofold, firstly it demonstrates the fundamental changes to neuronal phenotype that can occur in culture and secondly, it has clear ramifications for using capsaicin sensitivity to identify nociceptors.

The spatial arrangement of ion channels and other signalling molecules in cultured neurons is another confounding variable. It is certain that the distribution of such molecules is distinct from that that characterises the neuron *in situ*. This is true of all channel types, be it, say, glutamate receptors that may usually be confined to the microenvironment of the synaptic cleft or calcium channels that are normally differentially distributed between the axon and dendrites (Day *et al*, 1998). Whilst the redistribution of ion channels leads to uncertainty that a population of channels behave *in vitro* as they would *in vivo*, it is this rearrangement that allows the study of ion channels normally found only on the peripheral, sensory terminals of DRG neurons. Over the last 2 decades the use of cultured sensory neurons as a model of the receptive terminal has

grown considerably. In 1980, Krishtal and Pidoplichko described a proton-gated conductance in cultured sensory neurons and proposed that it "may serve as a pH-sensor in the sensory nerve endings". Baccaglini and Hogan (1983) showed that cultured trigeminal ganglia and DRG neurons showed a number of properties characteristic of nociceptors. Using sharp electrode intracellular recording, this study demonstrated that capsaicin and bradykinin caused membrane depolarisation and action potential generation in a subpopulation of cells and that prostaglandin E_2 sensitised the neuron to the excitatory effects of a high external K^+ concentration. Also in this year Jahr and Jessell (1983) described ATP activated currents in cultured sensory neurons. Subsequently many groups have used cultured sensory neurons to study voltage- and ligand-gated ion channels implicated in chemical activation of these cells' peripheral endings (see Wood, 2000). In 1996, Cesare and McNaughton produced evidence that the somata of a relevant subpopulation of cultured DRG neurons expressed a channel that was activated by heat. The demonstration that a thermally gated ion channel is expressed on the somatic membrane instigated a huge amount of interest into the possibility of using this system to investigate the mechanisms by which DRG neurons transduce physical stimuli.

1.3.2 Physical Transduction by DRG Neurons In Vitro

1.3.2.1 Heat Transduction

Cesare and McNaughton (1996) described how application of heated external solution (> 43°C) evoked an inward, non-selective cationic current in a subpopulation of small-diameter DRG neurons. The threshold of these responses and the proportion of small neurons that responded were both a good representation of the sensitivity and abundance of heat activated DRG fibres *in vivo* (Raja *et al*, 1999). This study also demonstrated that these currents were potentiated by the inflammatory mediator bradykinin, which is known to induce thermal hyperalgesia when administered peripherally (Dray and Perkins, 1993).

Caterina *et al* (1997) identified the channel that underlies heat-activated currents in cultured DRG neurons when they cloned the capsaicin receptor (TRPV1). This was achieved using an expression cloning strategy based on capsaicin-induced Ca^{2+} elevations in HEK293 cells transfected with a rodent DRG cDNA library. Heterologous expression of TRPV1 in HEK293 cells conferred to these cells sensitivity to both capsaicin and heat and capsaicin-evoked responses were augmented by drops in pH. Transcripts for TRPV1 were found exclusively in the trigeminal ganglia and DRG and expression was confined to a subset of small diameter neurons. This is consistent with the size distribution of heat- (Cesare and McNaughton, 1996) and capsaicin-sensitive neurons (Wood *et al*, 1988). Subsequent comparison of native capsaicin- and heat- evoked currents in cultured sensory neurons showed that all those that were capsaicin sensitive were also activated by noxious heat (Nagy and Rang, 1999) and that nearly all heat-sensitive neurons respond to capsaicin (Kirschstein *et al*, 1999; Nagy and Rang, 1999). It was also demonstrated that heat-activated currents were inhibited by the TRPV1 antagonists ruthenium red and capsazepine, albeit at significantly higher concentrations than for capsaicin-evoked responses (Kirschstein *et al*, 1999; Nagy and Rang, 1999). Nagy and Rang (1999) also demonstrated that Ca^{2+} permeability was greater for capsaicin than heat activated currents and that at the single channel level there was segregation of capsaicin and heat sensitivity; the authors suggested that this might be due to different functional forms of the TRPV1 gene product.

Tominaga *et al* (1998) showed that TRPV1 is present on sensory nerve endings and two papers published simultaneously by Caterina *et al* (2000) and Davis *et al* (2000), although not in complete agreement, showed that TRPV1 null mutants have a number of deficits in thermosensation. Both groups reported that neurons derived from nulls did not exhibit noxious heat activated currents in the 43-50°C range and that the nulls were hypoalgesic in tests of thermal hyperalgesia. The key difference was that Caterina *et al* (2000) found that mice lacking TRPV1 had behavioural deficits in acute thermosensation that were apparent at temperatures of 52.5-58°C, whereas Davis *et al*, (2000) found no significant difference between genotypes in similar hot plate assays. These data did however almost reach statistical significance (P = 0.053) and the authors made

speculations about the genetic diversity of their samples masking a difference. The Julius group also showed that in the skin nerve preparation there was a reduction in the number of and sensitivity of heat-sensitive C-fibres and extracellular recordings in the dorsal horn revealed an absence of thermal coding by spinal neurons. In both cases responses to mechanical stimuli were normal (Caterina *et al*, 2000). Interestingly, thermal coding deficits in both electrophysiology preparations were apparent at around 41-43°C, which equates to the thermal activation threshold of TRPV1. That behavioural deficits were only noticeable at temperatures of above 50°C is therefore somewhat paradoxical; it may represent a complex relationship between sensory input and behavioural responses.

Both papers show however, particularly at the behavioural level, that an ability to sense noxious temperatures is retained in the absence of TRPV1. The observation that isolated sensory neurons from TRPV1 null-mutants show major defects in heat-activated currents is therefore problematic. It seems to suggest that either not all heat sensitive ion channels are functionally expressed in the somata of cultured neurons or that other thermosensory mechanisms (possibly upregulated in the null mutant) are dependent on non-neuronal cells (see below).

Since the identification of TRPV1, a number of other TRP channels have been found to display thermosensitivity. TRPV2 was discovered due to its homology to TRPV1 and found to be gated by high temperatures (threshold ≈52°C). Such currents were sensitive to ruthenium red but not capsazepine and the channel was insensitive to capsaicin and protons (Caterina *et al*, 1999). Immunoreactivity for this protein was high in a subset of medium to large DRG neurons consistent with expression in high thermal threshold (Type I) Aδ-nociceptors (Raja *et al*, 1999). Ahluwalia *et al* (2002) showed that a subpopulation of cultured medium diameter, capsaicin insensitive DRG neurons express high threshold heat activated currents and that in an equivalent subpopulation of neurons, that did not express TRPV1, TRPV2 immunoreactivity was detectable. High threshold heat-activated currents were also present in the somata of neurons derived from TRPV1 null mutants (Caterina *et al*, 2000). These data thus support the hypothesis that TRPV2

underlies thermal activation of Type I Aδ nociceptors although data from TRPV2 knockout mice will be essential in further testing this hypothesis.

More recent studies have shown that TRPV3 and TRPV4 can also be activated by increases in temperature. TRPV4, which was identified as an osmotically gated channel (Section 1.2.3.2), when expressed heterologously is activated by temperature above 25°C (Watanabe *et al*, 2002a) or 34°C (Güler *et al*, 2002). TRPV4 may also have an integrative function as external osmolarity modulates the temperature sensitivity of this channel (Güler *et al*, 2002). Watanabe *et al* (2002a) showed that heat activation was dependent on the presence of N-terminal ankyrin domains and that activation at the single channel level was present in the cell-attached configuration but lost in inside-out patches suggesting it may be dependent on a diffusible cytosolic element. Whilst warm currents have been demonstrated in mouse aorta endothelial cells (Watanabe *et al*, 2002a) and keratinocytes (Chung *et al*, 2003), currents with a corresponding temperature sensitivity have not been reported in DRG neurons. No papers currently published on TRPV4 nulls report investigation of DRG thermosensation.

Three groups simultaneously reported the thermal sensitivity of TRPV3, demonstrating that heating evokes a non-selective cationic current through this channel with a threshold between 31°C and 39°C (Peier *et al*, 2002a; Smith *et al*, 2002; Xu *et al*, 2002). TRPV3 was also found to hetermultimerise with TRPV1 in heterologous systems (Smith *et al*, 2002). Again, no heat activated currents with similar thermal sensitivity have been reported in sensory neurons and the expression of TRPV3 in DRG is unresolved; Xu *et al* (2002) reported TRPV3 immunoreactivity in most sensory neurons of monkey DRG and Smith *et al* (2002) found TRPV3 mRNA in small neurons of human DRG often colocalised with TRPV1. However, Peier *et al* (2002a), looking in adult rat, failed to detect TRPV3 mRNA in the DRG using *in situ* hybridisation, although a signal was found using RT-PCR; this group reported high levels of expression in keratinocytes.

1.3.2.2 Cold Transduction

It has long been known that subpopulations of Aδ- and C-fibre DRG neurons respond to decreases in temperature (Hensel and Iggo, 1971; Kenshalo and Duclaux, 1977) and that these fibres can be sensitised or activated by menthol (Hensel and Zotterman, 1951). However, the mechanism by which this was achieved remained enigmatic. Recently, a number of studies using cultured DRG neurons have suggested that the primary excitatory mechanism is the direct gating of cationic channels by cooling (Reid and Flonta, 2001; 2002; McKemy *et al*, 2002; Peier *et al*, 2002b; Reid *et al*, 2002; Story *et al*, 2003). However, in addition, Viana *et al*, (2002) suggest a significant role in thermosensation for K^+ channel modulation by low temperatures.

Prior to electrophysiological characterisation, Reid and Flonta (2001) and McKemy *et al* (2002) selected cold sensitive sensory neurons by pre-screening using Ca^{2+} imaging; approximately 7% of DRG and around 14% of trigeminal ganglia neurons, respectively, responded to cooling with a robust increase in intracellular Ca^{2+}. These proportions are consistent with the frequency of cold receptors observed *in vivo* (Kenshalo and Duclaux, 1977). The electrophysiological properties of cold-sensitive neurons were then compared to insensitive neurons. Reid and Flonta (2001) showed that all cold sensitive neurons, but none of the insensitive population, expressed a cold activated mixed cationic current that was potentiated by menthol. Likewise, McKemy *et al* showed that in cold sensitive trigeminal ganglia neurons low temperatures (7°C) activated an outwardly rectifying, Ca^{2+} permeable cation channel. Furthermore, they found that menthol induced a current with almost identical properties in this same subpopulation. Thus, they used an expression cloning approach (trigeminal ganglia cDNA library expressed in HEK293 cells) to isolate a receptor that was activated by menthol. This receptor, a member of the TRP superfamily, which they termed CMR1, was found to be expressed appropriately in trigeminal ganglia and DRG and when expressed heterologously it recapitulated the key features of sensory neuron cold and menthol activated currents.

Interestingly, at the same time Peier *et al* (2002b) identified this same ion channel, which they termed TRPM8, via a bioinformatics approach. Having identified a number of novel TRP channels in genome databases, this group showed that TRPM8 was expressed in a subset of small diameter sensory neurons and that when it was expressed in CHO cells it gave rise to an increase in intracellular Ca^{2+} and a non-selective cationic currents in response to cold and menthol. Extending this approach the same group went on to identify another cold-activated TRP channel, ANKTM1 (Story *et al*, 2003). This channel is a distant relative of identified TRP channels that appears to be selectively expressed in a subpopulation of peptidergic nociceptors (3.6% of total DRG neurons) all of which express TRPV1. When heterologously expressed in CHO cells ANKTM1 was shown to induce sensitivity to cold temperatures (activation threshold $\approx$ 17°C); transfected cells responded to cold with an influx of Ca^{2+} and exhibited cold-evoked, outwardly rectifying cationic currents. ANKTM1 is insensitive to menthol but is gated by 100 μM icilin and the study demonstrated that a subpopulation of DRG neurons responded to cold temperatures in a manner consistent with ANKTM1 activation.

Gordon Reid and coworkers have produced an extensive body of work on native cold-induced responses in DRG neurons. Reid *et al* (2002) reported that cold-sensitive cells have a number of distinct properties from cold-insensitive nociceptors including shorter action potentials, smaller afterhyperpolarisations and more rapidly decaying sodium currents. It was shown that cold- and menthol-activated currents were carried mainly by Na^{+} ions in quasi-physiological solutions, were inhibited by extracellular Ca^{2+} and that adaptation of cold responses was dependent on Ca^{2+} passage through the channel. Also currents were blocked, albeit at relatively high concentrations, by the TRPV1 antagonists capsazepine (50 μM) and SKF 96365 (100 μM). It appears likely that the channel under investigation in these experiments was TRPM8 and this group did not report a second cationic conductance attributable to ANKTM1. Reid and Flonta (2002) recorded single channel currents gated by menthol and cold and demonstrated that individual channels were activated directly by both these stimuli. However, such currents had important properties that differed from whole-cell currents. Most saliently, the temperature threshold was 10°C colder than observed in intact neurons and single channel responses

failed to show adaptation. The latter finding is likely explained by an intracellular signalling effect of incoming Ca^{2+} but it remains to be determined how the intracellular environment modulates the channels' temperature sensitivity.

The other outstanding matter in this field is the precise role of K^+ channel inhibition by cooling. (Indeed it may well have been predicted *a priori* that neuronal excitation by cooling would be via inhibition of protein function.) Viana *et al* (2002) also pre-screened trigeminal ganglia neurons to identify cold-sensitive neurons (again small diameter neurons, in this case 9.3% of the total population) prior to electrophysiological characterisation. However, this study found that cold sensitive neurons were marked not by the expression of a specific cationic conductance but by their relative expression of K^+ currents. Thus, cold sensors were depolarised by inhibition of leak channels and this depolarisation generated firing that was limited by a reduction in inward rectification generated by I_h current. In cold insensitive neurons the prominent expression of another K^+ current, IK_D, acted as an *excitability brake* that prevented cold induced depolarisations eliciting action potentials and selective IK_D inhibition by 4-AP induced cold-sensitivity in previously unresponsive neurons. It should be noted that if this proposed mechanism is shown to be valid in controlling cold induced firing *in vivo* then not only do the somata of cultured neurons express channels that are normally found at their sensory terminals but they express them at a similar relative density also.

This study adds another layer of complexity to the study of cold transduction and is likely to be significant in accounting for important aspects of cold sensation. Firstly, whereas heat sensitive neurons respond with a fairly specific threshold (≈43°C) cold sensitive neurons tend to activate over a wider temperature range (15-28°C for innocuous cooling, <15°C for noxious cold). Therefore, the idea that multiple channel types contribute to setting a gradient of cold thresholds is appealing. It will be of great interest to observe how these data compare to studies using other approaches such as the skin-nerve preparation and gene ablation techniques, in particular in animals lacking the TRPM8 and ANKTM1 genes. The molecular identity of the cold-inhibited K^+ channel also remains to be determined.

1.3.2.3 Thermal Transduction Conclusion

The last eight years have seen a massive expansion in the use of isolated sensory neurons to study thermal transduction. This field has done much to validate the sensory competence of cultured neurons demonstrating that a number of subpopulations of neurons, consistent with *in vivo* data, show electrochemical responses to thermal stimuli with physiologically relevant thresholds of activation. This work has also been an integral part of the cloning of a number of thermosensitive ion channels, although the serendipitous finding that naturally occurring plant compounds, capsaicin and menthol, are agonists of key thermosensitive ion channels was clearly central.

The model that has emerged from the range of temperature thresholds of thermosensitive channels and their cellular distribution is one whereby thermosensitive TRP-related channels are capable of signalling information over a spectrum of temperatures from around 0 to 60°C (Jordt *et al*, 2003; Patapoutian *et al*, 2003, Fig. 1.8). In this system it is proposed that distinct cell populations differentially expressing thermosensitive channels will be able to encode temperatures ranging from noxious cold (ANKTM1), cool (TRPM8), moderate to warm (TRPV3, TRPV4), noxious heat (TRPV1) to intense noxious heat (TRPV2). This elegant hypothesis suggests that distinct classes of thermosensitive neurons have specific molecular phenotypes.

Analysis of single and multiple null mutants for each thermosensitive TRP channel will be fundamental to the testing of these hypotheses. Electrophysiological analysis of null mutants will be informative, however investigation will also require the implementation of novel behavioural assays for assessing responses to cooling and the temperature range over which TRPV3 and TRPV4 are purported to operate. So far only data regarding the phenotype of TRPV1 nulls have been published. Although there were some discrepancies between the studies of Caterina *et al* (2000) and Davis *et al* (2000) investigation of these animals verified a role for TRPV1 in heat sensation, particularly thermal hyperalgesia.

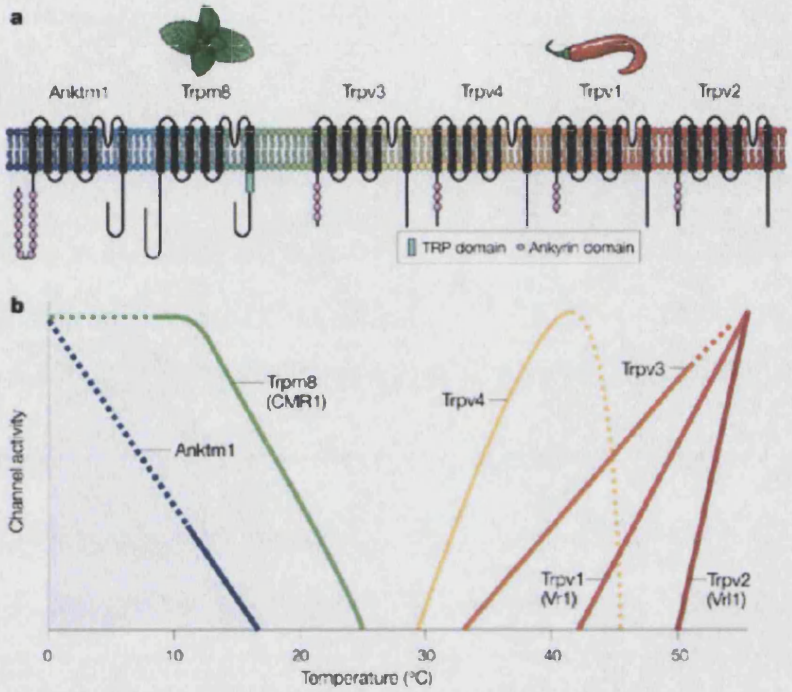

Fig. 1.8 Thermally gated TRP channels. The diagram shows the gating of TRP channels by temperatures ranging from noxious cold to noxious heat. As indicated, menthol and capsaicin activate Trpm8 and Trpv1, respectively. Activation thresholds and maximal activation are derived from studies of these channels expressed in heterologous systems; some thresholds are averages of values reported in different studies. Uncertainty in the exact slope of the lines is shown as dashed lines. (Figure from Patapoutian *et al*, 2003.)

There is still debate as to whether TRPV3 and TRPV4 are expressed in the DRG and no currents with thermal thresholds similar to these ion channels have been demonstrated in DRG neurons. If these channels do contribute to thermosensation at the nerve terminal it would undermine the use of cultured neurons as a model system. However, Alessandri-Haber *et al* (2003) recorded changes in membrane excitability attributable to TRPV4 in cultured neurons suggesting that the receptor is present at the soma. Potentially, the TRPV4 gene product may exist in multiple functional states as has been hypothesised for TRPV1 (Nagy and Rang, 1999). Another level of complexity in determining the role of each thermosensitive TRP channel in DRG physiology is the capability of different channel subunits to heteromultimerise, as demonstrated by Smith *et al* (2002) for TRPV3 and TRPV1 who showed this can produce channels with novel properties.

Finally it remains to be determined how thermosensitive TRPs are gated by temperature changes. Although, domains of TRPV1 responsible for gating by protons (Jordt *et al*, 2000) and capsaicin (Jordt and Julius, 2002) have been identified, no specific region has been attributed to thermosensitivity. That TRPM8 and ANKTM1 are activated by energy removal makes the biophysics of these channels particularly interesting.

1.3.2.4 Mechanotransduction

As discussed in Section 1.1 the majority of DRG neurons are sensitive to mechanical stimulation with different classes of neurons specialised to detect different forms of stimuli. The key differences lie in the thresholds of activation and the mechanically evoked firing pattern exhibited by different neuronal subpopulations (Perl, 1992; Koltzenburg *et al*, 1997). In an attempt to better understand how pressure generates neuronal activity a number of groups have investigated the responses of cultured sensory neurons to a range of mechanical stimuli using both Ca^{2+} imaging and electrophysiology.

In studies using ratiometric Ca^{2+} imaging neuronal stimulation using a rounded micropipette (Sharma *et al*, 1995; Gotoh and Takahashi, 1999; Raybould *et al*, 1999; Gschossmann *et al*, 2000), fluid jet (Sullivan *et al*, 1997) and hypoosmolarity-induced

cell swelling (Viana *et al*, 2001) has been shown to induce an increase in cytosolic Ca^{2+}. In each case the rise in Ca^{2+} was dependent on extracellular Ca^{2+} suggesting that it was mediated via a calcium permeable membrane channel rather than release from intra-cellular stores. One problematic issue with such studies has been the time course of the observed responses, in each case the rise in Ca^{2+} levels has been slow (occurring over many seconds or even minutes) and the return to baseline has consistently occurred considerably after the end of the stimulus. How these slow responses relate to the rapid encoding of mechanical stimulation by nerve endings *in vivo* is unclear. Furthermore, none of these studies were performed under voltage clamp conditions meaning that membrane depolarisations induced by mechanosensitive ion channel activation would likely have activated voltage-gated Ca^{2+} channels. Although some studies reported that calcium channel antagonists did not inhibit mechanically evoked responses (Sullivan *et al*, 1997; Gotoh and Takahashi, 1999; Gschossmann *et al*, 2000) as sensory neurons express a heterogeneous population of calcium channels (Yusaf *et al*, 2001) it cannot be guaranteed that all of them were blocked. Viana *et al* (2001) showed that the calcium channel blocker Ni^{2+} does inhibit swelling evoked responses.

These studies have consistently reported that Gd^{3+}, a blocker of a diverse range of mechanosensitive ion channels (Hamill and McBride, 1996), inhibited responses to mechanical stimulation. However the effective blocking concentration ranged from 5 μM (Gotoh and Takahashi, 1999) to 250 μM (Gschossmann *et al*, 2000). Moreover, it should be noted that Gd^{3+} might also antagonise voltage-gated Ca^{2+} channels (Boland *et al*, 1991). Gschossmann *et al* (2000) reported that amiloride (100 μM) and κ-opioid agonists reduced mechanically evoked Ca^{2+} increases whilst not affecting increases induced by capsaicin. Whilst, Drummond *et al* (1998, using the stimulation method of Sullivan *et al*, 1997) reported increases in intracellular Ca^{2+} were antagonised by 100 nM amiloride (see also Section 1.2.2.2).

Another variable that fluctuated widely between studies was the proportion of cells that responded; ranging from 25% (Raybould *et al*, 1999) to 93% (Gotoh and Takahashi, 1999) although this may simply reflect differences in the degree of pressure applied using

different stimulation protocols. Finally, none of the above studies demonstrate specificity of mechanically evoked Ca^{2+} increases by testing their stimulation methods on other populations of neurons or describe differences amongst subpopulations of DRG neurons. Viana *et al* (2001) did describe different temporal profiles of Ca^{2+} rises evoked by hypotonicity but did not identify if particular response types were associated with specific cell types (there was no association with capsaicin sensitivity).

To date three groups have published papers concerning electrophysiological studies of mechanically evoked responses of DRG neurons. McCarter *et al* (1999) reported whole cell currents evoked by stimulation of the cell soma with either a rounded micropipette or a fluid jet. Currents were detected in ≈70% of large neurons (>30 μm) and ≈35% of small neurons (≤30 μm), however no comparison of current amplitudes was made. Currents were inhibited by Gd^{3+} (IC_{50} ≈ 12 μM) and the amiloride analogue benzamil (IC_{50} ≈ 50 μM). The current-voltage relationship of responses (reversal potential +7 ± 7 mV in quasi-physiological solutions) indicated that they were non-selective cationic currents and, importantly, no such responses were seen in 23 sympathetic neurons tested.

Takahashi and Gotoh (2000) described, in neonatal DRG neurons, whole-cell currents that were activated by the application of positive pressure to the cell through the patch pipette, current amplitude being proportional to the level of applied pressure. Such responses were only seen in neurons over 20 μm and were of two types; either a Ca^{2+} current or a non-specific cation current, however no distinction was made between cells that expressed either current. Currents were sensitive to Gd^{3+} (concentration not given) but neither amiloride nor Ca^{2+} channel antagonists. Interestingly, pressure was applied for 0.5 sec but the peak current was seen between 0.5 and 1 sec after stimulation. What underlies this refractory period is unclear, possibly pressure within the system takes time to equilibrate and only reaches threshold levels after a delay or a second messenger intermediate could be involved although this is unlikely due to the dialysis of the cytoplasm when making whole cell recordings.

Finally, the group of Uhtaek Oh (Cho *et al*, 2002) have published an extensive study of DRG mechanosensitive ion channels at the single channel level that also compares the presence of these channels to that of whole-cell currents. Again whole-cell currents were evoked by positive pressure through the patch pipette and like Takahashi and Gotoh (2000) these currents were observed after a delay (this time 1-3 sec) and predominately in larger neurons.

Recording from cell-attached patches and applying negative pressure through the pipette two classes of mechanosensitive ion channels ("observed most frequently") were found. Firstly, low threshold (LT) channels were seen in 25.7% of patches that were activated at –10 to –20 mmHg with a $P_{1/2}$ of 60.6 mmHg and secondly high threshold (HT) channels (23.6% of patches) with a $P_{1/2}$ of 83.1 mmHg and a threshold of >60 mmHg. Current voltage relationships and ionic substitution experiments showed that both channel subtypes were non-specific cation channels with significant permeability to Ca^{2+}. LT channels were outwardly rectifying and HT channels had a more linear relationship. Both channels were blocked by Gd^{3+} but were insensitive to amiloride and arachidonic acid. Both channels were inhibited by pretreament of the patch with cytochalasin D (10 μM) or cholchicine (500 μM) or by excision of a cell-attached patch to the inside-out configuration. Interestingly in all three cases the inhibitory effect was significantly more pronounced for LT channels than it was for HT channels. Another interesting finding of this study was that HT, but not LT, channels showed a marked sensitisation following exposure to prostaglandin E_2 that was apparently mediated via a cAMP and protein kinase A dependent pathway.

A major consideration regarding this study is the cell size distribution of both channel types and the whole-cell currents. HT channels were found in a population of cells with diameters of 10-17.5 μm and LT channels in significantly larger cells; diameters 10-30 μm. However, whole cell currents were found in a population of cells (20-30 μm diameters) that, although having substantial overlap with those expressing LT channels, was significantly larger than both other populations. This therefore strongly suggests that the observed single channels do not underlie mechanically activated whole-cell currents.

Moreover, it is conspicuous that the largest cells tested (30-40μm), that would be expected to be low-threshold mechanoreceptors (Section 1.1), showed no mechanically evoked activity.

This body of work has demonstrated that cultured DRG (and nodose ganglia) neurons possess the capacity to respond to mechanical stimulation. The field is made complex by the fact that mechanical stimulation can be applied to neurons in a number of ways and from the available data (i.e. ionic permeability and pharmacology) it appears likely that different forms of stimulation result in activation of different species of ion channels. Although it is a distinct possibility that mechanotransduction at the nerve terminal *in vivo* is a complex process that involves multiple ion channel types, it is likely that some *in vitro* models of mechanosensation involve activation of channels that are not relevant to mechanosensation *in situ*.

Probably the most important control is to show specificity to DRG neurons; only McCarter *et al* (1999) showed that their stimulation protocol did not induce activity in another neuronal population (SCG neurons). This may be particularly relevant to single channel analysis where many ion channels, such as the voltage-gated K^+ channel Shaker (Gu *et al*, 2001), have been shown to be mechanosensitive but where no clear physiological relevance is apparent. Indeed, Gu *et al* (2001) suggest that mechano-sensitivity may be a common property of multi-conformation proteins (Section 1.2.1). Another important fact that has not been addressed, beyond cell size, is the physiological characterisation of the neurons that respond to pressure. Indeed the extensive expression of mechanosensitive ion channels in presumptive nociceptors and their absence in large cells in the Cho *et al* (2002) study is contrary to what would have been predicted. Conversely, McCarter *et al* (1999) found more large cells responded to mechanical stimulation. Here it should be considered that application of positive pressure through the patch pipette might well result in a significantly different form of mechanical stress on the membrane than does membrane compression induced by externally applied pressure.

Overall, a number of mechanically induced Ca^{2+} elevations and whole-cell and single channel currents have been characterised to lesser or greater degrees but remain entirely enigmatic at the molecular level. It may well be the case that different stimulation protocols activate distinct signalling pathways and it will not be until these pathways are identified molecularly that their relevance to somatosensory mechanotransduction will be determined.

Knowledge of mechanotransduction clearly lags behind that of thermosensation, particularly at the molecular level. Also there are more discrepancies between studies of this modality than there is between investigations of heat or cold responses. It is likely that this is due to the different modes of stimulation used and possibly due to the fact that multiple mechanosensitive cell types may respond to pressure differently. Also, to date the prediction that mechanosensitive ion channels exist within transduction complexes has negated the successful application of expression cloning techniques (see Section 1.2.2.1 and 1.3.3). However, the sensory competence of isolated DRG neurons suggests that they can be used as a model system of mechanosensation and that is what will be explored in this thesis.

1.3.3 Studying Mechanosensitive Ion Channels in Heterologous Systems

Complimentary to the study of ion channel physiology in cultured neurons are the techniques of expressing ion channels in heterologous systems such as cell lines, *Xenopus* oocytes or neurons that do not normally express the channel of interest. As described above this technique has successfully been employed in the study of thermally activated ion channels. In this section the applicability and possible caveats of this approach to studying mechanosensitive ion channels will be discussed.

To confirm that any channel is a mechanotransducer it is necessary to demonstrate that that channel is gated by mechanical force and so far this has not been achieved unequivocally for any eukaryotic channel. In invertebrate studies, loss of function data from mutant animals is persuasive for a key role of a number of ion channels in mechano-

transduction (Section 1.2). However, none of these channels have been shown to be rapidly mechanically gated when expressed exogenously, and so the possibility remains that these ion channels are *permissive* for mechanotransduction whilst not actually carrying the transduction current. Overcoming this issue is likely to be difficult. For example, NOMPC is expressed in the specialised cilia of *Drosophila* bristle cells (Walker *et al*, 2000) and so it is difficult to imagine a heterologous system that could recapture the morphological features of these cells. In addition, the extensive work on mechano-sensation in *C. elegans* has demonstrated that the gating of putative mechanosensory ion channels is very likely dependent upon their direct interaction with a number of intra- and extracellular proteins (Section 1.2.2.1). Hence, reconstitution of channel activity in a heterologous system may require the "rebuilding" of such a transduction complex. This issue is further complicated by the possibility that reconstitution of the correct extracellular matrix will be extremely difficult using an *in vitro* system. If this were the case it may be necessary to find novel ways of applying mechanical force to the ion channel. This key issue is a major reason why expression cloning, such as that used to identify heat and cold receptors, may be unable to be utilised in the search for mechanosensitive ion channels. Each necessary additional member of the ion channel complex makes the systematic division of cDNA pools underlying this procedure less and less likely to identify the proteins of interest.

In terms of functional studies the TRP channels TRPV4 (Liedtke *et al*, 2000; Strotmann *et al*, 2000) and Nan (Kim *et* al, 2003) have both been shown to be activated, when expressed in cell lines, by hypotonicity. Such activation occurs with a latency of tens of seconds and none of these studies has attempted to correlate the rate of change of cell volume with current activation. The temporal relationship between these two variables would be informative; if current activation closely follows membrane stretch it would support the hypothesis that membrane stretch is gating the channel whereas if the two variables have distinct temporal profiles it would argue that something downstream of membrane stretch (such as *Src* kinase activation, Xu *et al*, 2003) activates the channels. Zhang and Bourque (2003) have recently shown that cell volume increases in response to hypoosmolarity do occur over tens of seconds but also showed that different neuronal

types display distinct osmoregulatory responses and, thus, it is unclear how cell lines and DRG neurons respond.

With regards to members of the DEG/ENaC family, no mechanically activated whole cell currents have been recorded that are attributable to such channels. When Goodman *et al* (2002) expressed MEC4 and MEC10 in *Xenopus* oocytes (see Section 1.2.2.1) the induced amiloride sensitive sodium currents were not effected by hypotonicity-induced cell swelling either in the presence or absence of MEC2 and no other forms of mechanical stimulation were reported[6]. Likewise, no study has shown ASICs to be activated by mechanical stimulation in any heterologous system. Again, this suggests that the channels are not directly gated by pressure or that, by analogy to the work carried out in *C. elegans*, they are only mechanosensitive when expressed in the correct environment with the appropriate auxiliary proteins.

Due to these considerations, attempts to discover proteins that interact with ASICs have been undertaken, to do so several groups have searched for binding proteins using the yeast two-hybrid technique. Both the Welsh group (Hruska-Hageman *et al*, 2002) and the Corey group (Duggan *et al*, 2002) found that both ASIC1 and ASIC2 interact with the synaptic protein PICK1 (protein interacting with C kinase). It was shown that coexpression of ASIC2b and PICK1 mutually alters the distribution of each protein in COS-7 cells (Hruska-Hageman *et al*, 2002) and that the two proteins were colocalised in mechanosensory terminals (Duggan *et al*, 2002) and in central neurons (both studies). Anzai *et al* (2002) showed that the C terminus of ASIC3 interacts with CIPP (channel interacting PDZ domain protein). It was shown that CIPP is expressed widely in DRG (and throughout the body) and that coexpression of this protein with ASIC3 in COS-7 cells substantially increased the amplitude of proton-activated currents and slightly but significantly shifted the pH sensitivity of the channels to more alkaline values.

---

[6] Such experiments could be hampered by endogenous stretch activated currents in these *Xenopus* oocytesas reported by Saitou *et al* (2000) and Bryan-Sisneros *et al* (2003) although not all groups have observed such currents (see Zhang and Hamill, 2000).

Together these data suggest ASICs are dynamically regulated but only Eilers *et al* (2002), have found a protein homologous to a component of the proposed *C. elegans* mechanotransduction complex. In a preliminary report they presented evidence, from co-immunoprecipitation experiments, that ASIC2 (a and b) interacts with Nstom1, a neuron specific stomatin homologue also related to MEC-2. No study to date has reported experiments aimed at determining if any of these interacting proteins confer mechanosensitivity on heterologously expressed ASIC channels. Interestingly, all studies have identified proteins that interact with the C termini of ASIC channels, however, in *C. elegans* it appears that it is a conserved domain within the N terminus of MEC4 and 10 that is essential for normal channel function (Hong *et al*, 2000). Furthermore, the issue of whether an external binding protein is required to confer mechanosensitivity to ASICs remains a salient one. This is a complex matter as first it must be determined which cells normally synthesise this protein (i.e. which cDNA library would be appropriate for screening assays) and secondly would an expression system synthesise and translocate this protein in the correct manner.

That DRG neurons are mechanosensitive *in vitro* suggests that isolated cells *are* capable of functionally expressing mechanosensitive ion channels but it remains possible that there are multiple types of mechanosensitive channels some of which require complex extracellular matrices and/or auxiliary cell types to operate.

1.4 Aims

Initial data obtained in this lab by Paolo Cesare showed that mechanical stimulation of the somata of cultured sensory neurons evoked a cationic current that was proportional to the size of the stimulus. Neurons were stimulated using a rounded glass pipette (driven by a piezo electric device) that compressed the somatic membrane. The aims of my project were to characterise these mechanically activated currents and then to investigate the molecular identity of the channels that underlie them.

Characterisation of the currents would involve determining if different subtypes of DRG neurons (defined by established markers such as capsaicin sensitivity, cell diameter, IB4 binding and action potential duration) displayed distinct responses to mechanical stimulation as would be predicted from their *in vivo* functions. Characterisation would also involve investigation of the basic ionic permeability and pharmacology of these ion channels; comparison of these properties with those of known channels may yield clues as to the molecular identity of the sensory mechanosensitive ion channels (Chapters 3 and 4).

Having characterised mechanically activated currents, studies would be undertaken to attempt to uncover the molecular identity of the channels involved. Two routes would be taken; the first was to investigate the response properties of neurons derived from null mutants for candidate ion channel genes, i.e. members of the ASIC channel family (Chapter 4). Secondly, a project was initiated to isolate a single conopeptide antagonist of DRG mechanosensitive ion channels. Such a reagent would enable a number of approaches to cloning the ion channel (Chapter 5).

2 Methods & Materials

2.1 Cell Culture

2.1.1 Culture of Neonatal Rat DRG Neurons

Neonatal (P1) Sprague-Dawley rats were decapitated and 25-35 DRG taken from each animal. The ganglia were enzymatically digested in 1mg/ml collagenase D (Roche) in Ca^{2+}/Mg^{2+} free PBS for 25 minutes. Subsequently ganglia were washed three times (1x in PBS and 2x in culture medium) and then neurons were isolated by mechanical trituration using a 21-gauge hypodermic needle. Cells were passed through a 40 μm pore cell-strainer and then pelleted by centrifugation for 5 minutes at 1000 rpm. Cells were resuspended in culture medium and were cultured on poly-L-lysine and laminin (unless otherwise stated) coated 35 mm dishes in Dulbecco's Modified Eagle Medium (DMEM) containing 10% heat-inactivated foetal bovine serum (FBS, Gibco), 2 mM glutamine (Gibco), 10,000 IU/ml penicillin /streptomycin (Gibco) and 100 ng/ml NGF. Cultures were kept at 37°C in 5% CO_2. Neurons were (unless otherwise stated) used the day after preparation (i.e. 16-36 hours after plating).

2.1.2 Culture of Adult Mouse DRG Neurons

Null mutant and wild-type adult mice used in these studies were either 6-9 weeks old for ASIC2 and ASIC2/3 strains or 14-16 weeks old for the ASIC3 strain. Animals were killed by CO_2 inhalation followed by cervical dislocation and 20-25 DRG were dissected from each. Ganglia were digested in collagenase (Type XI, 0.6 mg/ml, reagents from Sigma unless stated otherwise), dispase (3.0 mg/ml) and glucose (1.8 mg/ml) in Ca^{2+}/Mg^{2+} free PBS for 40 minutes. Cells were washed once in culture medium and then mechanically triturated using a P1000 Gilson pipette. Cells were passed through a 60 μm pore cell-strainer, centrifuged for 5 minutes at 1000 rpm and then resuspended in DMEM containing 10% heat-inactivated FBS (Gibco), 2 mM glutamine (Gibco), 10,000 IU/ml penicillin/streptomycin (Gibco) and 100 ng/ml NGF. Cultures were plated on 35 mm

dishes coated with poly-L-lysine and laminin. Recordings were made 16-36 hours after plating.

2.1.3 Preparation of Superior Cervical Ganglia Neurons (prepared by Jo Riley)

Neurons were isolated from superior cervical ganglia (SCG) of adolescent Sprague-Dawley rats (P15-19) and cultured as described in Delmas *et al* (1998) and Marrion *et al* (1987). Briefly, rats were killed by CO_2 inhalation and decapitated. Both ganglia were removed and desheathed and then incubated first in collagenase and then in trypsin. The ganglia were then mechanically triturated and neurons collected by centrifugation. Cells were then resuspended and plated onto laminin-coated glass coverslips and incubated at 37°C with a 5% CO_2 atmosphere in L-15 culture medium (plus 10 % FBS, 2 mM glutamine, 24 mM $NaHCO_3$, 38 mM glucose, 50 U/ml penicillin/streptomycin, 25 ng/ml NGF). Neurons were used the day after plating.

2.2 Electrophysiology

Recordings of membrane currents and membrane voltage were made using the patch-clamp technique (Hamill *et al*, 1981). The vast majority of recordings made in this thesis were done using the perforated-patch technique whereby electrical access to the cell's interior is achieved through antibiotics forming monovalent ion channels in the membrane patch (see below). The basic circuit of the patch-clamp configuration is shown in Fig. 2.1. The command potential (V_{ref}) enters the high gain operational amplifier at its non-inverting input and the potential of the pipette (V_P) enters at the inverting input. A current is passed through the feedback resistor (i_f) so that the inputs are equal; due to the very high input resistance of the amplifier this current is equal to that passing across the membrane (i_P). In the whole-cell mode, the voltage output of the amplifier is hence $i_p R_f + V_{ref}$, where V_{ref} is known and R_f is constant and known.

The value of Vp recorded by the amplifier differs from that at the pipette tip because of a series resistance error. The primary source of error in the patch-clamp circuit is the

access resistance through the pipette, which means that the potential at the pipette tip will be different to the recorded V_P when the amplifier passes a current through the preparation. In this work access resistance typically varied between 3-10 MΩ and this was compensated for 40-60%, hence a common effective series resistance was 3.5 MΩ and the largest currents recorded in this study were typically around 2 nA. Therefore, Ohm's law dictates that the residual IR drop was around ($3.5 \times 10^3 \times 2 \times 10^{-9}$) 7 mV.

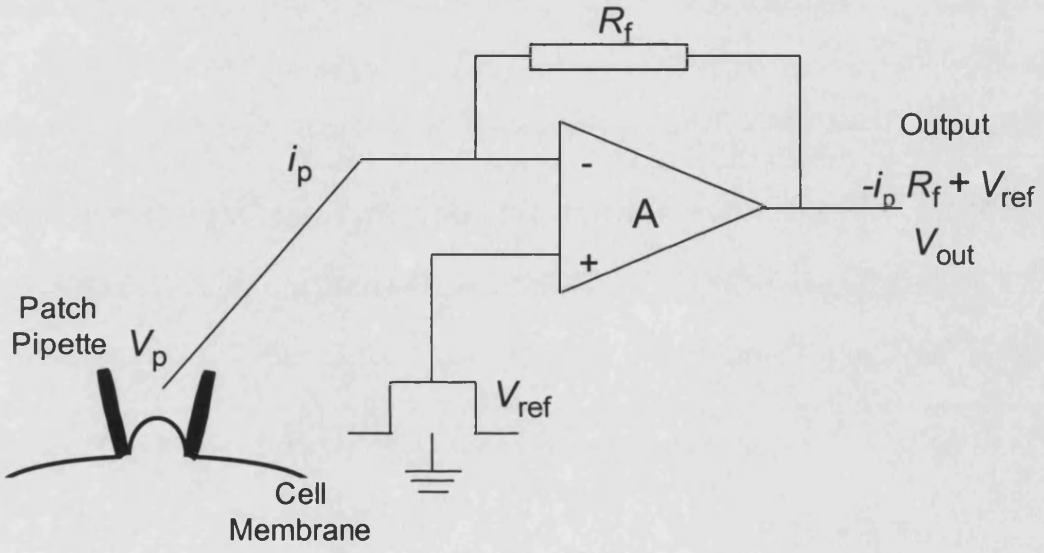

Fig. 2.1 The patch-clamp circuit. Current passing across the membrane, i_p, is measured as the voltage drop, v_p, across the feedback resistor, R_f, by the high gain amplifier, A. (Adapted from Aidley and Stanfield, 1996.)

2.2.1 Perforated-Patch Technique[7]

In the perforated patch technique antibiotic ionophores are used to perforate the membrane patch allowing electrical access to the cell. The most commonly used are the polyene antibiotics amphotericin B and nystatin; both compounds partition into cholesterol- or ergosterol-containing membranes and form channels permeable to mono-valent cations and chloride ions but not to multivalent ions. Chloride permeability is only

[7] See The Axon Guide, Chapter 5, Advanced Methods in Electrophysiology: Recording from Perforated Patches and perforated Vesicles and references therein. http://www.axon.com/MR_Axon_Guide.html

around a ninth of that for monovalent cations. However, if the chloride concentration is high, fluxes of this anion into the cell can induce cell swelling, therefore reduced concentrations of chloride (roughly equivalent to the cell's interior) are preferred and methanesulphonate can be used as a substitute anion.

The primary advantage of the perforated patch technique is that the cell's contents are disrupted to a much lesser degree than in conventional whole-cell recordings. Thus intracellular signalling pathways, the cytoskeleton and the concentration of multivalent ions are well preserved during recordings. Recordings can be made for long periods (upwards of 3 hours) and during experiments access resistance tends to remain stable and is only slightly higher than that seen in whole-cell recordings. The major disadvantage of the technique is the time taken for access resistance to become sufficiently low to commence experiments.

In this lab amphotericin B has been used to make perforated patch recordings (Rae *et al*, 1991). A stock solution of amphotericin B was made up at 50 mg/ml in DMSO and 8 µl aliquots were kept at -20°C for typically around 2-3 weeks with no appreciable diminution in activity. 6 µl of this solution was added to 1 ml of the pipette solution prior to recording to give a final concentration of 300 µg/ml, which is well above the predicted saturating concentration of this compound; 120 µg/ml (consistent with this, precipitation of amphotericin B was observed in these solutions). These solutions were kept at 4 °C and retained activity for 4-5 hours. As amphotericin B can interfere with seal formation, the tip of the electrode was filled with amphotericin B-free internal solution by dipping the pipette tip for 25-30 sec and then the electrode back-filled with the amphotericin solution.

After seal formation, voltage steps (+5 mV, 10 msec) were applied to the neuron every 15 sec to assess capacitance transients; as amphotericin B partitions into the membrane access resistance falls and thus capacitance transients increase in amplitude and decay of the transients becomes more rapid. Recordings were commenced when transients became stable and access resistance was below 10 MΩ; this typically took 10-20 minutes.

Access resistance remained stable or decreased slightly for at least up to 45 minutes. Occasionally, membrane patches would rupture during seal formation or recording, such events were apparent as a sudden jump in access resistance and such recordings were discarded. In a series of recordings (n = 4) lucifer yellow was included in the pipette solution and was shown to be excluded from the neuronal cytoplasm when making perforated-patch recordings; when the patch was ruptured the cell filled with this compound (Fig. 2.2).

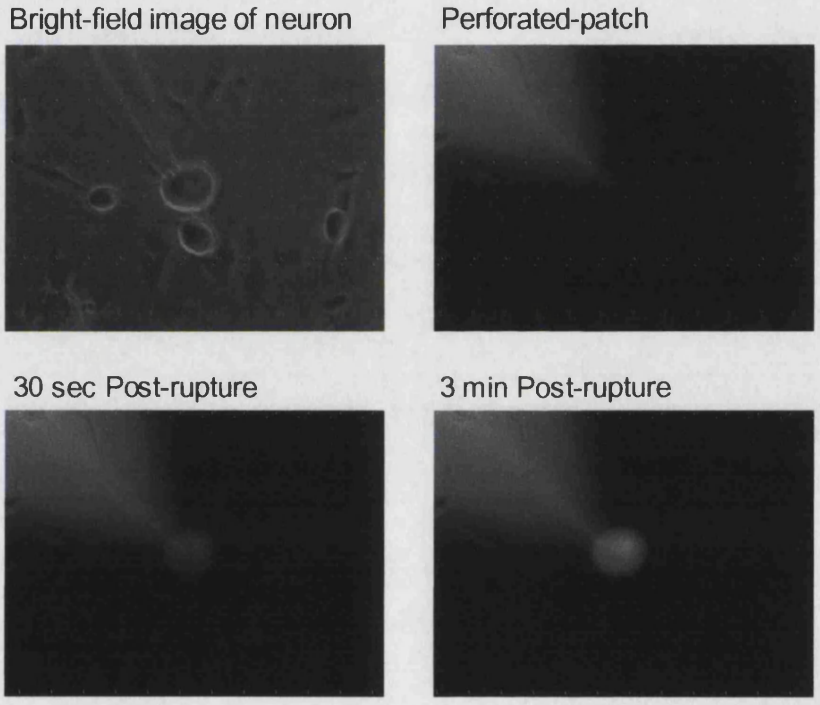

Fig. 2.2 Images demonstrating that during perforated-patch recordings the membrane patch was impermeant to lucifer yellow. Recordings were made as normal in the perforated-patch configuration, then the membrane was ruptured (access resistance dropped from 8.0 MΩ to 3.7 MΩ) and dialysis of the neuron's interior was observed through lucifer yellow fluorescence, seen here 30 seconds and 3 minutes after membrane rupture.

2.2.2 Cell Selection and Recording Configuration

Neurons whose soma was not in contact with those of other neurons were selected for recording. Whole-cell, perforated patch recordings were made using an Axopatch 200B

amplifier (Axon Instruments) controlled by pCLAMP 6 (Axon Instruments). Data was sampled at 5-20 kHz. Patch pipettes were made from thin-walled borosilicate glass capillaries (Harvard Apparatus) and had an initial resistance of 2-3 MΩ when filled with internal solution. Access resistance was typically 3-10 MΩ, compensated for by 40-60% (feedback lag; 15 μsec) in both voltage and current clamp experiments. Voltage-clamp recordings were made at a holding potential of –70 mV unless otherwise stated. A silver chloride pellet in the bath was used as the reference electrode.

IB4 labelling was achieved by incubating the cells in IB4-Alexa 488 (3 μg/ml, Molecular Probes) in standard external solution for 10 min prior to recording. Cells were then washed in external solution three times. For control experiments responses were recorded, and then 4.5 μg of IB4-Alexa in 100 μl was added to the 1.5 ml bath solution for 10 min before superfusion of the neurons with control solution.

2.2.3 Standard Solutions

Standard intracellular solution contained (in mM): 110 methanesulfonic acid, 30 KCl (BDH), 1 $MgCl_2$ and 10 HEPES, pH 7.35 (pH was corrected using KOH; final K^+ concentration ≈140 mM); 200 μg/ml amphotericin B was added immediately before recording. The standard external solution contained (in mM): 140 NaCl (BDH), 4 KCl (BDH), 2 $CaCl_2$ (BDH), 1 $MgCl_2$ and 10 HEPES, pH 7.4 (adjusted using NaOH). Alternative intra- and extracellular and drug solutions are given in the *Methods and Materials* sections of *Results* chapters.

2.2.4 Mechanical Stimulation and Drug Application

As discussed in Section 1.3.2.4 a number of methods have been employed to mechanically stimulate neurons and many of these protocols induce changes in membrane conductance and increases in intracellular Ca^{2+}. We opted to use a stimulation protocol that involved displacing the cell membrane as it was felt that a rapid, externally

applied mechanical stimulus may better reflect natural stimuli than does whole-soma membrane stretch derived from cell swelling.

Mechanical stimulation of neuronal somata was achieved using a heat-polished glass pipette (tip diameter approximately 5μm) controlled by a piezo-electric crystal drive (Burleigh). The probe was positioned at an angle of 70° to the surface of the dish and in a position so that when moved it made contact with the centre of the cell body (Fig. 2.3), i.e. the probe moved along a trajectory that was approximately perpendicular to the cell surface. Burleigh specifies that the application of a 10 V potential difference across the crystal would cause it to expand by 7 μm. Camplex controlled the device with its output, i.e. a voltage ramp was delivered to the piezo device via a preamplifier and the rate of change of voltage controlled the probe velocity. The probe was positioned so that a 10 μm movement did not visibly contact the cell but that a 12 μm stimulus produced an observable membrane indentation. A 12 μm movement was then defined as a 2 μm stimulation, 14 μm as a 4 μm stimulus, and so on. The probe was moved at a speed of 0.5 μm/msec (unless otherwise stated) and the stimulus was applied for 200 msec (unless otherwise stated). To assess the mechanical sensitivity of a neuron, a series of mechanical steps in 2 μm increments were applied (7 for neonatal rat neurons and in adult mice 9 for large cells and 7 for small-medium cells) at 15 sec intervals, which was sufficient for full current recovery between stimuli. To assess the effects of antagonists on MA currents a stimulus intensity that gave a reproducible response >200 pA were applied to the neuron at 20 sec intervals whilst the cell was constantly superfused with control or drug solution (except in the case of conopeptide experiments; see Chapter 5).

When studying the effects of compounds on MA currents, solutions were applied to the cell through a single tube, positioned around 300 μm from the neuron. Therefore, the angle of solution flow over the neuron did not change with drug application. The tube had multiple inputs and solutions were changed using a 6-way valve. To study agonist evoked currents in DRG neurons, drugs were applied using a multibarrel rapid solution changer (RSC-160, Biologic); exchange of solutions occurred in around 40 msec.

curves were fitted using a form of the Langmuir equation $B = B_{max}x_A/(x_A + K_D)$ where B is the current block, and B_{max} is the maximal fractional block, x_A is the concentration of the antagonist and K_D is the equilibrium constant for the antagonist.

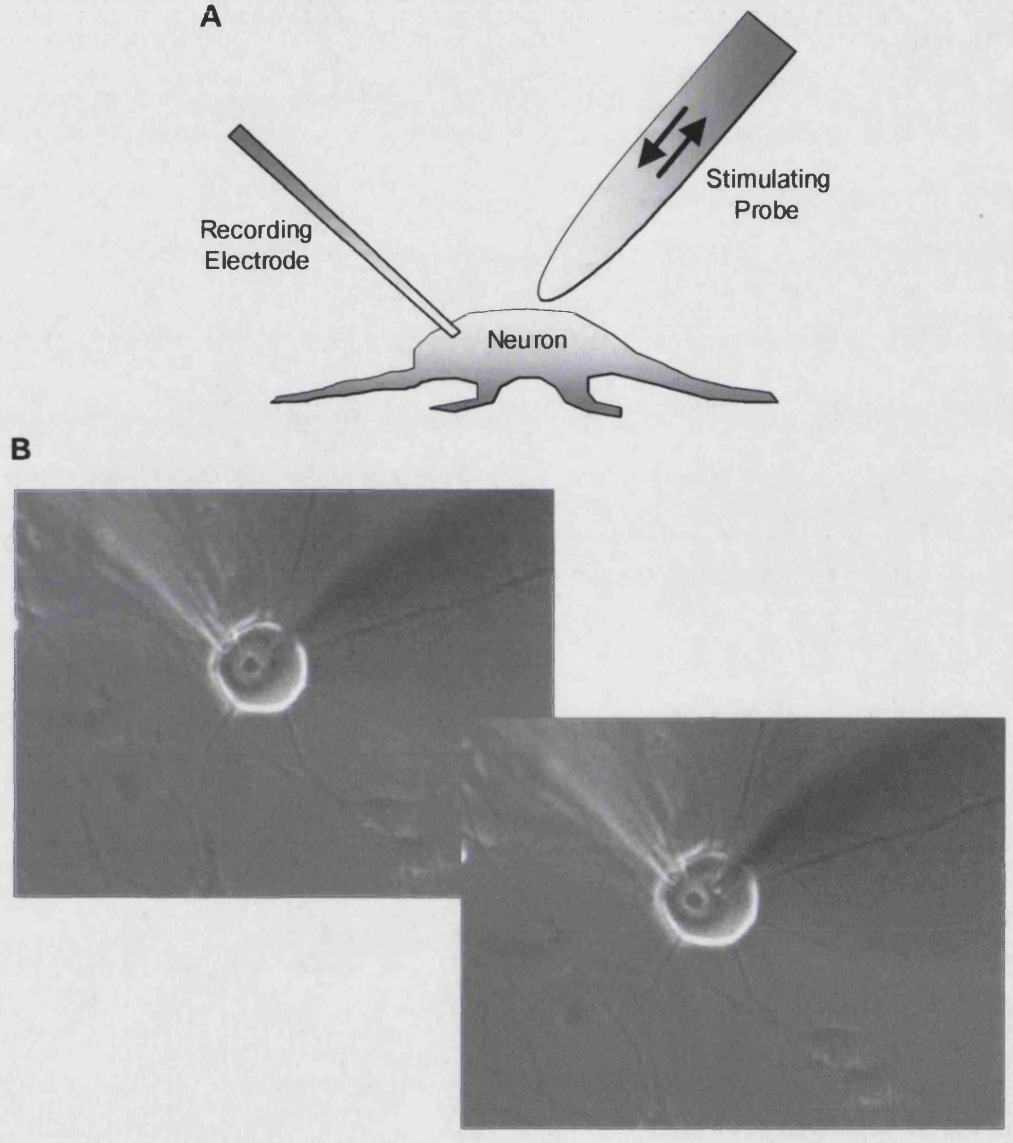

Fig. 2.3 Mechanical stimulation of neuronal cell bodies was achieved using a heat-polished glass probe controlled by a piezo-crystal drive. *A*, Schematic diagram of the experimental set-up and *B*, photos of an unstimulated neuron (*top, left*) and the neuron during the application of a 6 µm stimulus (*bottom right*). The recording electrode contacts the neuron on the top left and the stimulating probe comes from the top right of the picture to the centre of the neuron.

3 *Characterisation of Mechanically Activated Currents In Neonatal Rat DRG Neurons*

3.1 Introduction

Numerous studies have demonstrated that the cell bodies of cultured sensory neurons express ion channels that are sensitive to physical stimuli that are known to excite sensory neurons via their peripheral, sensory terminals *in vivo* (see Section 1.3.2). Amongst such studies a number have shown that mechanical stimulation of the somata of cultured sensory neurons can generate inward current and elevate intracellular Ca^{2+} levels. The range of stimulation protocols used include prodding of the somatic membrane with a glass probe (McCarter *et al*, 1999), fluid jet (McCarter *et al*, 1999), fluid injection through the patch pipette (Takahashi and Gotoh, 2000; Cho *et al*, 2002), negative pressure through the pipette (Cho *et al*, 2002) and osmotically induced cell swelling (Viana *et al*, 2001). We opted to use a glass probe to prod the somatic membrane, as we reasoned that applying acute mechanical stimulation externally to the neuronal membrane most closely resembled normal method of mechanically activating sensory terminals in the intact animal. Using a piezo crystal device to control the movement of the probe allowed fine, accurate manipulation of its position and speed.

Neonatal rat neurons were used for the initial characterisation of mechanically activated (MA) currents. Cesare and McNaughton (1996) used neonatal rat neurons to characterise heat-activated currents in sensory neurons; in their investigation it was found that a subpopulation of small diameter neurons responded to heating, consistent with the proportion of heat sensitive sensory fibres observed *in vivo*. It was also found that heat-activated currents were potentiated by bradykinin (Cesare *et al*, 2000). Together these studies suggested that neonatal neurons are a useful model for studying physical transduction and that the distribution and modulation of thermosensitive ion channels in neonatal and adult neurons is similar. One advantage of using neonatal neurons is that they appear to be more vigorous and healthy in culture than do adult neurons. In initial experiments (performed by Paolo Cesare) it was found that mechanically evoked

responses were more prevalent in neonatal neurons and the neurons were more robust in their responses to repeated stimulation.

Below is a description of work carried out to characterise the responses of sensory neurons to mechanical stimulation of their somatic membranes. In this work the response properties of distinct neuronal subpopulations was investigated and data are presented on the basic functional properties and pharmacology of MA currents.

3.2 Materials & Methods

Neonatal rat neurons were cultured as described in Section 2.1.1 and SCG neurons were prepared as described in Section 2.1.3.

Electrophysiology was conducted as described in Section 2.2 and mechanical stimulation applied following the protocols outlined in Section 2.2.4. Unless otherwise stated recordings were made in the perforated patch configuration using the standard internal and external solutions listed in Section 2.2.3. For ionic substitution experiments reported in Section 3.3.1 whole-cell recordings were made using the following solutions: Internal solution (in mM); 134 KCl/NaCl/CsCl, 0.2 $CaCl_2$, 1.6 $MgCl_2$, 2 BAPTA, 2.5 ATP(Mg), 0.3 GTP(Li) and 10 HEPES (pH 7.3). External with Na^+: 145 NaCl, 4 KCl, 1 MgCl and 10 HEPES (pH 7.4). External with Na^+: 145 N-methyl-*D*-glucamine (NMG), 4 KCl, 4 KCl, 1 MgCl and 10 HEPES (pH 7.4, corrected with HCl).

The effects of a number of compounds on MA currents were tested; in each case these drugs were applied to the neuron through a single static tube providing local superfusion (Section 2.2.4). Agonists of other receptors expressed by DRG neurons were applied using a multibarrel rapid solution changer (Section 2.2.4). In each case drugs were made as a stock solution in either standard external solution (*) or DMSO ($^{\nabla}$) and then dissolved in standard external solution to the working concentration. Stock were made to the following concentrations and stored at -20°C: Gd^{3+}* 50mM, ruthenium red* 750 μM, amiloride$^{\nabla}$ 200mM, gentamicin* 20mM, Zn^{2+}* 200mM, FM1-43$^{\nabla}$ 5mM, arachidonic

acid$^{\nabla}$ 50 mM, capsaicin$^{\nabla}$ 10 mM, capsazepine$^{\nabla}$ 20mM and α,β-methyl-ATP* 10 mM. The low pH solution used contained (in mM): 140 NaCl (BDH), 4 KCl (BDH), 2 $CaCl_2$ (BDH), 1 $MgCl_2$ and 10 MES, pH 5.15 (adjusted using NaOH).

When characterising the mechanosensitivity and chemosensitivity of a neuron, stimuli were applied as follows: mechanical stimulation (Steps1-7), capsaicin (1 μM), low pH, then α,β-methylene-ATP (10 μM). A reversible inward current of greater than 50 pA was considered a positive response to any of these stimuli.

Images of IB4 and FM1-43 fluorescence were taken using FITC filters (excitation 488 nm, emission 520 nm) using 50x oil immersion lenses. Images were captured using Openlab software with an exposure time of 2 sec.

3.3 Results

3.3.1 Mechanical Stimulation of the Somata of DRG Neurons Evokes a Cationic Current

Initial experiments showed that mechanical stimulation of the somata of cultured DRG neurons, voltage-clamped at -70 mV, evoked a reversible inward current. Currents were activated at displacements beyond a specific threshold displacement and all initially observed currents reached a peak amplitude at the cessation of probe movement and declined in amplitude during the stationary phase of the stimulus (but see below). Upon withdrawal of the probe the holding current rapidly returned to baseline (Fig. 3.1a).

To investigate if MA currents were specifically found in sensory neurons we stimulated SCG neurons using the same protocol. SCG and DRG neurons derive from common precursors in the trunk neural crest (Gilbert, 1994) and show similar growth and morphology in culture. Incrementing mechanical stimuli (2μm steps) were applied to these neurons until the recording was disrupted. In no case did mechanical stimulation of

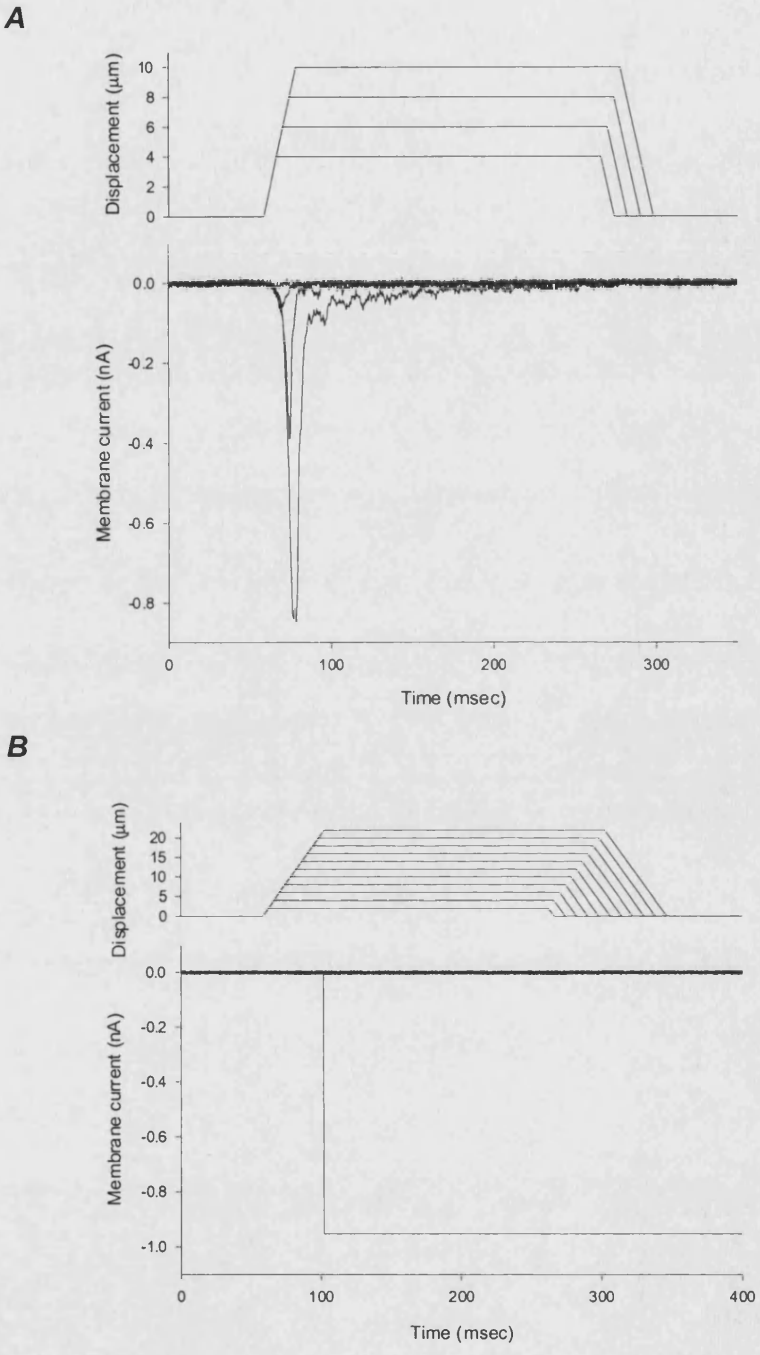

Fig. 3.1 Examples of the responses of DRG and SCG neurons to mechanical stimulation. *A*, Mechanical stimulation (4-10 µm displacements, *top trace*) of a DRG neuron, held at –70 mV, evokes a reversible inward current *(bottom trace)*. *B*, Mechanical stimulation (up to 22 µm, *top trace*) of a SCG neuron did not evoke a reversible, inward current (*bottom trace*). SCG neurons were stimulated up until the point that the recording was lost, as shown here.

17 (10 whole-cell recordings, 7 perforated patch recordings) SCG neurons evoke a reversible, inward current (Fig. 3.1b)

During early experiments it was found that MA currents recorded using the perforated patch technique were stable for considerably longer (commonly up to 30 minutes) than those recorded using the conventional whole-cell configuration. Currents recorded in the latter configuration tended to run down over 10-15 minutes (data not shown). Therefore, all subsequent experiments (except the ionic substitution studies described in this section) were performed using the perforated patch configuration.

To investigate the ionic selectivity of the ion channels underlying MA currents to monovalent cations we recorded currents at different membrane potentials whilst using different internal and external ionic solutions. In nominally Ca^{2+} free external solutions containing 145 mM Na^+, 4 mM K^+ and 1 mM Mg^{2+} the I-V relationship for MA currents was essentially linear when the internal solution was either Cs^+ (n = 2, Fig. 3.2a-c) or Na^+ (n = 1, Fig. 3.2d,e) based. Currents reversed at approximately 0 mV with the Na^+ based internal solution whereas they reversed between +8 and +14 mV with Cs^+ as the major intracellular ion. When external Na^+ was substituted by the impermeant cation NMG, MA currents recorded with a Cs^+ based internal solution reversed between –55 and –45 mV. The I-V relationship still appeared linear but had a shallower slope than when external Na^+ was present. With Na^+ inside the neuron currents reversed at around –50 mV and displayed an apparent linear IV relationship, approximately parallel to that seen when external Na^+ was present.

To assess if the ion channel underlying MA currents was permeable to Ca^{2+}, monovalent ions were removed from the external solution and MA currents were recorded in the presence of either 1.8 mM or 10 mM Ca^{2+} (plus 1 mM Mg^{2+} in each case) (Fig. 3.3a.). In two neurons replacement of Na^+ with NMG^+ reduced current amplitudes to 16.5% and 19.3% of control values, respectively. When the Ca^{2+} concentration was increased to 10 mM (NMG was correspondingly reduced), currents were larger; 26.3% and 42.6% of control, respectively. In addition, a series of experiments performed by Paolo Cesare,

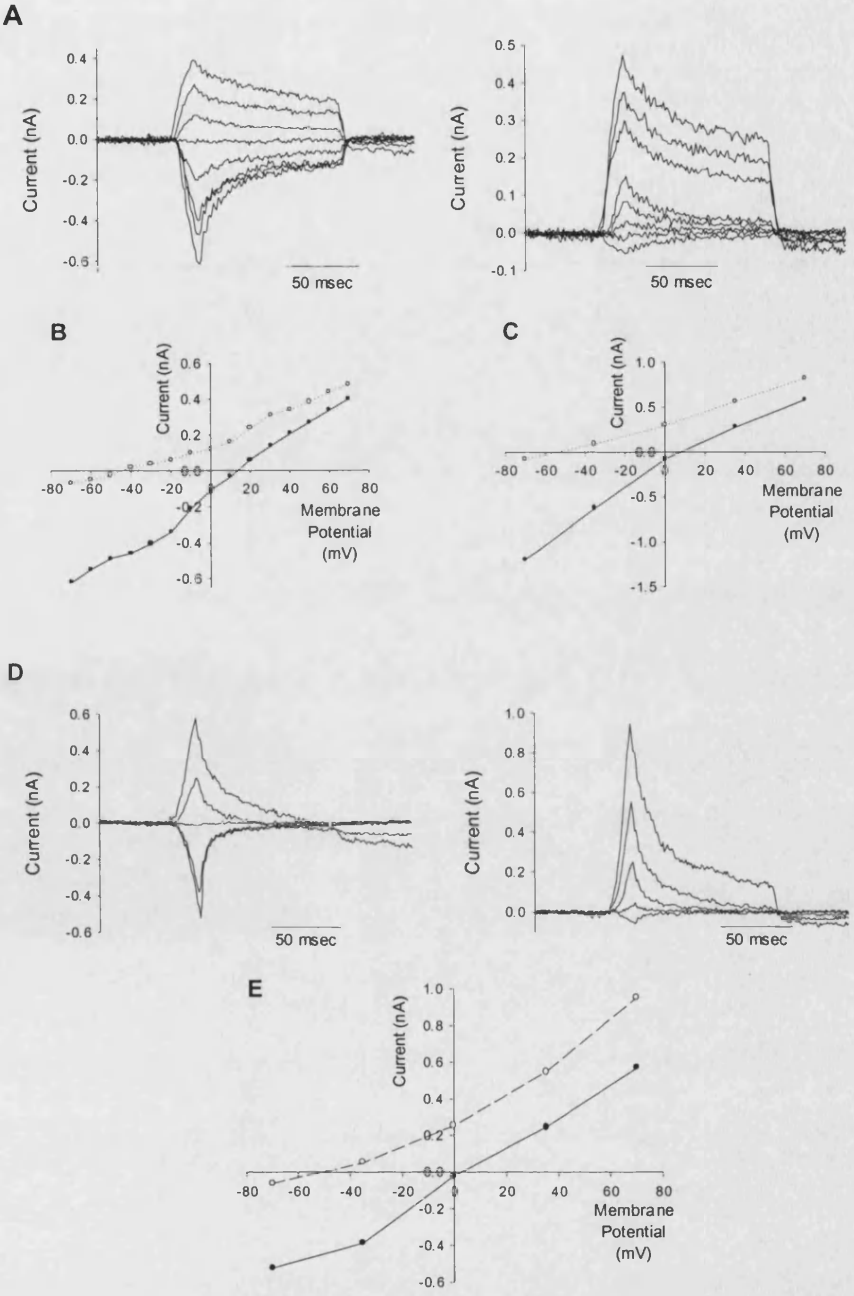

Fig. 3.2 Current-voltage relationships for MA currents. *A*, MA currents recorded at 20 mV steps (-70 - +70 mV) with a Cs^+ based internal solution. *Left*, the extracellular solution was nominally Ca^{2+} free and contained 145mM Na^+ as the principle ion. *Right*, the extracellular solution was nominally Ca^{2+} and Na^+ free. *B,C*, IV relationships for two neurons using the same solutions as in *A* (*B* is the neuron shown in *A*, *C* is a second neuron). *White circles, dotted line* Ca^{2+}/Na^+ free external, *black circles, solid line* 145 mM Na^+ external. *D*, MA currents recorded at 35 mV steps (-70 - +70 mV) with a Na^+ based internal solution. *Left*, the external solution contained 145 mM Na^+ and was nominally Ca^{2+} free. *Right*, the extracellular solution: nominally Ca^{2+}/Na^+ free. *E*, IV relationship for neuron in *D, White circles, dotted line* Ca^{2+}/Na^+ free external, *black circles, solid line* 145 mM Na^+ external.

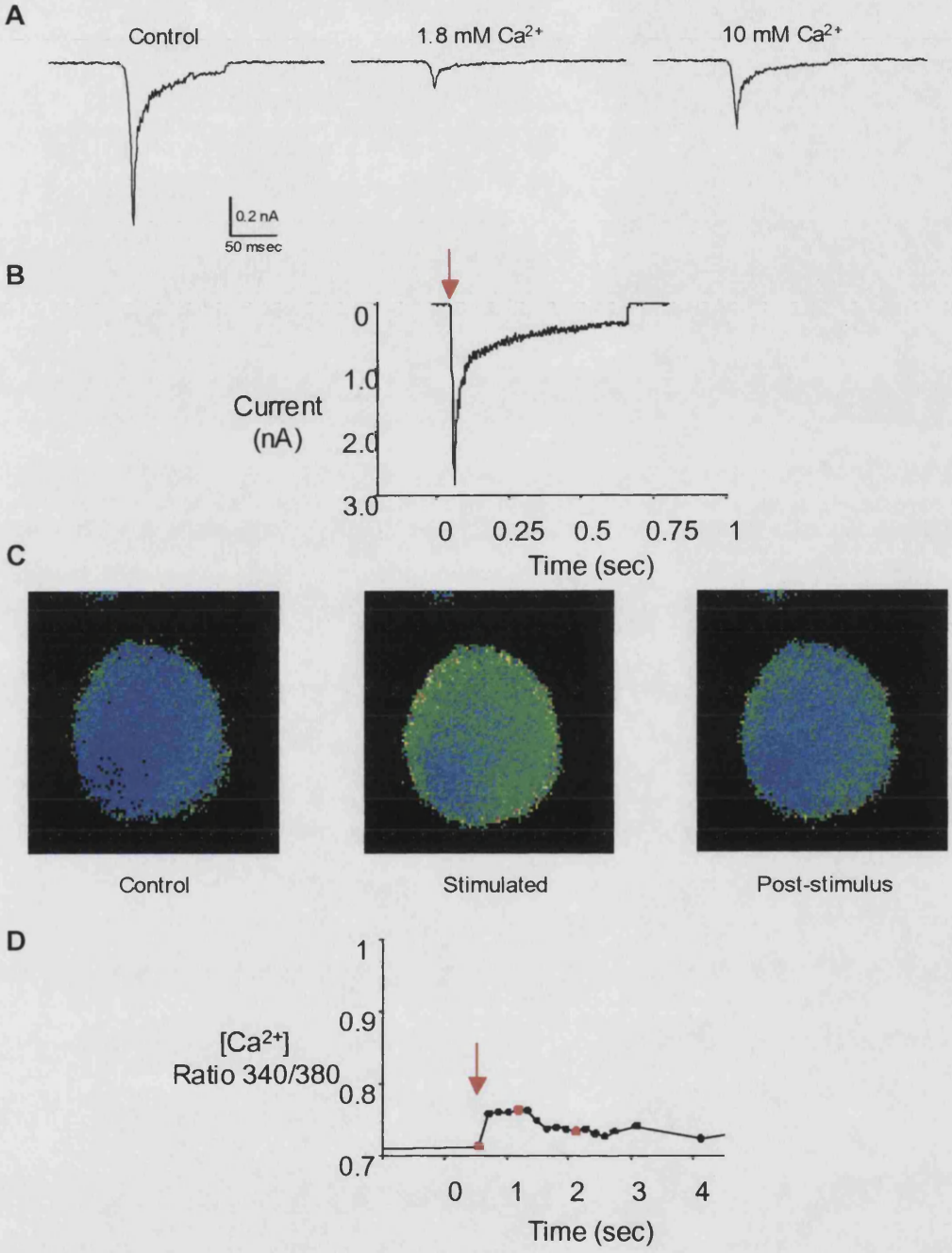

Fig. 3.3 The ion channels underlying MA currents are permeable to Ca^{2+}. *A*, Increasing the external Ca^{2+} concentration in the absence of Na^{+} increases MA current amplitude. *Left*, MA current trace recorded in control external solution (150mM Na^{+}, 1.8 mM Ca^{2+}, 1mM Mg^{2+}, 10 mM HEPES), *centre*, removal of Na^{+} decreases current to 16.5% of control amplitude and, *right*, increasing the Ca^{2+} concentration to 10 mM led to an increase in current amplitude (42.6% of control). *B-D*, Ca^{2+} imaging of a voltage-clamped neuron demonstrates Ca^{2+} entry into the neuron following mechanical stimulation. *B*, MA current. *C*, Ratiometric FURA-2 signal, reflecting intracellular level of Ca^{2+} before, during and after mechanical stimulation (*red arrow*), example images taken from time points as indicated (*red squares*) in *D*, which shows mean FURA-2 ratio for the whole neuron. (Imaging experiment by Paolo Cesare).

using electrophysiology and Ca^{2+} imaging combined, revealed that in voltage-clamped neurons (-70 mV) mechanical stimulation led to an increase in intracellular Ca^{2+} consistent with Ca^{2+} entry through the mechanically gated ion channels (Fig. 3.3b-d).

3.3.2 The Substrate on which Neurons are Grown Affects the Kinetics of MA Currents

Initial experiments were performed on neurons plated solely on poly-*L*-lysine but when neurons were plated on laminin and poly-*L*-lysine we found the adaptation kinetics of MA currents were quite different. To quantify this effect, neurons were plated on poly-*L*-lysine with or without laminin. Unlike currents observed in neurons plated only on poly-*L*-lysine, where the peak current amplitude was seen at the cessation of probe movement (Fig. 3.4a), some neurons plated on laminin displayed currents that increased in amplitude during the stimulus plateau (Fig. 3.4a). To quantify the kinetics of MA currents, current amplitude was measured when the probe stopped moving and then the percentage change in current amplitude 72 msec after this point was calculated. 72 msec was considered the point at which variability amongst currents was greatest. To decrease variability in the cells recorded from, only capsaicin insensitive neurons were compared (slowly adapting currents were not seen in capsaicin sensitive neurons, see below) and for each neuron currents evoked by a 10 μm stimulus were used for further analysis.

All currents generated by neurons plated on poly-*L*-lysine alone exhibited some degree of adaptation; the slowest declined in amplitude by around 30-40% whereas the majority of neurons (60%, 9/15) showed greater than 75% adaptation at 72 msec (Fig. 3.4b). In contrast, when cells were plated with laminin 6 of 16 (38%) of them displayed currents that declined slowly, with less than 20% adaptation at 72 msec. 2 neurons displayed currents that were larger 72 msec into the stationary phase of the stimulus than when the probed stopped moving. 38% (6/16) of neurons had currents that adapted by more than 75% (Fig. 3.4b). Overall, current adaptation was slower in neurons plated on a combination of laminin and Poly-*L*-lysine than on the latter alone ($P < 0.05$, Mann-

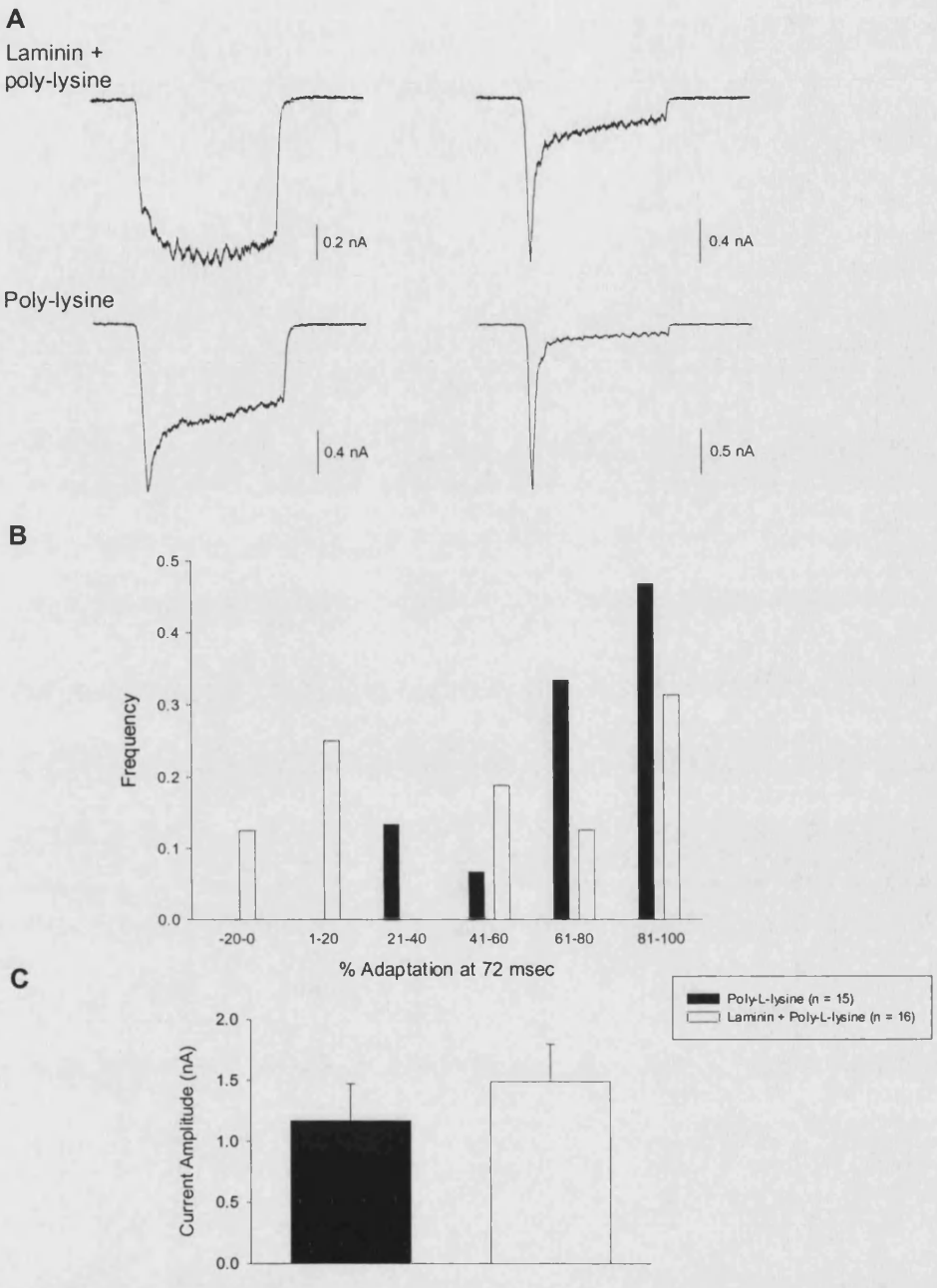

Fig. 3.4 Plating neurons on laminin affects adaptation kinetics of MA currents in capsaicin insensitive neurons. *A*, Example traces for MA currents generated by neurons plated on laminin and poly-*L*-lysine (*top*) or just poly-*L*-lysine (*bottom*). *Right*, rapidly adapting currents, both currents are in the 81-100% adaptation group. *Left*, The cell on laminin (*top*) displays slowly adapting kinetics and is in the –20-0% adaptation category. Current from cell plated without laminin *(bottom*) shows intermediate adaptation, this current was in the 41-60% adaptation group. *B*, Frequency histogram for current adaptation as % reduction in current amplitude at 72 msec after the cessation of probe movement. *Black bars*, neurons plated on poly-*L*-lysine only, *white bars*, neurons plated on poly-*L*-lysine plus laminin. Adaptation kinetics are slower in cells on laminin ($P < 0.05$, Mann-Whitney Rank Sum Test). *C*, Peak current amplitude was unaltered by substrate without laminin 1.17 ± 0.30 nA, with laminin 1.49 ± 0.30 nA ($P = 0.46$, unpaired *t*-test).

Whitney Rank Sum Test). Laminin appeared to affect only the current adaptation kinetics as there was no difference in the peak MA current amplitudes between the two groups (Fig. 3.4c, 1.49 ± 0.30 nA with laminin, 1.17 ± 0.30 nA without laminin, $P = 0.46$, unpaired *t*-test).

In subsequent experiments all neurons were plated on a combination of poly-*L*-lysine and laminin. The time for peak current to decline to half its amplitude of all currents demonstrating less than 30% adaptation at 72 msec was over 200 msec and this criterion (a $t_{0.5}$ of adaptation > 200 msec) was taken as the condition for defining a current as slowly adapting.

3.3.3 Subpopulations of DRG Neurons are Differentially Mechanosensitive

To address the question of whether distinct neuronal subpopulations of the DRG differed in their responses to mechanical stimulation neonatal rat neurons were divided according to size (soma diameter), capsaicin sensitivity, capsaicin sensitivity being indicative of a nociceptive phenotype (Sections 1.1.1.2 and 1.3.2.1) and, amongst smaller neurons, whether they bound IB4.

In medium-large neurons (> ≈29 μm), mechanical stimulation evoked an inward current in 92% (66 of 72) of cells. Of cells that responded the majority (86%, 57 of 66) generated currents that had an initially rapidly adapting (RA) phase that was followed at high stimulation intensities by a sustained component (Fig. 3.5a, *right*). The remaining 14% (9 of 66) of neurons expressed MA currents that were slowly adapting (SA) ($t_{0.5}$ of inactivation > 200 msec) (Fig. 3.5a, *left, bottom*).

Neurons were then divided according to capsaicin (1 μM) sensitivity. A similar number of neurons were mechanically responsive in either group; of those neurons that did not respond to capsaicin (Caps-) 95% (38 of 40) responded to mechanical stimulation and 88% (28 of 32) of capsaicin sensitive (Caps+) neurons responded. However, this division of neurons into presumptive nociceptive and non-nociceptive populations did reveal a

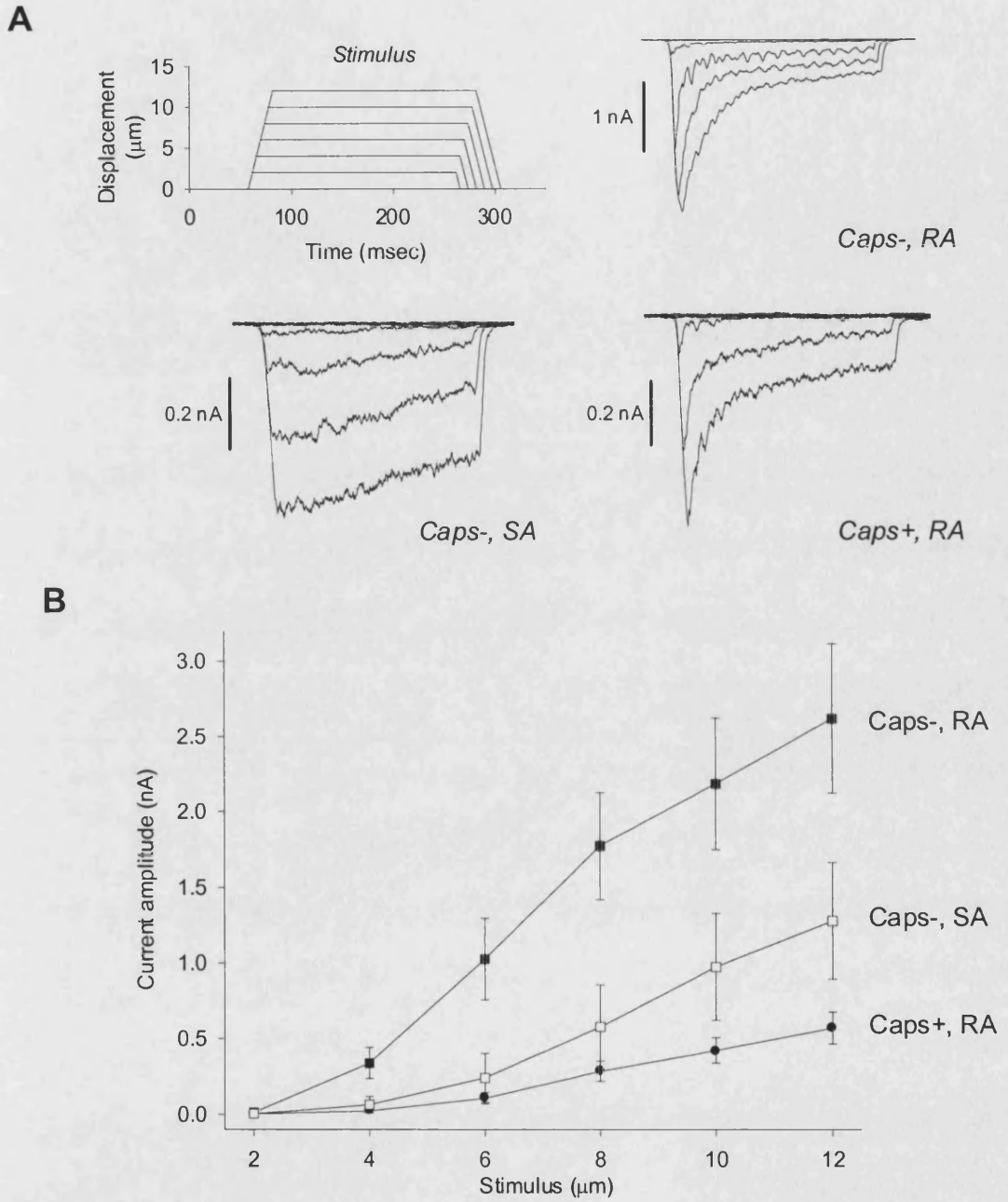

Fig. 3.5 Subpopulations of DRG neurons demonstrate different levels of mechanosensitivity. *A*, representative traces from 3 subpopulations of DRG neurons. *Right panel*, top and bottom traces show RA currents from Caps- and Caps+ neurons, respectively. The *left panel* shows a SA current; note the differences in scale. *B*, The mean amplitude of RA MA currents in Caps- neurons (*black squares*, $n = 31$) was significantly larger than in Caps+ neurons (*black circles*, $n = 32$). MA currents of Caps- neurons with SA responses (*white squares*, $n = 9$) were intermediate (2 way, repeated measures ANOVA, $P = 0.001$).

number of clear differences between groups. Firstly, whereas all neurons that responded to capsaicin exhibited RA currents, capsaicin insensitive neurons displayed either RA (76%, 29/38) or SA (24%, 9/38) currents. Subsequently, neurons that displayed SA currents were considered as a separate population for analysis.

The three groups also showed differing sensitivities to mechanical stimulation (2-way ANOVA, repeated measures, $P < 0.001$) (Fig. 3.5b). The most striking difference was in the amplitude of RA currents between Caps- and Caps+ populations of cells (Fig. 3.5b). In Caps- cells with RA MA currents, currents were consistently much larger than those in the Caps+ population (Fig. 3.5b). The amplitude of SA currents was intermediate between those of RA currents in the capsaicin sensitive and insensitive groups[8]. At the highest level of stimulation the mean amplitudes of MA currents were: Cap-, RA; 2.62 ± 0.50 nA, Caps-, SA; 1.28 ± 0.38 nA and Caps+; 0.57 ± 0.11 nA. All cells that responded to maximal mechanical stimulation with currents over 2 nA were Caps- (16 RA, 2 SA).

It was also seen that at low levels of stimulation significantly more non-nociceptive than nociceptive neurons displayed MA currents. At a 4 μm stimulation 48% (15/31) of Caps- RA neurons responded with currents over 50 pA compared to 13% (4/32) of capsaicin sensitive neurons and 11% (1/9) of neurons with slow kinetics (Fig. 3.6a, Chi-square, $P < 0.05$). Another method for assessing mechanosensitivity was to estimate the threshold of activation for MA currents. To do so the time taken for the holding current to deviate from the baseline after the stimulus had commenced was measured and then knowing the probe velocity the degree of membrane displacement was calculated (Fig. 3.6b). The mean threshold of activation of RA currents in Caps- neurons was 2.7 ± 0.3 μm, this was significantly lower than that for both SA currents (5.0 ± 0.3 μm, $P < 0.001$) and currents in Caps+ neurons (5.4 ± 0.4 μm, $P < 0.0001$, Student's *t*-test) (Fig. 3.6c).

[8] Using peak current as a measure of sensitivity is dependent on the rate at which the neuron is stimulated (see Section 3.3.9), consequently the relative differences shown between populations here is specific to a probe velocity of 0.5 μm/msec.

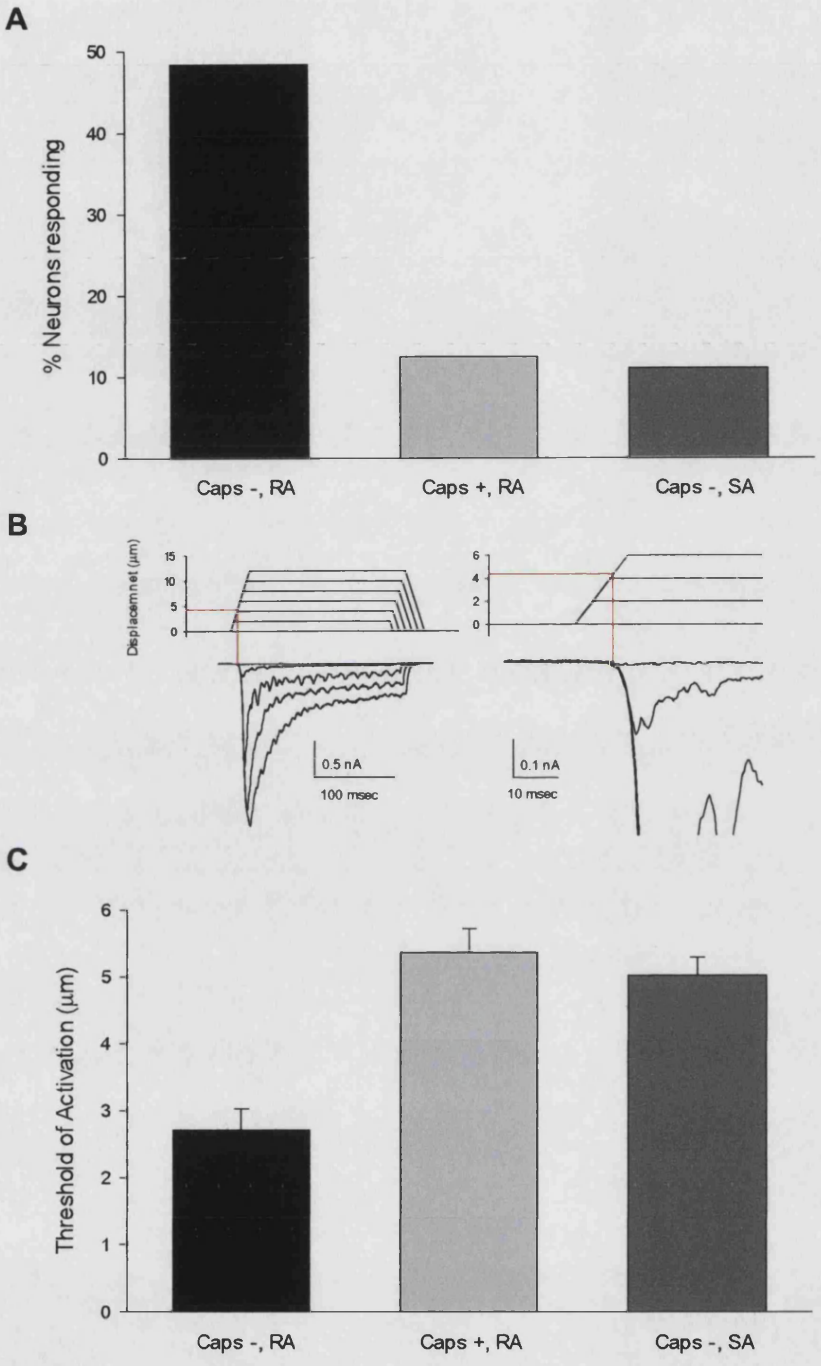

Fig. 3.6 MA currents in different DRG neuronal subpopulations have distinct thresholds of activation. *A*, Histogram showing the percentage of neurons in each population that generate currents of >50 pA in responses to a 4 µm stimulus. Significantly more Cap- neurons with RA currents responded than neurons in the other two populations (χ^2; $P < 0.05$). *B*, Example of how current thresholds were estimated; currents activate at a specific membrane displacement and so by measuring the time at which this occurs the displacement can be extrapolated. *C*, The threshold of activation for MA currents was significantly lower for RA currents in Caps- neurons (2.7 ± 0.3 µm) than for SA currents (5.0 ± 0.3 µm, $P < 0.001$) and currents Caps+ neurons (5.4 ± 0.4 µm, $P < 0.0001$, t-test).

The differences in mechanosensitivity were not attributable to cell size (Fig. 3.7a). Although Caps+ cells (diameter; 31.7 ± 0.6 μm) were significantly smaller than Caps- neurons with either RA (34.4 ± 0.7 μm) or SA (35.5 ± 0.7 μm) MA currents the difference was only 8.0% and 10.8%, respectively (t-test, $P < 0.05$). These small differences are unable to account for the large differences seen in current amplitude. Furthermore, MA current amplitude did not correlate with cell size either overall or within groups. Fig. 3.7b shows the mean somatic diameter of IB4 positive and negative neurons used in the next part of this study and Fig. 3.7c shows an example of fluorescent labelling using IB4 conjugated to Alexa Fluor® 488 .

Subsequently, the mechanically evoked responses of smaller capsaicin sensitive neurons were examined. Cells were further distinguished according to whether they bound IB4 (Fig. 3.8b, c), an isolectin that labels a subpopulation of non-peptidergic nociceptive neurons (see Molliver *et al*, 1997). It was found that the responses of Caps+, IB4- cells did not significantly differ from those of medium sized, Caps+ neurons. However, nociceptive neurons labelled with IB4 showed little or no response to mechanical stimulation (Fig. 3.8a, b). There was large variation in the size of MA currents in Caps+, IB4- cells but all were mechanically sensitive. It was not possible to determine if IB4+ neurons respond to higher levels of mechanical stimulation as stimuli greater than 12 μm are liable to dislodge the cell from the substrate or disrupt the seal. To control for the possibility that IB4 blocks the underlying ion channels mechanical responses were recorded in 6 capsaicin sensitive neurons prior to staining with IB4. Of these, two neurons that were unlabelled responded to a 10 μm mechanical stimulation with currents over 100 pA and to a 12 μm stimulus with currents of 254 pA and 389 pA, respectively. Conversely, of the 4 neurons that were labelled with IB4 2 did not respond to mechanical stimulation and of the other 2 the maximal evoked current was 160pA. Hence, the difference in MA current amplitude is unlikely to be due to IB4 directly interacting with the underlying channels.

There was also a large difference in the amplitude of currents evoked by 1 μM capsaicin between these two populations; IB4+ neurons had a mean current of 0.30 ± 0.04 nA

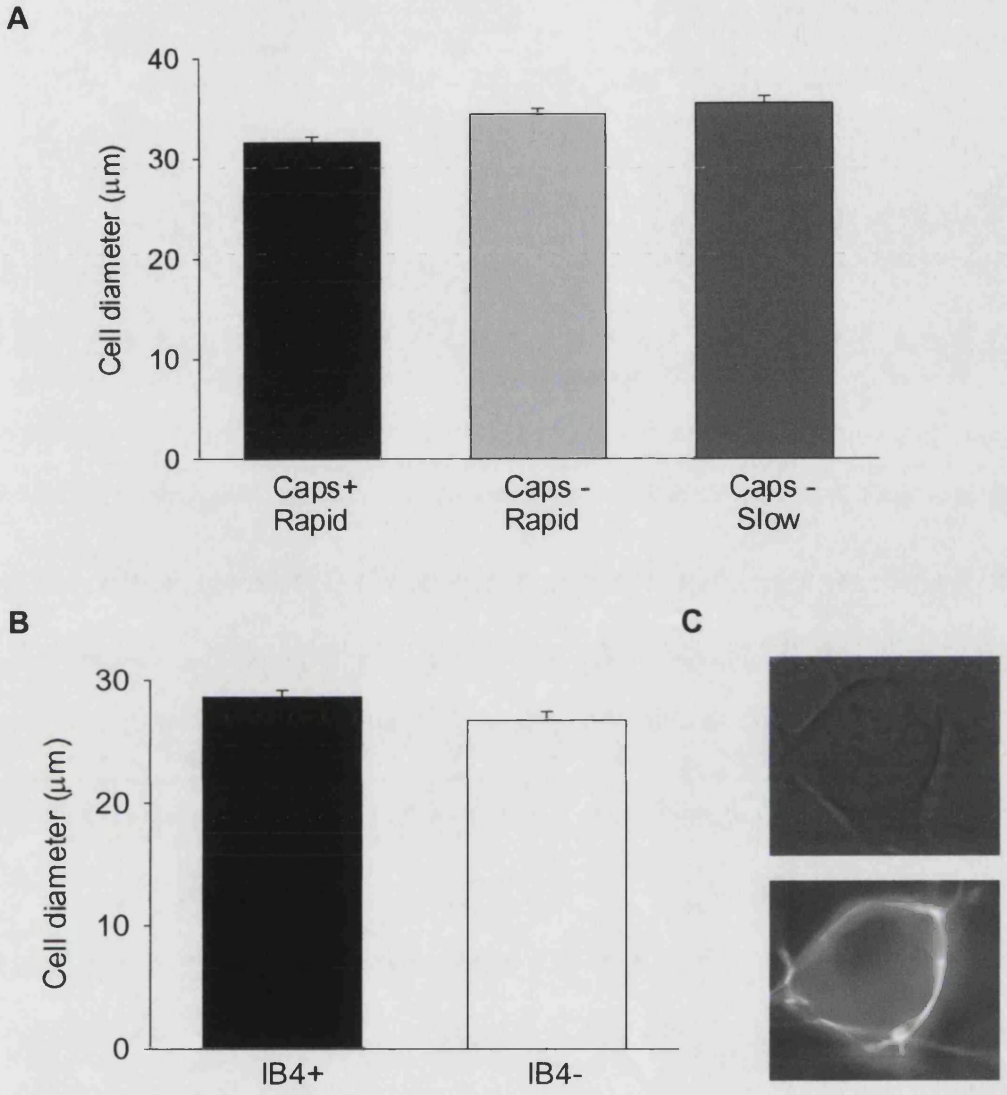

Fig. 3.7 Cell diameters of neurons studied. *A,* Medium-large neurons. Caps+ neurons (*black bar*, diameter; 31.7 ± 0.6 µm) were significantly smaller than Caps- neurons with either SA (*dark grey bar*, 35.5 ± 0.7 µm) or RA (*light grey bar*, 34.4 ± 0.6 µm) MA currents by 10.8% and 8.0%, respectively (t-test, $P < 0.001$and $P = 0.002$, respectively). *B*, Small-medium neurons. There was no significant difference in the diameter of IB4+ (*black bar*, 28.6 ± 0.6 µm) and IB4- (*white bar*, 26.7 ± 0.7 µm) neurons (t-test, $P = 0.053$). *C*, Example of IB4 labelling. T*op*, neuron seen in bright field and *bottom* fluorescent image of the same cell after incubation in IB4-Alexa Fluor® 488 conjugate.

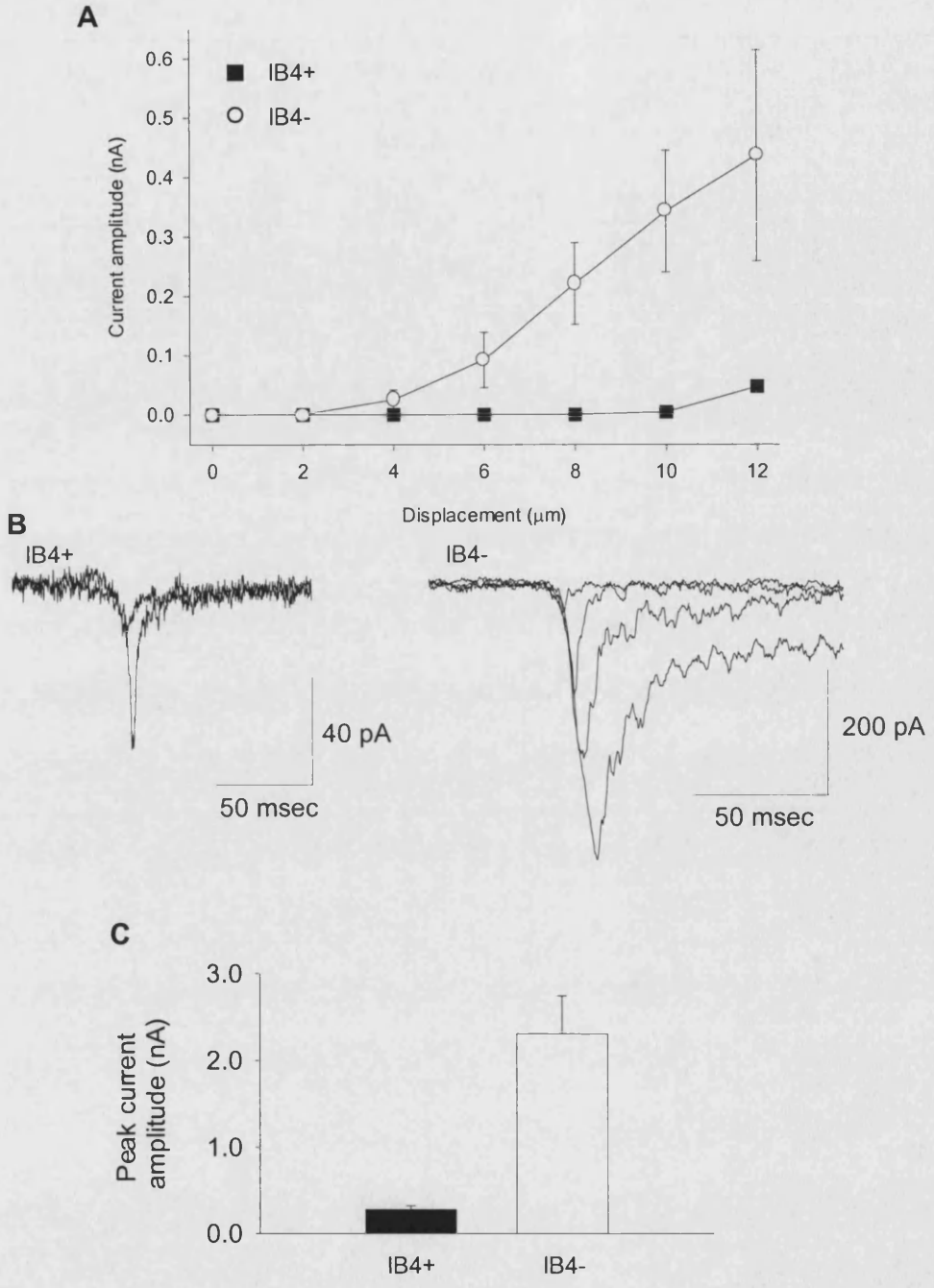

Fig. 3.8 IB4+ and - nociceptors respond differently to mechanical stimulation and capsaicin. *A*, The mean amplitude of MA currents in IB4-, Caps+ neurons (*white circles*, $n = 8$) was significantly larger than those seen in IB4+, Caps+ neurons (*black squares*, $n = 9$) (2 way, repeated measures ANOVA, $P < 0.001$). IB4+, Caps+ neurons were largely refractory to mechanical stimulation whereas the responses seen in IB4-, Caps+ small neurons were similar to those seen in medium sized Caps+ neurons. *B*, Representative traces from an IB4+ and an IB4- cell. *C*, The mean amplitude of responses evoked by 1μM capsaicin was significantly larger in IB4- cells (2.31 ± 0.44 nA, $n = 8$) than in IB4+ cells (0.30 ± 0.04 nA, $n = 9$) (t-test, $P < 0.001$).

whereas IB4- cells had a much larger mean response of 2.31 ± 0.44 nA (t-test, $P < 0.001$) (Fig. 3.8c).

3.3.4 MA Currents are Blocked by Ruthenium Red and Gadolinium

A number of compounds were tested for their ability to inhibit MA currents. As described by Hamill and McBride (1996), gadolinium (Gd^{3+}) (and other lanthanides), aminoglycoside antibiotics and amiloride (and its derivatives) block mechanosensitive ion channels in a range of systems. Therefore, the effects of Gd^{3+}, gentamicin and amiloride on MA currents were investigated. In addition it was determined if ruthenium red and capsazepine inhibited MA currents. Ruthenium red is an antagonist of ryanodine receptors and also broadly inhibits TRPV channels in the low micromolar range (see Gunthorpe *et al*, 2002), whereas capsazepine is a relatively selective antagonist of TRPV1 (Bevan *et al*, 1992). In addition to providing basic pharmacological data on the ion channels underlying MA currents, the identification of antagonists allowed comparison of the pharmacology of the channels mediating currents in different neuronal subpopulations.

Gd^{3+} and ruthenium red both blocked MA currents with IC_{50} values of less than 10 μM; in both cases drug actions were fully reversible. The blockade of RA MA currents by Gd^{3+} (1-100 μM) was very similar in Caps- and Caps+ cells (Fig. 3.9a, b); the derived IC_{50} values were 7.99 μM (Caps+) and 7.77 μM (Caps-). Normalising currents recorded in the presence of Gd^{3+} to the peak of the control current showed that Gd^{3+} did not alter current kinetics (Fig. 3.9c). Inhibition of MA currents by ruthenium red (0.6 – 100 μM) was also similar in all 3 subpopulations of neurons (Fig. 3.10a, b). The IC_{50} values derived for this compound were 2.97 μM (Caps +, RA), 2.71 μM (Caps-, RA) and 3.45 μM (SA). Again, normalisation of currents evoked in the presence of ruthenium red to control values showed this compound also did not affect the kinetics of MA currents (Fig. 3.10c).

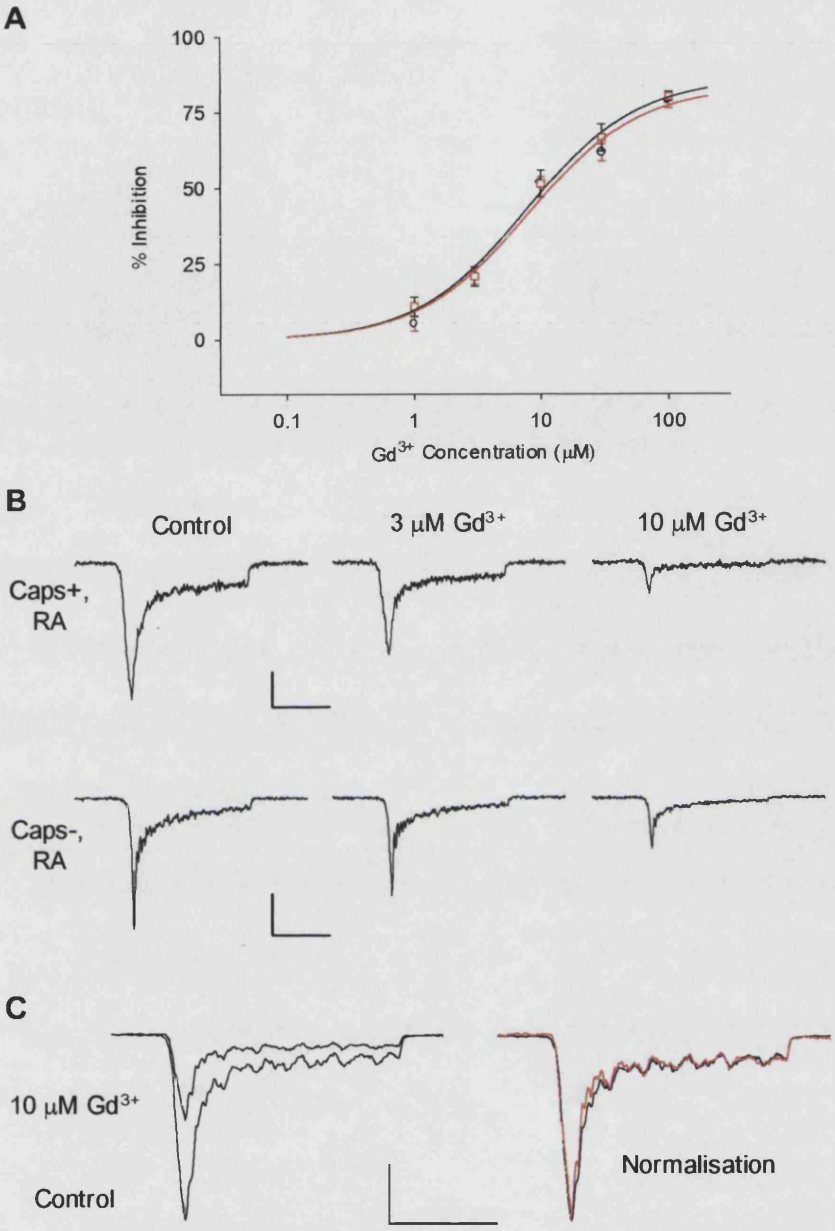

Fig. 3.9 Gd^{3+} inhibits RA MA currents equally in capsaicin sensitive and insensitive neurons. *A*, Concen-tration-inhibition curves for the blockade of RA in Caps+ (*red*) and Caps- (*black*) neurons by Gd^{3+} (1-100 μM). Activity in either group is indistinguishable. The derived IC_{50} values were 7.99 μM (Caps+) and 7.77 μM (Caps-). n = 3-6 for each data point. *B*, Examples of blockade of MA currents in a Caps+ neuron (*top*) and a Caps- neuron (*bottom*) by 3 μM (*centre*) and 10 μM (*right*) Gd^{3+}. *C*, Normalisation (*right*) of a current recorded in the presence of 10 μM Gd^{3+} (*left*) to peak control current amplitude. In all cases the vertical scale bar represents 0.2 nA and the horizontal bar indicates 50 msec.

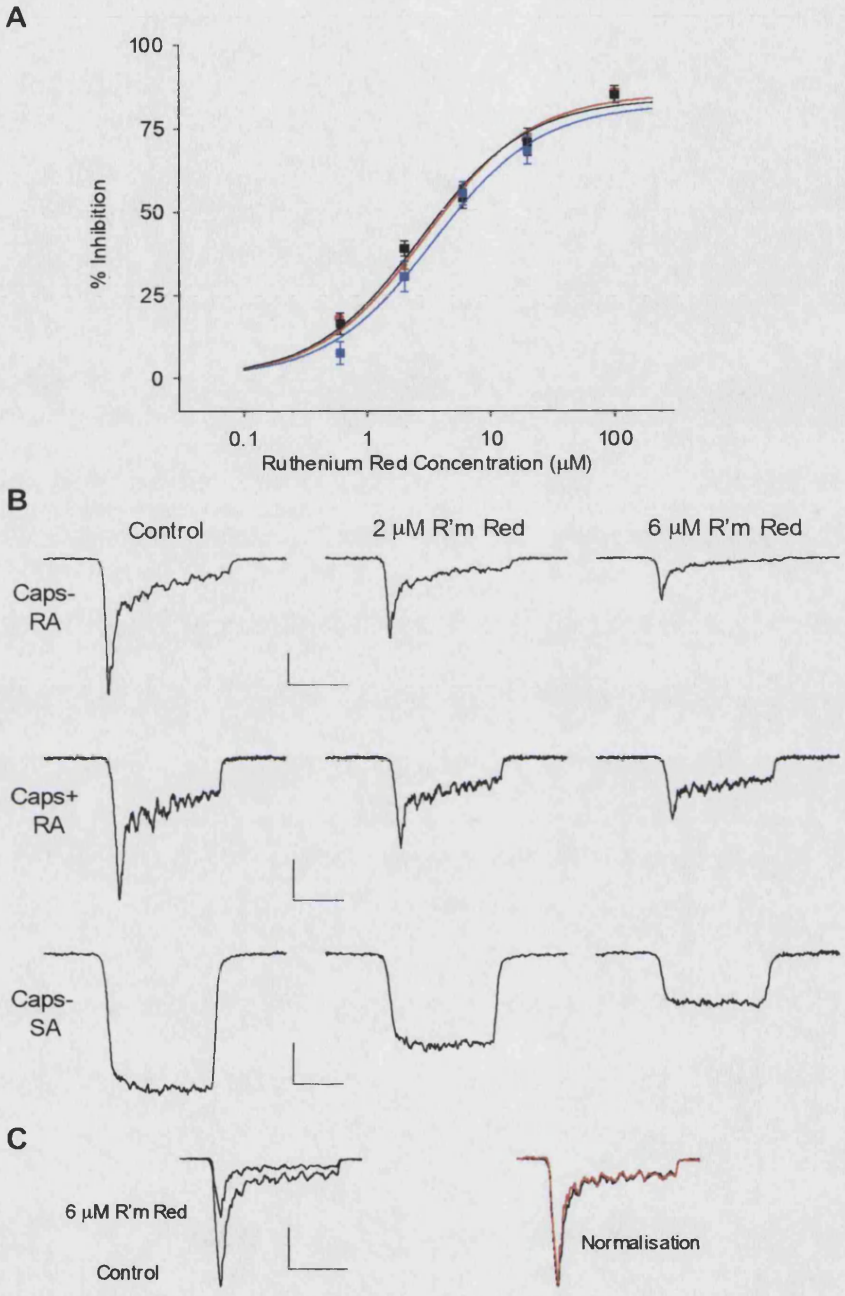

Fig. 3.10 Ruthenium red inhibits MA currents. *A*, Concentration-inhibition curves for the effect of ruthenium red (0.6-100 μM) on RA currents in Caps+ (*red*) and Caps- (*black*) neurons and SA currents (*blue*). Derived IC_{50} values were 2.97 μM (Caps+, RA), 2.71 μM (Caps-, RA) and 3.45 μM (SA). n = 2-7 for each data point. *B*, Example traces of ruthenium red inhibition of RA currents in Caps- (*top*) and Caps+ (*middle*) neurons and SA currents (*bottom*) at 2μM *(centre*) and 6 μM *(right*). *C*, Inhibition of RA (Caps- neuron) by 6 μM (left) and blocked current normalised to peak current. In all cases the vertical scale bar represents 0.2 nA and the horizontal bar indicates 50 msec.

Gentamicin and amiloride were also tested for their ability to inhibit MA currents. At 20 μM gentamicin had no effect; MA currents were 91.0 ± 9.8% of control values (P = 0.453, n = 3). However, at 100 μM gentamicin significantly blocked currents (P = <0.001, n = 10) although the effect was small with currents being inhibited by 16.7 ± 2.9% (Fig. 3.11a,b). In contrast amiloride, up to 500μM, did not significantly affect MA currents. In the presence of 100 μM amiloride peak current amplitude was 99.2 ± 8.5% (P = 0.629, n = 8) of control values whereas in 500 μM currents were 89.4 ± 5.7% (P = 0.245 , n = 5) of control amplitude (Fig. 3.11c,d).

Capsazepine inhibited MA currents at higher concentrations; at 50 μM currents were inhibited by 79.3 ± 3.7% (n = 4) and the IC_{50} of this compound was estimated to be around 25 μM (Fig. 3.12). Of the four neurons tested 2 were Caps+ and 2 Caps- (all currents were RA), there was no apparent difference in the potency of capsazepine between the 2 cell types.

3.3.5 MA Currents are Modulated by Extracellular Ca^{2+} and Zn^{2+}

Having determined that the mechanosensitive ion channels underlying MA currents in DRG neurons are non-selective cation channels (Section 3.3.1), a number of experiments were performed in which the external ion concentrations were manipulated to determine if MA currents in different neuronal subpopulations were similarly sensitive to changes.

Replacement of external Na^+ with the impermeant cation NMG led to a large reduction in the amplitude of RA currents in capsaicin sensitive and insensitive neurons (Fig. 3.13a,b). However, there was a significantly larger reduction in the amplitude of currents in Caps+ cells (currents decreased by 80.3 ± 0.9%) than in Caps- cells (68.3 ± 5.1%) (t-test, P < 0.05). It was apparent in some neurons that following the removal of Na^+ MA current activated significantly earlier than in control solution, i.e. at a lower level of mechanical displacement. This effect was quantified by extrapolating the threshold of activation from the point at which the current deviated from the baseline current (see Section 3.3.3,

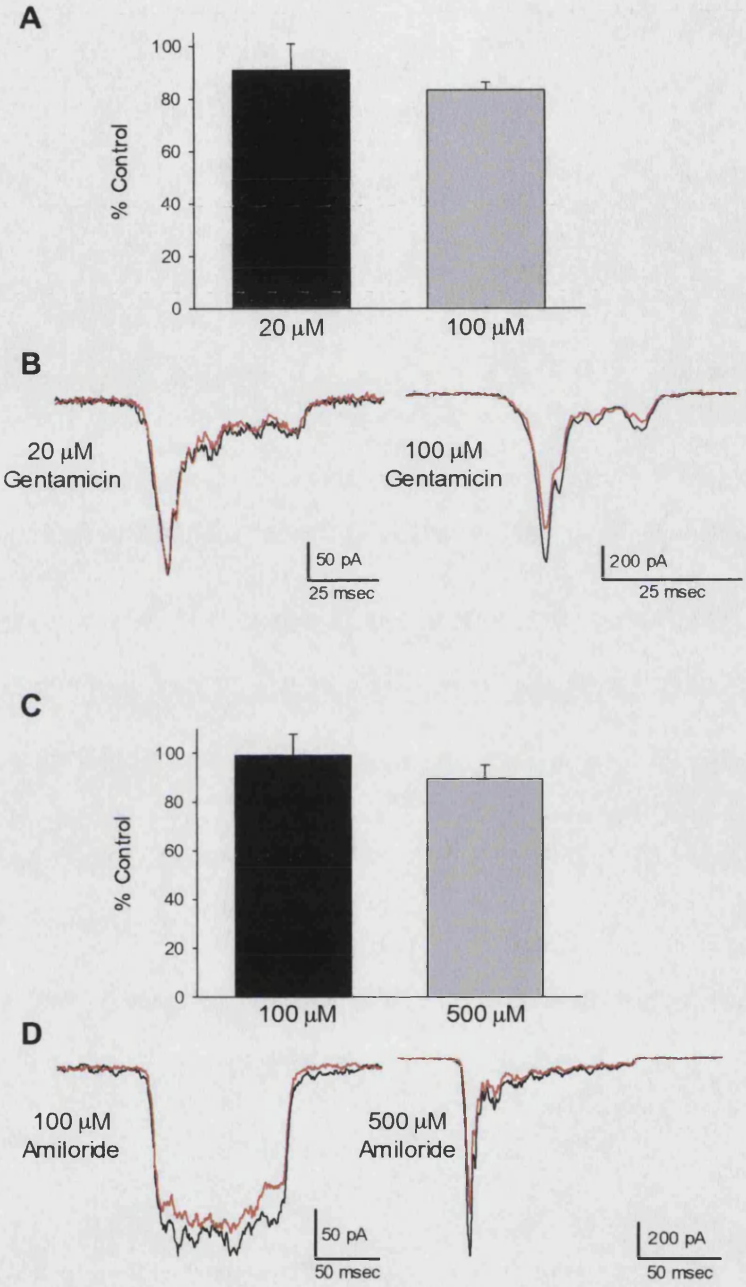

Fig. 3.11 Effect of gentamicin and amiloride on DRG MA currents. *A*, At 20 μM gentamicin had no effect on MA currents (91.0 ± 9.8% of control, $P = 0.453$, $n = 3$) whereas at 100 μM it significantly blocked currents ($P = <0.001$, $n = 10$) although the effect was small; currents were 83.3 ± 2.9% of control values. *B*, Example traces of control (*black*) and currents recorded in the presence of 20 μM (*left*) and 100 μM (*right*) gentamicin (*red*). C, Amiloride at 100 μM and 500 μM did not significantly affect MA currents. In 100 μM amiloride currents were 99.2 ± 8.5% ($P = 0.629$, $n = 8$) of control amplitude and in 500 μM currents were 89.4 ± 5.7% ($P = 0.245$, $n = 5$) of control amplitude. *D*, Example traces of control (*black*) and currents recorded in the presence of 100 μM (*left*) and 500 μM (*right*) amiloride (*red*).

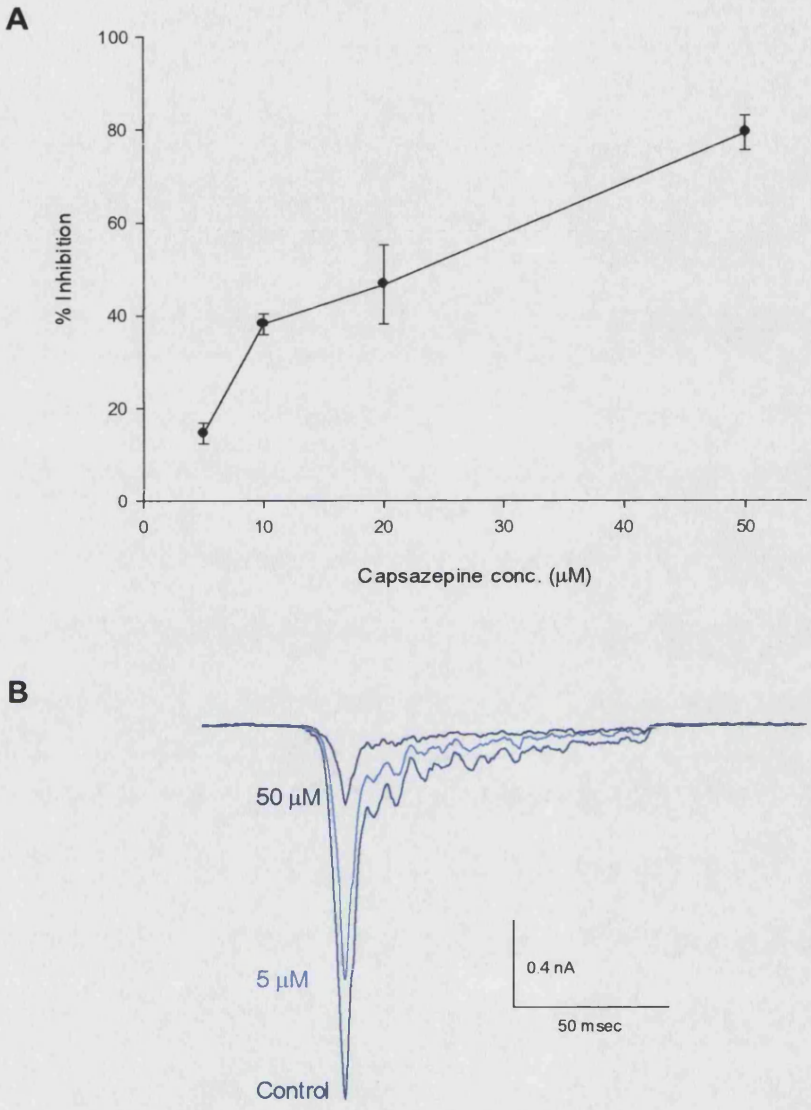

Fig. 3.12 High concentrations of capsazepine inhibit MA currents. *A*, Concentration-inhibition curve for capsazepine (5-50 μM) (n = 3-4 for each data point, data pooled from 2 Caps+ and 2 Caps– neurons; there was no apparent difference in drug efficacy between these cell types). Currents were inhibited by 79.3 ± 3.7% at 50 μM and the concentration producing 50% inhibition is estimated to be around 25 μM. *B*, Example traces of MA currents from a Caps- neuron showing the effect of 5 μM and 50 μM capsazepine.

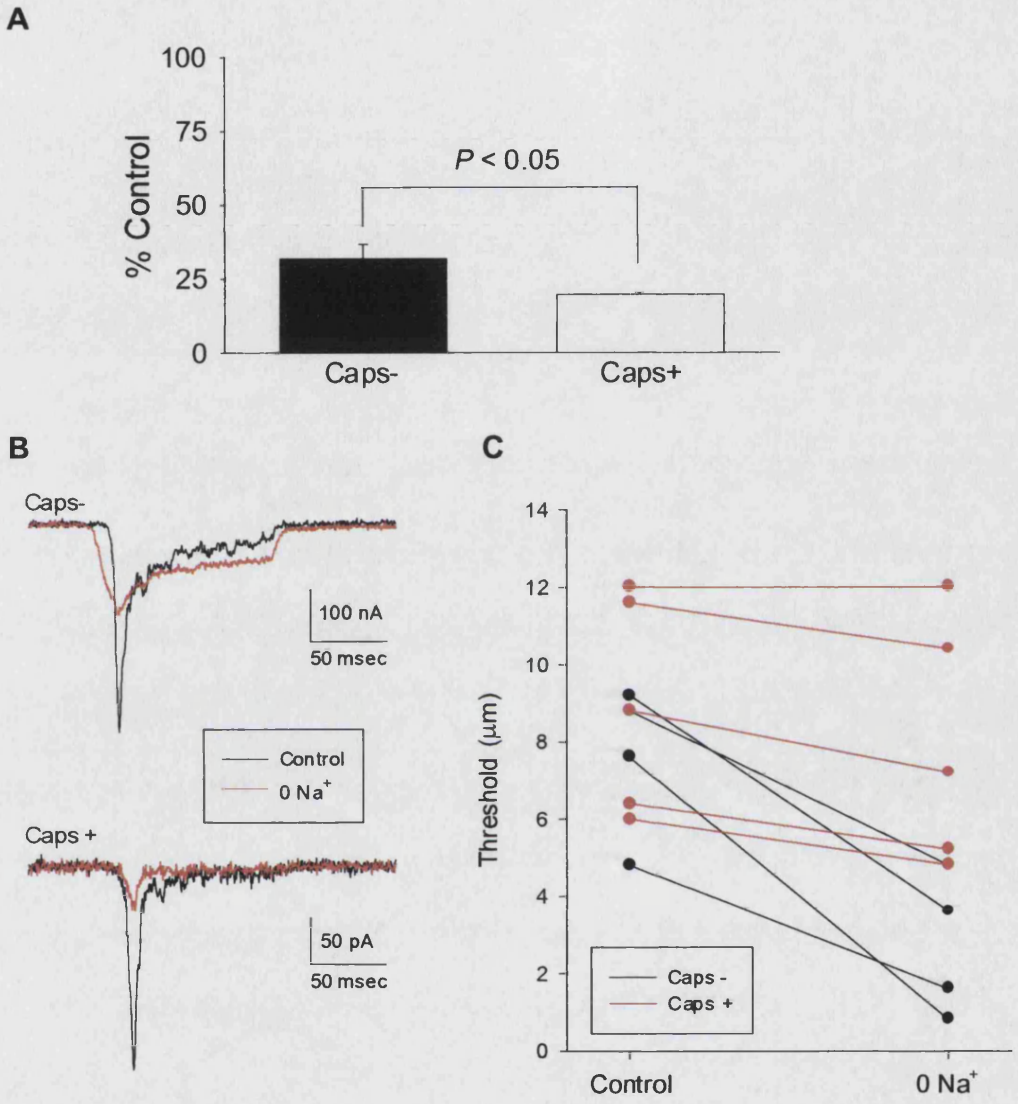

Fig. 3.13 The effect on MA currents of removing Na^+ from the external solution. *A*, Removal of Na^+ from the standard external solution (replaced with NMG^+) caused a reduction in MA currents of 80.3 ± 0.9% and 68.3 ± 5.1% in Caps+ (*white bar*, $n = 5$) and Caps- (*black bar*, $n = 5$) neurons, respectively. *B*, Example traces from a Caps+ (*top*) and Caps- (*bottom*) neuron, *black* traces were recorded in control solution and *red* traces in 0 Na^+. *C*, Shift in MA current threshold following Na^+ removal; lines in *black* from Caps- neurons and in *red* from Caps+ neurons. There is a significant reduction in threshold in Caps- (paired t-test, $P = 0.003$) but not in Caps+ ($P = 0.125$). NB. There are two black lines superimposed running from 4.8 – 1.6 μm.

Fig. 3.6b) and comparing Caps- and Caps+ neurons (Fig. 3.13c). Thresholds of activation fell significantly in Caps- neurons, on average by 4.5 μm (7.0 ± 1.0 to 2.5 ± 0.7 μm, $n = 5$, $P = 0.003$). Conversely, although there was a trend towards a small decrease in threshold in Caps+ neurons the effect was not significant (9.0 ± 1.3 to 7.9 ± 1.4 μm, $n = 5$, $P = 0.125$).

Manipulation of the external Ca^{2+} concentration revealed that this ion has an inhibitory effect on MA current amplitude (Fig. 3.14a, b). Moreover, this effect was significantly more pronounced in Caps- neurons than in Caps+ neurons (2-way ANOVA, $P < 0.05$). In nominally Ca^{2+} free external solution (containing no Ca^{2+} chelator) current amplitude increased, relative to 2 mM Ca^{2+}, by 80.1 ± 11.5% in Caps- neurons and by 32.8 ± 6.1% in Caps+ cells. Consistent with an effective blocking action of Ca^{2+}, increasing its concentration to 5 mM led to a reduction in current amplitude of 78.0 ± 6.6% and 38.3 ± 6.6% in Caps- and Caps+ cells respectively (Fig. 3.14a, b).

Interestingly, an opposite effect on MA current amplitude was observed when a Ca^{2+} free solution containing the divalent cation chelator EGTA (5 mM, Mg^{2+} raised to 1.6 mM) was used. Selectively in Caps- neurons, removal of Ca^{2+} and inclusion of EGTA led to a decrease in current amplitude whereas in Cap+ neurons currents were unchanged from control values. In Caps- neurons, RA and SA currents were reduced by 83.2 ± 8.3% ($n = 4$, paired t-test, $P = 0.002$) and 62.1 ± 6.9% ($n = 3$, $P = 0.01$), respectively, whereas RA currents in Caps+ neurons were 8.5 ± 11.8% ($n = 6$, $P = 0.51$) below control values (Fig. 3.14c, d). The reduction in current amplitude was not accompanied by any effect on current kinetics.

The divalent cation Zn^{2+} also inhibited MA currents and this effect was voltage dependent (Fig. 3.15). When the membrane potential was held at -70 mV, inward MA currents were reduced by 76.8 ± 8.7% ($n = 3$) in the presence of 200 μM extracellular Zn^{2+}; conversely, at a holding potential of +70 mV, outward MA currents were inhibited

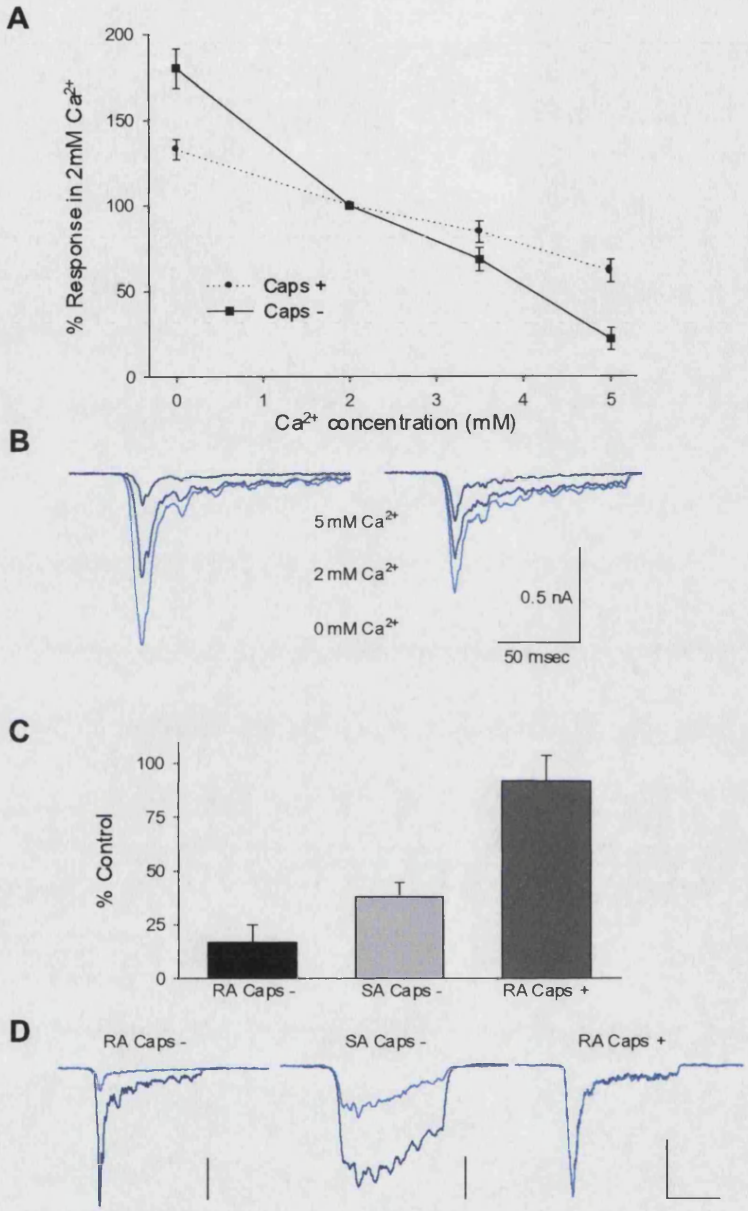

Fig. 3.14 External Ca^{2+} had a modulatory effect on MA current amplitude. *A*, The amplitude of MA currents was largest in nominally Ca^{2+} free solution (no divalent cation chelator) and increasing external Ca^{2+} concentration inhibited MA currents. The effect of Ca^{2+} was significantly greater in Caps- neurons than in Caps+ neurons (2-way ANOVA, $P < 0.01$) (n = 3-8 for each data point). *B*, Representative traces from a Caps- (*left panel*) and Caps+ (*right panel*) neuron showing MA currents evoked in nominally 0, 2 and 5 mM Ca^{2+}. *C*, Recording MA currents in a Ca^{2+} containing 5 mM EGTA selectively reduced current amplitudes in Caps- neurons; RA and SA currents were reduced by 83.2 ± 8.3% (n = 4, paired t-test, P = 0.002) and 62.1 ± 6.9% (n = 3, P = 0.01), respectively. Currents in Caps+ neurons were not significantly affected; 91.5 ± 11.8% (n = 6). *D*, Example traces of currents recorded in 0 Ca^{2+}/EGTA (*light blue*) versus control solutions (*dark blue*), vertical scale bars: 0.1nA, horizontal bar: 50 msec.

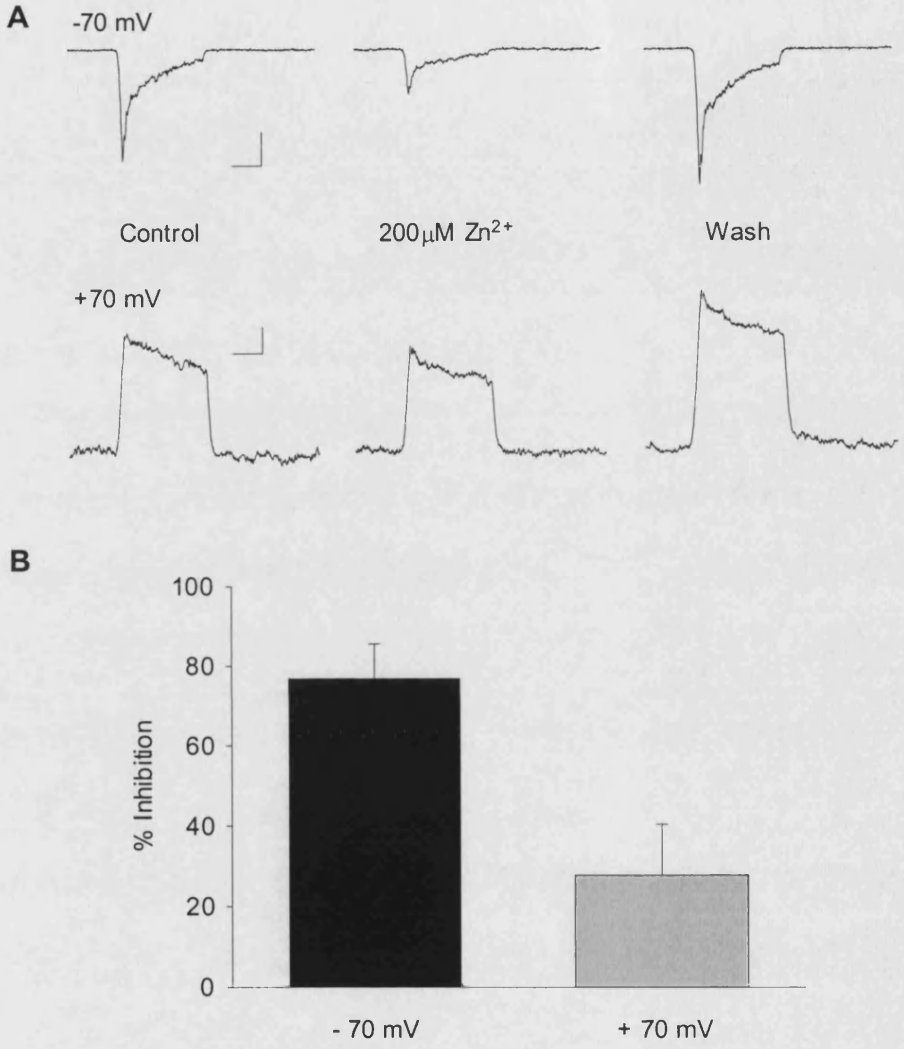

Fig. 3.15 Extracellular zinc voltage-dependently inhibits MA currents. *A*, Example traces of the effect of 200 μM Zn^{2+} on MA currents recorded at a membrane potential of either –70 mV (*top*) or +70 mV (*bottom*). Vertical scale bar; 0.2 nA, horizontal; 50 msec. *B*, The inhibitory action of Zn^{2+} was significantly greater at –70 mV (76.8 ± 8.7 % inhibition, $n = 3$) than at +70 mV (27.8 ± 12.6 %, $P < 0.05$, $n = 3$).

by only 27.8 ± 12.6% (n = 3). Hence, the blocking effect of Zn^{2+} is greater at negative membrane potentials (t-test, $P < 0.05$).

3.3.6 Cytochalasin B Inhibits MA Currents

The role of the actin cytoskeleton in the activation of mechanically evoked currents was examined by investigating the effects of cytochalasin B on MA currents; cytochalasin B is a fungal alkaloid that disrupts the actin cytoskeleton by inhibiting actin polymerisation. To investigate its effects, neurons were either cultured overnight in the presence of 100 nM of the compound (experiments performed by Paolo Cesare) or 10 μM was applied acutely to neurons whilst recording MA currents from them. It was found that neurons cultured in cytochalasin B were essentially unresponsive to mechanical stimulation whereas control neurons (neurons from the same preparation cultured as normal) all displayed MA currents (Fig. 3.16a) (Experiments were conducted without categorising neurons as capsaicin sensitive/insensitive). As a control it was found that voltage-gated currents were not significantly different between neurons cultured with or without cytochalasin (Paolo Cesare, personal communication).

Acute application of cytochalasin B (10 μM) also significantly inhibited MA currents. RA currents in both Caps+ and Caps- neurons were reduced below control levels, however, the effect of cytochalasin B was much greater in Caps- neurons ($P < 0.001$, t-test): MA currents were inhibited in Caps+ neurons by 19.5 ± 4.5% (n = 6, t-test, $P < 0.05$) but in Caps- neurons the level of reduction was 60.9 ± 4.7% (n = 6, $P < 0.001$) (Fig. 3.16b). Acute cytochalasin B changed neither the kinetics nor the threshold of activation of MA currents (Fig. 3.16c).

Acute application of colchicine (500 μM) did not have consistent effects on MA currents (n = 12, data not shown). On some occasions application of colchicine had no apparent effect on MA currents whereas sometimes it appeared to induce a gradual run-down of the current. Given the toxicity of colchicine, these data are difficult to interpret and

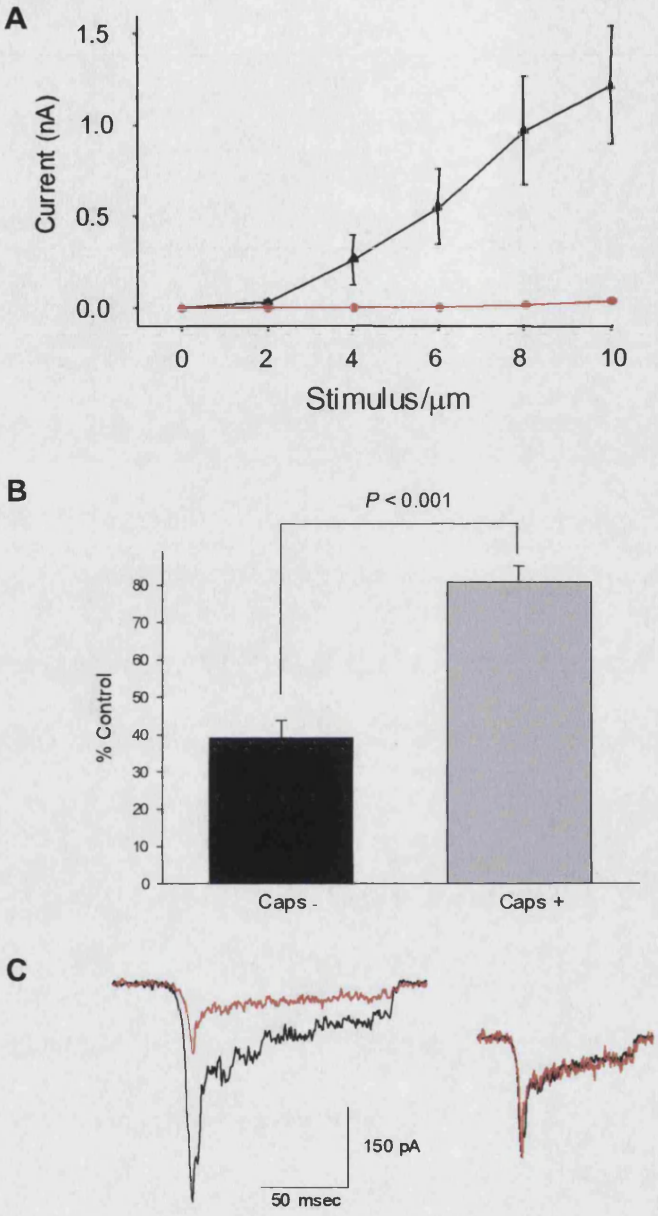

Fig. 3.16 Cytochalasin B had an inhibitory effect on MA currents. *A*, Culturing neurons overnight in 100 nM cytochalasin B leads to a severe reduction in mechanosensitivity. Neurons grown in cytochalasin B (n = 8, *red line*) had no or very small responses to mechanical stimulation, whereas control neurons from the same preparation (n = 8) all displayed MA currents (experiment by Paolo Cesare). *B*, Acute cytochalasin B (10 µM) had an inhibitory effect on MA currents that was more pronounced in Caps- neurons. In Caps- neurons (*black bar*) MA currents were inhibited by 60.9 ± 4.7% (n = 6) (significantly less than control, $P < 0.001$) and by 19.5 ± 4.5% in Caps+ cells (*white bar*, significantly less than control, $P < 0.05$, n = 6). Comparison of the drug effect in the two groups showed that the effect of cytochalasin B was significantly greater in the Caps- neurons ($P < 0.001$). *C, Left,* typical trace of inhibition by cytochalasin B (*red line*, control: *black)* in a Caps- neuron. *Right*, normalisation of current amplitude to peak control current amplitude.

provide inconclusive evidence of a role for microtubules in mechanosensitive channel gating in this preparation.

3.3.7 FM1-43 is a Permeant Blocker of DRG Mechanosensitive Ion Channels

Gale *et al* (2001) demonstrated that FM1-43 acts as a permeant blocker of the mechanotransduction channel in cochlear hair cells. Therefore, it was investigated if it had a similar action on mechanically gated ion channels in DRG neurons. MA currents were recorded in the presence of extracellular FM1-43 at range of concentrations from 0.6 to 15.0 μM. FM1-43 blocked MA currents with both RA and SA kinetics in Caps- and Caps+ neurons. The effect was relatively similar on all three classes of currents (Fig. 3.17a, b) although overall the inhibitory effect was greater on SA currents than either RA population (2-way ANOVA, $P < 0.001$). From the concentration-inhibition plots it can be estimated that 50% inhibition is achieved at around 3 μM for SA currents and around 5 μM for RA currents in Caps- and Caps+ neurons. Interestingly, the level of inhibition observed following FM1-43 application was not constant in neurons exhibiting SA currents; maximal inhibition was observed at the first stimulus applied in FM1-43 and subsequent stimuli evoked larger responses (Fig. 3.17c, 1^{st} vs 2^{nd} MA current, 2 way ANOVA, $P < 0.001$), subsequent responses remained constant (data not shown). There was a similar trend for RA currents in Caps- neurons although it was not statistically significant ($P = 0.1$) whereas MA currents evoked in FM1-43 remained constant in Caps+ neurons.

As FM1-43 is a fluorescent dye, permeation through an ion channel can be visualised as labelling of the cytoplasm. Fluorescent labelling of the neuronal cytoplasm was therefore assessed in neurons before and after mechanical stimulation in the presence of 5 μM FM1-43. Consistent with permeation through the mechanically gated channel, application of 10 mechanical stimuli resulted in a clear labelling of the neuronal cytoplasm in 4 neurons tested (see Fig. 3.17d).

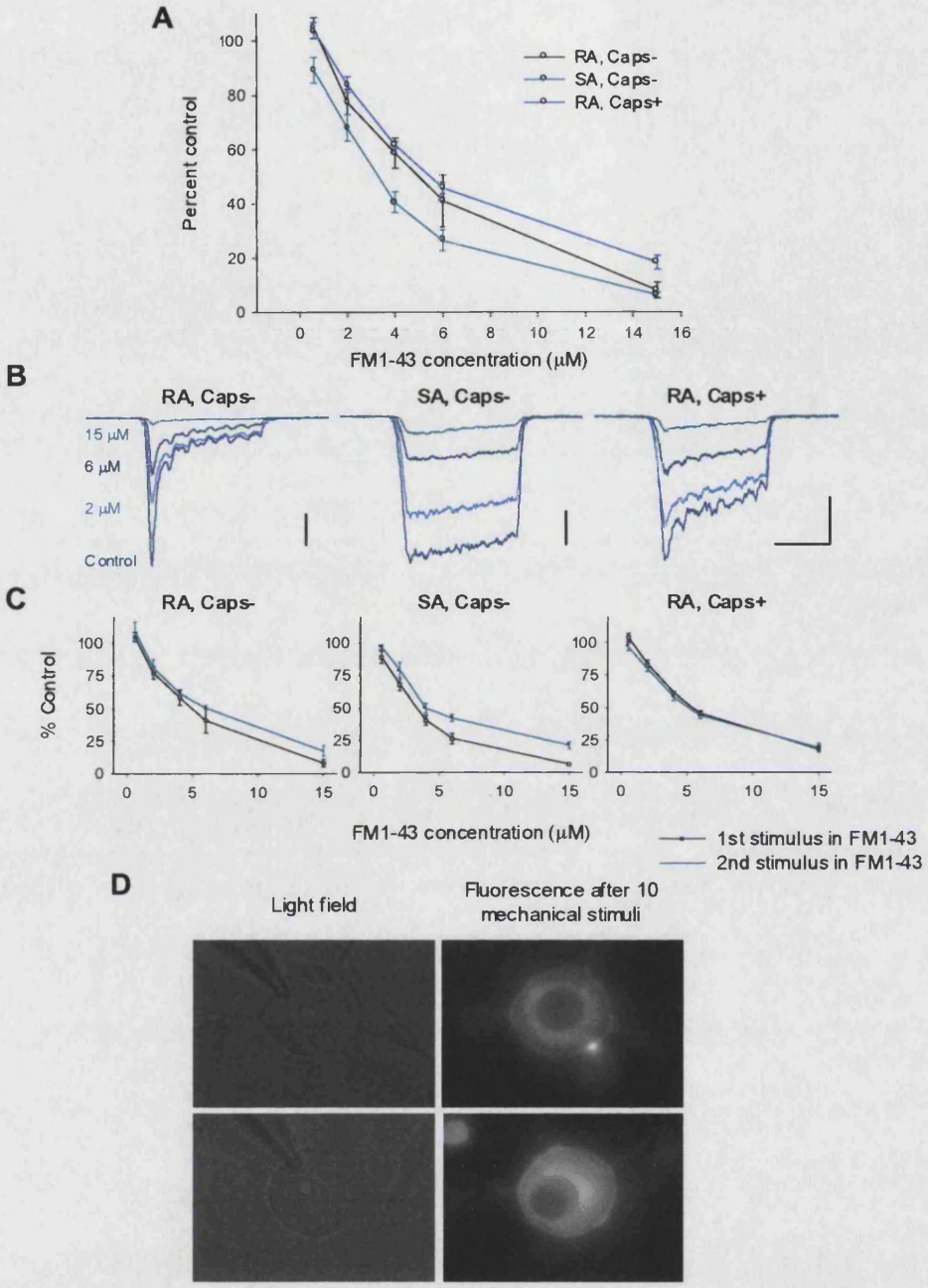

Fig. 3.17 FM1-43 is a permeant blocker of the ion channels underlying MA currents. *A*, Concentration-inhibition functions for FM1-43 (0.6-15 μM). Inhibition of RA currents in Caps- (n = 5) and Caps+ (n = 10) neurons and for SA currents (n = 6) (n = 3-10 for each data point, level of inhibition taken as the maximal change in current amplitude following FM1-43 application; see *C*). FM1-43 more potently inhibited SA currents than either population of RA currents (2-way ANOVA, $P < 0.001$). *B*, Example traces showing effect of 2, 6 and 15 μM FM1-43 on MA currents. *C*, Comparison of current amplitude evoked by 1st and 2nd mechanical stimuli following FM1-43 application. For SA currents, the second stimulus in FM1-43 evoked a larger current than the first (2-way ANOVA, $P < 0.001$). There was a similar (but not statistically significant) trend amongst RA, Caps- responses ($P = 0.1$) but no change in currents evoked in Caps+ neurons. *D*, Mechanical stimulation leads to an uptake of FM1-43 and thus fluorescent labelling of the neuronal cytoplasm. Two examples of labelling after 10 mechanical stimuli applied in the presence of 5 μM FM1-43.

Meyers *et al* (2003) showed that subcutaneous delivery of AM1-43 (a fixable analogue of FM1-43) resulted in labelling of all DRG neurons' cell bodies via uptake at the peripheral terminal. It was also shown that FM1-43 was taken up via stimulated $P2X_2$ and TRPV1 receptors, which could account for labelling of nociceptive neurons although these receptors are not expressed by large DRG neurons that are mainly low threshold mechanoreceptors. To test possible entry routes of FM1-43 into neurons it was determined if the dye was taken up passively by neurons or if it acted as a blocker of ASIC-mediated proton-gated currents or voltage-activated currents, and if there was labelling of neurons following activation of these currents. Perfusion of the neuron in 5 μM FM1-43 without stimulation produced a non-specific labelling of the membrane without uptake into the interior of the cell (Fig3.18a). Transient proton-gated currents (evoked by pH 5.4 external solution) were essentially unaffected by 5 μM FM1-43; their amplitudes were very slightly increased (peak amplitude was 107.3 ± 3.1% of control in 5 μM FM1-43, $n = 6$, $P = 0.07$) (Fig. 3.18b). In 3 neurons tested, there was no significant labelling of the cytoplasm following 6 stimulations with low pH (Fig 3.18c). Likewise, when two families of voltage-steps (14 steps in 10 mV increments from -70 mV to +70 mV) were applied to 2 neurons perfused in 5μM FM1-43 no subsequent labelling of the cytoplasm was detected (Fig. 3.18d). There was a slight decrease in the maximum inward current evoked in both neurons (10.3 nA to 9.4 nA and 15.0 nA to 14.2 nA, $P = 0.04$, data not shown). In one neuron a significant blocking effect of FM1-43 on capsaicin-evoked currents was observed (data not shown).

3.3.8 Arachidonic Acid Inhibits MA Currents

Arachidonic acid affects the behaviour of numerous ion channels (Meves, 1994). Also it can modulate the mechanical properties of cell membranes; due to its shape when this lipophilic compound inserts into the membrane it mimics the effect of membrane stretch (see Casado and Ascher, 1998). Consequently, the effect of arachidonic acid on MA currents was investigated. It was found that arachidonic acid had an inhibitory effect on these currents, at 10 μM peak current amplitude was reduced by 52.4 ± 7.2% and at 50

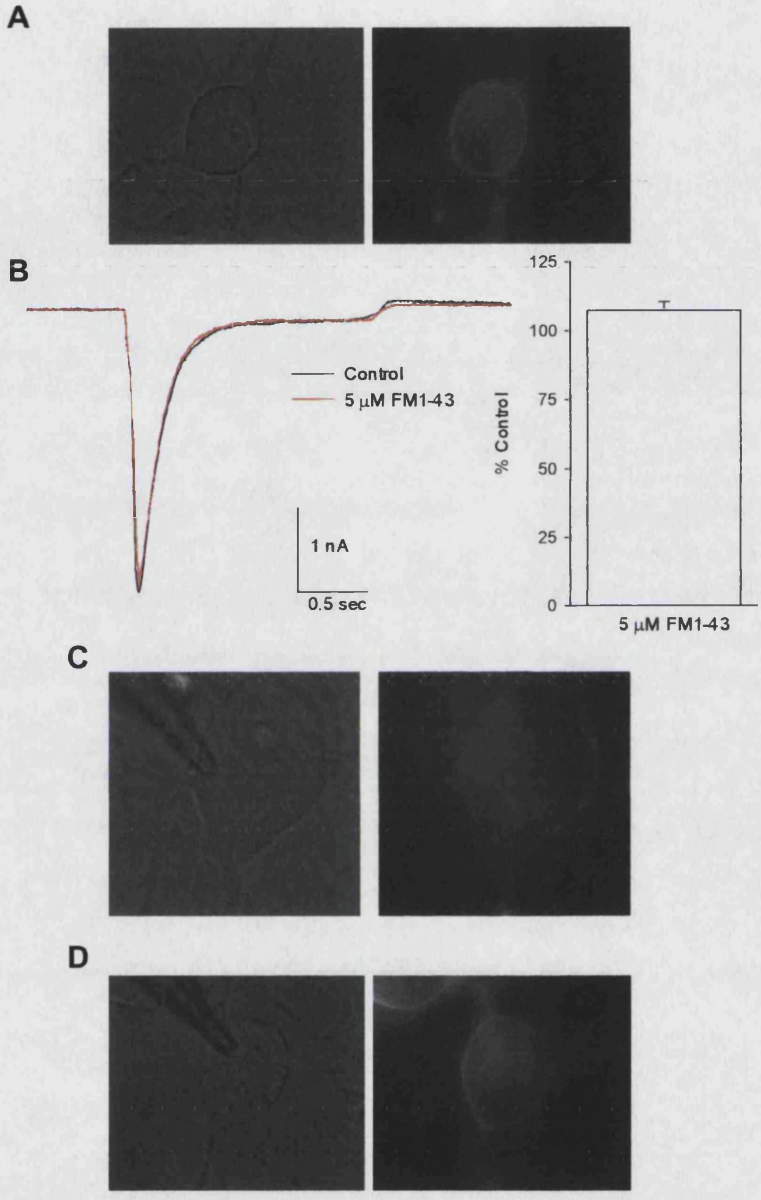

Fig. 3.18 *A*, FM1-43 is not passively taken up by neurons. Light field image of a neuron, *left*, and fluorescence image of the same cell after 5 minutes superfusion in 5 μM FM1-43. Note, labelling of membrane in the absence of cytoplasmic staining. *B*, 5 μM FM1-43 did not significantly affect transient proton-gated currents. *Left*, example traces of current recorded at pH 7.4 (*black*) and in FM1-43 (*red*). *Right*, Overall there was a slight potentiation of ASIC-mediated currents by 5 μM FM1-43; currents were 107.3 ± 3.1% of control (n = 6, P = 0.07). *C*, There was no cytoplasmic labelling of neurons following 6 applications of pH 5.4 (n = 3). *D*, There was no significant labelling of the cytoplasm following stimulation of voltage-activated currents in 2 neurons.

μM currents were inhibited by 81.3 ± 4.9% (Fig. 3.19a, b). There was a considerable degree of inter-cell variability in the level of inhibition produced by arachidonic acid. It is unclear what accounts for the variability; there was no relationship between the level of blockade and the kinetics of MA currents and these cells were not tested for capsaicin sensitivity.

The effect of arachidonic acid was either time or use dependent; the level of inhibition observed following application of this compound increased with each subsequent stimulus (Fig. 3.19c, d). At 10 μM the first stimulus in drug was 80.2 ± 5.5% of the control value whilst the fourth stimulus was 53.5 ± 10.5% of control ($P < 0.001$, one-way, repeated measures ANOVA). Likewise, the first MA current recorded in 50 μM arachidonic acid was inhibited by 59.5 ± 8.5% whereas the second was reduced by 71.4 ± 7.2% ($P < 0.001$, one-way, repeated measures ANOVA).

3.3.9 MA Currents Evoked by Different Probe Velocities

All experiments in this thesis were conducted using a probe velocity of 0.5 μm/msec. In this section the effects of altering the stimulus velocity on the properties of MA currents are reported. Stimuli were applied at 0.17, 0.25, 0.33, 0.50 and 1.00 μm/msec and the effects this had on peak and residual current amplitudes, peak current activation and adaptation rates, threshold of current activation and total charge transfer were analysed. Data are from 7 Caps- neurons with RA currents, 7 Caps+ neurons with RA currents and 6 neurons with SA currents.

The effects of altering the velocity of the probe on MA current properties were distinct according to the type of current. With regards to peak current amplitude, increasing probe velocity induced an increase in peak current amplitude in RA currents (Caps- and Caps+ neurons) but did not alter this property of SA currents (Fig. 3.20a, b). Moreover, the effect of probe velocity on peak current amplitude was more pronounced in Caps- neurons than in Caps+ neurons. Current amplitude was normalised for each neuron to

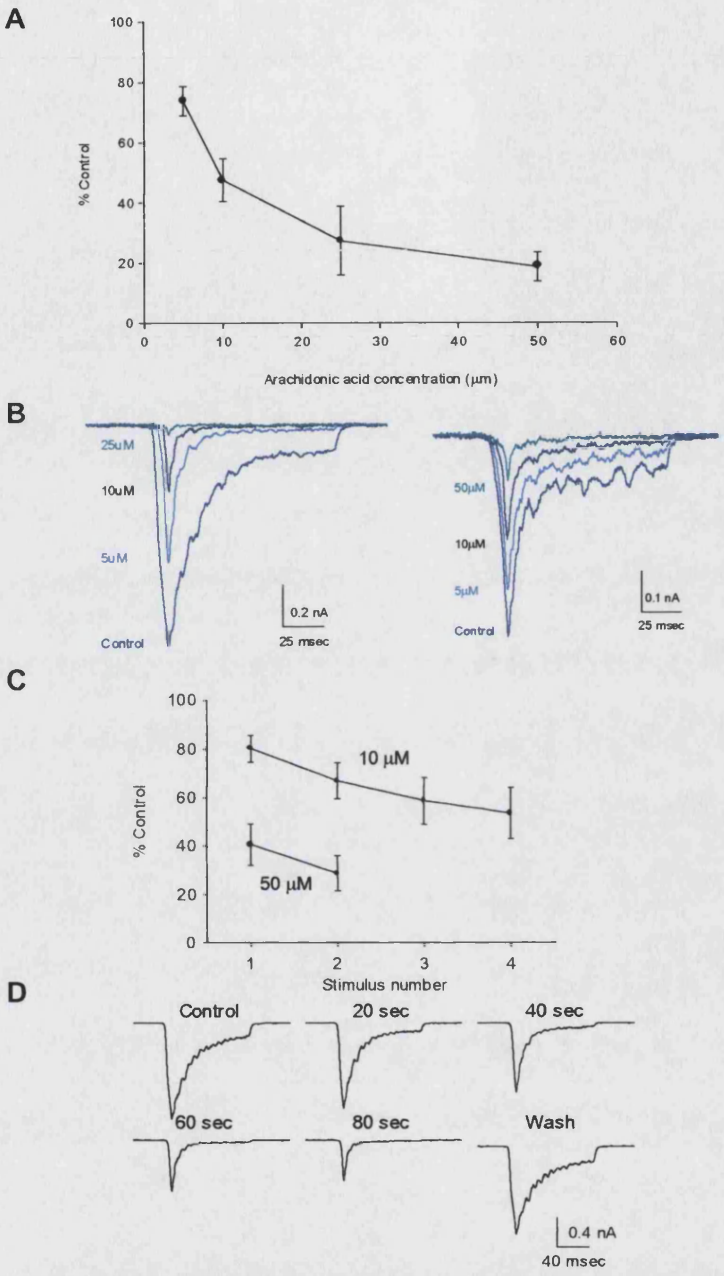

Fig. 3.19 Effect of arachidonic acid on MA currents. *A*, Concentration-inhibition relationship for arachidonic acid (5-50 μM). Inhibition taken as the maximal effect each concentration had on peak MA current amplitude. At 10 μM currents were inhibited by 52.4 ± 7.2%. *B*, Two example traces of the effects of arachidonic acid at various concentrations; traces show the variability in the blocking activity of this compound. *C*, The level of inhibition by arachidonic acid increased with repeated stimuli. Upper trace shows effect of 10 μM on MA currents 1, 2, 3 and 4 stimuli after drug application ($P < 0.001$, one-way, repeated measures ANOVA) and the lower trace shows the effect of 50 μM on the first and second stimuli after application ($P < 0.001$, one-way, repeated measures ANOVA). *D*, Example traces showing increasing blockade of MA currents by 10 μM.

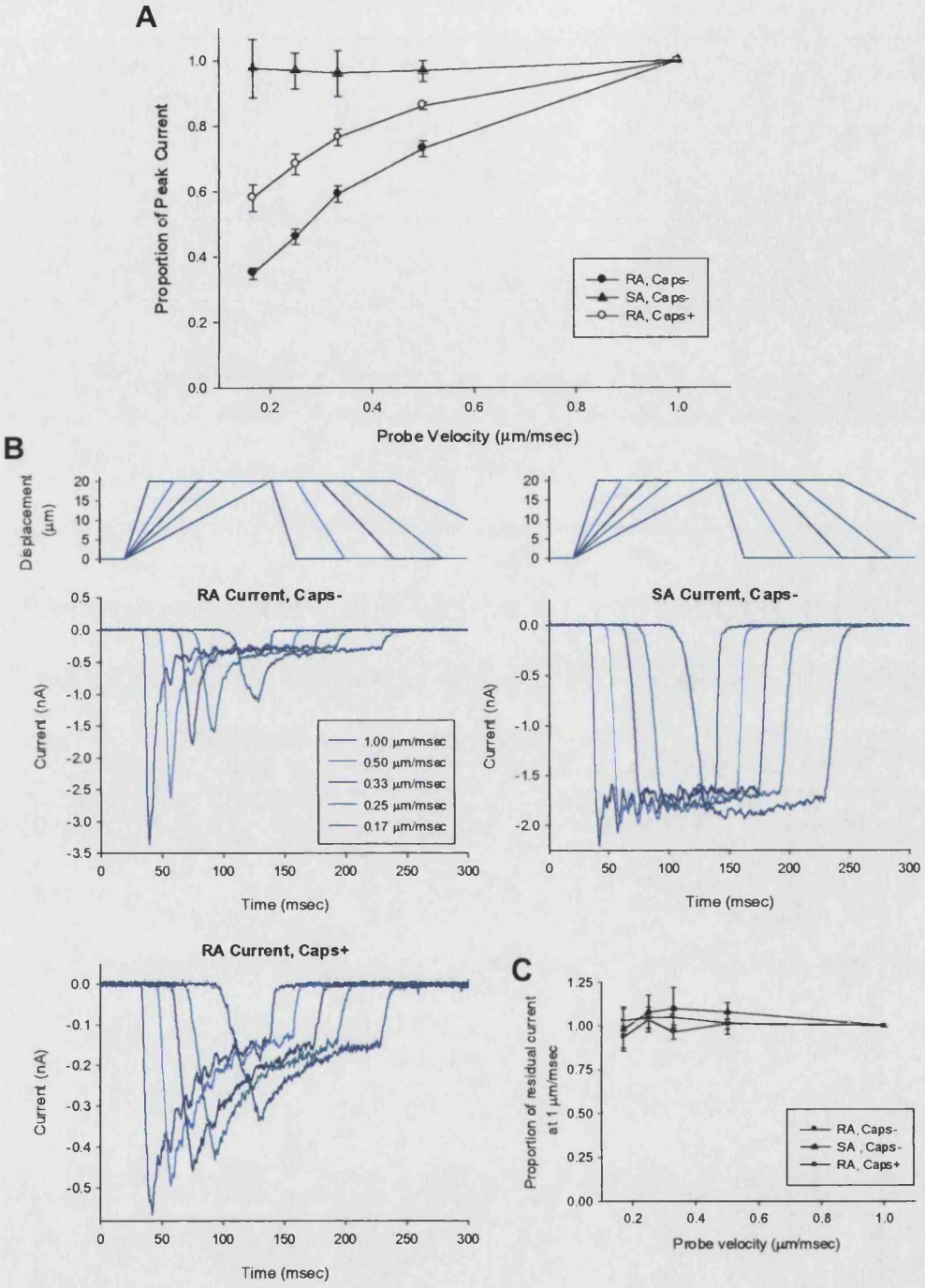

Fig. 3.20 Effects of varying the rate of mechanical stimulation on the amplitude of MA currents. *A*, Relationship between probe velocity and peak MA current amplitude. The size of SA, Caps- currents was unaffected by altering the rate of stimulation, whereas RA currents declined in amplitude as probe velocity was slowed. The effect was significantly more pronounced in Caps- neurons than in Caps+ neurons (2-way ANOVA, $P < 0.001$). *B*, Example MA currents evoked by different probe velocities. *C*, Relationship between the amplitude of the residual current and probe velocity. In all current types the magnitude of the residual current was independent of the rate of stimulation.

that evoked by a 1 μm/msec stimulus. At the 4 lower stimulation rates (0.17 – 0.50 μm/msec) the mean peak SA current amplitude remained between 96.1% and 97.6% of control values. Conversely, at 0.17 μm/msec peak RA current amplitude was 34.9 ± 4.7% and 58.1 ± 10.8% of control in Caps- and Caps+ neurons, respectively, and overall, the relationship between probe velocity and peak current amplitude was significantly steeper in RA current Caps- neurons than in Caps+ neurons (2-way ANOVA, $P < 0.001$). The pattern observed for both RA current groups was different to that seen for SA currents (2-way ANOVA, $P < 0.001$).

The residual current amplitude was also measured for each current type (current amplitude ≈2 msec before probe withdrawal[9]). In all three current classes there was no relationship between probe velocity and this property of the current, i.e. in all cases currents declined to, or remained at, a steady state current that was independent of the initial probe velocity (Fig. 3.20c).

It was then determined how the peak rate of current activation and current decline related to probe velocity (peak rates were assessed as it was not possible to accurately fit exponentials to all currents). In all cases the peak rate of current activation increased with increasing velocity, however the slope of this relationship again varied with current type; the steepest relationship was seen for RA currents in Caps- neurons whereas the shallowest was for SA currents (Fig. 3.21a). At 0.17 μm/msec peak activation rates were 10.9 ± 2.7%, 21.7 ± 6.6% and 44.2 ± 16.7% of those seen at 1.00 μm/msec for Caps- RA, Caps+ RA and SA currents, respectively (All groups different, 2-way ANOVA, $P < 0.001$). The relationship of peak rate of current decline was measured for RA currents in Caps- and Caps+ neurons (Fig. 3.21b) and again it was found that the relationship was steeper for Caps- neurons than for Caps+ neurons. At 0.17 μm/msec the rate was 18.8 ± 3.3% of the rate at 1.00 μm/msec in Caps- neurons whereas this value was 39.6 ± 15.5% for Caps+ neurons (2-way ANOVA, $P < 0.001$).

[9] Often there were oscillations in current amplitude at this stage of the current (these are likely attributable to probe oscillations and were more evident at higher probe velocities); therefore an attempt was made to measure current amplitude at the mid point of the final oscillation.

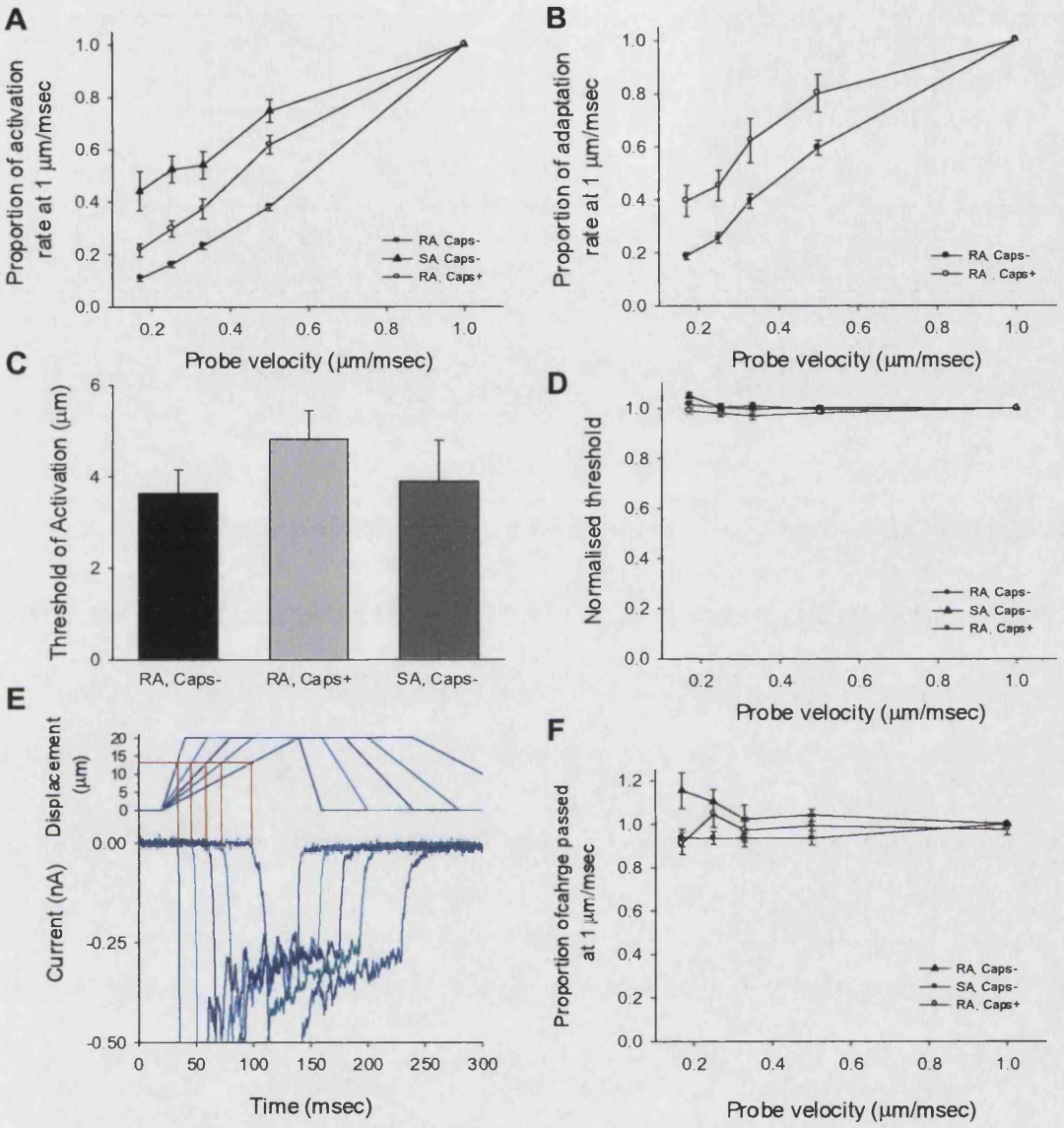

Fig. 3.21 Effect of altering the rate of mechanical stimulation on MA current activation rate, adaptation rate, threshold of activation and total charge transfer. *A*, As probe velocity was increased the maximal rate of activation increased for all current types. However, the relationship was steepest for RA, Caps- currents and shallowest for SA, Caps- currents (all groups different, 2-way ANOVA, $P < 0.001$). *B*, Maximal adaptation rates for RA currents decreased as probe velocity was slowed. The effect of probe velocity was greater on RA currents from Caps- neurons than Caps+ neurons (2-way ANOVA, $P < 0.001$). *C*, Estimated activation thresholds of MA currents used in this study. *D*, Changing the rate of stimulation had no effect on the threshold of current activation, as shown in an example in *E*. *F*, Total charge transfer over the full stimulus duration was unaffected by changing probe velocity.

The final two current properties investigated with regard to probe velocity were the threshold of activation of MA currents and the total charge transfer during the stimulus (determined as the integral of the current waveform). (The difference in thresholds of activation was not statistically significant for the three types of currents assessed here due to rejection of small/high threshold MA currents for these experiments, Fig. 3.21c) Both these attributes remained constant at all rates of stimulation; current thresholds changed very little at any probe velocity (Fig. 3.21d, e) whereas total charge transfer showed a larger degree of variation but on average was largely unchanged at different probe velocities (Fig. 3.21f).

3.3.10 Relationship of MA Currents to Neurons' Chemosensitivity

It was observed that the majority (19/22) of neonatal rat neurons responded to pH 5.15 with transient, ASIC-like currents (Fig. 3.22a). Similarly, most neurons (29/30) responded to application of α,β-methyl-ATP (10 μM), an agonist at homomeric $P2X_1$ and $P2X_3$ receptors and $P2X_{2/3}$ heteromers; 75.9% (22/29) of responding neurons exhibited predominately rapidly desensitising kinetics indicative of $P2X_3$ receptors, whereas the remaining 24.1% (7/29) neurons displayed currents with slowly desensitising kinetics likely to be mediated by $P2X_{2/3}$ receptors (Fig. 3.22b). However, it should be noted that a number of neurons had mixed kinetics (as indicated in Fig. 3.22b also); they were classified according to the major component.

The amplitude of MA currents did not correlate with the magnitude of proton-gated currents observed in DRG neurons in response to application of a pH 5.15 external solution (Pearson's product moment, correlation coefficient (r) = -0.24, P = 0.28, Fig. 3.22c). Nor was there a relationship observed between the kinetics of MA currents exhibited by a neuron and the kinetics of its proton-gated current. Likewise, the amplitude and kinetics of MA currents bore no relationship to the neuron's response to α,β-methyl-ATP (Pearson's product moment for current amplitude, r = -0.02, P = 0.93, Fig. 3.22d). With regards to capsaicin sensitivity there was a small overall negative correlation between the amplitude of MA and capsaicin-evoked currents (r = -0.31, P =

0.02, Fig. 3.22e), however amongst capsaicin sensitive neurons the magnitude of responses to capsaicin were unrelated to the size of MA currents (r = -0.14, P = 0.47, Fig. 3.22e).

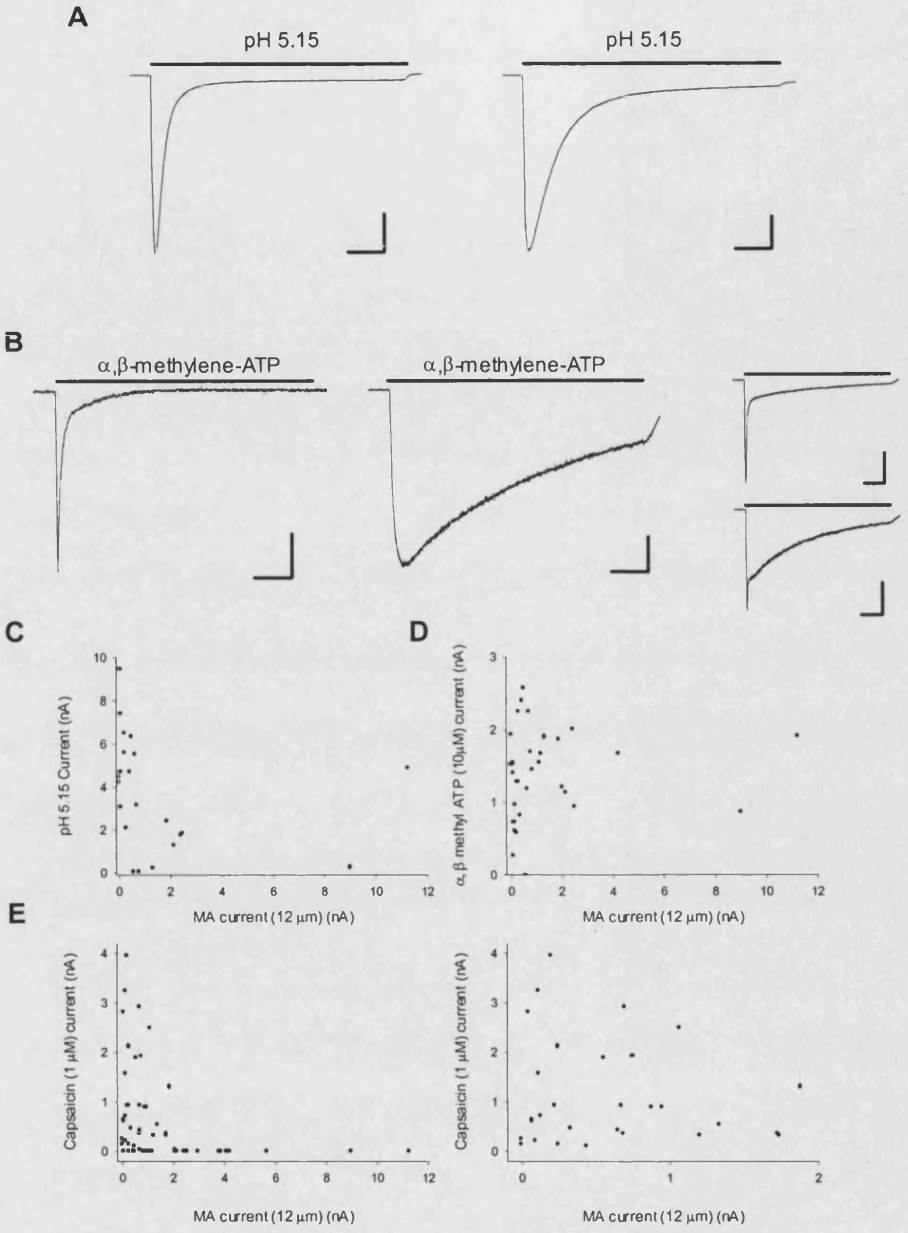

Fig. 3.22 Comparison of neuronal mechanosensitivity and responses to pH 5.15, α β-methylene-ATP (10 mM) and capsaicin. *A*, Example traces of responses to pH5.15, *left*, example from Caps- neuron and, *right*, example from Caps+ neuron. Vertical scale bar: 1 nA, horizontal: 1 sec. *B*, Example responses to α β-methylene-ATP. *Left*, a rapidly desensitising response, NB. full desenitisation during stimulus application. *Centre*, a slowly desensitising current. *Right*, two examples of "mixed" current, *top*, a predominately rapidly desensitising current with a small sustained component and, *bottom,* a predominately slowly desensitising current with an initial rapid component. Vertical scale bar: 0.5 nA, horizontal: 1 sec. *C*, Relationship between amplitude of maximum MA current (stimulus: 12 mm) and amplitude of pH5.15-evoked current. *D*, Relationship between amplitude of maximum MA current and amplitude of α, β-methylene-ATP-evoked current. *E*, Relationship between amplitude of maximum MA current and amplitude of capsaicin-evoked current. *Left*, all neurons, *right*, capsaicin sensitive neurons.

3.4 Discussion

3.4.1 DRG Neuronal Subtypes have Distinct Mechanosensitive Phenotypes in vitro

Focal mechanical stimulation of the cell soma evoked cationic currents (Section 3.4.2) in the majority of sensory neurons and the properties of such currents varied according to cell type. Mechanosensitivity was shown to be a specific characteristic of DRG neurons as related peripheral, sympathetic neurons of the SCG failed to show any electrical response to the same stimulation protocol. Medium-large neonatal neurons (≥ 30 μm) were divided into presumptive nociceptive (capsaicin sensitive) and non-nociceptive (capsaicin insensitive) populations; all capsaicin sensitive neurons that responded to mechanical stimulation generated rapidly adapting MA currents whereas MA currents in capsaicin insensitive neurons were either rapidly or slowly adapting. Consistent with capsaicin insensitive neurons mainly giving rise to low threshold mechanoreceptors *in vivo*, rapidly adapting currents in capsaicin insensitive neurons were larger than the other two classes and activated at significantly lower thresholds. Slowly adapting MA currents (evoked at a probe velocity of 0.5 μm/msec, see Section 3.3.10) were slightly larger than currents in capsaicin sensitive neurons although activation thresholds were similar for both these current types. The phenotype of neurons exhibiting slowly adapting currents is unclear; despite being insensitive to capsaicin, the higher activation thresholds seen in these cells is suggestive of a nociceptive function. One possibility is that they could represent a population of high threshold Aδ-mechanoreceptors[10]. Determination of whether these neurons are likely to have A-fibres by staining for NF200 after recording of MA currents would be informative.

Amongst smaller neurons, there was a clear divergence in mechanical sensitivity between IB4+ and IB- cells in the capsaicin sensitive population. IB4+ cells were mostly refractory to mechanical stimulation, whereas all IB4-, capsaicin sensitive cells responded to pressure. However, it is known that IB4+ neurons respond to high levels of mechanical

[10] Data from adult mouse neurons further indicates a nociceptive function for these neurons in that they all expressed wide, inflected action potentials; see Section 4.4.1.

stimulation *in vivo* (Gerke and Plenderleith, 2001). It is possible that IB4+ cells have higher mechanical thresholds that were not reached because of the danger of detaching the cell from the substrate or losing the seal. Other possibilities include that there are developmental changes in mechanosensitivity in IB4+ neurons (Section 4.4.3), whilst it is also possible that these neurons respond to high levels of pressure via the release of a chemical mediator (see Section 1.2.4). One candidate for this role is ATP. Approximately 90% of IB4+ neurons display $P2X_3$ or $P2X_{2/3}$ currents (Burgard et al., 1999), and there is evidence that $P2X_3$ receptors are central to mechanosensation in the bladder through activation by mechanically evoked ATP release (Vlaskovska et al., 2001).

In these experiments capsaicin sensitivity was used as an indicator of a nociceptive phenotype. Although action potential properties are a better indicator of mechano-receptive properties (Sections 1.1.1.1 and 1.3.1), action potentials in neonatal neurons are immature (the vast majority of neurons have wide inflected action potentials), only reaching a mature state in the third postnatal week (Fitzgerald and Fulton, 1992). Capsaicin sensitivity is however restricted to nociceptive neurons (Sections 1.1.1.2 and 1.3.2) and expression of the capsaicin receptor, TRPV1, is found in between 75% and 83% of rat nociceptors (Guo *et al*, 1999; Michael and Priestley, 1999). Therefore, it can be assumed that all capsaicin sensitive neurons are nociceptors but that the capsaicin insensitive population also contains a fraction of nociceptors; these neurons could account for the neurons in this group that did not respond to mechanical stimulation or that expressed small MA currents. Within the capsaicin sensitive class there was no correlation between mechanosensitivity and the magnitude of capsaicin-evoked currents. Interestingly, capsaicin-evoked currents in smaller neurons were much larger in IB4- neurons than in IB4+ neurons. In adult rat neurons the opposite pattern is observed (see Priestley *et al*, 2002), this is consistent with the data of Guo *et al* (2001) who showed a developmental upregulation of TRPV1 in IB4+ neurons, coincident with increased Ret expression.

Mechanosensitivity showed no relationship with responses to protons (pH 5.15) or the P2X receptor agonist, α,β-methyl-ATP. A lack of correlation with low pH-evoked responses, and the pH-insensitivity of MA currents, suggests that the ion channels

underlying MA currents are not gated or regulated by protons. However, Welsh *et al* (2001) have suggested that ASICs contained within a mechanotransduction complex maybe be resistant to pH changes and there is evidence that post-translational alterations to TRPV1 make the gene product either heat or capsaicin sensitive (Nagy and Rang, 1999). An absence of a relationship between $P2X_3$ and $P2X_{2/3}$ mediated currents and mechanosensitivity, suggests that the mechanical stimulus used here does not induce the release of ATP from the neurons which could modulate or even mediate MA currents, as has been suggested in some systems (Nakamura and Strittmatter, 1996). This conclusion was further supported in adult sensory neurons (Section 4.3.9) when MA currents were shown to be normal when recorded in the presence of the nucleotidase apyrase, which breaks down extracellular ATP.

That $P2X_3$ and/or $P2X_{2/3}$ mediated currents were observed in nearly all DRG neurons would suggest that $P2X_3$ is expressed in the majority of sensory neurons at P1. This is in contrast to the adult population where the expression of this receptor is largely confined to small, IB4+ neurons (Burgard *et al*, 1999), however when Boldogköi *et al* (2002) investigated its embryonic expression they found $P2X_3$ immunoreactivity across all DRG neurons at E14.5 suggesting that its expression pattern is gradually refined through development.

3.4.2 Mechanical Stimulation Evokes a Cationic Current

In a number of neurons exhibiting rapidly adapting MA currents (but not tested for capsaicin sensitivity) the IV relationships of these currents were investigated. In nominally Ca^{2+} free external solutions and Na^+ or Cs^+ based internal solutions IV plots were essentially linear (from -70 to +70 mV) and reversed around 0 mV. The replacement of external Na^+ with the impermeant cation NMG, shifted the reversal potential to close that expected for the internal cation. Hence, these data suggest the underlying channel is non-selective with regards Na^+ and Cs^+ permeability. The underlying ion channel is also permeable to Ca^{2+}; when the external solution was free of monovalent cations, MA currents were proportional to the external Ca^{2+} concentration

and, using FURA-2 imaging, Paolo Cesare showed that in voltage-clamped neurons mechanical stimulation induced a rise in the level of intracellular Ca^{2+}. To further study Ca^{2+} permeability it would be beneficial to study shifts in current reversal potentials in the presence of different extracellular Ca^{2+} concentrations, although, as discussed below Ca^{2+} has modulatory effects on MA currents that may affect such experiments.

A number of other experimental manipulations of external cation concentrations were performed where neurons were distinguished according to capsaicin sensitivity. Replacement of Na^+ with NMG in an otherwise standard external solution led to a large reduction in rapidly adapting MA current amplitudes in both cell types, however this effect was significantly greater for capsaicin sensitive neurons (80% versus 68% reduction). Larger MA currents in the absence of Na^+ may suggest that the underlying ion channels in capsaicin insensitive neurons are more Ca^{2+} permeant than those in nociceptive neurons. However, the removal of Na^+ had another interesting effect on MA currents; in capsaicin insensitive neurons the absence of Na^+ induced a decrease in the activation threshold and a reduction in the rate of MA current adaptation. The mechanism by which these effects are achieved is unclear, however, a decrease in activation threshold could account for the relatively smaller decrease in MA current amplitude in these neurons.

Modulation of MA currents by Ca^{2+} was demonstrated in experiments where external levels of this ion were altered. Removal of Ca^{2+} (in the absence of a divalent cation chelator) caused an increase in MA current amplitude and increasing Ca^{2+} concentration up to 5 mM showed that in this concentration range there was an inverse, linear relationship between MA current amplitude and Ca^{2+} levels. Such an effect could be attributable to slow permeation by Ca^{2+} effectively blocking the more rapid passage of Na^+. Such a mechanism has been demonstrated for other non-selective cation channels such as the hair cell transduction channel (Ricci and Fettiplace, 1998) and certain nicotinic acetylcholine receptors (for example $\alpha 9$, Katz *et al*, 2000). Moreover, Ca^{2+} has been shown to have similar effects on receptor potentials recorded from mechanosensory nerve endings (Section 1.1.2.2). Interestingly, this relationship was significantly steeper in

capsaicin insensitive neurons than in capsaicin sensitive neurons possibly due to a higher Ca^{2+} permeability of mechanosensitive channels in capsaicin insensitive neurons.

In contrast, when 5 mM EGTA was added to the Ca^{2+}-free solution slowly and rapidly adapting MA currents in capsaicin insensitive neurons declined in amplitude whereas currents in capsaicin sensitive neurons were essentially unaffected. It is likely, due to impurities (either in the water source or in the chemicals used), that in the absence of a chelator there are tens of micromoles of Ca^{2+} in the external solution whereas with 5mM EGTA there are subnanomolar levels of this ion. Hence, it would appear that although Ca^{2+} has an inhibitory action on MA currents, its presence at low levels is necessary for the functioning of the underlying ion channel selectively in capsaicin insensitive neurons. This may be due to a direct interaction of Ca^{2+} with the channel or possibly because EGTA dysregulates another Ca^{2+} dependent process, such as protein-protein or membrane-protein interactions specific to these neurons. It should be noted that EGTA also chelates other metal ions and it is possible that such actions could underlie this effect; to test this possibility other chelators with low Ca^{2+} affinity should be investigated.

It is of interest to note that manipulation of external Ca^{2+} levels did not affect the kinetics of MA current adaptation, as has been observed for the hair cell transduction channel (Ricci and Fettiplace, 1998). However, when external Na^{+} was removed a reduction in the rate of adaptation was seen in rapidly adapting currents in capsaicin insensitive neurons. This observation coupled with the reduced MA current activation threshold in these neurons could mean that Na^{+} has an inhibitory action on the ion channels. Testing the effects of intermediate Na^{+} concentrations on MA currents amplitude and kinetics would be instructive.

3.4.3 MA Currents, the Cytoskeleton and Laminin

Whereas bacterial mechanosensitive ion channels are directly sensitive to stretch in the plane of the membrane, the majority of research on metazoan mechanosensation suggests that mechanosensitive ion channels are gated through their interaction with cytoskeletal and/or extracellular matrix proteins (see Section 1.2). Here, it was found that disruption

of the actin cytoskeleton by cytochalasin B inhibited MA currents. Overnight incubation in 100 nM cytochalasin B essentially ablated responses to mechanical stimulation (Paolo Cesare, personal communication) whereas acute application of 10 μM of this compound significantly reduced MA current amplitude. Interestingly, the degree of inhibition caused by acute cytochalasin B application varied significantly between currents in capsaicin sensitive and insensitive neurons; currents in capsaicin insensitive neurons were inhibited by around 60% whereas in neurons that responded to capsaicin currents were reduced by only 20%. Acute application of the microtubule disruptor colchicine did not clearly inhibit MA currents. The importance of the cytoskeleton was further emphasised indirectly by the observation that MA currents were more stable when recorded in the perforated patch configuration than in the conventional whole-cell mode. Complete dialysis of the cell in the latter configuration is likely to disrupt the integrity of the cytoskeleton to a much greater degree than recordings made using a membrane perforant to gain electrical access to the cell.

These data clearly suggest that the gating of DRG mechanosensitive ion channels is dependent on the integrity of the actin cytoskeleton and also raise the possibility that the differential mechanosensitivity of capsaicin sensitive and insensitive neurons may be due in part to differential tethering of the ion channel to the cytoskeleton. Distinct mechanisms for tethering the channel to cytoskeletal proteins may exist or perhaps the two cell populations express distinct cytoskeletal proteins. Consistent with the latter hypothesis, non-nociceptive neurons are often distinguished by their expression of neurofilament-200, a heavy chain neurofilament, whereas nociceptors are characterised by high expression of peripherin, which is an intermediate neurofilament (see Section 1.1.1.1). It would be of interest to determine the effects of phalloidin, which binds to and stabilises actin filaments, on MA currents.

The data suggesting mechanosensitive channels' interact with actin filaments rather than microtubules is consistent with previous findings suggesting that at the likely site of mechanotransduction on a Pacinian corpuscle afferent the cytoplasm is dominated by neurofilaments whereas microtubules are absent (Zelena, 1994). It also contrasts with the

situation in *C. elegans* where body touch receptors are characterised by a distinctive arrangement of microtubules that are required for normal mechanosensation (Section 1.2.2). This discrepancy is evidence of a distinct mechanism of mechanotransduction operating in mammalian cells.

Regulation of MA currents by an extracellular matrix protein was seen when neurons were plated on laminin in addition to poly-*L*-lysine. Interaction with laminin resulted in a slowing of current adaptation and in particular a subpopulation of capsaicin insensitive cells displayed MA currents that showed very slow or no adaptation. The peak amplitude of such currents typically occurred during the plateau phase of the stimulus and had higher activation thresholds than rapidly adapting currents in capsaicin insensitive neurons.

Laminins are a major component of basal laminae and are prevalent in the end organs of mechanoreceptors (Chouchkov *et al*, 2003), they are heterotrimeric structures made up of an α, a β and a γ subunit. There are 5 α, 3 β and 3 γ isomers respectively and, up to now, 12 naturally occurring trimeric compositions have been identified (Bosman and Stamenkovic, 2003). The receptors for laminins are transmembrane integrins. These are heterodimeric molecules consisting of an α and a β subunit and again diversity is generated by multiple α and β genes (18 and 8, respectively). At least ten integrin dimers bind laminins (others bind different extracellular matrix proteins such as collagens and fibronectin). Furthermore, ligand binding can be promiscuous; different laminin receptors tend to bind to a range of laminin subtypes, with differing affinities, and $\alpha1\beta1$ integrins, for example, bind laminin and collagen (Belkin and Stepp, 2000).

Integrins expressed by sensory neurons have important roles in neurite outgrowth (Tomaselli *et al*, 1993) where ligand binding regulates aspects of cytoskeletal arrangement (for example see Schmidt *et al*, 1995). The laminin used here was laminin 1 ($\alpha1\beta3\gamma2$) extracted from Engelbreth-Holm-Swarm mouse sarcomas which in terms of axon growth in DRG neurons interacts preferentially with $\alpha1\beta1$ integrins (Tomaselli *et al*, 1993). Regulation of neurite outgrowth by laminin is seen in the majority of DRG

neurons whist the main effect of laminin observed here was a dramatic slowing of MA current kinetics in a relatively small subpopulation of neurons. It may, therefore, be the case that neurons exhibiting slowly adapting MA currents in the presence of laminin express a specific complement of integrins that modulate mechanosensitive ion channels. It would be of interest to investigate this hypothesis; this could be achieved immunocytochemically or by single-cell PCR after recording a neuron's mechanically induced responses or by culturing neurons in the presence of function blocking antibodies against specific integrin subunits. Given the ambiguity regarding the phenotype of these neurons (see Sections 3.4.1 and 4.4.1), if these neurons did express specific integrins it could serve as a molecular marker of these neurons *in vivo*.

The mechanism by which integrins modulate MA currents is unclear. Integrins have been implicated in certain forms of mechanosensation, although typically in slow processes, such as altered gene expression or tissue remodelling in response to forces such chronic shear stress or cell migration. It is uncertain if mechanosensation in such cases is dependent on activation of mechanosensitive ion channels (see Alenghat and Ingber, 2002; Geiger and Bershadsky, 2002). Integrins are at the core of focal adhesions that give mechanical continuity between the cytoskeleton and the extracellular matrix; they exist in large complexes that include proteins that link them to the actin cytoskeleton (e.g. vinculin, paxillin) and also key molecules in intracellular signalling pathways (Belkin and Stepp, 2000;Alenghat and Ingber, 2002; Geiger and Bershadsky, 2002). Hence, changes in intracellular messengers and in gene expression could underlie the effects of laminin, however, the effects of integrin activation on membrane elasticity are of interest. Ligand binding to integrins leads to recruitment of actin and actin-binding proteins to focal adhesion complexes and to a subsequent stiffening of the membrane, i.e. the membrane shows heightened resistance to displacement (Matthews *et al*, 2004 and references therein). It remains to be determined if membrane elasticity is important in determining the rate at which MA currents adapt; experiments aimed at manipulation of membrane stiffness may shed light on adaptation and the effects of laminin (see Section 3.4.6). Membrane/cytoskeleton rearrangement in response to integrin activation occurs in minutes (Plopper and Ingber, 1993) so acute ligand application could be used. It is

unclear if a DRG mechanosensitive channels would be closely juxtaposed to or contained within focal adhesions or if effects on membrane tension could act at a distance on the channel.

In considering the mechanism of action of laminin there is a need to understand where on the cell membrane ion channels are being activated by the mechanical stimulus. If activated integrins are part of a transduction complex (be their function active or structural) or if cytoskeletal rearrangements induced by laminin binding are local, given that laminin is bound to the surface of the culture dish this would suggest that the site of channel activation is on the base of the neuron. Although mechanical stimulation is applied to the top of the cell (Fig. 2.1), and thus membrane stretch is greatest at this site, if there is a requirement for external membrane anchoring (either non-specifically by poly-*L*-lysine or at integrins by laminin) then the likely site of transduction would be the base of the cell. Alternatively, if sheering between the membrane and cortical cytoskeleton is sufficient to activate the mechanosensitive channel then integrin activation would have to induce more global changes in the neuron to affect channel behaviour. The site of transduction may be difficult to determine, although high resolution Ca^{2+} imaging using confocal microscopy may give insights into the point of ion influx.

The effect of laminin is interesting given that it has been detected close to the site of transduction at the nerve terminal *in situ* (Chouchkov *et al*, 2003). Further investigation could include determination of the effects on MA currents of plating DRG cultures on other components of the extracellular matrix, including different laminin isoforms and types of collagens or fibronectin. Moreover, if other proteins had modulatory effects it would be interesting to know if these effects were seen in the same population of cells that respond to laminin 1 or if MA currents in different cell types are regulated by interactions with distinct components of the extracellular milieu.

3.4.4 MA Current Pharmacology

There are no known selective, high affinity antagonists of mechanosensitive ion channels (Section 1.2.1; Chapter 5). Blockers of stretch-activated, cation channels come from three families represented by amiloride, gentamicin and Gd^{3+} (see Hamill and McBride, 1996). In the experiments presented in this chapter, a number of non-specific channel blockers were found to inhibit MA currents.

The compounds found to block MA currents with the greatest affinity were Gd^{3+}, ruthenium red and FM1-43, all of them inhibiting currents with IC_{50} values of less than 10 μM. Gd^{3+} displayed an IC_{50} of approximately 8 μM for rapidly adapting currents in both capsaicin insensitive and sensitive neurons. Likewise, the IC_{50} for MA current inhibition by ruthenium red was more or less 3 μM for blockade of all current types. Hence the similarity in affinity of both compounds for the ion channels underlying different types of MA currents would suggest that very closely related ion channels mediate currents that differ in kinetics and sensitivity. Moreover, the accurate fitting of these data by a curve defined by the Langmuir equation is consistent with these antagonists functionally interacting with a single class of binding sites, implying that a single population of ion channels underlie currents in each cell type. This conclusion is supported by the demonstration that when currents in the presence of drug are normalised to the peak control current it can be seen that the same proportion of current is blocked during the transient and sustained components.

Gd^{3+} and ruthenium red are both multivalent cations that act as channel pore blockers. Neither is selective for a single class of channels. Gd^{3+} has widely been reported to block mechanosensitive cation channels in a variety of systems (Hamill and McBride, 1996). In addition to these activities, this ion has been demonstrated to block channels from other classes including voltage-gated Ca^{2+} channels (Boland *et al*, 1991), TRP channels (Liedtke *et al*, 2000; Strotmann *et al*, 2000; Lee *et al*, 2003), and some ASICs (Babinski *et al*, 2000; Allen and Attwell, 2002). In contrast ruthenium red (to the best of my knowledge) has not been previously reported to block channels that are unequivocally

mechanically gated. The channels it is known to block include ryanodine receptors (see Koulen and Thrower, 2001), a variety of TRP-related channels (see Clapham *et al*, 2001; Gunthorpe *et al*, 2002) including TRPV1 (Caterina *et al* 1997) and TRPV4 (Liedtke *et al*, 2000; Strotmann *et al*, 2000) and voltage-gated Ca^{2+} channels (Cibulsky and Sather, 1999). Thus, the blocking activity of these two compounds did not give a strong indication as to the likely class of ion channels that mediate MA currents (see below for discussion). Consistent with ruthenium red blocking MA currents by entering the channel pore due to its charged nature, its inhibitory action was shown to be voltage dependent in adult mouse neurons (see Sections 4.3.4 and 4.4.5). Hence, it seems that the ruthenium red binding site must lie within the membrane electric field.

A number of other compounds were tested for their ability to inhibit MA currents. Saliently, it was found that amiloride (up to 500 μM) did not block mechanically evoked responses and that gentamicin had only a minor inhibitory effect (17% block) at 100 μM. This is in contrast to the blocking activity these compounds display at a variety of mechanosensitive channels (see Hamill and McBride, 1996). Gentamicin (affinity in the low micromolar range) and amiloride (affinity around 50 μM) both block the transduction channel of mammalian hair cells (see Strassmaier and Gillespie, 2002) suggesting that the mechanosensitive ion channel in DRG neurons is different from those in the cochlea. In addition, amiloride also blocks members of the DEG/ENaC family of ion channels (Kellenberger and Schild, 2002; see below) albeit via a different mechanism than that responsible for its inhibition of hair cell mechanosensors (Section 1.2.2.2).

FM1-43 was found to act as a permeant blocker of the ion channels underlying DRG MA currents. FM1-43 is a cationic (+2 charge) styryl pyridinium dye that has traditionally been used to label biological membranes in order to study processes such as endocytosis, exocytosis and endosome trafficking, in particular synaptic vesicle recycling (Betz *et al*, 1996; Ryan, 2001). In 2001, Gale *et al* published an account of how FM1-43 acted as a permeant blocker of the mechanotransduction channel in mammalian hair cells. FM1-43 applied to the extracellular surface of hair cells was taken up by the cell (resulting in fluorescent labelling of the cytoplasm) at a site close to the proposed site of transduction

in a manner that was dependent on mechanical stimulation. FM1-43 was also shown to inhibit mechanically activated currents (blockade showed some voltage dependence, affinity was greatest at –4 mV with an IC_{50} of 1.2 μM).

Subsequently, Meyers et al (2003) reported similar effects of FM1-43 on hair cells and also described a series of experiments in which they injected mice subcutaneously with AM1-43 (a fixable analogue of FM1-43) and discovered, after 1-2days, staining of a variety of mechanosensory structures throughout the animal. These structures included the cell bodies of the DRG and trigeminal ganglia. The authors demonstrated that ligation of the ipsilateral infraorbital branch of the trigeminal nerve prevented labelling of trigeminal neuronal somata following local subcutaneous delivery of the drug; strongly suggesting that uptake was via the peripheral nerve terminal. Here it was found that FM1-43 slowly permeated, and effectively blocked, the ion channel underlying MA currents. The IC_{50} for inhibition by FM1-43 was in the low micromolar range, however, in contrast to ruthenium red and Gd^{3+}, the potency of this compound differed between neuronal subpopulations, thus it inhibited slowly adapting (IC_{50} approximately 3 μM) more effectively than it did RA currents in either capsaicin sensitive or insensitive neurons (IC_{50} approximately 5 μM).

Given that all cell bodies in the DRG are labelled (to some degree) following administration of FM1-43 (Meyers *et al*, 2003), the mechanosensitive ion channel under study here is a strong candidate for mediating, at least in part, the uptake of this compound by sensory neurons. Meyers *et al* (2003) showed that FM1-43 permeated TRPV1 and $P2X_2$, suggesting that FM1-43 may pass through most or all non-selective cation channels. However, whilst numerous channels of this type are associated with polymodal transduction (and sensitisation) in nociceptive neurons (Julius and Basbaum, 2001), none are known to be expressed in low threshold mechanoreceptors. Here it was found that FM1-43 does not block or permeate ASICs and nor did it inhibit inward voltage-activated currents. Therefore, although FM1-43 may enter nociceptors via TRPV1 and other known channels, mechanosensitive ion channels may also contribute to nociceptor labelling and may be the sole entry mechanism for the labelling of low

threshold mechanoreceptors. Future experiments to test if dye uptake in the animal is dependent on mechanical stimulation may include administration of FM1-43 (or AM1-43) to anaesthetised animals and then comparing uptake (in either the ganglia or nerve endings) following mechanical stimulation of a paw relative to an unstimulated or electrically stimulated paw. Additionally, the ability of FM1-43 to inhibit mechanically evoked activity in DRG nerve fibres could be tested.

Zinc and capsazepine also inhibited MA currents. At a concentration of 200 μM Zn^{2+} inhibited MA currents by approximately 80% at -70 mV and block also showed voltage dependence; outward currents recorded at +70 mV were reduced by only around 30%. Again, the hypothesised mechanism of Zn^{2+} blockade is that it is pulled into the channel by the electric field at negative holding potentials and occludes the passage of other permeant ions. Capsazepine was identified as a competitive antagonist at the capsaicin receptor (TRPV1) with an IC_{50} of around 400nM (Bevan *et al*, 1992). In addition, applied to DRG neurons at higher concentrations it also inhibits cold-induced currents (94% at 50 μM, Reid *et al*, 2002) and voltage-gated Ca^{2+} currents (Docherty *et al*, 1997). Here it blocked MA currents by around 80% at 50 μM. In DRG neurons capsazepine blocks heat-activated currents much less efficiently than it does capsaicin-evoked currents; Kirchstein *et al* (1999) estimate an IC_{50} of around 10 μM whereas Nagy and Rang (1999) saw only slight inhibition at this concentration. Hence, the ability of capsazepine to block heat-, cold- and mechanically evoked currents in DRG neurons are comparable.

In conclusion, it has been shown that a number of molecules, already identified as ion channel blockers, inhibit MA currents in DRG neurons. Although no antagonist identified is specific to any single class of ion channels the comparison of the effects of multiple compounds allows the properties of this channel to be contrasted with known channel families. Thus, in comparison to the hair cell transduction channel, the DRG channel is similarly blocked by FM1-43 (Gale *et al*, 2001) and Gd^{3+} but not by amiloride or gentamicin (see Strassmaier and Gillespie, 2002). In addition adaptation of DRG MA currents is not clearly modulated by Ca^{2+}, as is the case in hair cells (Ricci and Fettiplace,

1998), hence there are significant differences in the properties of these channels. As discussed in Section 1.2 there is strong evidence that members of the DEG/ENaC and TRP channel superfamilies are invertebrate mechanotransducers, and thus it is hypothesised that vertebrate homologues of these channels are mechanically gated. A defining feature of DEG/ENaC-related channels is their sensitivity to amiloride (Goodman and Schwarz, 2002) and therefore the inactivity of amiloride provided evidence that DRG MA currents are not mediated by members of this class of channels. However, when ENaC activity in lipid bilayers was mechanically potentiated its affinity for amiloride decreased dramatically from 150 nM to over 25 μM (Awayda *et al*, 1995; Section 1.2.2.2) suggesting that this form of stimulus may induce structural changes in the channel that decrease amiloride affinity, leaving open the possibility that MA currents are mediated by DEG/ENaC related channels. Nevertheless, the effects on DEG/ENaC channels of other compounds that block MA currents argue against their direct involvement in mediating these currents. Ruthenium red is inactive at ASICs (Alvarez de la Rosa *et al*, 2002) and although Gd^{3+} blocks ASIC2a/3 heteromers with an IC_{50} of about 40 μM it is inactive at other channel compositions (Babinski *et al*, 2000). Zn^{2+} has contrastingly been shown to potentiate ASIC mediated currents (Baron *et al*, 2001) although Allen and Attwell (2002) report that it blocks such currents; effects may be dependent on the subunit composition of the channel. Finally, FM1-43 did not permeate or block ASIC channels.

In contrast, TRP-related channels share many features of MA current pharmacology. Primarily, inhibition by ruthenium red in the low micromolar range is a characteristic of many TRP channels including most TRPV channels (see Gunthorpe *et al*, 2002) and TRPM6 (Voets *et al*, 2003). Moreover, like the blockade of MA channels, inhibition of TRPV4 (Watanabe *et al*, 2002b) and TRPM6 (Voets *et al*, 2003) by ruthenium red is voltage dependent. In addition, Gd^{3+} has been shown to act as an antagonist at TRPV4 (Liedtke *et al*, 2000; Strotmann *et al*, 2000) and TRPC3 (Trebak *et al*, 2002) and FM1-43 permeates (and presumably blocks) TRPV1 (Meyers *et al*, 2002). Finally, capsazepine inhibited MA currents with a similar potency to that observed for heat (TRPV1 mediated)

and cold (TRPM8 mediated) currents in DRG neurons. Together these findings suggest that the ion channels that underlie MA currents may be TRP-related channels.

3.4.5 Inhibition of MA Currents by Arachidonic Acid

Arachidonic acid inhibited MA currents in neonatal rat neurons with an IC_{50} of around 10 μM. This compound has modulatory effects on a wide range of ion channels, inhibiting many and potentiating others (see Meves, 1994). Analysing the effects of arachidonic acid are hugely complicated by the fact that it is a substrate in many signalling pathways. To define its role in regulating channel activity one must determine whether the compound itself or one of its metabolites is the active molecule (see for example Vellani *et al*, 2000). Casado and Ascher (1998) observed that arachidonic acid mimicked the effect of membrane stretch (induced by hypotonic solution, Paoletti and Ascher, 1994) in potentiating NMDA receptor activity and that lysophospholipids inhibited NMDA receptor activity by reproducing the effect of membrane compression. They hypothesised that this was due to the shape of these compounds and the consequent effects of their insertion into the outer leaflet of the membrane, i.e. owing to their "cone" shapes, lysophospholipids are expected to compress integral membrane proteins whereas, due to its large hydrophobic tail, arachidonic acid is believed to recapitulate membrane stretch. In inhibiting DRG MA currents, arachidonic acid had the opposite effect to its action on NMDA receptors. This could possibly have been because the stimulation protocol here induces membrane compression, essentially the opposite of the effect induced by cell swelling, however, lysophosphatidylinositol had minor and inconsistent effects on MA currents (data not shown), suggesting this is not the case. Casado and Ascher (1998) found that the effects of these amphiphilic compounds is independent of an interaction of NMDA receptors with the cytoskeleton whereas data presented here (Sections 3.3.6 and 3.4.3) suggest that gating of the ion channel underlying MA currents is dependent on the cytoskeleton.

Inhibition of MA currents by arachidonic acid may have been due to a direct inhibitory effect of arachidonic acid, or one of its metabolites, on the channel. Inhibition of MA

currents increased with time (or possibly repeated stimulation) following arachidonic acid application, this observation argues against a direct interaction of this compound with an extracellular domain of the channel as such a mechanism would likely be rapid. Rather it would suggest that either there is metabolism of arachidonic acid to an active compound or that the effect is dependent upon integration of arachidonic acid into the cell membrane. Due to the extensive experiments required to study arachidonic acid effects, these investigations were not continued.

3.4.6 MA Currents at Different Probe Velocities: MA Current Kinetics

To study the relationship between the rate of stimulus application and the characteristics of evoked responses, a number of properties of MA currents were analysed following mechanical stimulation at probe velocities ranging from 0.17 to 1.00 μm/msec. Data were analysed separately for currents from capsaicin sensitive neurons and for rapidly and slowly adapting currents from capsaicin insensitive neurons. The most striking finding was that the peak amplitude of both classes of rapidly adapting currents correlated positively with the speed of stimulation whereas the amplitude of slowly adapting currents was independent of this variable. The amplitude of the residual current (that measured at the end of the stimulus plateau) in neurons with rapidly adapting currents and the total charge transfer (as measured by the integration of the current) in all neurons were also independent of probe velocity. Moreover, the threshold for current activation was unaffected by the probe velocity. Finally, the peak rate of current activation was positively correlated with probe velocity in all classes of neurons and for rapidly adapting currents the peak rate of adaptation also increased as the velocity of the probe increased. These experiments also revealed clear differences between the behaviour of rapidly adapting MA currents in capsaicin sensitive and insensitive neurons; the relationship between probe velocity and peak current amplitude, peak rate of current activation and peak rate of current adaptation was in each case steeper for currents in capsaicin insensitive neurons than in capsaicin sensitive neurons.

The stimulation protocol used in this study negates studying the rate of MA current activation independently of the rate of adaptation, i.e. the measured macroscopic rate of activation is dependent on the relative rates of channel opening and closing. The rate of activation observed for slowly adapting currents is the least affected by channel closure as the probability of channel closing is very low. The amplitude and rate of activation of rapidly adapting currents falls sharply when the probe velocity is decreased as there is presumably significant channel closing during stimulus application. Differences between rapidly adapting currents in capsaicin sensitive and insensitive neurons suggest that there is a lower rate of channel closing in the former population[11].

The data suggest that the probability of individual mechanosensitive ion channels opening is determined by the magnitude of displacement independently of the rate of displacement and the rate of channel closing is distinct in each of the three current types. Consistent with this, the total charge transfer was also independent of probe velocity suggesting mean channel open-time (and hence rate of closure) was unaffected by this variable. Hence for slowly adapting MA currents, where the probability of channel closing is low, the peak current amplitude and rate of activation are determined, respectively, by the number of channels available and the rate at which they open. Conversely, for rapidly adapting currents, channels open at a given stimulus intensity and then rapidly close, hence peak current amplitude and rate of activation are determined by the rates at which channels both open and close; the slower the rate of displacement, the slower the rate of channel opening and the greater the effect of channel closing. These properties mean that rapidly adapting whole-cell currents encode both the size and the rate of displacement, whereas slowly adapting currents only encode the magnitude of displacement.

The amplitude of the residual portion of rapidly adapting currents was independent of the probe velocity. It is unclear if neurons tend to contain a mixture of both slowly and

[11] Comparison of adaptation rates between these two populations (at 0.5 μm/msec) did not show a significant difference; although there was a trend towards capsaicin sensitive neurons having slower adaptation (data not shown), variance was high and analysis was complicated by the tendency for adaptation to slow with increasing current size (Section 4.3.2).

rapidly closing ion channels or, as residual currents are more apparent at higher stimulus intensities, if at higher levels of membrane tension the rate of channel closing is reduced or channels can reopen. The lack of a pharmacological agent that distinguishes between rapidly and slowly adapting currents makes this difficult to test.

Focal stimulation of the somatic membrane produces a local indentation of the membrane (Fig. 2.1), hence membrane stretch is greatest in the region adjacent to the probe and will decrease with increasing distance from the probe. However, as discussed in Section 3.4.3 MA currents may be mediated by channels at the base of the neuron and so would be dependent on force transmission through the cell and stretching of the membrane adjacent to anchored points. Nevertheless, increasing the stimulus size will increase the degree of stretch adjacent to and opposite the probe and also apply tension to an increasing area of membrane. Therefore, the membrane of the cell (and the population of mechanosensitive channels expressed therein) is exposed to a gradient of tension. It remains to be determined if mechanosensitive channels in each cell type tend to be fairly homogenous in terms of sensitivity and current amplitude grows with increasing stimulus intensity as the area of membrane at a suprathreshold tension increases or if more and more channels are activated in the same area of membrane.

What determines the rate of channel closing is unclear. It may be an intrinsic property of the channel (analogous to the inactivation mechanism of voltage-gated sodium channels), it may be dependent upon the interaction of permeant ions with the channel pore (as demonstrated for the hair cell transduction channel) or it may be due to the elastic properties of the cell membrane in response to stretch. In the first model, periods of decreased sensitivity would be expected if the channel entered an inactivated state, therefore either application of a second mechanical stimulus rapidly after the first or the application of double steps (i.e. stimulate to, say, 10 μm and then to 14 μm without withdrawing the probe) may be informative. In the second instance, ionic substitution experiments would be useful; for those performed in this study, the data suggest that adaptation is Ca^{2+} independent but there is some evidence that removal of Na^{+} from the external solution slows adaptation. This idea is further supported by the apparently

slower adaptation kinetics of outward currents (mediated by Cs^+) than inward currents (mediated primarily by Na^+) when membrane polarity is switched (see figure 4.6). The possibility of membrane stiffness affecting current adaptation is supported by the observation that laminin can modulate adaptation kinetics (Section 3.4.3). To test this possibility further neurons could be plated on other integrin ligands or such compounds could be applied to the cell acutely whilst recording. Finally, it may also be of interest to record MA currents when the cell membrane has been pre-stretched by hypo-osmolarity.

4 *Analysis of Mechanically Activated Currents in Adult Mouse DRG Neurons: Effect of ASIC gene Ablation*

4.1 Introduction

As discussed in Section 1.2, no eukaryotic ion channel has been shown to be both unequivocally mechanically gated and key to sensory mechanotransduction. The work described in Chapter 3 demonstrated that stimulation of the somata of sensory neurons evoked whole-cell currents that were absent from non-sensory, peripheral (SCG) neurons. Moreover, it was found that the amplitude of these currents and their thresholds of activation co-varied with capsaicin sensitivity, in a manner compatible with the predicted *in vivo* mechanosensory phenotypes of the neurons. Thus these data strongly implicate the underlying mechanosensitive ion channel in the process of somatosensory mechanotransduction. We therefore sought to investigate the molecular identity of this ion channel and two approaches were employed to do this. One approach was to attempt to identify a high affinity, conopeptide ligand for this ion channel (Chapter 5) and the other was to examine MA currents in neurons derived from mice lacking the genes for candidate ion channels. In this section work is reported investigating the response properties of neurons taken from ASIC2 and ASIC3 null mutants and from double knockouts lacking both of these genes. Also briefly reported are MA currents in ASIC1 nulls.

Work in *C. elegans* demonstrating that two members of the DEG/ENaC ion channel superfamily, MEC-4 and MEC-10, are required for sensing light touch has stimulated much interest in the idea that related ion channels may function as mechanosensors in vertebrates (Section 1.2.2). There is now excellent evidence that in nematodes MEC-4 and MEC-10, with MEC-6, form an ion channel at the core of a mechanotransduction complex including intra- and extracellular binding proteins (Tavernarakis and Driscoll, 1997; Ernstrom and Chalfie, 2002). The first known vertebrate homologues of these channels were the ENaC channels and much work has been undertaken to assess if these channels are mechanosensitive, although as yet the results of these studies remain

ambiguous (see Section 1.2.2.2). The identification of ASICs and the finding that these channels are highly expressed in sensory neurons, in some cases selectively, led to the hypothesis that they function in mammalian mechanosensation (Section 1.2.2.3).

Two lines of evidence support a function for ASICs in sensory mechanotransduction. Firstly, ASIC2 (Price *et al*, 2000; García-Añoveros *et al*, 2001) and ASIC3 (Price *et al*, 2001) immunoreactivity is detectable in a number of peripheral mechanosensory structures. Secondly, ASIC2 and ASIC3 null mutants, assessed with the skin-nerve preparation, have a number of aberrations in mechanosensation (Price *et al* 2000; 2001; Fig. 1.5). In ASIC2 knockouts mechanically evoked firing rates of rapidly adapting, and to a lesser degree slowly adapting, Aβ mechanoreceptors were lower than wild-type responses. In ASIC3 knockouts, mechanosensory abnormalities were also observed although responses to heat and acid were also altered; Aδ-nociceptors showed reduced firing frequencies in response to mechanical stimulation and increased activation thresholds, whereas rapidly adapting mechanoreceptors exhibited increased firing. In C-fibres, responses to pH 5 and noxious heat were both reduced. These data thus suggest a role for ASICs in sensory transduction; however, no direct evidence has been presented demonstrating mechanical activation of ASICs. ASICs could modulate mechanosensory function by either regulating mechanosensitive ion channel expression or function, by actually transducing mechanical stimuli or by acting downstream of mechano-transduction. It was therefore decided to assess MA currents in ASIC2 and/or ASIC3 null mutant neurons to determine if aspects of these currents were altered by loss of these genes.

In these experiments action potential duration was used to define subpopulations of neurons as this parameter is a strong predictor of the mechanosensitive phenotype of DRG neurons; narrow, uninflected action potentials being indicative of low threshold, A-fibre mechanoreceptors whereas wide action potentials with an inflection on the falling phase are generally associated with high threshold mechanoreceptors and nociceptors (Rose *et* al, 1986; Koerber *et al*, 1988; Ritter and Mendell, 1992; Sections 1.1.1.1 and 1.3.1). The use of this parameter to classify neurons is only possible in adult animals as

membrane properties of sensory neurons reach a mature state after around postnatal week 3 (Fitzgerald and Fulton, 1992). Moreover, the use of capsaicin sensitivity to categorise murine neurons is problematic due to the apparently less abundant expression of TRPV1 in mice relative to rats (see Section 1.3.1).

4.2 Materials & Methods

4.2.1 Generation of ASIC1, ASIC2 and ASIC3 Null Mutants (ASIC2 by Margaret P Price and ASIC1 and 3 by Daniel K Rohrer)

The ASIC1 null mutants were generated by ablation of a 341 base pair sequence (nucleotides 1434-1774 corresponding to amino acids 297-410) by insertion of a 7kb lacZ-neo insert into the ASIC1 gene. This region is expressed in both splice variants (ASIC1a and 1b) of this gene. The ASIC2 null mutants used in this study were described in Price *et al* (2000). Briefly, a neo cassette was inserted into the ASIC2 gene to replace two exons encoding the entire second transmembrane domain and part of the putative pore forming domain.

Genetic disruption of the mouse ASIC3 gene was carried out by a standard positive-negative selection scheme (Mansour *et al*, 1988) in mouse R1 embryonic stem cells (Nagy *et al*, 1993). The targeting vector contained a 2.3 kb Hind3/Nsi1 5' arm of homology (-2211 to +83 relative to the initiator ATG codon) and a 6.2 kb Sph1/Sph1 3' arm of homology (+1880 to +8083 relative to ATG), flanking the TK-neo positive selection cassette (Fig. 4.1a). This led to the deletion of the first two coding exons (containing amino acids 28-229). Speed Congenics (Jackson Laboratories, Bar Harbor, ME, see http://jaxmice.jax.org/library/communication/communication06.pdf) was applied to ASIC3 gene-targeted mice, utilizing C57Bl/6J mice as the backcross strain. ASIC3 heterozygous null mice, determined to be genetically >99% C57Bl/6J by marker-assisted backcrossing, were then intercrossed to generate ASIC3 homozygous-null mice.

In both cases experimental animals were the offspring of matings of either KO or wild-type pairings from the offspring of heterozygous parents. To generate mice lacking both genes ASIC2 nulls were bred to ASIC3 nulls to generate animals heterozygous for both genes. These animals were then crossed and double KOs and wild-type offspring were selected from the resultant offspring to breed lines of wild-type and double KO mice. Therefore, in all experiments wild-type and KO mice were "first cousins".

4.2.2 ASIC3 Expression Studies (performed by Dr Daniel K Rohrer)

Total RNA was isolated using the Trizol® reagent (InVitrogen, Carlsbad, CA). 2 mice were used for each tissue tested, with the exception of dorsal root ganglia (DRG), which, owing to their small size, were pooled for sufficient RNA template. Reverse transcriptase-polymerase chain reaction (RT-PCR) amplification of ASIC3 mRNA was done using 1μg of total RNA in the Supercript™ One Step RT-PCR system (InVitrogen). Glyceraldehyde phosphate dehydrogenase (GAPDH) was used as an internal standard. RT-PCR was carried out under the following thermal cycling conditions: 50°C, 30 min; followed by 94°C, 3 min. This first step was then followed by 30 cycles of 94°C, 30 sec; 60°C, 1 min; 72°C 2.5 min and a final extension step of 72°C, 10 min. Primer sequences spanned exon-intron boundaries so that products of the expected size could only be derived from properly spliced mRNA templates. Primer sequences used for RT-PCR were as follows:

ASIC3 sense primer = 5'ATGAAACCTCCCTCAGGACTGGAG 3'

ASIC3 antisense primer = 5' TTCCTCCTGGCCGTGGATCTGCAC 3'

Expected amplicon = 741 bp

GAPDH sense primer = 5' TCAACGACCCCTTGATTGACC 3'

GAPDH antisense primer = 5' GGATGCAGGGATGATGTTCTGG 3'

Expected amplicon = 534 bp.

Products were electrophoresed on 1% agarose gels stained with ethidium bromide, and photographed. Gels were then subjected to Southern blot transfer, and ^{32}-P labelled probes specific for ASIC3 and GAPDH were used to verify the amplification products.

4.2.3 Genotyping of ASIC1/2/3 Mice (done mainly by Karen E Blaver)

To genotype mice, genomic DNA was extracted from tissue samples taken from the tip of the animals' tails. Following digestion of the tails in proteinase K (0.1 mg/ml in Tris buffer with 2% SDS, incubated overnight at 55°C), DNA was extracted using isopropanol and then washed twice in 70% ethanol.

In each case PCRs for the products of the knockout and wild-type gene sequences were carried out in separate reactions. Primers and thermal cycling conditions used for PCR were as follows:

ASIC1

Wild-type primers: 5' CCTGCAATGCTGTTACCATGGACT 3'
5' GATCTGCACACTCCTTGTACTGCT 3'
Expected amplicon = 500 bp

Knockout primers: 5' CTTGGGTGGAGAGGCTATTC 3'
5' AGGTGAGATGACAGGAGATC 3'
Expected amplicon = 280 bp

94°C, 90 sec, then 35 cycles of 94°C, 30 sec; 55°C, 45 sec and 72°C, 45 sec and a final extension step of 72°C, 2 min.

ASIC2

Wild-type primers: 5' GAAGAGGAAGGGAGCCATGATGAG 3'
5' AGTCCTGCACGGTGGGAGCTTCTA 3'
Expected amplicon = 350 bp

Knockout primers: 5' TGG ATG TGG AAT GTG TGC GA 3'
5' ATG GTT TGC GAG TGG TTT GGC ATT GTG 3'
Expected amplicon = 450 bp

94°C, 3 min, then 40 cycles of 94°C, 45 sec; 60°C, 45 sec and 72°C, 1 min and a final extension step of 72°C, 2 min.

ASIC3

Wild-type primers: 5' ATGAAACCTCCCTCAGGACTG 3'

5' CACTGTGAAGTTCTCAGGTCC 3'

Expected amplicon = 536 bp

Knockout primers: 5' ATGAAACCTCCCTCAGGACTG 3'

5' GCTTCCTCTTGCAAAACCACACTGC 3'

Expected amplicon = 257 bp

94°C, 3 min. Then 41 cycles of 94°C, 30 sec; 66°C, 1 min and 72°C, 1 min and a final extension step of 72°C, 2 min.

PCR products were visualised using gel electrophoresis (1 agarose gels) and ethidium bromide staining. Examples of PCR products for ASIC2 and ASIC3 wild-type, heterozygous and knock out animals are shown in Fig. 4.1c.

4.2.4 Electrophysiology, Mechanical Stimulation and Drug Application

DRG cultures from adult mice (ASIC2 and ASIC2/3 KOs: 6-9 weeks, ASIC3 KOs: 14-16 weeks) were prepared as described in Section 2.1.2. All experiments with ASIC2 mice and the majority of other experiments were performed *blind* to the genotype of the animal used.

Electrophysiological recordings were made as described in Section 2.2, application of drugs and mechanical stimulation was as outlined in Section 2.2.4 and IB4 staining was performed as described in Section 2.2.2. Standard solutions (Section 2.2.3) were used for nearly all experiments except when testing the blocking efficiency of ruthenium red on inwards and outwards currents where a caesium based internal solution was used (in mM): 110 $CsMetSO_4$, 30 CsCl, 1 $MgCl_2$, 10 HEPES, pH 7.3 (adjusted using CsOH).

Following seal formation, a series of incrementing mechanical stimuli were applied to the neuron in voltage-clamp. The recording configuration was then switched to current-clamp and incrementing, depolarising currents were passed to elicit action potentials.

Subsequently, in voltage clamp the presence or absence of tetradotoxin resistant (TTX-r) voltage-activated sodium currents was noted and the characteristics of the cell's responses to protons and capsaicin were determined.

Action potentials were evoked by 1 msec (20 msec for ASIC2 mice) square waves of depolarising current. TTX-r Na^+ currents were evoked by applying an incrementing family of 10 msec depolarising voltage steps (-70 - +70 mV) whilst the neuron was perfused in 300nM TTX. Capsaicin (1 μM) and low pH (pH 5.3) were applied for 4 sec using a multibarrel rapid solution changer (Biologic) and ruthenium red was applied through a single tube with multiple inputs superfusing the neuron.

Neuron diameters were determined as the mean of the shortest and longest "diameters" measured using imaging software (Openlab). Action potential amplitude was measured from a baseline potential of -70 mV to the peak potential change and the duration was measured as the width of the action potential at half the peak amplitude. For analysis of adaptation kinetics, exponentials were only fitted to currents over 150 pA. Data are presented as mean ± SEM.

4.2.5 Immunocytochemistry (done with Karen E Blaver)

Neurons were cultured from adult mice on 13 mm glass coverslips and after one day in culture were washed twice with PBS and then fixed using 4% paraformaldehyde (10 min). Cultures were washed (PBS, 3x) and then blocked and permeablised for 30 min in 10% goat serum and 0.1% Nonidet P-40 (NP40). Cells were then incubated in N52 monclonal primary antibody (1:800 in PBS + 10% goat serum) overnight at 4°C, washed (3x in PBS + 0.1% NP40) and then incubated in goat anti-mouse secondary antibody conjugated to FITC (1:400). Images were acquired with Openlab software using FITC filters (excitation 488 nm, emission 520 nm) and 40× dry lens. Diameters were taken as the mean of the shortest and longest "diameters". Experiments were performed *blind* to the genotypes of the cultures.

4.3 Results

4.3.1 Generation of ASIC3 Null Mutants (work by Dr Daniel K Rohrer)

ASIC3 null mutants were generated by using homologous recombination to delete amino acids 28-229 of the ASIC3 genes (Fig. 4.1b). This corresponds to removal of the majority of exon 1 and the whole of exon 2 which encode approximately the last third of the amino terminus, the first transmembrane domain and nearly half of the extracellular loop.

Using RT-PCR ASIC3 mRNA was detected in brain, spinal cord and DRG of wild-type animals but was absent from null mutants (Fig. 4.1d). ASIC3 nulls were indistinguishable from wild-type littermates in terms of gross morphology, behaviour and fertility.

4.3.2 Mechanically Activated Currents in Large, Wild-Type DRG Neurons

As shown previously (McCarter *et al*, 1999; Chapter 3) cultured sensory neurons responded to focal mechanical stimulation of their somata with an inward, cationic current. Overall, 70.2% (66/94) of large wild-type neurons (> 35 μm, mean 41.05 ± 0.29 μm) displayed mechanically activated (MA) currents. To determine if properties of the MA currents correlated with other aspects of neuronal phenotype neurons were divided into subpopulations.

Neurons were classified according to diameter, action potential properties and IB4 binding. In addition, responses to a low pH stimulus (pH 5.3) and capsaicin (1 μM) were recorded and the presence or absence of TTX-r voltage-activated sodium currents was noted. Others have described a robust correlation between action potential properties and the peripheral receptor type of DRG neurons: Low threshold mechanoreceptors have

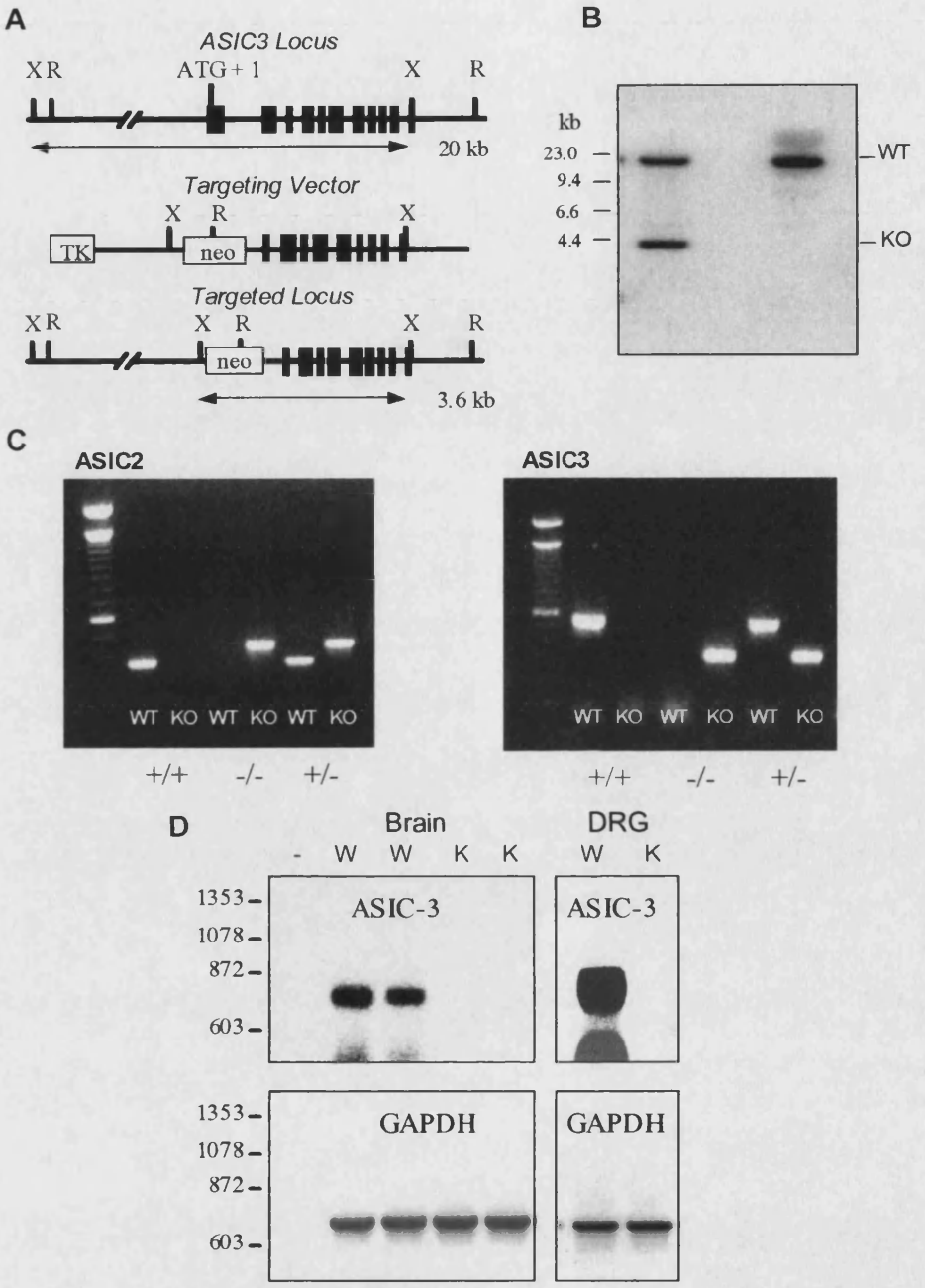

Fig. 4.1 Disruption of the ASIC3 gene in mice. *A*, The wild-type ASIC3 gene has 11 identified exons (rectangles). The wild-type ASIC3 locus is bounded by two XbaI sites, ~20 kb apart (X=XbaI, R=EcoR1). The middle panel shows the ASIC3 gene targeting vector that deletes most of exon 1 and all of exon 2. Targeted constructs acquired a new XbaI site, 3.6 kb upstream from the endogenous 3' XbaI site. *B*, Southern blot analysis of ASIC3 gene targeted ES cells. Wild-type and gene-targeted fragment sizes are indicated. *C*, Electrophoresis of the products of genotyping PCRs for the ASIC2 (*left*) and ASIC3 (*right*) strains of mice. PCRs for KO and WT genes were performed in separate reactions and an in parallel on the gel; shown for each strain are the products for a wild-type (*left*), knockout (*centre*) and heterozygous (*right*) mouse. *D*, RT-PCR analysis of mRNA expression in wild type and ASIC3 null mice. Separate reactions were carried out for GAPDH and ASIC3, under identical amplification conditions. Amplification products were electrophoresed, Southern blotted, and probed with ^{32}P cDNA probes. W = wild-type, K = ASIC3 null, (-) = no RNA.

narrow, uninflected action potentials and high threshold mechanoreceptors and nociceptors have wide, inflected action potentials (Koerber *et al*, 1988; Ritter and Mendell, 1992; Lawson, 2002). Therefore, large neurons were categorised into those with action potential durations of less than or equal to 1 msec (narrow action potentials) and those with action potentials of longer duration (wide action potentials). The majority of narrow action potentials had uninflected falling phases although some had very minor inflections whereas all wide action potentials showed prominent inflections during repolarisation (Fig. 4.2a). This was strongly correlated with the expression of TTX-r sodium currents; only 6.2% (2/32) of narrow action potential neurons expressed TTX-r currents while these currents were present in 97.9% (47/48) of neurons with wide action potentials.

Amongst large DRG neurons from wild-type animals a clear distinction was observed between MA currents expressed by narrow and wide action potential neurons (Fig. 4.2b). Of neurons with narrow action potentials 96.5% (55/57) expressed MA currents and of these 96.4% (53/55) responded to mechanical stimulation with rapidly adapting (RA) currents (Fig. 4.2c). The other two neurons that responded exhibited currents with significantly slower adaptation kinetics. Of the two neurons with narrow action potentials that expressed TTX-r sodium currents one was unresponsive and one had more slowly adapting MA currents.

In contrast, in neurons with wide action potentials, MA currents were only seen in 29.7% (11/37) of cells (Chi-square; $P < 0.001$) (Fig. 4.2b). Moreover, the neurons that responded displayed MA currents that were much smaller in amplitude and that exhibited distinctly slower adaptation kinetics than those seen in narrow action potential neurons (Fig. 4.2c) and (Fig. 4.2d) (2-way, repeated measures ANOVA; $P = 0.02$). The mean maximal response of narrow action potential neurons was 1.57 ± 0.21 nA compared to 0.37 ± 0.17 nA by wide action potential cells. Typical rapidly adapting MA currents in neurons with narrow action potentials were unaffected by exposure to 300 nM TTX; the currents in TTX were $99.1 \pm 1.4\%$ of control amplitude values ($n = 3$, Fig. 4.2e).

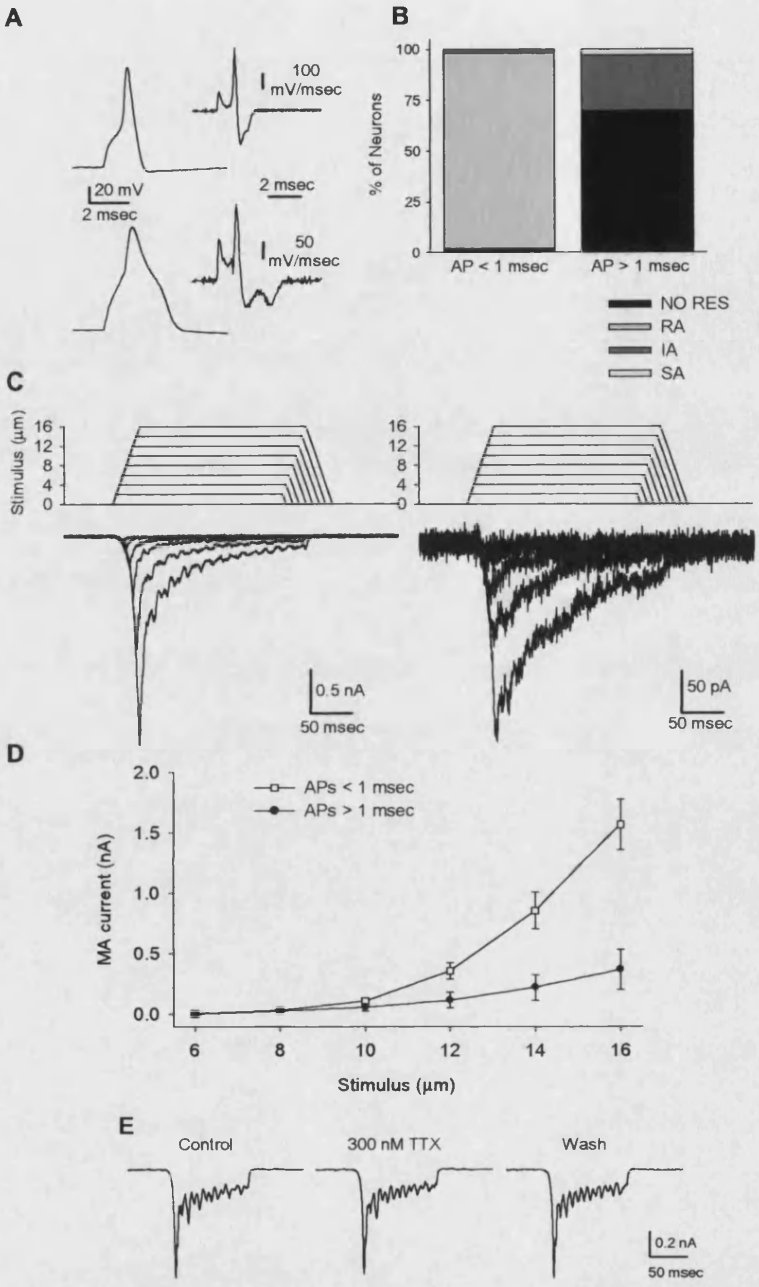

Fig. 4.2 Action potentials and mechanically activated currents of large, wild-type DRG neurons. *A*, Examples of narrow (*top*) and wide (*bottom*) action potentials of large DRG neurons. Action potential traces (*left*) and the differentials of these waveforms (*right*), allowing easier observation of inflections, are shown. *B*, Frequency histograms indicating the proportion of neurons with narrow (*left*) and wide (*right*) action potentials that respond to mechanical stimulation with rapidly adapting (RA), slowly adapting (SA), intermediately adapting (IA) or no (No Res) currents. *C*, Examples of MA currents (suprathreshold traces only). *Left*, RA current from a narrow action potential neuron. *Right*, IA current from a neuron with a wide action potential. *D*, Relationship between stimulus and MA current amplitude in neurons with narrow (*white squares*) and wide (*black circles*) action potentials. *E*, Example traces showing lack of effect of 300 nM TTX on rapidly adapting MA currents in neurons with narrow action potentials; *left*, control current, *centre*, current in the presence of 300 nM TTX and, *right*, currents after TTX removal.

Analysis of MA current kinetics revealed that the adaptation of RA currents was well fitted by two exponentials (Fig. 4.3a). Of the two derived tau values, tau 1 was 2.93 ± 0.07 msec (n = 126) and described the initial very rapidly adapting component of the current. Tau 2 was significantly longer, 53.05 ± 2.10 msec (n = 126) and described the later more slowly adapting part of the current. The amplitude of the component defined by tau 1 accounted for most of the current (77.6 ± 1.3%) whereas the more slowly declining component accounted for 22.2 ± 0.7%. Peak MA current amplitude for a 16 μm stimulus for each narrow action potential neuron was compared to the size of tau 1 and 2 to determine if the kinetics of the current changed as the amplitude increased. Current amplitude had a small positive correlation with tau 1 (Pearson's Product moment; r = 0.40, P < 0.01; Fig. 4.3b) and a much stronger correlation with tau 2 (r = 0.88, P < 0.001; Fig. 4.3c), i.e. current adaptation slowed with increasing current amplitude.

The kinetics of MA currents expressed by wide action potential neurons showed considerably more variation in their adaptation kinetics than did RA currents. Most MA currents were well fitted by a single exponential (example shown in Fig. 4.2c) whilst some were well fitted by 2 exponentials with a short tau 1 that accounted for only a minor fraction of the current amplitude (i.e. < 20%). Such cells were pooled in the category of intermediately adapting (IA) currents. One wide action potential cell responded with a slowly adapting (SA) MA current, such currents declined very little in amplitude over 200 msec and were also characterised by current amplitude reaching a peak during the stationary part of the stimulus (see for example Fig. 4.7e). This contrasts with both RA and IA currents where peak current amplitude occurred concurrently with cessation of probe movement.

4.3.3 Mechanically Activated Currents were Unchanged in Large DRG Neurons Derived from ASIC2 and/or ASIC3 Null Mutants

Price *et al* (2000) have shown that Aβ-fibres from ASIC2 null mutants had decreased firing rates in response to mechanical stimuli. Therefore a comparison was made of the MA currents of large neurons with narrow action potentials derived from ASIC2 KOs to

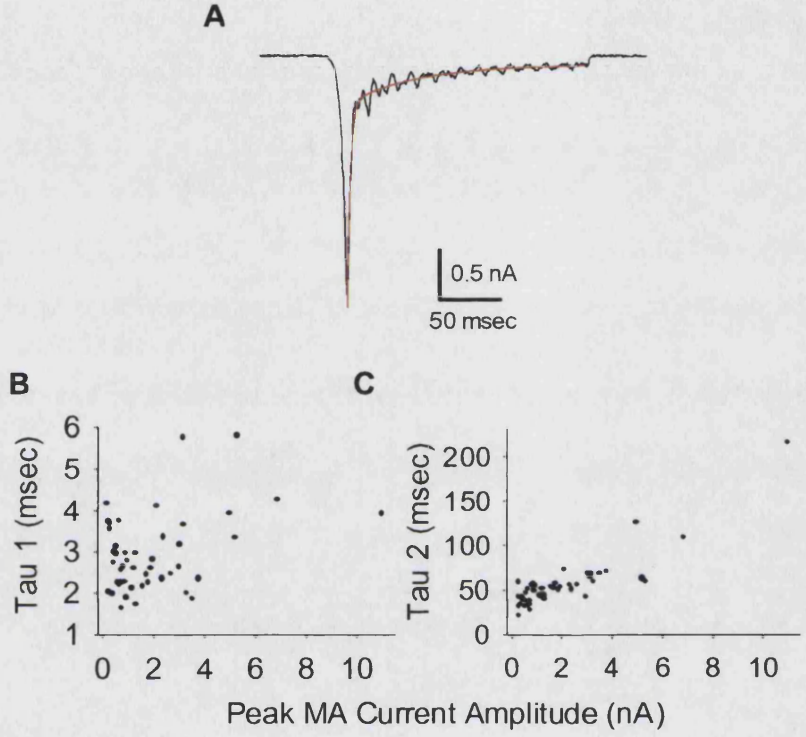

Fig. 4.3 Decay of rapidly-adapting MA currents is well described by two exponentials. *A*, Example of the fitting of two exponentials (*red* line) to the decay of a MA current (*black* line). *B*, *C*, Graphs show the relationship between peak current amplitude and the duration of Tau 1 (*B*) and Tau 2 (*C*) for RA MA currents evoked by a 16 mm stimulus (n = 46). In both cases there is a significant positive correlation between each variable for Tau 1, $r = 0.40$ (Pearson's Product Moment, $P < 0.01$) and for Tau 2 $r = 0.88$ ($P < 0.001$).

wild-type controls. As can be seen in Fig. 4.4a the mechanosensitivity of neurons from these two genotypes was not significantly different (2-way, repeated measures ANOVA; $P = 0.82$). The mean maximal amplitudes of MA currents were 2.66 ± 0.51 nA for KOs ($n = 21$) and 2.15 ± 0.55 nA for wild-types ($n = 21$). Similarly the kinetics of MA currents were unaltered by the deletion of the ASIC2 gene (Fig. 4.4b, 4.5b); ASIC2 KO vs wild-type; tau 1 = 3.00 ± 0.10 ($n = 63$) vs 2.89 ± 0.08 msec ($n = 56$), tau 2 = 62.03 ± 4.77 ($n = 63$) vs 57.36 ± 4.17 msec ($n = 56$). All neurons with narrow action potentials from the ASIC2 KOs and 21/22 from wild-type controls were mechanosensitive and generated RA currents (Fig. 4.5a).

Despite strong evidence that ASIC2 subunits coassemble into heteromeric ASIC channels that mediate transient low-pH gated currents, such currents in ASIC2 KOs show almost indistinguishable kinetics and amplitudes from wild-type currents (Price *et al*, 2000; Benson *et al*, 2002). In contrast, proton-gated currents are significantly slowed by the removal of ASIC3 (Price *et al*, 2001; Benson *et al*, 2002; Xie *et al*, 2002) and there is some alteration of mechanically evoked firing in RA Aβ-mechanoreceptors from these mutants (Price *et al*, 2001). The slowing of proton-gated currents in ASIC3 nulls was confirmed (see below) and then MA current characteristics were assessed. It was found that there was no change in either current amplitude (Fig. 4.4a) or in the response kinetics (Fig. 4.4b, 4.5d). Of neurons with narrow action potentials derived from ASIC3 nulls 88.9% (8/9) were mechanosensitive and all had RA currents (Fig. 4.5a). The mean evoked current of responding neurons by a 16 μm stimulus was 1.45 ± 0.46 nA ($n = 8$) for ASIC3 nulls and 1.51 ± 0.74 nA ($n = 8$) for wild-types. Neither tau 1 nor tau 2 differed significantly: ASIC3 KO vs wild-type; tau 1 = 3.51 ± 0.25 ($n = 20$) vs 3.02 ± 0.18 msec ($n = 15$), tau 2 = 52.71 ± 3.48 ($n = 20$) vs 47.06 ± 5.55 msec ($n = 15$).

It has been suggested that there may be a significant amount of functional redundancy amongst the ASIC ion channel family or that in null mutants there is functional compensation by related channels (Welsh *et al*, 2001). Therefore subsequent work focussed on the properties of MA currents of double knockout (DKO) mice lacking the genes for both ASIC2 and ASIC3. Comparison of MA currents from large neurons with

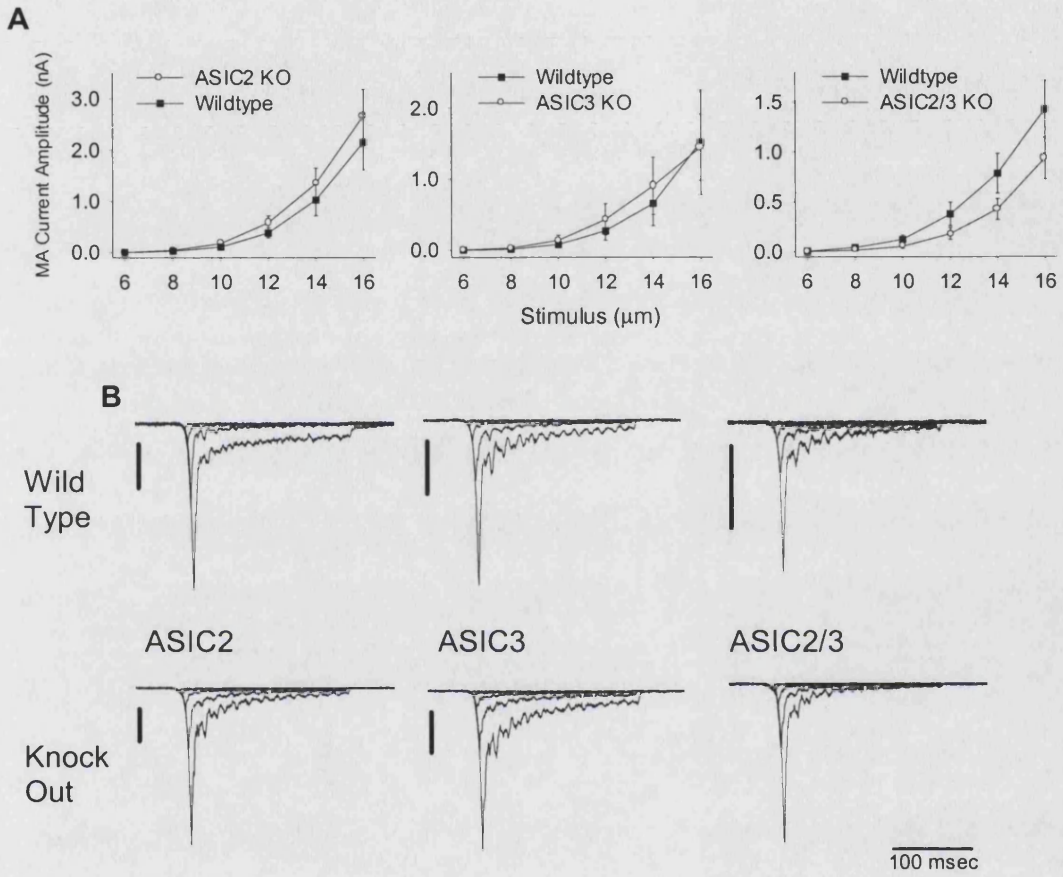

Fig. 4.4 Comparison of MA currents in large neurons from wild-type and ASIC2 and/or 3 null mutants. *A*, Graphs showing comparison knock outs' versus wild-type controls' stimulus-response relationships for MA currents from neurons with narrow action potentials; *left*, ASIC2 (KO; n = 21, WT; n = 21), *centre*, ASIC3 (KO; n = 8, WT; n = 8) and *right*, ASIC2/3 (KO; n = 25, WT; n = 25) (n = 21, 8 and 25, respectively). *B*, Example traces of RA MA currents from narrow action potential neurons (all vertical scale bars: 1 nA). *Bottom*, traces from null mutants and, *top*, from wild-types for ASIC2 (*left*), ASIC3 (*middle*) and ASIC2/3 (*right*).

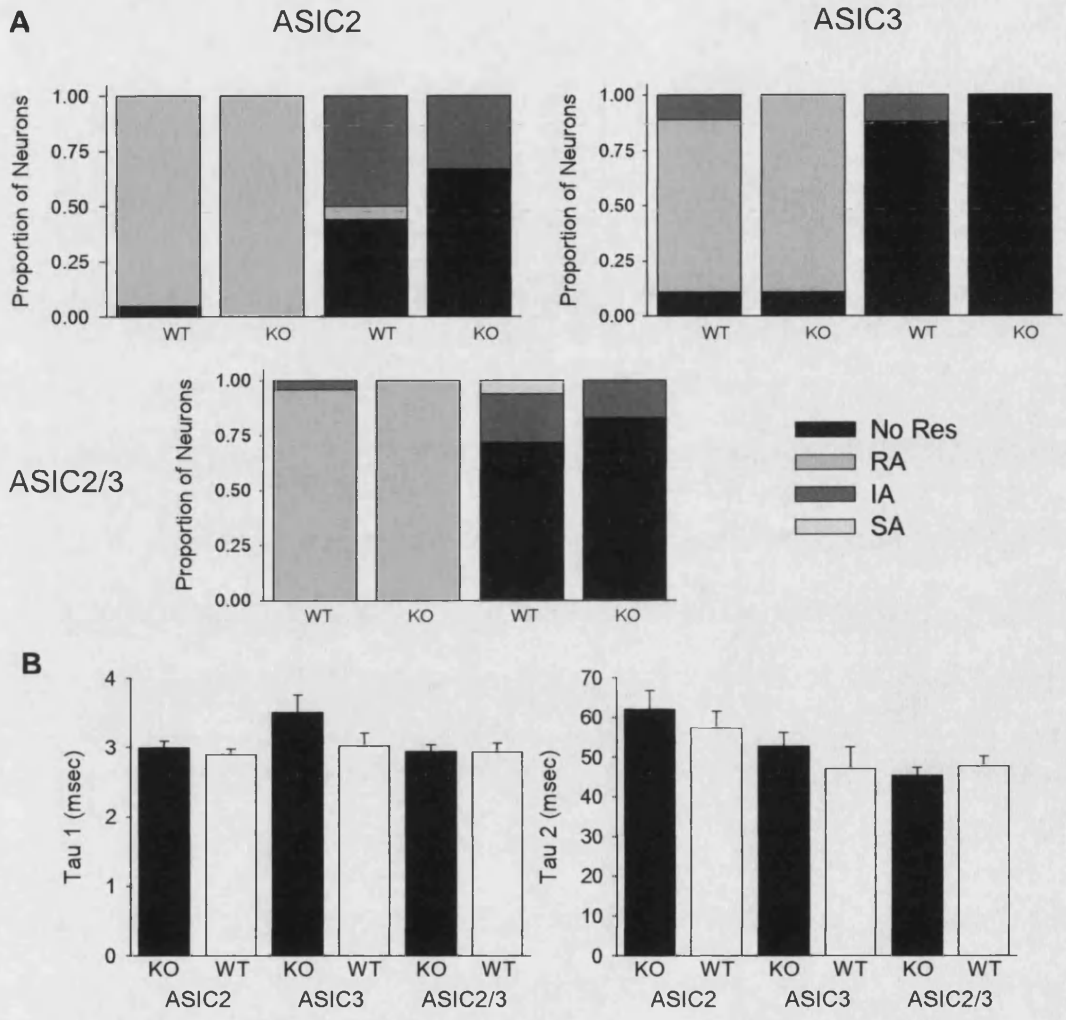

Fig. 4.5 Comparison of MA currents in large neurons from wild-type and ASIC2 and/or 3 null mutants. *A*, Frequency histograms for responses to mechanical stimulation of narrow (*left*) and wide (*right*) action potential neurons for null mutants (*right*) and wild-type controls (*left*). When comparing knockouts to wild-types there were no significant differences between distributions. *B*, Comparison of Tau 1 (*left*) and Tau 2 (*right*) values for RA MA currents between wild-type controls (*white*) and null mutants (*black*): ASIC 2 (*left*), ASIC3 (*centre*) and ASIC2/3 (*right*). The adaptation of currents in knockout neurons did not significantly differ from that of currents in wild-type neurons.

narrow action potentials showed that there was a trend towards currents being of smaller amplitude in the ASIC2/3 DKOs but this difference was not significant (Fig. 4.4a, 2-way, repeated measures ANOVA; $P = 0.09$). Peak MA current amplitude in wild-types was 1.43 ± 0.28 nA ($n = 25$) compared to 0.93 ± 0.21 nA ($n = 25$) in DKOs. The removal of these two genes together did not alter the kinetics of the observed MA currents (Fig. 4.4b, 4.5d). ASIC2/3 DKO vs wild-type: tau 1 = 2.94 ± 0.10 ($n = 44$) vs 2.94 ± 0.13 msec ($n = 55$), tau 2 = 45.37 ± 2.11 ($n = 44$) vs 50.95 ± 2.09 msec ($n = 55$).

In all three KO strains large neurons with wide action potentials were either unresponsive to mechanical stimuli up to a 16 μm displacement (ASIC2 KO 44.4% (8/18); ASIC3 KO 100.0% (8/8); ASIC2/3 DKO 83.3% (5/6)) or displayed MA currents with IA kinetics, except for one ASIC2 KO neuron which had RA MA currents (AP width: 1.1 msec). In no mouse strain were the proportions of cells that did not respond different from that found for wild-type controls (Fig.4.5a). Also the mean amplitude of evoked responses did not differ between each KO strain and control (data not shown).

Comparison of neuronal resting potential, action potential duration, action potential amplitude and action potential maximal rate of rise (dV/dt_{max}) between genotypes for each strain revealed only one difference (Table 4.1); dV/dt_{max} was significantly smaller in ASIC2/3 DKO narrow action potential neurons versus wild-type; 368.00 ± 12.66 vs 432.20 ± 24.21 mV/msec (Student's, unpaired t-test, $P = 0.02$). The functional significance of this finding is unclear.

4.3.4 Ruthenium Red Voltage-Dependently Blocks Mechanically Activated Currents

Ruthenium red blocked all MA currents in neonatal rat neurons with an IC_{50} value of around 4 μM (Section 3.3.4). Here the ability of 5 μM ruthenium red to inhibit MA currents was tested in neurons that displayed RA inward currents from wild-type and ASIC2/3 DKOs. At a holding potential of –70 mV this concentration reduced responses by 43.27 ± 4.57% ($n = 5$) and 47.08 ± 2.15% ($n = 4$), respectively (Fig. 4.6a, b), indicating that there was no difference in phenotypes. The ability of ruthenium red to

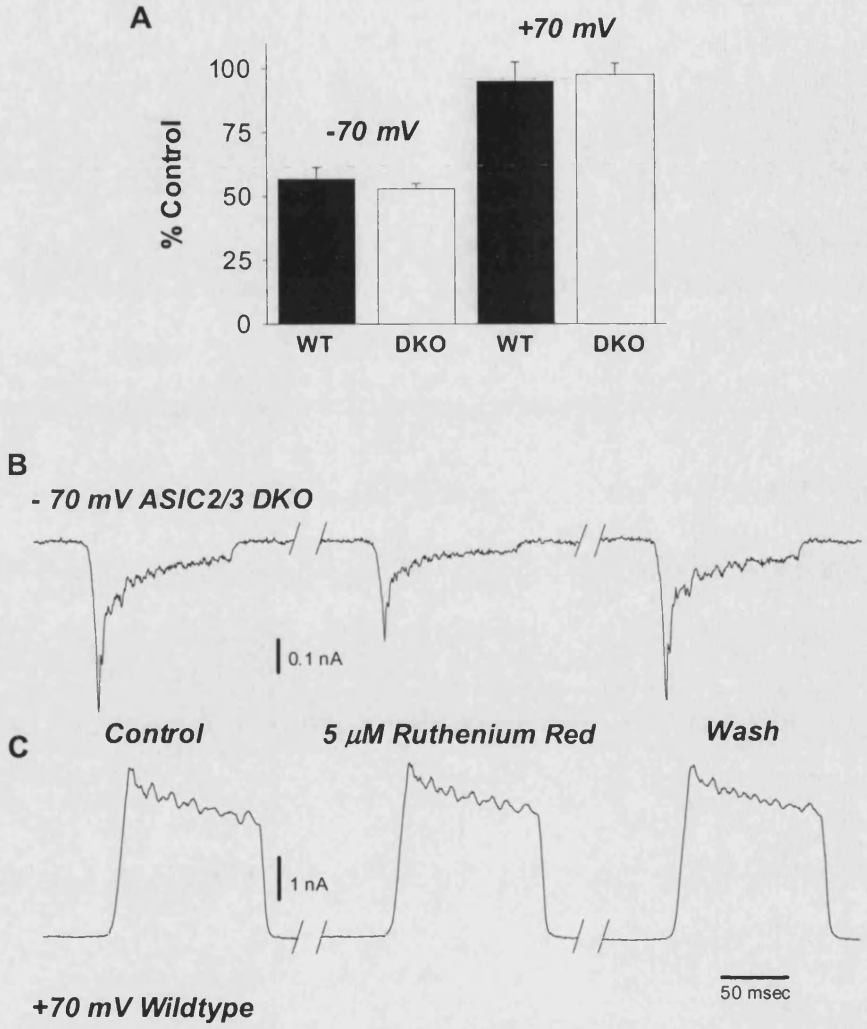

Fig. 4.6 RA MA currents are voltage dependently blocked by ruthenium red. *A*, Inhibition of RA MA currents by 5 μM ruthenium red at a holding potential of –70 mV (*left*) and +70 mV (*right*) in wild-type (*black*) and ASIC2/3 DKOs (*white*). *B*, Example traces of ruthenium red blockade of MA currents in a wild-type neuron held at –70 mV. *C*, Example traces showing no effect of ruthenium red at +70 mV in an ASIC2/3 DKO neuron.

block outward MA currents evoked at positive holding potentials (Section 3.3.1) was then tested. Interestingly, it was observed that ruthenium red block of MA currents was strongly voltage dependent. When 5 μM ruthenium red was applied to neurons held at +70 mV, outward MA currents were not inhibited in either genotype (ASIC2/3 DKO: 97.53 ± 4.53%, $n = 3$, of control vs wild-type 95.02 ± 7.52%, $n = 2$) (Fig. 4.6a, c).

Cell Type	*n*	Diameter (μm)	Resting Potential (mV)	Action Potential Duration (msec)	Action Potential Amplitude (mV)	dV/dt_{max} (mV/msec)
2/3 KO Large						
RA – KO	25	42.43 ± 0.60	-63.10 ± 0.48	0.72 ± 0.02	126.40 ± 1.47	368.00 ± 12.66
RA – WT	25	42.21 ± 0.72	-64.37 ± 0.53	0.70 ± 0.03	127.77 ± 2.62	432.20 ± 24.21
Non-RA KO	6	44.14 ± 1.66	-61.04 ± 0.73	1.78 ± 0.16	135.58 ± 2.00	304.17 ± 29.84
Non-RA WT	19	40.70 ± 0.45	-60.01 ± 0.92	1.91 ± 0.12	133.97 ± 1.35	268.29 ± 17.17
2/3 KO IB4-						
RA – KO	3	31.92 ± 1.33	-55.41 ± 2.62	1.40 ± 0.70	135.25 ± 6.00	353.33 ± 56.00
RA – WT	6	31.45 ± 0.94	-60.88 ± 2.05	0.68 ± 0.07	131.88 ± 3.59	410.00 ± 23.13
S/IA – KO	9	29.97 ± 0.83	-58.47 ± 1.38	2.13 ± 0.30	136.22 ± 2.54	236.88 ± 32.07
S/IA – WT	11	31.01 ± 0.66	-59.09 ± 0.87	1.95 ± 0.22	136.75 ± 1.98	245.91 ± 17.01
No – KO	13	29.75 ± 0.75	-59.25 ± 1.05	3.18 ± 0.50	136.23 ± 1.05	233.85 ± 23.86
No - WT	18	30.25 ± 0.50	-57.18 ± 1.04	1.88 ± 0.17	139.39 ± 1.75	285.83 ± 15.20
Wide AP KO	22	29.73 ± 0.54	-58.49 ± 0.79	2.87 ± 0.33	136.54 ± 1.39	230.48 ± 17.36
Wide AP WT	29	30.48 ± 0.40	-58.03 ± 0.76	1.92 ± 0.13	139.29 ± 1.09	272.41 ± 12.32
2/3 KO IB4+						
IA – KO	10	26.62 ± 0.48	-49.48 ± 1.24	3.00 ± 0.42	144.56 ± 1.65	219.50 ± 10.53
IA – WT	9	26.57 ± 0.60	-52.22 ± 1.35	2.83 ± 0.14	145.42 ± 1.09	231.11 ± 11.48
No – KO	10	27.83 ± 0.92	-50.40 ± 1.25	3.46 ± 0.40	142.80 ± 2.88	208.25 ± 15.38
No – WT	7	27.46 ± 0.88	-51.54 ± 1.06	2.88 ± 0.37	145.82 ± 1.36	233.57 ± 12.18
Wide AP KO	20	27.22 ± 0.53	-49.94 ± 0.86	3.23 ± 0.29	143.68 ± 1.68	213.88 ± 9.16
Wide AP WT	16	26.96 ± 0.50	-51.92 ± 0.87	2.85 ± 0.17	145.59 ± 0.83	232.19 ± 8.10
2 KO Large						
RA – KO	22	39.87 ± 0.81	-62.04 ± 0.79	0.76 ± 0.03	141.39 ± 1.85	471.14 ± 13.55
RA – WT	21	41.05 ± 0.45	-62.70 ± 0.56	0.78 ± 0.02	138.80 ± 2.56	459.29 ± 15.37
Non-RA KO	17	39.75 ± 1.12	-61.33 ± 0.88	1.72 ± 0.19	143.53 ± 2.02	350.28 ± 21.44
Non-RA WT	16	40.72 ± 0.63	-61.27 ± 0.69	1.77 ± 0.16	147.09 ± 2.15	313.13 ± 23.13
3 KO Large						
RA – KO	9	40.79 ± 0.63	-61.94 ± 0.87	0.60 ± 0.03	123.53 ± 2.75	409.44 ± 31.54
RA – WT	8	40.79 ± 0.85	-60.75 ± 0.44	0.61 ± 0.02	129.81 ± 2.95	467.50 ± 22.97
Non-RA KO	5	37.54 ± 1.01	-60.55 ± 1.17	1.35 ± 0.21	139.60 ± 2.25	314.00 ± 17.92
Non-RA WT	8	38.95 ± 0.72	-58.59 ± 2.38	1.34 ± 0.27	136.06 ± 2.65	340.63 ± 29.02

Table 4.1 Physiological properties of neurons defined by their genotype, size and their response to mechanical stimulation. The table shows the mean (± standard error) diameter, resting potential, action potential amplitude and duration and the maximum rate of change of membrane potential for each subpopulation of neurons. Action potentials were evoked at a membrane potential of –70 mV. Action potential duration measured at half maximal amplitude.

4.3.5 Mechanically Activated Currents in Small-Medium Neurons from Wild-type and ASIC2/3 Null Mutants

Responses of small-medium diameter (< 35 μm, mean 29.52 ± 0.38 μm) DRG neurons to mechanical stimulation were also tested and wild-type responses were compared to those of ASIC2/3 DKOs. Nearly all small-medium neurons exhibited wide action potentials (88.2%, 45/51) and overall 51.0% (26/51) of them responded to mechanical stimulation up to a 12 μm displacement. For analysis, neurons were first subdivided according to whether they bound the isolectin IB4.

The mechanical response properties of neurons that did not bind IB4 (IB4-) fell into four categories: 51.4% (18/35) of wild-type neurons did not respond to displacements up to 12 μm, 17.1% (6/35) responded with RA currents, 14.3% (5/35) had IA currents and 17.1% (6/35) displayed SA currents (Fig. 4.7a, c-e). The kinetics of RA currents and IA currents were similar to those observed in large neurons. RA currents (Fig. 4.7c) were well fitted by two exponentials, tau 1 (2.64 ± 0.21 msec, n = 8) described the initial very rapidly adapting component and the longer tau 2 (48.90 ± 6.39 msec, n = 8) described the second slowly decaying part of the response. IA currents (Fig. 4.7d) were again a mixture of those well described by a single exponential and those apparently better described by two but with the fast tau accounting for a minor part of the current. SA currents (Fig. 4.7e) were more prevalent amongst small nociceptive neurons than amongst large neurons.

MA currents observed in small IB4- neurons derived from ASIC2/3 DKO showed no significant differences from those seen in wild-type neurons. The proportion of neurons found to fall into each category was not altered: 52.0% (13/25) did not respond, 12.0% (3/25) showed RA currents, 24.0% (6/25) had IA currents and 12.0% (3/25) had MA currents that adapted slowly (Chi square; P = 0.73, Fig. 4.7a). Similarly, within each group the kinetics of the responses were not altered by the gene deletions (Fig. 4.7c-e). For RA currents tau 1 was 2.92 ± 0.37 msec (n = 6) and tau 2 was 49.81 ± 8.04 msec (n = 6). The mean evoked current amplitude of this class of neurons was unaltered in the

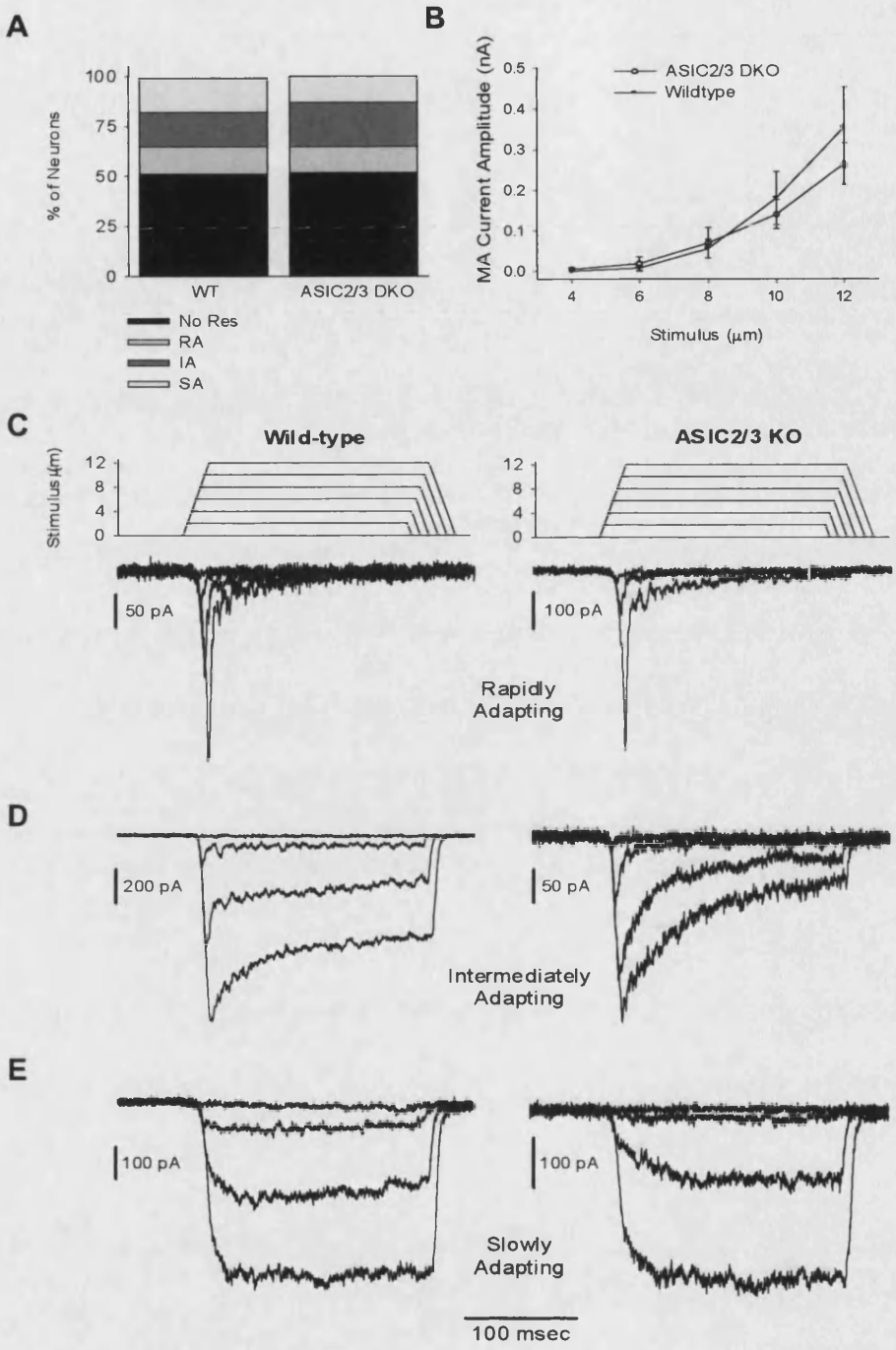

Fig. 4.7 MA currents exhibited by wild-type and ASIC2/3 DKO IB4- small-medium DRG neurons. *A*, Frequency histograms for responses of wild-type and ASIC2/3 DKO neurons; responses were of four types either slowly (SA), rapidly (RA) or intermediately (IA) adapting currents or neurons were unresponsive (No Res). *B*, Comparison of stimulus-response relation-ships for pooled data from IA and SA currents of wild-type (*black*, $n = 11$) and ASIC2/3 DKO (*white*, $n = 9$) neurons. *C-E* Example traces of RA, IA and SA currents, respectively, from wild-type (*left*) and ASIC2/3 DKO (*right*) neurons.

DKOs. The stimulus-response curves for pooled IA and SA MA currents are shown in Fig. 4.7b (2-way ANOVA, repeated measures; P = 0.37). No differences were seen between RA, SA and IA groups when analysed separately (data not shown).

Examination of the physiological properties of neurons classified according to their responses to mechanical stimulation revealed some trends within groups (Table 4.2). The majority of neurons that expressed RA currents also fired narrow APs (4/5 in wild-types and 2/3 in DKOs) and none responded to capsaicin. Neurons with SA currents were largely capsaicin insensitive (wild-type: 5/6, DKO: 2/2) but all expressed wide action potentials. Nearly all unresponsive neurons (wild-type: 17/18, DKO: 11/12) and IA MA current neurons (wild-type: 6/6, DKO: 4/4) had wide action potentials. Within these groups, in both genotypes, approximately half of the cells responded to capsaicin (Table 4.2).

MA Current	Genotype	AP > 1 msec	TTX-r	Capsaicin	pH 5.3	T:S:M
RA	WT	1/6	1/5	0/5	5/5	4:1:0
	DKO	1/3	2/3	0/3	2/2	1:1:0
SA	WT	6/6	5/5	1/5	5/5	3:1:1
	DKO	3/3	2/2	0/2	1/2	0:1:0
IA	WT	5/5	5/5	2/5	5/5	4:1:0
	DKO	5/5	5/5	2/4	4/4	2:2:0
No	WT	17/18	15/16	8/16	16/16	8:5:3
Response	DKO	11/12	12/12	5/11	10/10	6:4:0

Table 4.2 Response properties of IB4- small-medium neurons defined by their response to mechanical stimulation. Table shows the fraction of neurons in each category that have action potential durations over 1 msec, respond to capsaicin (currents > 50 pA), express TTX-r sodium currents and respond to pH 5.3 (currents > 50 pA). The final column indicates the kinetics of responses to pH 5.3: T = transient current, S = slow (persistent currents/TRPV1 mediated responses) and M = mixed currents.

Interestingly, action potentials of IB4- nociceptors were significantly longer in DKO neurons than in wild-type neurons (2.87 ± 0.33 msec (n = 22) vs 1.92 ± 0.13 msec (n = 29), Student's, unpaired t-test P = 0.01), which may in part be related to a lower maximal

rate of change of membrane potential in DKO neurons (230.48 ± 17.36 mV/msec vs 272.41 ± 12.32 mV/msec, $P < 0.05$).

In IB4+ neurons it was found that both wild-type and ASIC2/3 DKOs neurons were either unresponsive to mechanical stimulation or responded with IA currents. In each case the proportion was approximately 50%; in wild-type neurons 56.3% (9/16) responded whilst in DKOs 50.0% (10/20) responded (Fig. 4.8a). The mechanosensitivity of responding neurons was not significantly different between genotypes (2-way ANOVA, repeated measures; $P = 0.70$, Fig. 4.8b). Mean maximal currents were 434.05 ± 76.45 pA in DKOs and 360.88 ± 105.70 pA in wild-types. Residual currents were observed in these neurons that persisted after the withdrawal of the mechanical stimulus (e.g. Fig 4.8c). Such currents were not observed in other cell types and there significance is unclear. There were no differences in the physiological parameters of IB4+ neurons between genotypes or between those that responded to mechanical stimulation and those that did not (Table 4.1).

In neonatal rat, IB4+ neurons were essentially refractory to mechanical stimulation (Section 3.3.3) suggesting that there is either a species or a developmental difference that accounts for the observation of MA currents in the adult mouse IB4+ cells. To distinguish between these possibilities IB4+ neurons from young adult (p28) rats were mechanically stimulated. In 16 neurons tested, 43.8% (7/16) exhibited MA currents and of these 85.7% (6/7) displayed IA currents whilst the other cell had SA kinetics (Fig. 4.8a, c). The mean maximal evoked current was 0.30 ± 0.08 nA. Hence, there were no significant differences in MA currents exhibited by adult mouse and rat IB4+ neurons

Comparison of wild-type IB4+ and – nociceptors (i.e. neurons selected for having wide, inflected action potentials) revealed a number of differences between these two groups of cells. As previously reported by Stucky and Lewin (1999) IB4+ neurons had significantly longer action potentials than IB4- neurons (2.85 ± 0.17 msec vs 1.92 ± 0.13 msec, Student's, unpaired t-test, $P < 0.001$). However, in our recording configuration a number of other differences were apparent most notably the resting membrane potential

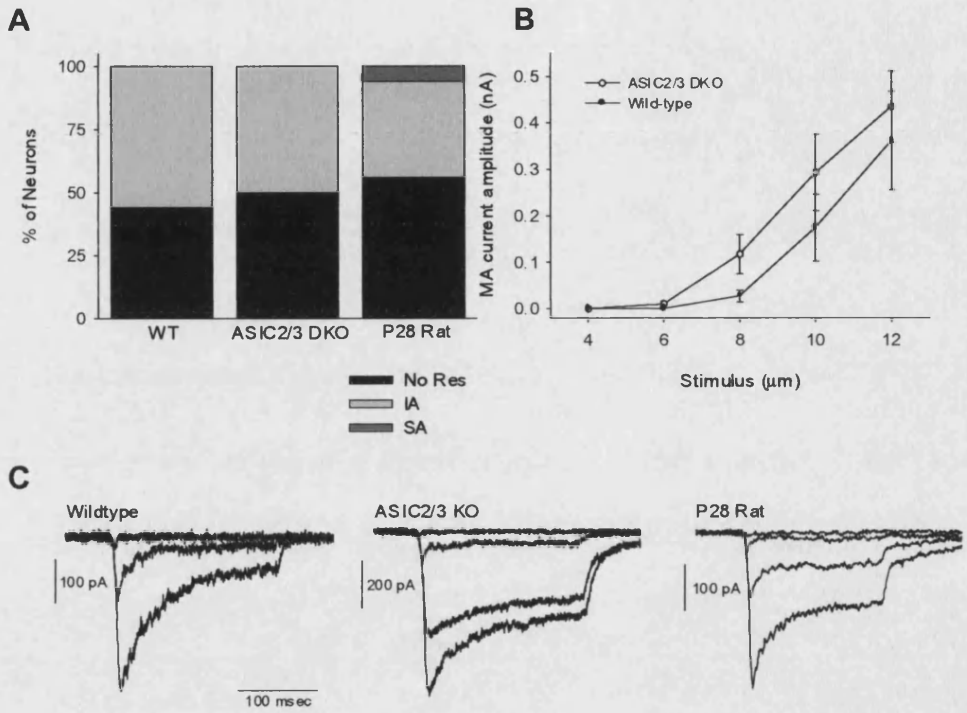

Fig. 4.8 MA currents exhibited by adult rat, wild-type mouse and ASIC2/3 DKO mouse IB4+ DRG neurons. *A*, Frequency histogram showing that approximately half of IB4+ neurons from wild-type (56.3%, *left*) and ASIC2/3 DKO (50.0%, *centre*) mice exhibited intermediately adapting MA currents whilst the remainder were unresponsive to mechanical stimulation. In the adult rat 56.3% of neurons did not respond; of those that did 6/7 had intermediately adapting kinetics and the seventh was slowly adapting. *B*, Comparison of stimulus-response relationships for wild-type (*black*, $n = 9$) and ASIC2/3 DKO (*white*, $n = 10$) neurons showing no significant difference between these populations. *C*, Example MA current traces from a wild-type (*left*), an ASIC2/3 DKO (*centre*) and an adult rat (*right*) neuron.

of IB4+ neurons was more depolarised than that of IB4- neurons (-51.92 ± 0.87 mV vs –58.03 ± 0.76 mV, Student's, unpaired t-test $P < 0.001$). Action potentials (recorded at a potential of –70 mV) were also significantly larger in IB4+ cells (145.59 ± 0.83 mV vs 139.29 ± 1.09 mV, $P < 0.001$) and the maximal rate of change of membrane potential was higher in IB4- neurons (272.41 ± 12.32 vs 232.19 ± 8.10 mV/msec, $P < 0.05$) (Table 4.1).

4.3.6 Low pH and Capsaicin Evoked Currents in Wild-type and ASIC2/3 Null DRG Neurons

As well as studying the association between ASICs and mechanosensitivity, the responses of different classes of DRG neuron to low pH (pH 5.3) were categorised and the response properties of neurons lacking the genes for ASIC2 and 3 to protons were recorded. As before, neurons were classified according to size, action potential duration and IB4 binding. Responses to low pH fell into three classes: Transient ASIC-like responses, slowly activating, persistent currents or mixed currents (in which a small transient current was activated prior to a slowly activating, persistent component) (see Fig. 4.9b, 4.10b).

Application of pH 5.3 solution to wild-type, large neurons evoked an inward current in 90.7% (49/54) of cells; the proportion of positive responses was similar amongst wide (85.7%; 18/21) and narrow (93.9%; 31/33) action potential classifications. However, division of responses according to desensitisation kinetics revealed significant differences between the two neuronal classes. Amongst neurons with narrow action potentials the predominant response was a slowly activating, persistent current seen in 71.0% (22/31) of responding neurons (Fig 4.9a, b). In contrast, no neurons with a wide action potential showed such a response in the absence of a transient component. Instead amongst this population 77.8% (14/18) neurons expressed transient currents typical of those mediated by ASICs (Fig. 4.9a, b). Transient proton-gated currents were seen in only 16.1% (5/31) of narrow action potential neurons. Moreover, the amplitudes of transient currents were significantly larger in neurons with wide action potentials, 2.67 ± 0.60 nA, than in narrow action potential neurons, 0.39 ± 0.12 nA (t-test, $P < 0.05$, Fig. 4.9c). In both groups the

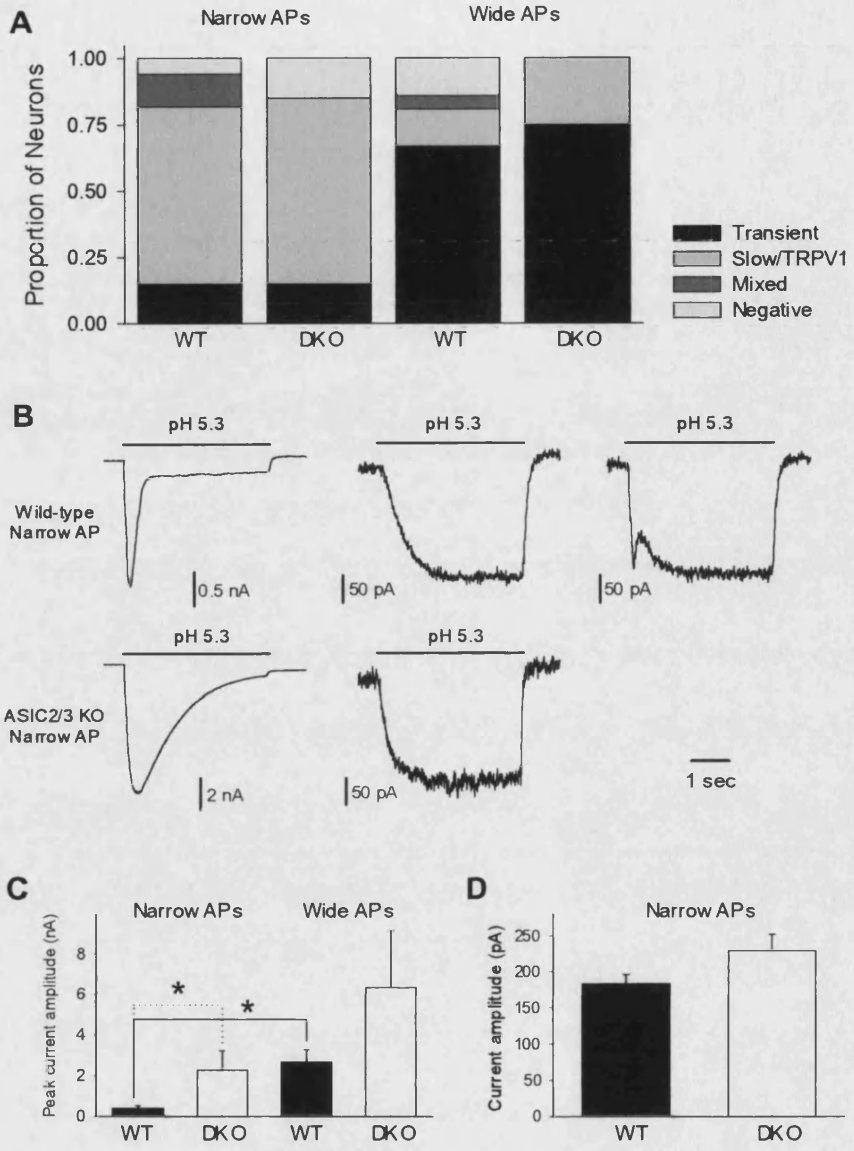

Fig. 4.9 pH 5.3-activated currents in large DRG neurons; ASIC2/3 DKO versus wild-type neurons. *A*, Frequency histograms of responses of different neuronal populations. *Left*, large neurons with narrow action potentials; *right*, large neurons with wide action potentials, *left,* wild-type and, *right*, nulls. Responses were classified as Transient, Slow or TRPV1 (slowly, activating persistent currents or currents likely TRPV1-mediated), Mixed (transient peak followed by slowly, activating persistent current) or Negative (non responsive). Mixed currents were absent in ASIC2/3 DKO neurons otherwise the proportions of each type of response were similar in each population. *B*, Example traces from wild-type (*top*) and ASIC2/3 DKO (*bottom*) large, narrow action potential neurons. *C*, Peak amplitudes of transient proton-gated currents; large neurons with narrow action potentials (*left*) and wide action potentials (*right*); wild-type (*black*) and ASIC2/3 DKO (*white*). Wild-type responses in wide action potential cells were larger than those of narrow action potential cells ($P < 0.05$). ASIC2/3 DKOs had larger currents than wild-types in narrow action potential neurons ($P < 0.05$) and there was a similar trend between wide action potential neurons ($P = 0.054$). *D*, Amplitudes of persistent proton-gated currents in large neurons with narrow action potentials; wild-type (*black*) and ASIC2/3 DKO (*white*).

duration and profile of the transient component was similar (Tau desensitisation, narrow action potential; 126.8 ± 16.6 msec, wide action potential; 194.2 ± 26.4 msec, $P = 0.12$) whereas the fractional amplitude of the sustained component varied. The amplitude of persistent currents was consistently small, the mean maximal amplitude amongst wild-type neurons with narrow action potentials was 197.4 ± 18.6 pA ($n = 22$, Fig. 4.9d). This also suggests in some neurons persistent currents may not have been apparent due to masking by concurrent activation of larger transient proton-gated currents. "Mixed" currents were seen in 12.9% (4/31) of narrow action potential neurons and 5.6% (1/18) of wide action potential cells (Fig. 4.9a, b). In three capsaicin-sensitive wide action potential neurons the response kinetics indicated that the currents were likely to be mediated solely by TRPV1 (data not shown). Consistent with previous observations (Section 3.3.10) there was no correlation between the amplitude or type of response to low pH and the response to mechanical stimulation.

In large ASIC2/3 DKO neurons the proportions of neurons with slow and transient currents were similar to wild-type although mixed currents were not observed. Amongst narrow action potential cells 85.0% (17/20) responded to low pH; 82.4% (14/17) had persistent currents and 17.6% (3/17) had transient responses (Fig. 4.9a, b). Four of four neurons with wide action potentials responded; 3/4 had transient currents and the remaining neuron displayed a slowly activating persistent current. The desensitisation kinetics of transient currents were similar in neurons generating narrow and wide action potentials but were much slower in DKO neurons than in wild-type neurons (Fig. 4.9b). The tau of desensitisation was 1.06 ± 0.08 sec for narrow action potential neurons and 1.15 ± 0.02 sec in wide action potential cells. There was a tendency for transient currents to be of larger amplitude in DKO neurons; in neurons with narrow action potentials the mean amplitude was 2.28 ± 0.96 (DKO) versus 0.39 ± 0.12 nA (wild-type) ($n = 3$, $P = 0.04$, Fig. 4.9c) and in wide action potential neurons it was 6.33 ± 2.82 versus 2.67 ± 0.60 nA ($n = 3$, $P = 0.054$, Fig. 4.9c). Slowly activating persistent currents were slightly larger in DKO neurons but the difference was not statistically significant; mean amplitude was 229.4 ± 21.2 pA ($P = 0.07$ versus wild-type, Fig. 4.9d). Changes in transient low pH evoked currents' kinetics in ASIC2 and ASIC3 knockouts were consistent with the

effects published by Benson *et al* (2001) and Xie *et al* (2002) (data not shown). However, while mixed kinetic currents were present in ASIC2 knockout neurons, they were absent from ASIC3 knockouts.

Only 4.3% (2/46) of large wild-type neurons with narrow action potentials responded to capsaicin (both responses were small, < 250 pA, and one of these cells generated a TTX-r sodium current). However, 25.0% (8/32) of large, wide action potential neurons were capsaicin sensitive. These responses varied widely in amplitude but tended to be larger than those of narrow action potential cells; the mean evoked current was 4.05 ± 2.36 nA (data not shown).

Next pH 5.3-evoked currents in small-medium nociceptive neurons, i.e. those with wide action potentials, were examined. Nearly all IB4- nociceptors responded to a pH 5.3 stimulus (wild-type; 100.0% (26/26) and ASIC2/3 DKO; 93.3% (15/16)). Responses to pH 5.3 in relation to responses to mechanical stimulation are summarised in Table 4.2. Amongst wild-type neurons, transient proton-gated currents were present in 50.0% (13/26) of cells, mixed currents in 15.3% (4/26) and persistent currents in 34.6% (9/26), where three examples of the latter class were likely TRPV1-mediated (Fig. 4.10a, b). In ASIC2/3 DKO neurons only sustained and transient currents were observed, transient in 46.7% (7/15) of responding neurons and sustained currents in 53.3% (8/15) (Fig. 4.10a, c), two of which were likely to be due to TRPV1 activation. Amongst either mutant or control nociceptors (neurons with wide action potentials), the desensitising components of transient currents were kinetically similar whereas the sustained components of these currents were more varied often due to the slow activation of TRPV1 receptors (data not shown, example shown in Fig. 9c was capsaicin insensitive). Between genotypes the tau of transient current desensitisation differed significantly. In wild-types it was 130.49 ± 6.56 msec (n = 13) compared to 1.41 ± 0.01 sec (n = 7) in DKOs. Transient currents were on average larger in ASIC2/3 DKO neurons, 5.25 ± 0.93 nA vs 2.06 ± 0.58 nA (Student's, unpaired t-test, $P < 0.01$), due mainly to a large reduction in the number of cells that expressed small (< 0.5 nA) transient currents in the mutant genotype. The amplitude of persistent currents was similar in DKO (116.1 ± 25.8 pA) and wild-type

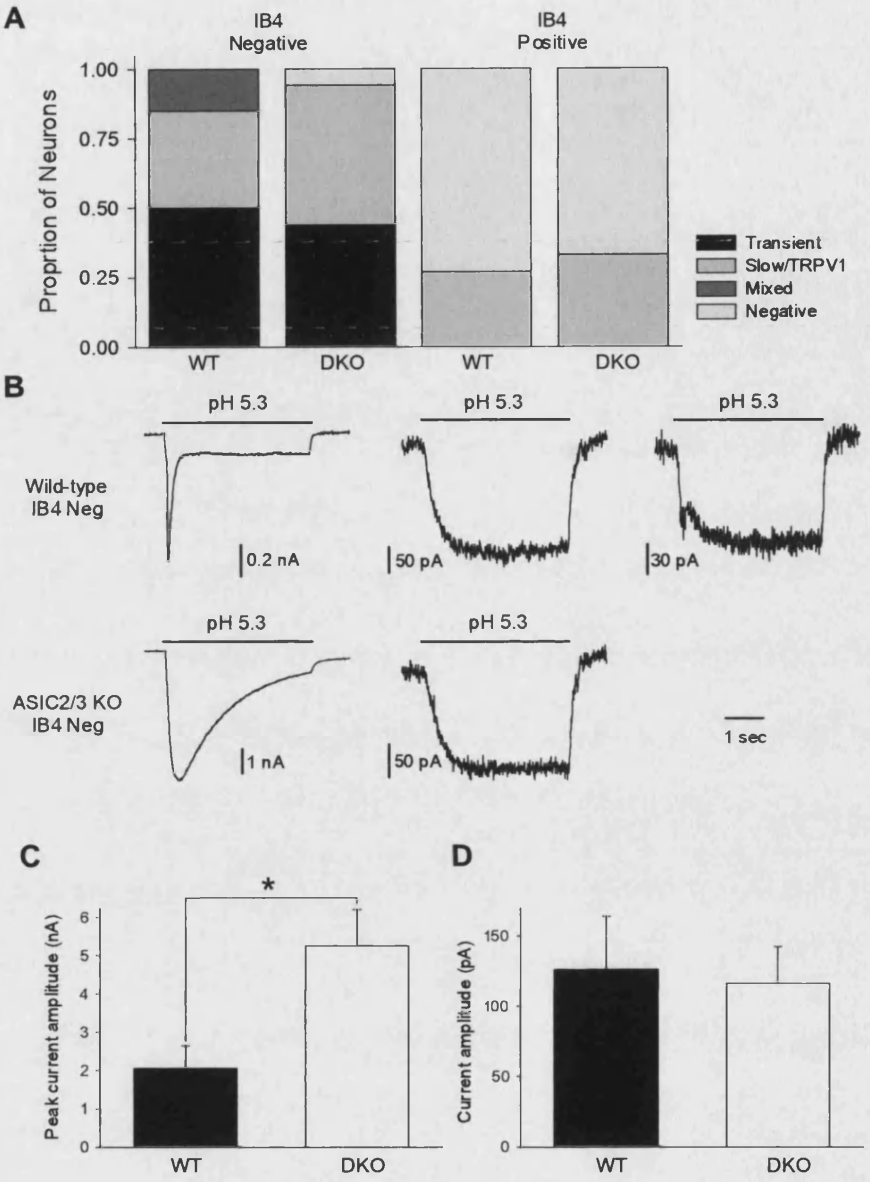

Fig. 4.10 Currents activated in small-medium DRG neurons by pH 5.3; comparison of ASIC2/3 DKO and wild-type neurons. *A*, Frequency histograms of the responses of different neuronal populations to pH 5.3. *Left*, IB4- nociceptors and, *right*, IB4+ nociceptors; wild-type columns are on the *left* and nulls on the *right*. Responses were classified as Transient, Slow/TRPV1, Mixed or Negative. In IB4- neurons the proportion of cells displaying transient currents was similar between genotypes (wild-type, 50.0%; DKO, 43.8%); mixed currents were absent from ASIC2/3 DKO neurons. The majority of IB4+ neurons did not respond to acidification and transient proton-gated currents were not observed in these cells. No distinction between genotypes was seen. *B*, Example traces from wild-type (*top*) and ASIC2/3 DKO (*bottom*) IB4- neurons with wide action potentials. *C*, Mean peak amplitude of transient currents in wild-type (*black*) and ASIC2/3 DKO (*white*) IB4- nociceptors; currents were significantly smaller in wild-type neurons ($P < 0.01$). *D*, Mean amplitude of persistent currents in capsaicin-insensitive wild-type (*black*) and ASIC2/3 DKO (*white*) IB4- nociceptors. No difference was found between genotypes.

(125.8 ± 37.9 pA, $P = 0.84$) neurons and mixed kinetics currents were consistently small (69.4 ± 5.2 pA).

As observed by Dirajlal *et al* (2002) transient acid evoked currents were absent from IB4+ neurons (Fig. 4.10a). In wild-type neurons 26.7% (4/15) tested for proton sensitivity showed small (<100 pA) sustained responses and 26.7% (4/15) were sensitive to capsaicin, 3 neurons responded to both. In DKO neurons 40.0% (6/15) responded to low pH (5/6 currents < 100 pA and the sixth (248 pA) had kinetics characteristic of a TRPV1 mediated response) and 16.7% (3/18) responded to capsaicin, 1 cell was sensitive to both (data not shown).

4.3.7 MA and Proton-Gated Currents in ASIC1 Null Mutant Neurons

Recordings were made from six medium-large neurons derived from an ASIC1 null mutant. Action potentials and responses to low pH were recorded from all neurons and responses to mechanical stimulation were recorded from five. Four of the six neurons had narrow action potentials (resting potential; -63.3 ± 1.1 mV, action potential duration; 0.58 ± 0.01 msec, amplitude; 131.3 ± 3.7 mV, dV/dt_{max}; 438.8 ± 54.0 mV/msec). Of these neurons, all responded to mechanical stimulation with RA currents; currents showed large variation in amplitude but did not differ significantly from currents recorded from any other strain of mouse, the mean amplitude to a 12 μm stimulus was 393.1 ± 218.7 pA. MA current kinetics were indistinguishable from other strains of mice tested (Fig. 4.11a). Of the two neurons with wide action potentials (1.7 msec and 2.3 msec) only one was tested for mechanical responsiveness; it generated a maximal current of 124.5 pA in response to a 16 μm displacement and the kinetics of the response were rapidly adapting. While this phenotype was rare, such characteristics were also found amongst some wild-type neurons.

In response to stimulation with pH 5.0, 5 of the 6 neurons responded with an inward current and in all 5 cases this current was slowly activating and persistent. (The neuron

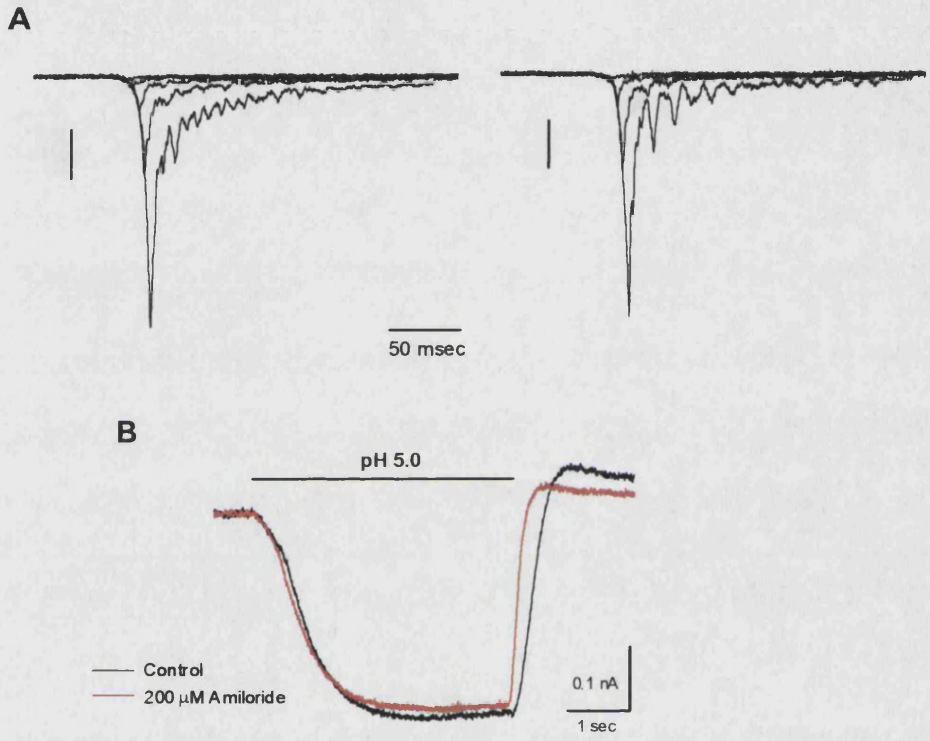

Fig. 4.11 Mechanically evoked and proton-gated currents in neurons derived from ASIC1 null mutants. *A*, Two examples of RA currents evoked by mechanical stimulation in 2 neurons with narrow action potentials. Vertical scale bars: 0.2 nA. *B*, Slowly activating, persistent proton-gated currents are present in ASIC1 nulls (*black*) and are not inhibited by 200 μM amiloride (*red*, n = 3), note however that currents inactivate more rapidly in the presence of amiloride.

that did no respond had a wide action potential.) In 3 neurons, these currents were recorded in the presence of 200 μM amiloride; the drug had no significant effect on current amplitude (paired t-test, $P = 0.65$) although it did have a small effect on the inactivation kinetics following the withdrawal of the stimulus, increasing the rate at which the current inactivated (Fig. 4.11b).

4.3.8 Deletion of ASIC2 and 3 does not Affect Cell Diameter of NF-200 Positive Neurons (work done with Karen Blaver)

Another aspect of the phenotype of ASIC mutants that was examined was the size distribution of neurons. It was considered that a putative mechanosensitive ion channel may play a role in cell growth and/or that changes in size may affect the ability of parts of a neuron to respond to pressure and/or its ability to conduct action potentials. To do so, the diameters of cell bodies of NF200 positive wild-type and ASIC2/3 DKO DRG neurons (Fig. 4.12b) were compared. Measurement of the diameters of 118 wild-type and 138 knockout NF200 positive neurons derived from 2 mice of each genotype revealed no difference in the size distribution of these neurons (Fig. 4.12a). Wild-type neurons were on average 32.2 ± 0.6 μm in diameter whereas knockout neurons were 32.5 ± 0.5 μm (t-test, $P = 0.69$).

4.3.9 MA Currents are not Mediated via Mechanically Evoked ATP Release

Mechanical stimulation evokes ATP release from a number of distinct cell types and ATP may then act in an autocrine or paracrine fashion (for examples see Nakumara and Strittmatter, 1996; Shiga *et al*, 2001; Birder *et al*, 2002). For example, in attempting to identify a mechanosensor using expression cloning in *Xenopus* oocytes Nakumara and Strittmatter (1996) isolated a cDNA encoding $P2Y_1$ as mechanical stimulation was activating this receptor through the release of ATP from the oocytes. Therefore, to test if MA currents in DRG neurons are mediated by or modulated by mechanically evoked ATP release, neurons were mechanically stimulated in the presence of apyrase (5 U/ml);

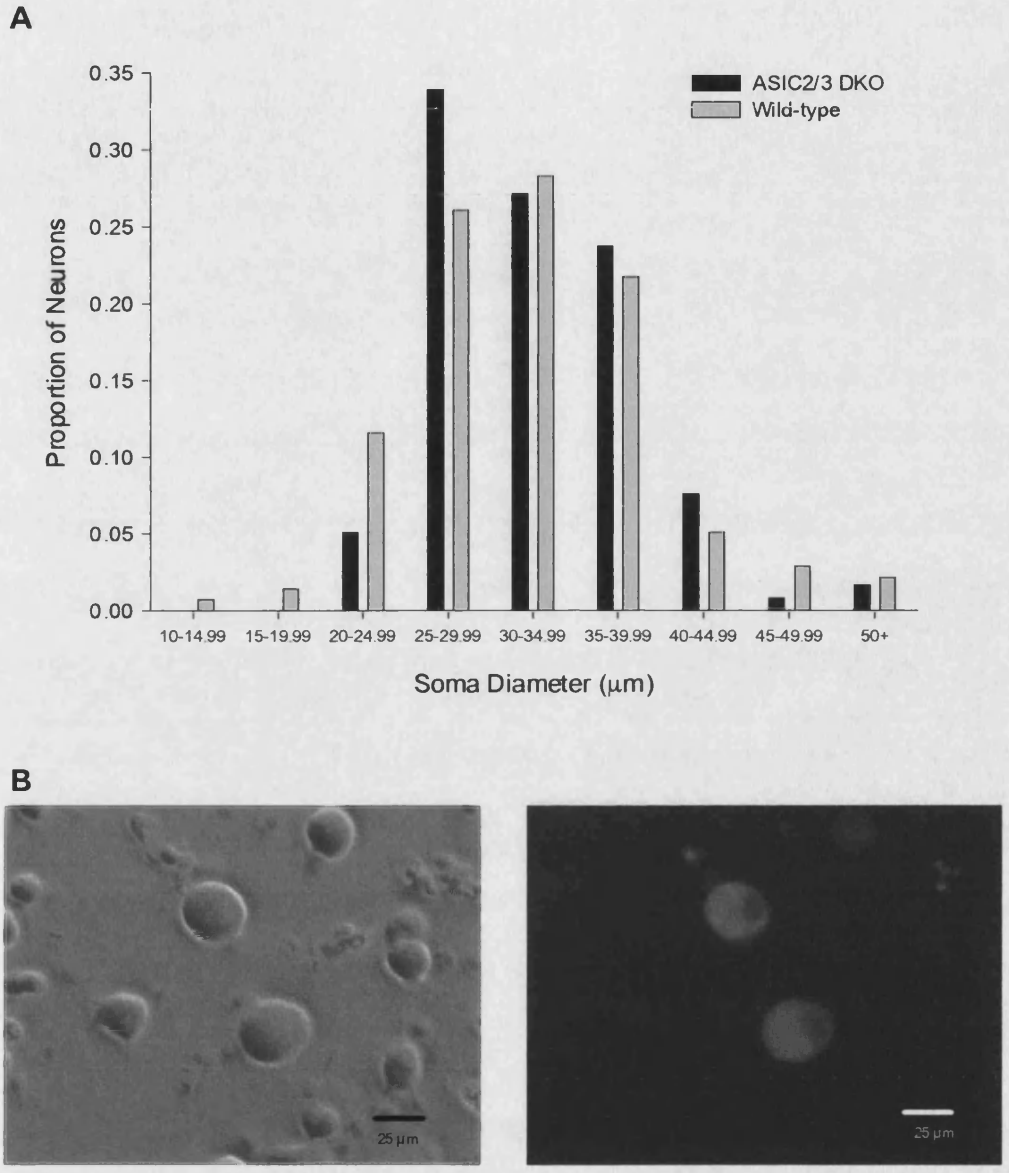

Fig. 4.12 The diameters of the cell bodies of NF-200 positive DRG neurons were not different between ASIC2/3 double knockouts and wild-types. *A*, Distribution of soma diameters for ASIC23 DKOs and WT neurons. Data from 118 DKO neurons and 138 WT neurons cultured from 2 KO mice and 2 WT mice. *B*, Example of NF-200 staining. *Left*, Light field image of a number of neurons, *right*, fluorescent detection of NF-200 immunoreactivity.

apyrase has ATPase/ADPase activity and so will reduce the concentration of ATP (and ADP) in the extracellular space. MA currents (3 RA, 1 SA) recorded in the presence of apyrase did not differ significantly from those recorded in control solution (n = 4). The mean peak amplitude of control currents was 0.53 ± 0.10 nA compared to 0.52 ± 0.08 nA (t-test, P = 0.97, Fig. 4.13). (Experiments discussed in Section 3.4.1)

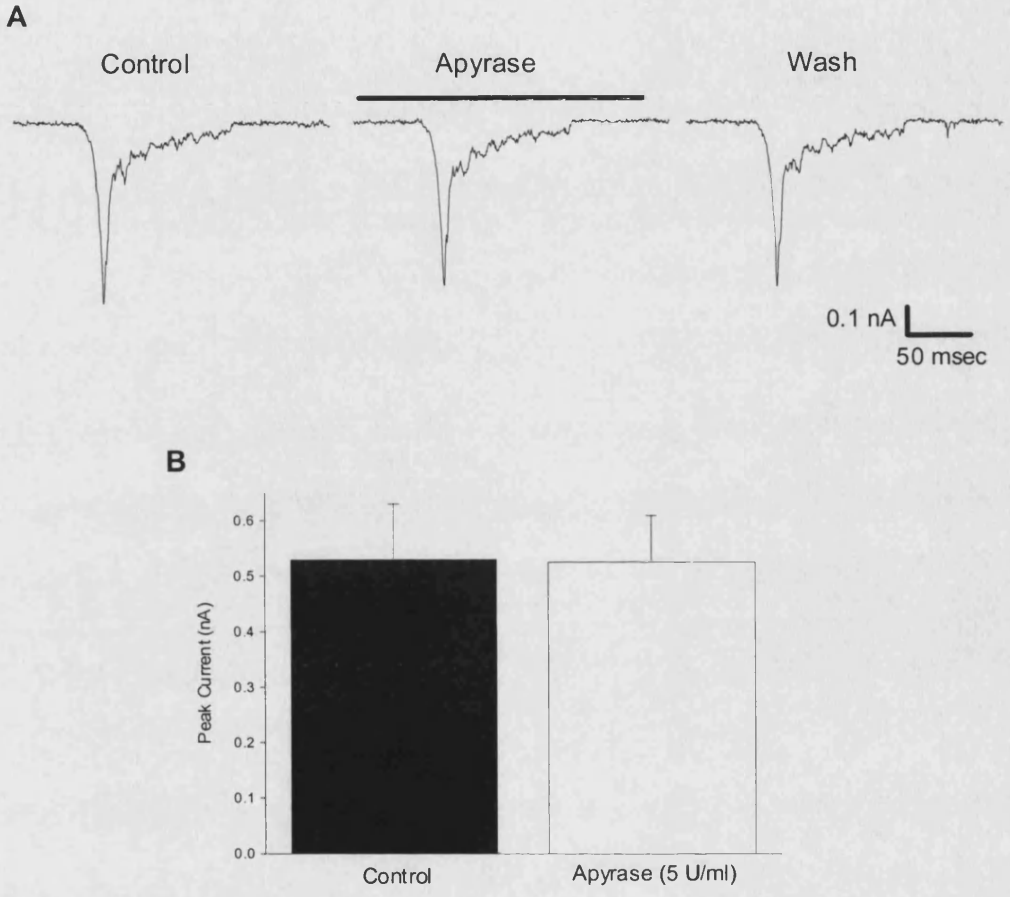

Fig. 4.13 Apyrase, an enzyme with ATPase activity, did not affect MA currents. *A*, Example traces of MA currents before, during and after application of apyrase (5 U/ml) to the neuron. RA current from neuron with a narrow action potential. *B*, Comparison of peak amplitude of MA currents recorded in control solution and in apyrase ($n = 4$). Mean control value: 0.53 ± 0.10 nA, mean apyrase value; 0.52 ± 0.08 nA (t-test, $P < 0.97$).

4.4 *Discussion*

4.4.1 MA Currents in Wild-Type Adult Mouse Sensory Neurons

Extending the work presented in Chapter 3, it was found that clearly defined subsets of adult, sensory neurons have distinct responses to mechanical stimulation. In this chapter, cell size, action potential duration and IB4 binding were used to classify neurons. *In vivo* studies have shown a robust correlation between action potential duration and mechanical sensitivity; receptors with high mechanical thresholds and mechanically insensitive neurons express wide, inflected action potentials regardless of fibre type whereas narrow action potentials are displayed almost exclusively by Aβ- and Aδ-fibre low threshold mechanoreceptors (Rose *et* al, 1986; Koerber *et al*, 1988; Ritter and Mendell, 1992; see Lawson, 2002; Section 1.1.1.1). Here a striking relationship between action potential duration and responses to mechanical stimulation *in vitro* was observed. Nearly all large neurons expressing narrow action potentials displayed substantial inward cationic currents on membrane displacement that adapted rapidly. By comparison, similar sized neurons with wide, inflected action potentials responded much less frequently to mechanical stimulation (within the testing range) and overall had currents that were much smaller and adapted more slowly, classified as intermediately adapting.

Small-medium neurons, the vast majority of which exhibited wide action potentials indicative of nociceptors, exhibited four categories of responses to mechanical stimulation. Approximately half were unresponsive when subjected to displacements (up to 12 μm) whilst the remainder had responses that were classified as rapidly, intermediately or slowly adapting. MA currents with intermediate adaptation kinetics were observed most frequently; such responses were seen in IB4- neurons and were characteristic of all responding IB4+ neurons. Hence intermediately adapting currents appear to be the response of the majority of nociceptive neurons to membrane displacement. Approximately half of unresponsive neurons and neurons with intermediately adapting currents were capsaicin sensitive; this is consistent with the observation by Caterina *et al* (2000) that approximately half of C-fibres in the mouse are activated by

capsaicin and also underlines the unsuitability of the use of responses to this compound as an indicator of nociceptive function in mouse neurons.

Subpopulations of IB4- neurons also displayed slowly and rapidly adapting currents. The identity of neurons that display slow responses remains unclear (Section 3.4.1); again, nearly all neurons displaying such currents were insensitive to capsaicin however, a nociceptive phenotype is supported by the observation that they all generated wide, inflected action potentials. Hence, these data along with the observed size distribution and frequency of such neurons is consistent with them being Aδ-mechanonociceptors (Koltzenburg *et* al, 1997). The majority of small-medium neurons that exhibited MA currents with rapidly adapting kinetics also displayed narrow action potentials and were capsaicin insensitive, thus, it is possible that these smaller neurons are also low threshold mechanoreceptors (Djouhri *et al*, 1998; Lawson, 2002). Their smaller size suggests they may be the somata of Aδ-fibres. Low threshold mechanoreceptors with Aδ-fibres are predominately D-hair receptors which selectively express $Ca_V3.2$ (Shin *et al*, 2003), so future experiments may include testing these neurons for the presence of voltage-gated Ca^{2+} currents consistent with expression of this channel.

Overall, the data are consistent with investigations of mechanosensitivity in the intact animal. Moreover, observations here extend the findings of the previous chapter because the classification system is more phenotypically valid and in mature sensory neurons MA currents of nociceptive neurons have adaptation kinetics that are clearly distinct from those of non-nociceptive neurons.

The adaptation of rapidly adapting currents was well described by two exponentials indicating a rapidly adapting initial phase followed by a slowly adapting component. The slow phase tended to slow as current amplitude increased, suggesting that the rate of adaptation slows at higher stimulus intensities, the reasons for this however remain elusive (see Section 3.4.6). Adaptation profiles of intermediately adapting currents were highly variable (but were always clearly distinct from rapidly and slowly adapting currents). Some were described well by a single exponential whereas many appeared

better described by two. In the latter case, currents typically contained a rapidly adapting initial component that varied in magnitude between cells (compare Figs. 4.2c, *left* and 4.7d, *left*). This might mean that neurons express more than one type of channel that adapt at different rates. Whether different channels would have distinct molecular identities or be distinctly modified post-translationally is unknown (Section 6.3).

In a number of neurons rapidly adapting MA currents were recorded in the presence of TTX to demonstrate that neurons were sufficiently space clamped, indicating the site of mechanosensitive channel activation is likely to be in the cell body and not due to movement of processes that are likely to contain the same channels.

4.4.2 ASIC2 and ASIC3 Do Not Contribute to MA Currents in Sensory Neurons

To investigate the molecular basis of MA currents in DRG neurons it was determined if neurons derived from ASIC2 and ASIC3 null mutants showed altered responses to focal mechanical stimulation. First, MA currents in low threshold mechanoreceptor neurons were investigated. Price *et al* (2000; 2001) observed that mechanically evoked firing in Aβ-fibres from ASIC2 nulls was reduced and that there was an increase in firing rates in RA-mechanoreceptors from ASIC3 knockout mice. Although an *in vitro* system prohibits direct comparison of the different subclasses of Aβ-fibres characterised by Price *et al* (2000; 2001), the data demonstrate that the deletion of these genes, alone or together, had no significant effect on either the sensitivity of large neurons with narrow action potentials to mechanical stimulation or on the kinetics of evoked responses. It is therefore concluded that neither of these ion channels contributes to the generation of MA currents in isolated neurons. Mechanically evoked responses of small-medium and other large neurons also showed no differences between wild-type and double knockout neurons. Price *et al* (2001) showed a reduced sensitivity of Aδ-nociceptors in ASIC3 nulls but no subpopulation showed any decrease in sensitivity in our assay.

There was a small difference in the mean amplitude of MA currents between ASIC2 nulls and their wild-type controls and the ASIC3 nulls and their controls. This may be due to

the different genetic backgrounds of these mouse strains (Section 4.2.1 and Price *et al*, 2000) and variation introduced by crossing the two lines may account for the small difference between ASIC2/3 double knockouts and controls.

It is widely hypothesised that ASICs are mechanosensitive ion channels and that failure to demonstrate mechanical gating of them is due to mechanosensitivity being conditional on their inclusion in a multi-protein transduction complex (Lewin and Stucky, 2000; Welsh *et al*, 2001). In this work it has been shown that ASICs do not contribute to MA currents in their native host cells, which would be expected to express the majority of components of the putative mechanosensory complex, for instance all but one (MEC-5, a collagen) of the structural components the *C. elegans* complex are expressed by the body touch receptor cells (Section 1.2.2.1). Hence, these data are the strongest evidence available that ASICs are not mechanosensitive. It is notable that ASICs lie on a branch of the DEG/ENaC phylogenetic tree quite distant from MEC-4 and MEC-10 and the other putatively mechanosensitive *C. elegans* channels (Goodman and Schwarz, 2002) and as discussed in Section 1.2.2 they do not contain the extracellular regulatory domain that is hypothesised to be central to mechanical gating (García-Añoveros *et al*, 1995).

In a small number of recordings it was also apparent that MA currents appeared normal in ASIC1 null mutants, negating a role for this channel subunit in the generation of MA currents. This is consistent with normal response properties of DRG nerve fibres in ASIC1 knockouts when assayed with skin-nerve preparation (GR Lewin, personal communication). It was also found that somatic diameters of NF200-positive neurons were normal in ASIC2/3 double mutants suggesting that these channels are not important in the development of these neurons.

4.4.3 Developmental Changes in MA Currents

The observation that around half of IB4 positive neurons generate MA currents in adult mouse and rat, but not neonatal rat (Section 3.3.3) suggests that developmental changes occur in the mechanosensitivity of these neurons. One possibility is that neurotrophic

signalling modulates mechanosensitivity as such signalling undergoes major postnatal changes in IB4 positive neurons (Molliver *et al*, 1997). BDNF has been shown to regulate the mechanosensitivity of slowly adapting mechanoreceptors (Carroll *et al*, 1998) and in IB4 positive neurons Stucky *et al* (2002) have shown that GFRα2 null mutants have a selective reduction in their sensitivity to heat stimuli. Alternatively, as IB4 binds a greater proportion of neurons in the adult than the neonate (Bennett *et al*, 1996) it may be the case that with development IB4 comes to label a population of mechanically sensitive neurons. Detailed studies of the mechanosensitivity of IB4+ neurons at a range of developmental stages and the ability of GDNF and related neurotrophic factors, such as neurturin, to regulate mechanosensitivity would be informative.

Although, comparison of data in this chapter with that in Chapter 3 is compromised due to a change in both age and species, it is interesting to note that in adult neurons the rates of adaptation were clearly different between nociceptive and non-nociceptive neurons, with an apparent quickening of adaptation in non-nociceptive neurons and a slowing in nociceptors. The expression of slowly adapting currents appeared constant. Given that currents in rat and mouse adult IB4+ neurons were similar this would suggest this is a developmental rather an interspecies phenomenon. Given the poverty in understanding of the mechanisms underlying MA current kinetics (Section 3.4.6) it is difficult to postulate if such changes are likely to be due to changes in the molecular make up of the channels in either cell type or due to changes in the way channels are regulated potentially due to changes in membrane composition or the arrangement of the cortical cytoskeleton.

4.4.4 Proton-Gated Currents

The investigation of responses to low pH revealed that distinct current types are differentially distributed amongst the categories of DRG neurons that were defined. The major currents observed in response to extracellular acidification were ASIC mediated transient currents and a slowly activating persistent current, although (at least) a small

number of cells displayed both types of currents. The data suggest that functional expression of ASIC-like proton-gated currents is found predominately in IB4 negative neurons likely to have a nociceptive function. Amongst large neurons approximately 75% of those with wide action potentials (almost certainly IB4 negative due to the size distribution of IB4 binding neurons, Molliver *et* al, 1997; Dirajlal *et al*, 2003) displayed transient proton-gated currents whereas in those with narrow action potentials the expression frequency was below 20%. In small-medium neurons, approximately 50% of IB4 negative nociceptors (neurons with wide action potentials) exhibited transient proton-gated currents whereas such currents were absent in IB4 positive cells. These observations are in agreement with Dirajlal *et al* (2003) who found ASIC mediated currents in 35% of IB4- nociceptors and in no IB4+ neurons.

Two aspects of the data here support the hypothesis that ASIC1, 2 and 3 subunits usually coassemble in heteromeric ion channels (Benson *et al*, 2001; Xie *et al*, 2002): Firstly, in wild-type neurons the rate of desensitisation of all transient currents was rapid, consistent with the coexpression of all three subunits (Benson *et al*, 2001), whereas in double knockout neurons transient currents all displayed desensitisation kinetics consistent with the expression of ASIC1 (Waldmann *et al*, 1997a; Chen *et al*, 1998) (although it is unclear if ASIC1a or 1b or a combination of the two mediated the responses observed). Secondly, transient currents were seen in similar proportions of neurons derived from wild-type and ASIC2/3 double knockouts; this is at odds with a significant subpopulation of neurons solely expressing functional ASIC2 and/or 3 subunits alone. However, it was notable that neurons lacking ASIC3 did not generate mixed currents suggesting ASIC3 is sometimes expressed without other ASIC subunits, albeit the transient components of mixed currents were consistently of small amplitude (< 200 pA). Furthermore, small diameter neurons (<25 μm), not tested in this study, may selectively express ASIC3 in the absence of other ASIC subunits. The tendency for pH 5.3 evoked currents to be larger in ASIC2/3 double knockouts may reflect an upregulation of ASIC1 transcripts, although the slowed rate of desensitisation would likely contribute to the increase in peak current.

There is much debate as to the distribution and coassembly of ASIC subunits in DRG neurons (Section 1.2.2.3). Data presented here support the conclusions of Benson *et al* (2001) that proton-gated currents in DRG neurons are mediated by receptors containing at least one subunit of each ASIC1, 2 and 3. Localisation of subunits using immunocyto-chemistry and *in situ* hybridisation have suggested that there is a non-overlapping distribution of subunits (Section 1.2.2.3), however no laboratory has triple labelled DRG for all three subunits. Analysis may be complicated if splice variants of ASIC1 and 2 are differentially distributed but are functionally analogous in the assembly of heteromeric channels. In nociceptive neurons, the recording of proton-gated currents is almost certainly complicated by concurrent activation of TRPV1 and in all neuron types by activation of the slowly activating, persistent currents recorded here.

The other major response to acidification that was observed was a slowly activating, persistent current. Interestingly, this was the most common response of presumptive low threshold mechanoreceptors to pH 5.3 (seen in around 70-80% of neurons) although it was also seen in all other neuronal subtypes. Persistent currents have been reported before in capsaicin insensitive cells (Petruska *et al*, 2000) but have not been functionally characterised. The channel that underlies this response is unknown; such currents were present in ASIC2/3 double knockouts and also in ASIC1 nulls and were insensitive to 200 μM amiloride. The slow kinetics of current activation were similar to those observed for TRPV1 gating, however this current was observed mainly in capsaicin insensitive neurons. We found such currents most frequently in large neurons with narrow action potentials (although they may have been present, but masked, in neurons with large ASIC mediated currents). The absence of large transient proton-gated currents in the majority of presumptive low threshold mechanoreceptors is consistent with the acid insensitivity of their peripheral endings (Lewin and Stucky, 2000), although the activation of a persistent inward current by low pH could have important consequences for neuronal excitability. Identification of the channel that underlies these responses awaits further investigation, although inhibition of a K^+ conductance has been ruled out by analysis of the current-voltage relationship of such responses (MD Baker, personal communication).

4.4.5 Ruthenium Red Blockade of MA Currents

In neonatal neurons ruthenium red blocked all types of MA currents with an IC_{50} of around 3 μM. At 5 μM, rapidly adapting MA currents were inhibited by around 45% in both wild-type and ASIC2/3 double knockout neurons when they were held at a potential of -70mV. The equal potency of ruthenium red in both populations is consistent with ASIC2 and 3 forming no part of the mechanosensitive ion channel. Furthermore, this block was shown to be voltage-dependent; when outward currents were evoked at a holding potential of +70 mV, 5 μM ruthenium red had no significant effect on current amplitude. These data are consistent with this highly charged compound acting as a pore blocker that requires a negative membrane potential to enter into the channel, i.e. the binding site is within the membrane electric field. Ruthenium red blockade of TRPV4 (Watanabe *et al*, 2002b) and TRPM6 (Voets *et al*, 2003) also been found to be voltage-dependent; see Section 3.4.4 for discussion.

4.4.6 ASICs and Mechanosensation

The role of ASICs in mammalian mechanosensation remains to be determined. Whilst the selective mechanical activation of ASICs at the sensory terminal remains a possibility, data presented here argue against such gating and so, given the studies of Price *et al* (2000; 2001), emphasis is put on other possible roles for these channels in mammalian mechanosensation. That ablation of single ASIC subunits induced mechanosensory deficits in selective afferent fibre types (Price *et al*, 2000; 2001) is interesting given that the results of this study and of others (Benson *et al*, 2001; Xie *et al*, 2002) suggest that in DRG neurons ASIC1, 2 and 3 subunits all coassemble in heteromeric ion channels. Another notable finding of this study is that only a small percentage (< 20%) of low threshold mechanoreceptor neurons expressed transient ASIC-mediated currents in response to external acidification; this is in contrast to a number of studies that have found ASIC subunit mRNA and immunoreactivity in large neurons of the DRG (Section 1.2.2.3). One possible explanation of this discrepancy is that ASIC channels were localised to internal membranes of the neurons and ASICs could modulate

the (axonal) transportation of mechanosensitive ion channels, although an action upstream of membrane insertion of these channels would have been expected to be apparent in the protocol used here.

Altered firing rates in ASIC3 nulls were not limited to mechanoreceptors as acid- and heat-evoked activity was reduced in C-fibres (Price *et al*, 2001). A function downstream of transduction events may be apparent in ASIC3 knockouts if ASIC3 is expressed in C-fibres in the absence of other ASIC subunits. Although a mechanism for ASIC modulation of membrane excitability is not immediately obvious, this possibility could be tested using the skin-nerve preparation by investigating the response properties of afferent fibres in response to electrical stimulation.

Interestingly, the recently cloned zebra fish family of ASICs has an extensive distribution throughout the central nervous system but is very sparsely expressed peripherally (Paukert *et al*, 2004). It should be noted that these ion channels are located throughout mammalian nervous systems and that their physiological functions in other neural systems remain as enigmatic as it does in sensory neurons (see for example Alvarez de la Rosa *et al*, 2003). Although the gross physiological systems in which ASICs operate is becoming apparent (i.e. mechanosensation, pain, learning and memory, fear conditioning) further research will be required to understand how these channels contribute to each system.

4.4.7 Physiological Properties of Neuronal Subclasses

Few differences became apparent when comparing resting membrane potentials, action potential duration and amplitude and maximal rates of depolarisation between wild-type neurons and those derived from null mutants. Given the number of variables recorded and the number of groups compared, such differences might be attributable to random variation in the data. Nevertheless, dV/dt_{max} was smaller in narrow action potential neurons from ASIC2/3 double mutants than wild-type controls but the significance of this is uncertain, especially given that this variable is unchanged in either single knockout.

Amongst IB4 negative nociceptive neurons, those lacking the ASIC 2 and 3 genes displayed action potentials approximately 50% longer than those in the equivalent wild-type population (they also had slower maximal rates of depolarisation). Again the significance of this is unclear and comparison of single knockout neurons would be informative. However, if the difference is "real" it may imply that properties of voltage-activated currents are affected by deletion of ASIC subunits and this could have implications for firing rates in C-fibres.

Amongst wild-type neurons, narrow action potentials were typically of smaller amplitude than wide action potentials and had higher maximal rates of depolarisation. Additionally, the resting potentials of large neurons with narrow action potentials tended to be more negative than nociceptive neurons. Comparison of the properties of IB4 negative and positive nociceptors showed similarities and differences with the work of Stucky and Lewin (1999). In agreement it was found that the action potentials of IB4 positive neurons were longer than those of IB4 negative nociceptors and this was consistent with a higher rate of depolarisation in IB4 negative neurons found here. Additionally, unlike the previous study, it was found that IB4 positive neurons had more depolarised resting potentials and slightly larger action potentials than IB4 negative nociceptors.

5 *Conopeptide Antagonists of DRG Mechanosensitive Ion Channels*

5.1 Introduction

There are currently no known high affinity (K_d < 100 nM) ligands of mechanosensitive ion channels. The value of discovering a selective, high affinity compound is manifest. Firstly, it could provide a route to uncovering the molecular identity of such channels. Secondly, it would be an invaluable pharmacological tool for studying the physiological functions of mechanosensitive channels and finally, blockade of mechanosensory transduction may be of therapeutic value.

There is a mass of evidence suggesting that the gating of eukaryotic mechanosensitive ion channels is dependent upon an interaction with auxiliary proteins (Section 1.2) a high affinity biochemical "tag" for such a channel would therefore provide an attractive approach to cloning it, as the methods employed would not initially involve functional assays. Such a compound, if found, could be employed in a number of ways. The most direct technique would be to use it as a probe for screening a cDNA library. Labelling of the ligand (either by inclusion of a radioactive isotope or via covalent attachment of readably detectable side group, such as biotin) would enable the screening of a heterologously expressed cDNA library. Such an approach was used to isolate the δ-opioid receptor (Kieffer *et al*, 1992); Tyr-*D*-Thr-Gly-Phe-Leu-Thr, an agonist at native δ-opioid receptors ($K_d \approx 1$ nM), was tritiated and used as a probe for screening a random-primed cDNA library prepared from NG 108-15 cells expressed in COS cells. After four rounds of selection, a single cDNA was identified that conferred strong agonist binding to COS cells.

Alternatively, a high affinity ligand could be used to isolate the protein of interest directly. In the late 1970s and early 1980s α-bungarotoxin(see Heidmann and Changeux, 1978) and *Tityus* gamma toxin (Norman *et al*, 1983) were used to purify nicotinic acetylcholine receptors and sodium channels, respectively, from electric fish such as

Torpedo californica and *Electrophorus electricus*. Such ligands were covalently bound to insoluble matrices allowing isolation of their receptors from protein preparations rich in that receptor. Such an isolation system would allow sequencing of the amino acid structure of the target receptor. The yeast 2-hybrid assay could be employed if the peptide ligand were cloned and used as a bait for screening an appropriate cDNA library. Although such an approach has not been used to identify novel proteins before it is a robust system for uncovering protein-protein interactions (for example see Malik-Hall *et al*, 2003).

The approach we took to searching for a novel antagonist of DRG mechanosensitive ion channels was to screen the venom of the marine snail *Conus ventricosus* for a peptide that blocked MA currents in cultured sensory neurons. The venom of *Conus* snails has previously been a rich source of peptide toxins. Conopeptides have been identified that inhibit a variety of voltage-gated and ligand-gated ion channels including Na^+, K^+ and Ca^{2+} channels and nicotinic acetylcholine, 5-HT_3 and NMDA receptors (see Olivera and Cruz, 2001; Harvey, 2002; Terlau and Olivera, 2004). In addition, conotoxins that inhibit G-protein coupled receptors (e.g. α_1-adrenoreceptors) and noradrenaline transporters have been identified (Sharpe *et al*, 2001). There is also a group of conotoxins, the δ class, that slows inactivation Na^+ channels (see Terlau and Olivera, 2004). Conotoxins tend to be between 13 and 35 amino acids in length and nearly all contain a number of disulphide bridges (up to 5 but typically 2 or 3). The number and positioning of the cysteines within the toxin, and hence the structure of the disulphide bonds, determine the classification of toxins into distinct subclasses (see Olivera and Cruz, 2001; Harvey, 2002; Terlau and Olivera, 2004). The venom of each species of *Conus* snails is thought to contain over 100 distinct peptides; hence with 500 identified species, upwards of 50,000 peptides are believed to exist. It is therefore likely that many other active toxins and targets will be identified in the future (Olivera and Cruz, 2001).

Conus ventricosus is a worm hunting snail found in the Mediterranean and Red Seas. To date one active peptide has been isolated from the venom of this organism; Contryphan-Vn is a nonapeptide with a single disulphide bridge (Massilia *et al*, 2001) that at a

relatively high concentration (20 μM) modulates Ca^{2+} activated K^+ channels (Massilia *et al*, 2003).

The group of Fred Sachs (Suchyna *et al*, 2000) has previously identified a peptide toxin that inhibits stretch-activated cation channels expressed by astrocytes and cardio-myocytes. A 35 amino acid peptide, termed GsMTx-4, was isolated from the venom of the tarantula *Grammostola spatulata* by fractionation of whole venom using inhibition of astrocyte stretch-activated channels as the functional assay. GsMTx-4 had an approximate equilibrium dissociation constant (K_d) of 630 nM for these channels and also inhibited whole-cell swelling-activated currents in astroctyes and cardiomyocytes. Subsequent work by this group (Bode *et al*, 2001) showed, using perfused rabbit hearts, that GsMTx-4 inhibits atrial fibrillation induced by high intraatrial pressures applied at high frequency. This study hence demonstrated a pivotal role for stretch activated channels in modulating cardiac function and also suggested a potential therapeutic role for antagonists of these channels.

5.2 Materials & Methods

Adult *Conus ventricosus* snails were taken from the northern Red Sea. Lyophilised venom was extracted in ammonium acetate. Initial fractionations were performed on Sephadex G-50 columns. Subsequent high performance liquid chromatography (HPLC) fractionations were done using reverse phase chromatography on C18 columns (see Fainzilber *et al*, 1994). Work done in the Fainzilber laboratory.

Lyophilised crude venom and fractionated venom was resuspended in the standard external solution (140 mM NaCl, 4 mM KCl, 2 mM $CaCl_2$, 1 mM $MgCl_2$, 10 mM HEPES, pH 7.4) including 0.1% BSA. Given the small amount of venom available to us peptides had to be resuspended in relatively small volumes. Typically 25-50 μl of peptide solution was applied to the neuron through a Gilsson pipette tip (p20-200) positioned within 100-150 μm of the cell body. The pipette tip was attached to a Gilsson p100 via a length of tubing so that it could be front filled and evacuated using the dial on

the pipette. Neurons were stimulated every 20 seconds at a stimulus intensity giving a reproducible response >200 pA, solutions were "dialled" on over approximately 30-40 sec, with application suspended whilst the stimulus was given.

5.3 Results

5.3.1 Crude Conus ventricosus *Venom Inhibits MA Currents*

Application of crude *Conus ventricosus* venom to DRG neurons reversibly inhibited MA currents in a dose-dependent fashion (Fig.5.1). 0.2 venom equivalents (VE) of crude venom applied to two neurons inhibited MA currents by 100% and 96%, respectively (Fig. 5.1a,b,d). Immediately after venom application blockade was partial and maximal 30 sec later; maximal inhibition was sustained for 1-2 min before current amplitudes returned to baseline over 2-3 min (Fig. 5.1b). There appeared to be no significant difference in the ability of the venom to inhibit SA and RA currents. When 0.07 VE were applied to one neuron the response to mechanical stimulation was maximally inhibited by 64% and in another 0.02 VE inhibited MA currents by 33% (Fig. 5.1c,d).

5.3.2 Fractionation of Crude Venom

The first fractionation of the crude venom divided it into 12 fractions each of which was tested for activity at mechanosensitive channels. Each fraction was initially applied twice (except 4a applied once and 5 applied three times) to neurons at 1 VE. Fig. 5.2a shows the peak current amplitude (as percentage of control value) of the first mechanically evoked response after venom application and Fig. 5.2b shows the maximal change in current amplitude. Although there tended to be a significant degree of variation in MA current amplitude following drug application the only fraction that consistently inhibited MA currents by a large amount with a time course similar to that observed for the crude venom was fraction 4 (Fig. 5.3). The reduction in MA current amplitude seen after application of fraction 5 was transient and was accompanied by a large increase in the holding current hence this effect was discarded. Fraction 4 was applied to 4 neurons at

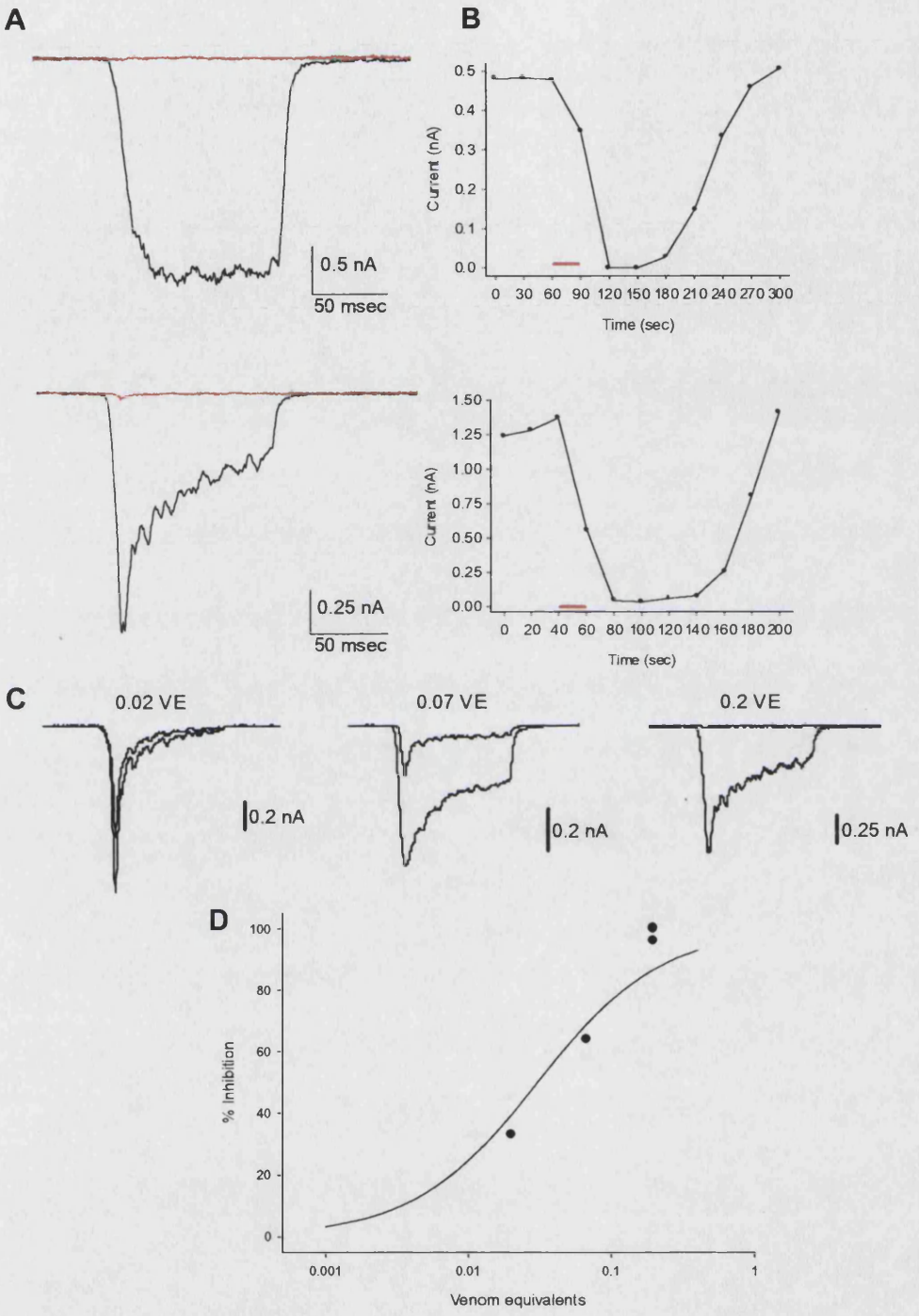

Fig. 5.1 Effect of crude *Conus ventricosus* venom on MA currents. *A*, *B*, Two examples of the effect of 0.2 VE of crude venom on MA currents. *A*, Example traces showing recording in control solution (*black*) and the maximally inhibited response in the presence of the venom (*red*). *B*, Time course of inhibition following application of venom, indicated by *red bar*. *C*, *D*, Concentration inhibition relationship for venom effect. *C*, Traces showing the application of 0.02 VE *(left)*, 0.07 VE (*centre*) and 0.2 VE (as in *A*, *right*); smaller currents in presence of venom. *D*, Graphical representation of the effect of the venom (Each data point represents a single cell).

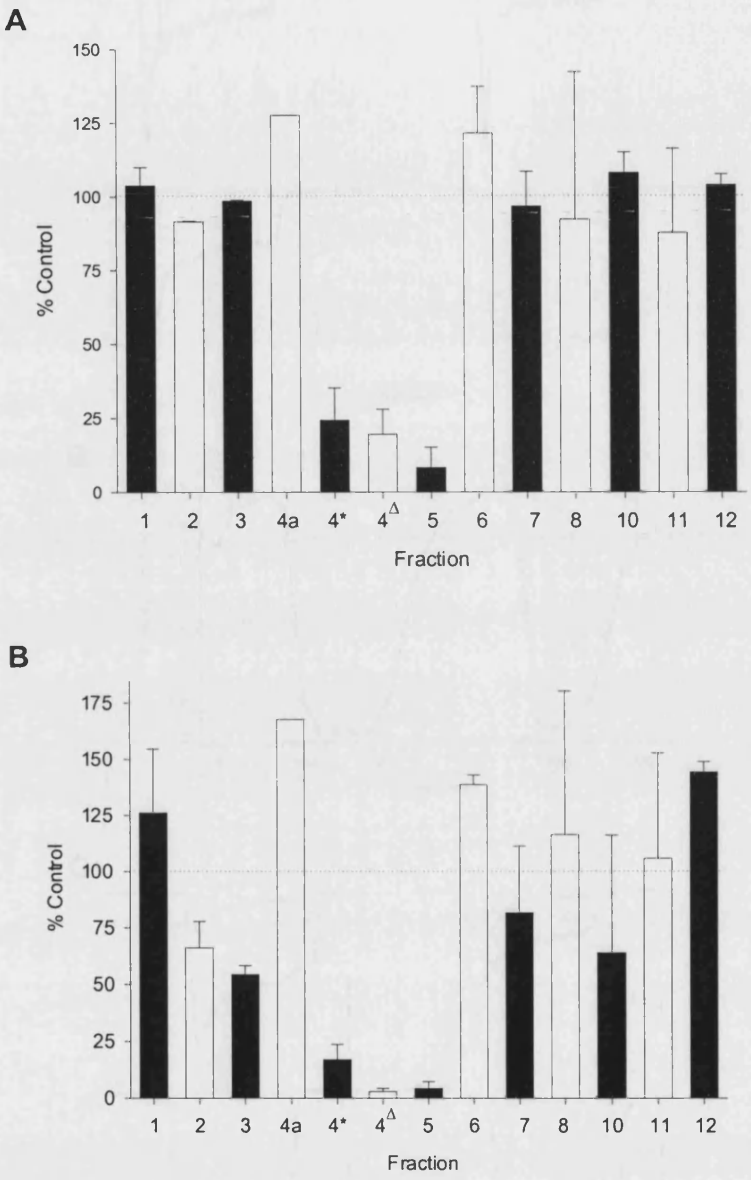

Fig. 5.2 Screening of the first round of venom fractions revealed that Fraction 4 significantly inhibited MA currents. *A*, Bar graph showing the amplitude of MA currents, as percentage of control value, evoked by the first mechanical stimulus after application of each fraction (1 VE, except 4*; 0.2 VE, 4^{Δ}; 0.65 VE, 4a is a distinct fraction to 4). *B*, Graph showing maximal change in MA current amplitude, as percentage of control value, after fraction application. Typically each fraction was tested twice, except, Fraction 4*; ×4, 4^{Δ}; ×4, 5; ×3, 4a; ×1.

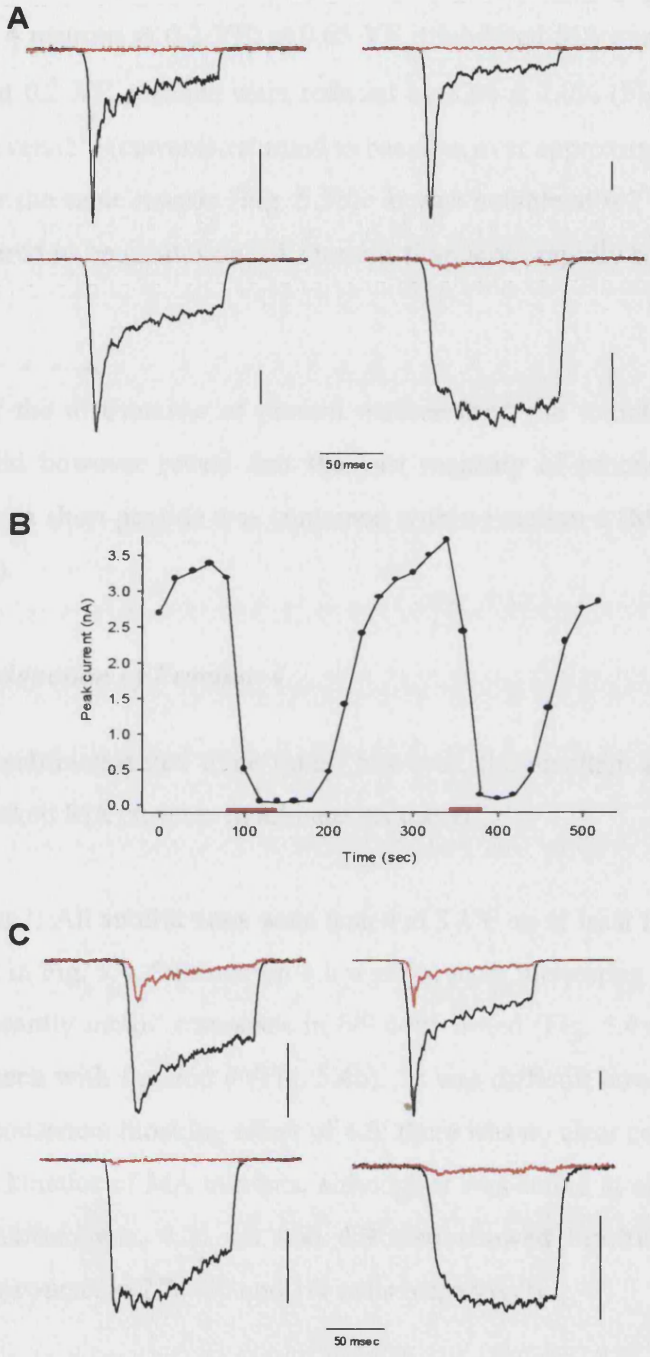

Fig. 5.3 Effects of Fraction 4 on MA currents. *A*, MA current traces from the 4 neurons that 0.65 VE of Fraction 4 was applied to showing control traces (*black*) and the maximal inhibition induced by the venom (*red*). *B*, Example of the time course of the action of 0.65 VE of Fraction 4 on MA currents. Two applications of Fraction 4 (*red bars*) to the same neuron are shown. *C*, Traces from neurons receiving 0.2 VE of Fraction 4, again, control; *black*, venom; *red*. In all traces vertical scale bars: 0.5 nA.

0.65 VE and to 4 neurons at 0.2 VE; at 0.65 VE it inhibited MA currents by 97.3 ± 1.3% (Fig.5.3a) and at 0.2 VE currents were reduced by 82.6 ± 7.0% (Fig. 5.3c). In all cases blockade was reversible (currents returned to baseline over approximately 2 min) and was reproducible for the same neuron (Fig. 5.3b). It was notable at 0.2 VE that the effect of fraction 4 appeared to be greater on SA currents than more rapidly adapting currents (Fig. 5.3c).

Examination of the distribution of protein masses from the initial fractionation of the crude venom did however reveal that the vast majority of protein material of a size corresponding to a short peptide was contained within Fraction 4 (M Fainzilber, personal communication).

5.3.3 Subfractionation of Fraction 4

Fraction 4 was subfractionated three times, however, the resultant subfractions failed to consistently blocked MA currents in all neurons tested.

Subfractionation 1: All subfractions were tested at 3 VE on at least two neurons. Results are summarised in Fig. 5.4. Subfraction 4.6 was the most interesting subfraction as it was found to significantly inhibit responses in 6/9 cells tested (Fig. 5.4a) with a time course similar to that seen with fraction 4 (Fig. 5.4b). It was difficult however to discern what underlay the inconsistent blocking effect of 4.6; there was no clear correlation between its activity and the kinetics of MA currents, although it was active at all SA currents tested. Of the other subfractions, 4.2, 4.3 and 4.9 also showed blocking activity, with an appropriate time course, in 2/6, 3/6 and 1/4 cells respectively.

Subsequent to obtaining this data we were sent a further subfractionation of subfractions 4.2, 4.3 and 4.4 in four samples labelled A, B, C and D. Of these none showed substantial inhibition but "B" showed some blocking activity. We were subsequently sent another tube containing "an identified peptide mass" which showed no activity (data not shown).

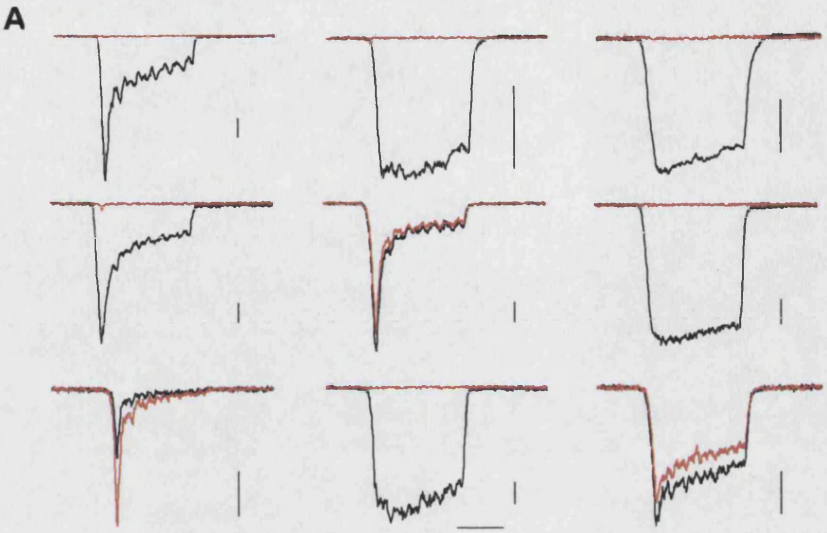

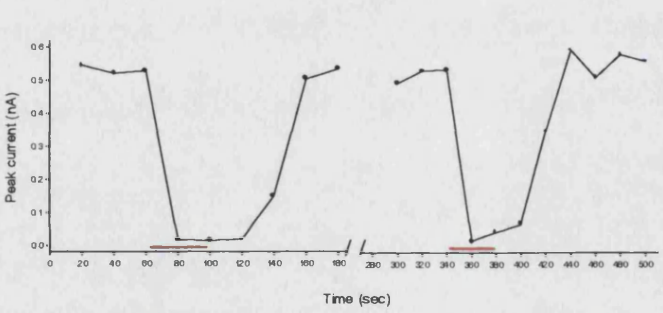

C

4.1	4.2	4.3	4.4	4.5	4.7	4.8	4.9	4.10	4.11	4.12
-	⇓	⇓	↓	-	↑	-	↓	-	-	-
-	⇓	⇓	↓	↓	↓	-	⇓	↓	-	↓
	↓	↑			-		↓			
	-	-					↓			
	-	⇓								
	↓	-								

Fig. 5.4 Testing of subfractions of fraction 4 for blocking activity on MA currents. *A*, Subfraction 4.6 was applied to nine neurons; blocking activity was observed in 6/9 neurons. All SA currents tested were inhibited however activity of 4.6 was inconsistent on RA currents. Vertical scale bars: 0.2 nA, Horizontal bar: 50 msec. *B*, Time course of blocking activity of 4.6 following 2 applications to the same neuron (SA current). *C*, Summary of the effects of the other subfractions; each box represents a neuron. Solid arrow indicates an inhibitory action (> 50%) with an appropriate time course, thin arrows indicate transient or minor effect on MA currents, - indicates no effect.

Subfractionation 2: A second set of subfractions derived from fraction 4 was screened at 3.8 VE per neuron with each subfraction applied to 2 neurons; no activity was seen in any subfraction (data not shown).

Subfractionation 3: A third set of subfractions was tested at 5 VE per neuron (2 neurons each). In the first round of screening inhibitory action (with an appropriate time course) was seen with subfractions 4.3b, 4.6 and 4.9 in 1 of the two neurons. This was consistent with the data from the first subfractionation, however in further testing (2 neurons for each subfraction) only 4.9 again showed a significant blocking effect (data not shown). Of these subfractions a further 4 subfractions of 4.3b were further tested (each on 3 neurons), however no significant blocking activity was observed (data not shown).

5.3.4 Psalmotoxin 1 does not Inhibit MA Currents

Escoubas *et al* (2000) identified psalmotoxin 1 (PCTx1) as a 40 amino acid tarantula toxin that inhibits ASIC1a mediated currents with an IC_{50} of 0.9 nM. We tested if this toxin had any blocking activity of MA currents in DRG neurons. As shown in Fig. 5.5, PCTx1 had no affinity for the ion channels underlying MA currents; it was tested on 5 neurons displaying MA currents that varied in sensitivity and adaptation kinetics (Fig. 5.5a). The first MA current evoked in toxin was 99.5 ± 4.9% of control, whereas the second was 96.0 ± 2.0% of control (Fig. 5.5b).

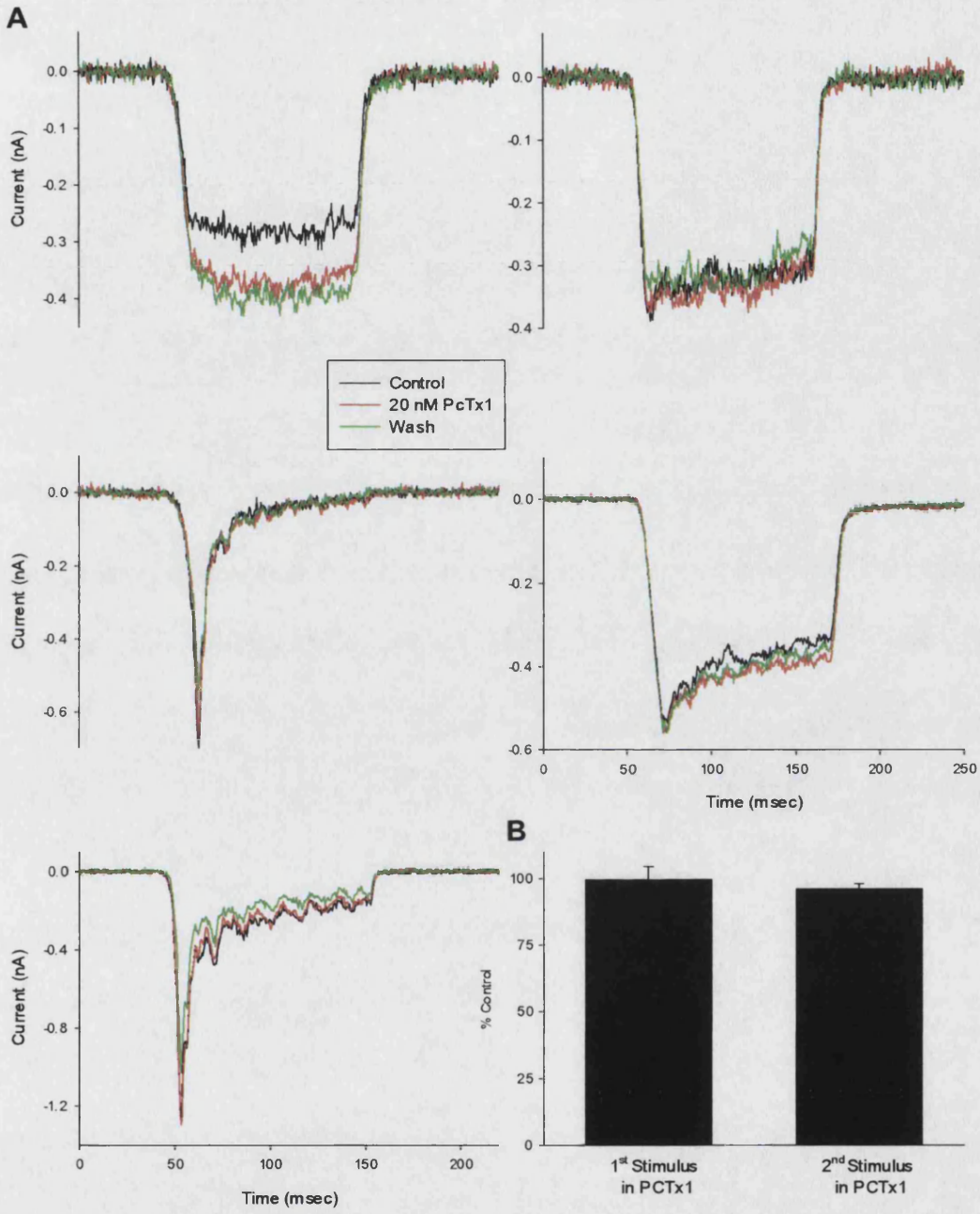

Fig. 5.5 20 nM PCTx1 had no effect on MA currents in DRG neurons. *A*, PCTx1 was applied to five neurons; control traces are in *black*, recordings made in the presence of 20 nM PCTx1 are in *red* and *green* traces show wash out. *B*, Summary of the effect of PCTx1 on MA currents; the first MA current evoked in PCTx1 was 99.5 ± 4.9% of control, whereas the second was 96.0 ± 2.0% of control (*n* = 5).

5.4 *Discussion*

The results of this screening process suggest that the venom of *Conus ventricosus* contains a peptide that blocks the mechanosensitive ion channel underlying MA currents in DRG neurons. The active molecule blocks mechanosensitive ion channels from the extracellular side and the near maximal blockade of the first response following peptide application suggests that the mechanism is use independent. We were, however, unable to identify a single active peptide as inhibitory activity diminished with subsequent fractionation of the venom. At the first round of fractionation a clear blocking effect was evident; however this was to be expected given that the vast majority of peptidergic material in the venom was contained in fraction 4. The subfractionation of fraction 4 gave no single subfraction that consistently blocked MA currents. Of 9 neurons tested subfraction 4.6 inhibited currents in 6. It is uncertain why activity was observed in only two thirds of the neurons; although SA currents were blocked in all (4/4) neurons tested, in the remaining neurons there was no clear relationship between current kinetics and blocking activity. There was also inconsistent activity observed in subfractions 4.2 and 4.3

It is uncertain why blocking activity was lost with repeated fractionation of the venom. Perhaps, the most likely explanation is that the active peptide is present at a low concentration in the crude venom and was lost in the fractionation process, possibly it is highly charged and liable to bind to charged surfaces, conversely its water solubility could be poor and it could have been lost due to this. Another possibility, albeit an unprecedented one, is that more than one component of the venom is required to fully inhibit currents. Moreover, the reason for the inconsistent effects of subfractions of fraction 4 is unclear; potentially with the application of small volumes of solution the amount of peptide reaching the cell varied although this is unlikely given that the same apparatus was used each time. The possibility that the molecular composition of the underlying channel varied from cell to cell (see Section 6.3), with the putative toxin targeting perhaps a single subunit, is attractive but although there was a trend towards greater activity on SA currents there was no robust correlation between kinetics and

blocking activity. The worst-case scenario is that there was a contaminant (such as an inorganic ion) introduced by the extraction or purification process that inhibited mechanosensitive ion channels and that subsequent purification reduced the concentration of this molecule. Although, it may be expected that such a contaminant would be distributed equally amongst all fractions, i.e. each would have had a similar blocking activity, if the contaminant interacted with peptidergic matter its concentration may have been significantly higher in fraction 4.

The delivery of small volumes of solution to neurons in this series of experiments was somewhat problematic. Primarily, this type of application makes it uncertain what concentration of compound exists in the vicinity of the neuron. Usually the cell would be superfused in a constant concentration of the drug of interest and then washed in a flow of control solution, here the test solution is relatively rapidly applied in close proximity to the neuron but then is free to diffuse from the cell. Hence, the rate at which current amplitude recovers is dependent both on the affinity of the peptide for the receptor and the rate at which the concentration of peptide available for binding changes (the bath volume was 3 ml and so a 30 µl volume would be diluted 100 times). Other issues with this method of application are that although every effort was made to be constant, variation would occur in the rate of application and a transient application of solution could move the cell from its initial position. Such effects could account for transient fluctuations in current amplitude occasionally observed following solution application.

It is unclear what the affinity of the putative peptide antagonist for the mechanosensitive ion channel is. As the application system used precluded rapid concentration jumps accurate estimations of on and off rates of antagonist binding were not possible. Examination of the relief of block, by either crude venom (Fig. 5.1b) or fraction 4 (Fig. 5.3b) would suggest a dissociation time constant of around 30 seconds, this is similar to that of observed for saxitoxin at sodium channels (in experiments using rapid concentration jumps), which has an affinity of approximately 1-5 nM (Hille, 2001). However, the true time constant will be less (i.e. the affinity lower) as the concentration of peptide around the cell does not fall immediately to zero. There is, though, evidence

that a process operated to rapidly clear the peptide. That there is almost complete blockade of MA currents with 0.65 VE of fraction 4, suggests that the initial concentration of peptide at the receptor is well in excess of the K_D50 for the channel, typically by around two orders of magnitude. However, there is complete recovery of current amplitude despite the fact that the dilution factor of the applied volume is only 100; this would suggest that another factor also reduces peptide concentration. One possibility is that, despite the presence of 0.1% BSA, non-specific binding of the peptide (perhaps to poly-lysine, the plastic culture dish or cell membranes) drastically reduces the free peptide concentration by acting as a "sink" for the peptide.

PCTx1, which blocks ASIC1a (Escoubas *et al*, 2000), did not inhibit MA currents. This finding is consistent with observations in ASIC null mutants showing no change in the properties of MA currents. It would be interesting to test the ability of GsMTx1 (Suchyna *et al*, 2000) to inhibit MA currents in sensory neurons; such an experiment would give information regarding the relatedness of stretch-activated cation channels in different cell types.

The search for a peptide ligand for the ion channels underlying MA currents in sensory neurons remains attractive both as a route to the molecular identification of the channel and as a useful pharmacological tool. To use a ligand-binding based system for cloning the receptor would however require a high affinity, such as Tyr-*D*-Thr-Gly-Phe-Leu-Thr at δ-opioid receptor ($K_D \approx 1$ nM, Kieffer *et al*, 1992). It is, for example, unlikely that GsMTx1 ($K_D \approx 500$ nM) is of high enough affinity to bind the astrocyte/cardiomyocyte stretch-activated ion channel through the process of gene isolation. The constraints over this experimental system did not allow a confident estimation of the affinity of the blocking agent from *Conus ventricosus* venom to be made. If the affinity were too low for the peptide to form the basis of a screening strategy, the compound may nevertheless be a useful pharmacological tool (dependent on it's selectivity) for the study of sensory neuron mechanosensitive ion channels. Finally, if the affinity were relatively low, it may be the case that the basic structure of the identified peptide could be manipulated to

develop a more potent antagonist. Alternaitively, screening of related snail (or other animals') venoms may prove fruitful in isolating a high affinity peptide antagonist.

6 Discussion & Conclusions

6.1 *Comparison of Thesis Work with Published* In Vitro *Studies of Sensory Neuron Mechanotransduction*

As discussed in Section 1.3.2.4, there have been a number of electrophysiological studies published on mechanotransduction in cultured sensory neurons. The techniques used in this thesis most closely resemble those used by McCarter *et al* (1999); who also made whole-cell recordings from neurons stimulated with a rounded glass probe. This group reported that mechanical stimulation evoked a non-specific cationic current in adult DRG neurons that was sensitive to Gd^{3+} and high concentrations of the amiloride analogue, benzamil. It was also observed that more large neurons (>30 μm, 70%) than small neurons (≤30 μm, 35%) responded to mechanical stimulation. Hence, the data acquired here are consistent with those findings; MA currents recorded in this lab were also inhibited by high concentrations of benzamil (P Cesare, personal communication). The key differences between this study and that of McCarter *et* al (1999) are that the system used here for manipulation of the glass probe allowed fine calibration of the stimulus and that here a number of functional classification systems were used that allowed the categorisation of sensory neurons and thus to distinguish their differential responses to mechanical stimulation.

The study of Takahashi and Gotoh (2000) used pressure application through the patch pipette and reported two types of mechanically activated currents; one a calcium current, the other a non-specific cation current. This type of stimulus seems analogous to cell swelling generated by hypo-osmotic shock as it involves the injection of pipette solution into the cell's interior. Neurons with diameters less than 20 μm did not respond to mechanical stimulation but currents were seen in the majority of cells larger than this; this is essentially consistent with data herein although in this study neurons less than 20 μm in diameter were not tested. No comparison of the properties of neurons exhibiting

the two types of currents was made (such as resting potential or size) and neurons were not tested for capsaicin sensitivity. The authors report (without showing data) that the currents were sensitive to gadolinium and not amiloride but the relative affinity of gadolinium for the two current types was again not reported. Without knowing the effective concentration of gadolinium comparison cannot be made with MA currents observed here. The striking difference between Takahasi and Gotoh's work and that presented here is the observation that increasing intracellular pressure evoked calcium currents in some neurons; in this study, despite differences in calcium sensitivity between MA current subtypes, all currents observed were non-selective cation currents. This discrepancy strongly suggests that these two stimulation protocols activate different classes of ion channels. It should be noted however that Cho *et al* (2002) used a similar stimulation protocol and reported only the activation of non-selective cationic conductances but in their study whole cell currents were, in contrast to work here, absent in neurons larger than 30 μm. Finally, it is unclear if this method of stimulation evokes currents in non-sensory neurons.

At the single-channel level, Cho *et al* (2002) extensively characterised ion channels in neonatal rat DRG neurons that were activated by pressure applied through the patch pipette. Their primary findings were that sensory neurons expressed two classes of non-selective cation channels, which were activated by low and high levels of pressure, respectively. It is however uncertain if these channels underlie the whole-cell currents that have been recorded here; there are a number of similarities between the currents observed in the two preparations but there are also key differences. In common, currents were blocked by similar concentrations of Gd^{3+} and were insensitive to amiloride. Also, in each study currents were reduced by cytochalasin treatment; interestingly in the study of Cho *et al* (2002) the effect of cytochalasin was greater on low than high threshold channels and here the effect of this compound was greater on MA currents in capsaicin insensitive than sensitive neurons. Likewise, the ionic permeability of the ion channels studied by Cho *et al* (2002) is compatible with the currents observed here. Conversely, the inhibitory effects of arachidonic acid observed here were absent in the single-channel study and here no clear inhibitory action of colchicine was observed. Cho *et al* (2002)

also found a pronounced sensitisation of high threshold channel activity by PGE2 but in this lab PGE2 did not potentiate MA currents (data not shown). In contrast to the rapid adaptation of the majority of MA currents observed here, Cho *et al* (2002) found no adaptation in single channel activity of either channel; this may be attributable to differences between the behaviour of membrane patches in a pipette and whole cell membranes. The clearest difference between the two studies is in the size distribution of neurons that displayed mechanically evoked activity. Cho *et al* (2002) found mechano-sensitive channels in neurons with diameters under 30 μm and no activity was observed in larger neurons (diameters 30-40 μm); in this study whole-cell MA currents were found most abundantly in large neurons (diameters >30 μm in neonatal rat neurons and >40 μm in adult mouse neurons). The distribution observed here for whole-cell currents is therefore more in line with the mechanoreceptive properties known for small and large neurons (Section 1.1). As discussed in Section 1.2.1, mechanosensitive ion channels have been observed in the single-channel recording configuration that do not have a clear physiological function in the host cell and Cho *et al* (2002) did not show if their simulation protocol evoked similar channel activity in non-sensory neurons. The absence of single channel activity in larger neurons may indicate that mechanosensitive ion channels in these cells (activated in this study) require some form of external membrane anchoring for activation. Finally, although prostaglandin E_2 induces mechanical hyperalgesia much data suggests that this form of sensitisation is centrally mediated (Costigan and Woolf, 1998), hence studies, perhaps using the skin nerve preparation, to determine if prostaglandin E_2 lowers the mechanical thresholds of afferent fibres would be informative.

Numerous studies have used calcium-imaging techniques to demonstrate that mechanical stimulation of sensory neurons evokes an increase in intracellular Ca^{2+} (Section 1.3.2.4). A number of these studies also applied pressure to the somatic membrane using a rounded glass probe (Sharma *et al*, 1995; Raybould *et al*, 1999; Gotoh and Takahashi, 1999; Gschossmann *et al*, 2000) and it would be expected that the same population of mechanosensitive ion channels would have been activated that underlay the MA currents in the present study. In Section 1.3.2.4, I argued that the slow increases and decreases in

intracellular Ca^{2+} levels recorded in these studies limited the usefulness of this approach for studying the rapid process of mechanotransduction and that these studies are compromised by the fact that neurons are not voltage-clamped. Data obtained in this lab (Paolo Cesare, personal communication), using FURA-2 imaging of voltage-clamped neurons, showed that the kinetics of changes in intracellular Ca^{2+} levels are distinct to changes in membrane current. The initial transient component of MA currents is not apparent in the Ca^{2+} signal and Ca^{2+} levels remain above baseline beyond the cessation of the stimulus, albeit for significantly less time than observed in published studies. Concurrent monitoring of membrane current using electrophysiology allowed us to know that there was no damage to the membrane in our stimulation protocol that could underlie prolonged increases in Ca^{2+}. However, the primary distinction is that electrophysiology (being essentially real-time) gives considerably more information about the dynamic behaviour of mechanosensitive ion channels than does Ca^{2+} imaging, which is compromised by slow sampling rates and lower signal to noise sensitivity. Moreover, data herein demonstrate that in quasi-physiological solutions the major charge carrier in MA currents is Na^{+}. Again, the system of stimulus delivery in published imaging studies was cruder than that used here. Inhibition of Ca^{2+} increases by gadolinium in these studies is consistent with observations here, although effective concentrations did vary widely; the reasons for this are unclear.

Other stimulation protocols used in Ca^{2+} imaging studies are fluid jet (Sullivan *et al*, 1997; Drummond *et al*, 2000) and hypotonic shock (Viana *et al*, 2000); whether such stimuli activate the same ion channels as stimulation with a glass probe is uncertain. Drummond *et al* (2000) suggested ENaC channels underlay responses to a fluid jet as these were inhibited by 100 nM amiloride; this is in sharp contrast to the inactivity of amiloride in this study. Inhibition by this level of amiloride is somewhat indicative of this class of channels, although amiloride may block other channel types at this level and ENaCs are not typically Ca^{2+} permeant. Given the lethality of ENaC subunit gene ablation, tissue specific knockouts would be informative in addressing the role of ENaCs in sensory neurons (Section 1.2.2.2). Exposure to hypotonic stimuli evoked Ca^{2+} influxes in sensory neurons (Viana *et al*, 2001). Neurons that responded to this stimulus did so

with either a fast, large response or a smaller, slow response and there was no association between responses and capsaicin sensitivity. Ca^{2+} fluxes were sensitive to gadolinium and also to nickel, although if nickel acted at the primary transducer or at voltage-gated Ca^{2+} channels is unclear. It would be of interest to determine the contribution of TRPV4 to these responses (Section 1.2.3.2). Again it is unclear if hypotonicity activates the same population of ion channels that underlie MA currents; an informative experiment would be to record the responses of neurons to all three stimuli (glass probe, fluid jet and hypo-osmolarity) and determine the relationship between them.

6.2 Discovering the Molecular Identity of Sensory Neuron Mechanotransducing Ion Channels

Genetic screening has proved remarkably fruitful in the discovery of ion channels critical for mechanosensation in invertebrates (Section 1.2). However, despite convincing analysis of mutant animals, none of these channels, with the possible exception of hypotonic activation of Nan (Kim *et al*, 2003), have been shown to be directly gated by mechanical stimuli. Analysis of homologous channels in vertebrates has shown an important role for NOMPC in zebra fish mechanosensation (Sidi *et al*, 2003) but in mammals data regarding the role of TRP and ENaC/DEG channels in mechanosensation is equivocal (Section 1.2). We await an analysis of TRPV4 null mutants using the skin-nerve preparation and currently mechanical activation of ASICs remains purely hypothetical.

Here it has been demonstrated that cultured DRG neurons express mechanosensitive ion channels that generate MA currents with key features consistent with the mechano-receptive phenotypes of the host cell. How could the molecular identity of this channel be investigated? We attempted to discover a high affinity conopeptide ligand for these channels, and although this attempt failed, such an approach remains attractive as it would bypass the likely functional dependence of these channels on binding to auxiliary proteins (see Chapter 5).

TRPV1 (Caterina *et al*, 1997) and TRPM8 (McKemy *et al*, 2002) were identified by the Julius lab through expression cloning. However, the serendipitous evolution of capsaicin and menthol sensitivity of these channels was central to these studies and no known compounds mimic the sensation of touch or painful pressure, hence such an approach is infeasible for mechanosensors. Using a similar approach but applying pressure to large numbers of cells requires, one, the development of an appropriate stimulus and two, would depend on the ability of the channel to function in a heterologous system; a dependence on specific protein-protein interactions would also make this approach unsuitable . Caprini *et al* (2003) attempted to isolate a mechanotransducing protein from sensory neurons using an expression cloning approach; a DRG cDNA library was expressed in HEK293 cells and intracellular Ca^{2+} levels were measured following a hypotonic stimulus (see Viana *et al*, 2001). Unexpectedly, GAP43 was identified as an osmosensitive signalling molecule. In HEK293 cells over-expressing GAP43, exposure to hypotonic stimuli caused an association of GAP43 with phospholipase C-δ_1 resulting in IP_3 formation and the induction of Ca^{2+} release from intracellular stores. This is unlikely to play a role in DRG mechanotransduction for a number of reasons; firstly, Viana *et al* (2001) found that increases in intracellular Ca^{2+} evoked by hypotonicity were dependent on external Ca^{2+}, secondly, the pattern of GAP43 expression in mature DRG neurons is inappropriate (Chong *et al*, 1992; Andersen and Schreyer, 1999) and, thirdly, a second messenger based system is too slow to underlie sensory mechanotransduction. The significance of GAP43 osmosensitivity is unclear; however, the failure of this study to identify an ion channel gated by membrane stretch may indicate the futility of this approach in seeking to identify molecules that depend on complex anchoring for their functioning[12].

The approach of Peier *et al* (2002b) and Story *et al* (2003) to identifying cold-activated ion channels was to heterologously express uncharacterised TRP channels (identified from database searches) and test them for cold sensitivity. Similarly, the heat-sensitive channel TRPV2 was cloned due to its homology to TRPV1 (Caterina *et al*, 1999). Again

[12] Other technical reasons may have prevented the isolation of such a protein; the failure of this screen to identify TRPV4 is of interest as in other studies this channel was activated by hypo-osmolarity when expressed in cell lines (see Section 1.2.3.2).

reconstitution in a heterologous system of a functional mechanosensitive ion channel was required. We have used expression of putative mechanosensors in SCG neurons as a possible approach to doing this, as SCG neurons are morphologically similar to DRG neurons and will likely have the most similar cytoarchitecture and membrane properties (see England *et al*, 1998). However, neuronal transfection is difficult and time consuming[13]. Alternatively, upon identification of candidate molecules, their expression in DRG neurons could be down regulated using antisense or siRNA and the effect on endogenous MA currents assessed. Using this approach (or the ligand binding approach) would generate candidate molecules that would necessarily have to be functionally reconstituted; the yeast-2-hybrid system may be a useful approach to uncovering required interacting proteins.

6.3 Conclusions

The work presented in this thesis has characterised mechanically activated currents evoked by focal stimulation of the somatic membrane of cultured sensory neurons of the DRG. Compression of the cell membrane using a finely calibrated system for moving a heat polished glass probe has revealed that mechanical stimulation activates mechanosensitive non-selective cation channels, selectively in these neurons. When neonatal rat neurons were defined as nociceptive or non-nociceptive according to capsaicin sensitivity, it was found that MA currents were larger and activated at lower thresholds in the capsaicin insensitive population. Likewise, in adult mouse neurons identification of low threshold mechanoreceptors by their narrow action potentials showed that these neurons had larger MA currents than nociceptors and these currents displayed rapid adaptation. Moreover, currents in different cell types were kinetically distinct; most nociceptors exhibited intermediately adapting MA currents whilst a subpopulation generated slowly adapting currents. Overall these data show that cultured neurons retain mechanosensitivity and aspects of their responses to mechanical stimulation are consistent with their *in vivo* phenotypes; future work may involve

[13] In this lab SCG neurons have been transfected with various ENaC/DEG and TRP channels using nuclear microinjection; in no case were MA currents evoked.

clarification of the phenotype of neurons expressing slowly adapting currents and the characterisation of MA currents in more extensively subclassified sensory neurons (see Section 1.3.1; Petruska *et al*, 2000; 2002). Future work will also include determining why MA currents differ in different cell types. Possibilities include expression of distinct channel types (they may be encoded by different genes, splice variants of a common gene product or due to distinct heteromeric compositions of channels), differences in the binding of auxiliary proteins to common channels or due to different cytoskeletal or membrane specialisations.

A number of compounds that inhibit MA currents in the low micromolar range have been identified. Whilst none have selectivity for mechanosensitive ion channels, they have allowed a basic pharmacological characterisation of the channels underlying MA currents and have revealed that channels underlying currents in distinct cell types are mediated by closely related channels and have showed that mechanosensitive channels share a number of properties with the TRP family of ion channels (Section 3.4.4).

Dependence of mechanosensitive ion channel function in DRG neurons on the actin cytoskeleton was demonstrated and regulation of channel kinetics by laminin was demonstrated (Section 3.4.3). This is consistent with the prevalent model of eukaryotic mechanotransduction that purports that mechanosensitive ion channels are tethered to extracellular and intracellular components that function to transmit tension to the gating mechanism of the channel. Future work would involve further identification of cytoskeletal proteins required for channel operation and modulation of currents by other integrin activating ligands.

It has been found that mechanosensitive ion channels have non-selective cation permeability. This is consistent with investigations of the sensory terminals of DRG nerve fibres using extracellular recording techniques that suggested generator currents were mediated by cation channels permeable to both sodium and calcium (Section 1.1.2.2). Data suggested that there is distinct Ca^{2+} regulation of MA currents in capsaicin sensitive and insensitive neurons, hence a more detailed study of Ca^{2+} permeability and

determination of how Ca^{2+} chelation inhibits MA currents in the latter population would be informative.

Using neurons derived from knockout mice, it was demonstrated that ASIC2 and ASIC3, and probably ASIC1, did not contribute to MA currents in DRG neurons. This is strong data that ASICs are not mechanically gated and their function in neuronal signalling generally and specifically in mechanosensation awaits clarification. The screening of null mutant neurons is a powerful tool for assessing the function of ion channels and will likely be used again in this field to investigate candidate mechanosensitive channels.

Whilst the use of mechanical stimulation of cultured neurons has revealed information about mechanosensitive ion channels expressed by sensory neurons, proof of concept will only be achieved if and when it is shown that the ion channels under investigation here are responsible for sensory mechanotransduction *in vivo*. There are a number of reasons to believe that this will be the case: firstly, TRPV1 is activated by heat when expressed in the somatic membrane of cultured neurons (Cesare and McNaughton, 1996) and is located at the sensory terminals of sensory fibres (Tominaga *et al*, 1998). Furthermore, ablation of the *trpv1* gene causes deficits in thermosensation (Caterina *et al*, 2000; Davis *et al*, 2000). Secondly, MA currents were absent from non-sensory SCG neurons and had distinct properties in different classes of sensory DRG neurons. Thirdly, although the cell bodies of DRG neurons are not normally mechanosensitive, axotomy of the sciatic nerve has been shown to induce mechanosensitivity in the neuroma and in the ganglion (Burchiel, 1984); this is consistent with aberrant insertion of mechanosensitive channels into axonal and somatic membranes when their normal trafficking is disrupted[14]. *In vivo* studies of the effects of compounds that block MA currents on mechanosensation would be informative; no mammalian studies have been published demonstrating a selective blockade of mechanosensation by a drug; this may be related to poor drug penetration to the site of transduction due to the encapsulation of mechanosensory terminals in complex end organs (Section 1.1.2). Related to this, it is notable that the compounds that blocked

[14] An interesting control experiment would be to determine if neuromas formed on transected spinal roots of the DRG were mechanosensitive.

MA currents were all charge-dense molecules, although FM1-43 may be useful for such studies (Meyers *et al*, 2003). Only when the molecular identity of the ion channel is determined will full resolution of this issue be possible.

Overall, the work in this thesis has characterised the properties of a novel class of mechanically activated currents in sensory neurons, which are hypothesised to represent the primary mechanism by which mechanical stimuli impinging on the bodies of mammals are detected.

6.4 Publications

Drew LJ, Wood JN, Cesare P (2002) Distinct mechanosensitive properties of capsaicin-sensitive and -insensitive sensory neurons. *J Neurosci*, 22; RC228.

Drew LJ, Rohrer DK, Price MP, Blaver K, Cockayne DA, Cesare P, Wood JN (2004) ASIC2 and ASIC3 Do Not Contribute to Mechanically Activated Currents in Mammalian Sensory Neurons. *J Physiol*, 556; 691-710.

Ding Y, Cesare P, Drew L, Nikitaki D, Wood JN (2000) ATP, P2X receptors and pain pathways. *J Auton Nerv Syst*, 81; 289-94.

Wood JN, Beggs S, Drew LJ (2004) Sensing damage. www.wellcome.ac.uk/pain

7 *References*

Adams CM, Anderson MG, Motto DG, Price MP, Johnson WA, Welsh MJ (1998) Ripped pocket and pickpocket, novel *Drosophila* DEG/ENaC subunits expressed in early development and in mechanosensory neurons. *J Cell Biol*, 140; 143-152.

Adrian ED (1928) *The basis of sensation: The action of the sense organs*. Christophers, London.

Ahluwalia J, Rang H, Nagy I (2002) The putative role of vanilloid receptor-like protein-1 in mediating high threshold noxious heat-sensitivity in rat cultured primary sensory neurons. *Eur J Neurosci*, 16; 1483-1489.

Aidley, DJ, Stanfield PR (1996) *Ion channels: Molecules in action*. Cambridge University Press.

Ainsley JA, Pettus JM, Bosenko D, Gerstein CE, Zinkevich N, Anderson MG, Adams CM, Welsh MJ, Johnson WA (2003) Enhanced locomotion caused by loss of the *Drosophila* DEG/ENaC protein Pickpocket1. *Curr Biol*, 13; 1557-1563.

Akoev GN (1982) The effect of Mg^{2+} and Ca^{2+} on the excitability of Pacinian corpuscles. *Brain Res*, 239; 391-399.

Akoev GN, Alekseev NP, Krylov BV (1988) *Mechanoreceptors, their functional organization*. Springer-Verlag, Berlin.

Akopian AN, Abson NC, Wood JN (1996a) Molecular genetic approaches to nociceptor development and function. *Trends Neurosci*, 19; 240-246.

Akopian AN, Sivilotti L, Wood JN (1996b) A tetrodotoxin-resistant voltage-gated sodium channel expressed by sensory neurons. *Nature*, 379; 257-262.

Akopian AN, Chen CC, Souslova V, Okuse K, Wood JN (2000a) Sensory neuron-specific ion channels and receptors. In *Molecular basis of pain induction* (Ed. Wood, JN), pp. 113-128, Wiley-Liss, New York.

Akopian AN, Chen CC, Ding Y, Cesare P, Wood JN (2000b) A new member of the acid-sensing ion channel family. *Neuroreport*, 11; 2217-2222.

Alenghat FJ, Ingber DE (2002) Mechanotransduction: all signals point to cytoskeleton, matrix, and integrins. *Sci STKE*, 119; PE6.

Alessandri-Haber N, Yeh JJ, Boyd AE, Parada CA, Chen X, Reichling DB, Levine JD (2003) Hypotonicity induces TRPV4-mediated nociception in rat. *Neuron*, 39; 497-511.

Allen NJ, Attwell D (2002) Modulation of ASIC channels in rat cerebellar Purkinje neurons by ischaemia-related signals. *J Physiol*, 543; 521-529.

Alvarez de la Rosa D, Zhang P, Shao D, White F, Canessa CM (2002) Functional implications of the localization and activity of acid-sensitive channels in rat peripheral nervous system. *Proc Natl Acad Sci U S A*, 99; 2326-2331.

Alvarez de la Rosa D, Krueger SR, Kolar A, Shao D, Fitzsimonds RM, Canessa CM (2003) Distribution, subcellular localization and ontogeny of ASIC1 in the mammalian central nervous system. *J Physiol*, 546; 77-87.

Andersen LB, Schreyer DJ (1999) Constitutive expression of GAP-43 correlates with rapid, but not slow regrowth of injured dorsal root axons in the adult rat. *Exp Neurol*, 155; 157-164.

Anzai N, Deval E, Schaefer L, Friend V, Lazdunski M, Lingueglia, E (2002) The multivalent PDZ domain-containing protein CIPP is a partner of acid-sensing ion channel 3 in sensory neurons. *J Biol Chem*, 277; 16655-16661.

Askwith CC, Cheng C, Ikuma M, Benson C, Price MP, Welsh MJ (2000) Neuropeptide FF and FMRFamide potentiate acid-evoked currents from sensory neurons and proton-gated DEG/ENaC channels. *Neuron*, 26; 133-141.

Awayda MS, Ismailov II, Berdiev BK, Benos DJ (1995) A cloned renal epithelial Na^+ channel protein displays stretch activation in planar lipid bilayers. *Am J Physiol*, 268; C1450-9.

Awayda MS, Subramanyam M (1998) Regulation of the epithelial Na^+ channel by membrane tension. *J Gen Physiol*, 112; 97-111.

Babinski K, Catarsi S, Biagini G, Seguela P (2000) Mammalian ASIC2a and ASIC3 subunits co-assemble into heteromeric proton-gated channels sensitive to Gd^{3+}. *J Biol Chem*, 275; 28519-28525.

Baccaglini PI, Hogan PG (1983) Some rat sensory neurons in culture express characteristics of differentiated pain sensory cells. *Proc Natl Acad Sci USA*, 80; 594-598.

Baker MD, Bostock H (1997) Low-threshold, persistent sodium current in rat large dorsal root ganglion neurons in culture. *J Neurophysiol*, 77; 1503-13.

Baker MD, Chandra SY, Ding Y, Waxman SG, Wood JN (2003) GTP-induced tetrodotoxin-resistant Na^+ current regulates excitability in mouse and rat small diameter sensory neurons. *J Physiol*, 548; 373-382.

Barker PM, Nguyen MS, Gatzy JT, Grubb B, Norman H, Hummler E, Rossier B, Boucher RC, Koller B (1998) Role of gammaENaC subunit in lung liquid clearance and electrolyte balance in newborn mice. Insights into perinatal adaptation and pseudohypoaldosteronism. *J Clin Invest*, 102; 1634-1640.

Baron A, Schaefer L, Lingueglia E, Champigny G, Lazdunski M (2001) Zn^{2+} and H^+ are coactivators of acid-sensing ion channels. *J Biol Chem*, 276; 35361-35367.

Belkin AM, Stepp MA (2000) Integrins as receptors for laminins. *Microsc Res Tech*, 51; 280-301.

Bennett DL, Averill S, Clary DO, Priestley JV, McMahon SB (1996) Postnatal changes in the expression of the trkA high-affinity NGF receptor in primary sensory neurons. *Eur J Neurosci*, 8; 2204-2208.

Benson CJ, Xie J, Wemmie JA, Price MP, Henss JM, Welsh MJ, Snyder PM (2002) Heteromultimers of DEG/ENaC subunits form H^+-gated channels in mouse sensory neurons. *Proc Natl Acad Sci U S A*, 99; 2338-2343.

Betz WJ, Mao F, Smith CB (1996) Imaging exocytosis and endocytosis. *Curr Opin Neurobiol*, 6; 365-371.

Bevan S, Yeats J (1991) Protons activate a cation conductance in a sub-population of rat dorsal root ganglion neurones. *J Physiol*, 433; 145-161.

Bevan S, Hothi S, Hughes G, James IF, Rang HP, Shah K, Walpole CS, Yeats JC (1992) Capsazepine: a competitive antagonist of the sensory neurone excitant capsaicin. *Br J Pharmacol*, 107; 544-552.

Birder LA, Nakamura Y, Kiss S, Nealen ML, Barrick S, Kanai AJ, Wang E, Ruiz G, De Groat WC, Apodaca G, Watkins S, Caterina MJ (2002) Altered urinary bladder function in mice lacking the vanilloid receptor TRPV1. *Nat Neurosci*, 5; 856-860.

Black JA, Dib-Hajj S, McNabola K, Jeste S, Rizzo MA, Kocsis JD, Waxman SG (1996) Spinal sensory neurons express multiple sodium channel alpha-subunit mRNAs. *Brain Res Mol Brain Res*, 43; 117-131.

Black JA, Langworthy K, Hinson AW, Dib-Hajj SD, Waxman SG (1997) NGF has opposing effects on Na^+ channel III and SNS gene expression in spinal sensory neurons. *Neuroreport*, 8; 2331-2335.

Blair NT, Bean BP (2002) Roles of tetrodotoxin (TTX)-sensitive Na^+ current, TTX-resistant Na^+ current, and Ca^{2+} current in the action potentials of nociceptive sensory neurons. *J Neurosci*, 22; 10277-10290.

Blount P, Moe PC (1999) Bacterial mechanosensitive channels: integrating physiology, structure and function. *Trends Microbiol*, 7; 420-424.

Bode F, Sachs F, Franz MR (2001) Tarantula peptide inhibits atrial fibrillation. *Nature*, 409; 35-36.

Boland LM, Brown TA, Dingledine R. (1991) Gadolinium block of calcium channels: influence of bicarbonate. *Brain Res*, 563; 142-150.

Boldogkoi Z, Schutz B, Sallach J, Zimmer A (2002) $P2X_3$ receptor expression at early stage of mouse embryogenesis. *Mech Dev*, 118; 255-260.

Bosman FT, Stamenkovic I (2003) Functional structure and composition of the extracellular matrix. *J Pathol*, 200; 423-428.

Boucher TJ, Okuse K, Bennett DL, Munson JB, Wood JN, McMahon SB (2000) Potent analgesic effects of GDNF in neuropathic pain states. *Science*, 290; 124-127.

Brock JA, McLachlan EM, Belmonte C (1998) Tetrodotoxin-resistant impulses in single nociceptor nerve terminals in guinea-pig cornea. *J Physiol*, 512; 211-217.

Bryan-Sisneros AA, Fraser SP, Djamgoz MBA (2003) Electrophysiological, mechanosensitive responses of *Xenopu laevis* oocytes to direct, isotonic increase in cell volume. *J Neurosci Meth*, 125; 103-111.

Burgard EC, Niforatos W, van Biesen T, Lynch KJ, Touma E, Metzger RE, Kowaluk EA, Jarvis MF (1999) P2X receptor-mediated ionic currents in dorsal root ganglion neurons. *J Neurophysiol*, 82; 1590-1598.

Burnstock G (1999) Release of vasoactive substances from endothelial cells by shear stress and purinergic mechanosensory transduction. *J Anat*, 194; 335-342.

Cain DM, Khasabov SG, Simone DA (2001) Response properties of mechanoreceptors and nociceptors in mouse glabrous skin: an *in vivo* study. *J Neurophysiol*, 85; 1561-1574.

Caldwell JH, Schaller KL, Lasher RS, Peles E, Levinson SR (2000) Sodium channel $Na_v1.6$ is localized at nodes of Ranvier, dendrites, and synapses. *Proc Natl Acad Sci U S A*, 97; 5616-5620.

Canessa CM, Schild L, Buell G, Thorens B, Gautschi I, Horisberger JD, Rossier BC (1994) Amiloride-sensitive epithelial Na^+ channel is made of three homologous subunits. *Nature*, 367; 463-467.

Caprini M, Gomis A, Cabedo H, Planells-Cases R, Belmonte C, Viana F, Ferrer-Montiel A (2003) GAP43 stimulates inositol trisphosphate-mediated calcium release in response to hypotonicity. *EMBO J*, 22; 3004-3014.

Cardenas CG, Del Mar LP, Scroggs RS (1995) Variation in serotonergic inhibition of calcium channel currents in four types of rat sensory neurons differentiated by membrane properties. *J Neurophysiol*, 74; 1870-1879.

Carr MJ, Gover TD, Weinreich D, Undem BJ (2001) Inhibition of mechanical activation of guinea-pig airway afferent neurons by amiloride analogues. *Br J Pharmacol*, 133; 1255-1262.

Carroll P, Lewin GR, Koltzenburg M, Toyka KV, Thoenen H (1998) A role for BDNF in mechano-sensation. *Nat Neurosci*, 1; 42-46.

Casado M, Ascher P (1998) Opposite modulation of NMDA receptors by lysophospholipids and arachidonic acid: common features with mechanosensitivity. *J Physiol*, 513; 317-330.

Caterina MJ, Schumacher MA, Tominaga M, Rosen TA, Levine JD, Julius D (1997) The capsaicin receptor: a heat-activated ion channel in the pain pathway. *Nature*, 389; 816-824.

Caterina MJ, Rosen TA, Tominaga M, Brake AJ, Julius D (1999) A capsaicin-receptor homologue with a high threshold for noxious heat. *Nature*, 398; 436-441.

Caterina MJ, Julius D (1999) Sense and specificity: a molecular identity for nociceptors. *Curr Opin Neurobiol*, 9; 525-530.

Caterina MJ, Leffler A, Malmberg AB, Martin WJ, Trafton J, Petersen-Zeitz KR, Koltzenburg M, Basbaum AI, Julius D (2000) Impaired nociception and pain sensation in mice lacking the capsaicin receptor. *Science*, 288; 306-313.

Caterina MJ, Julius D (2001) The vanilloid receptor: a molecular gateway to the pain pathway. *Annu Rev Neurosci*, 24; 487-517.

Catton WT (1970) Mechanoreceptor function. *Physiol Rev*, 50; 297-318.

Cesare P, McNaughton P (1996) A novel heat-activated current in nociceptive neurons and its sensitization by bradykinin. *Proc Natl Acad Sci U S A*, 93; 15435-15439.

Cesare P, Dekker LV, Sardini A, Parker PJ, McNaughton PA (1999) Specific involvement of PKC-epsilon in sensitization of the neuronal response to painful heat. *Neuron*, 23; 617-624.

Chalfie M, Sulston J (1981) Developmental genetics of the mechanosensory neurons of *Caenorhabditis elegans*. *Dev Biol*, 82; 358-370.

Chalfie M, Sulston JE, White JG, Southgate E, Thomson JN, Brenner S (1985) The neural circuit for touch sensitivity in *Caenorhabditis elegans*. *J Neurosci*, 5; 956-964.

Chalfie M, Thomson JN (1982) Structural and functional diversity in the neuronal microtubules of *Caenorhabditis elegans*. *J Cell Biol*, 93; 15-23.

Chelur DS, Ernstrom GG, Goodman MB, Yao CA, Chen L, O' Hagan R, Chalfie M (2002) The mechano-sensory protein MEC-6 is a subunit of the *C. elegans* touch-cell degenerin channel. *Nature*, 420; 669-673.

Chen CC, Akopian AN, Sivilotti L, Colquhoun D, Burnstock G, Wood JN (1995) A P2X purinoceptor expressed by a subset of sensory neurons. *Nature*, 377; 428-431.

Chen CC, England S, Akopian AN, Wood JN (1998) A sensory neuron-specific, proton-gated ion channel. *Proc Natl Acad Sci U S A*, 95; 10240-10245.

Chen CC, Zimmer A, Sun WH, Hall J, Brownstein MJ, Zimmer A (2002) A role for ASIC3 in the modulation of high-intensity pain stimuli. *Proc Natl Acad Sci U S A*, 99; 8992-8997.

Cho H, Shin J, Shin CY, LeeS-Y, Oh U (2002) Mechanosensitive ion channels in cultured sensory neurons of neonatal rats. *J Neurosci*, 22; 1238-1247.

Chong MS, Fitzgerald M, Winter J, Hu-Tsai M, Emson PC, Wiese U, Woolf CJ (1992) GAP-43 mRNA in rat spinal cord and dorsal root ganglia neurons: Developmental changes and re-expression following peripheral nerve injury. *Eur J Neurosci*, 4; 883-895.

Chouchkov C, Andreev D, Dandov A (2003) Localization and distribution of laminin in the basal lamina of certain mechanoreceptors - an immunogold study. *Somatosens Mot Res*, 20; 265-270.

Chung YD, Zhu J, Han Y, Kernan MJ (2001) *nompA* encodes a PNS-specific, ZP domain protein required to connect mechanosensory dendrites to sensory structures. *Neuron*, 29; 415-428.

Chung MK, Lee H, Caterina MJ (2003) Warm temperatures activate TRPV4 in mouse 308 keratinocytes. *J Biol Chem*, 278; 32037-32046.

Cibulsky SM, Sather WA (1999) Block by ruthenium red of cloned neuronal voltage-gated calcium channels. *J Pharmacol Exp Ther*, 289; 1447-1453.

Clapham DE, Runnels LW, Strubing C (2001) The TRP ion channel family. *Nat Rev Neurosci*, 2; 387-396.

Clapham DE (2003) TRP channels as cellular sensors. *Nature*, 426; 517-524.

Cockayne DA, Hamilton SG, Zhu QM, Dunn PM, Zhong Y, Novakovic S, Malmberg AB, Cain G, Berson A, Kassotakis L, Hedley L, Lachnit WG, Burnstock G, McMahon SB, Ford AP (2000) Urinary bladder hyporeflexia and reduced pain-related behaviour in $P2X_3$-deficient mice. *Nature*, 407; 1011-1015.

Colbert HA, Smith TL, Bargmann CI (1997) OSM-9, a novel protein with structural similarity to channels, is required for olfaction, mechanosensation, and olfactory adaptation in *Caenorhabditis elegans*. *J Neurosci*, 17; 8259-8269.

Collo G, North RA, Kawashima E, Merlo-Pich E, Neidhart S, Surprenant A, Buell G (1996) Cloning of $P2X_5$ and $P2X_6$ receptors and the distribution and properties of an extended family of ATP-gated ion channels. *J Neurosci*, 16; 2495-2507.

Cook SP, McCleskey EW (2002) Cell damage excites nociceptors through release of cytosolic ATP. *Pain*, 95; 41-47.

Cummins TR, Dib-Hajj SD, Black JA, Akopian AN, Wood JN, Waxman SG (1999) A novel persistent tetrodotoxin-resistant sodium current in SNS-null and wild-type small primary sensory neurons. *J Neurosci*, 19; RC43.

Davies, AM (2000) Neurotrophic factor requirements of developing sensory neurons. In *Molecular basis of pain induction* (Ed. Wood, JN), pp. 23-42, Wiley-Liss, New York.

Davis JB, Gray J, Gunthorpe MJ, Hatcher JP, Davey PT, Overend P, Harries MH, Latcham J, Clapham C, Atkinson K, Hughes SA, Rance K, Grau E, Harper AJ, Pugh PL, Rogers DC, Bingham S, Randall A, Sheardown SA (2000) Vanilloid receptor-1 is essential for inflammatory thermal hyperalgesia. *Nature*, 405; 183-187.

Day NC, Volsen SG, McCormack AL, Craig PJ, Smith W, Beattie RE, Shaw PJ, Ellis SB, Harpold MM, Ince PG (1998) The expression of voltage-dependent calcium channel beta subunits in human hippocampus. *Brain Res Mol Brain Res*, 60; 259-269.

Delmas P, Abogadie FC, Dayrell M, Haley JE, Milligan G, Caulfield MP, Brown DA, Buckley NJ (1998) G-proteins and G-protein subunits mediating cholinergic inhibition of N-type calcium currents in sympathetic neurons. *Eur J Neurosci*, 10; 1654-1666.

Delmas P, Nomura H, Li X, Lakkis M, Luo Y, Segal Y, Fernandez-Fernandez JM, Harris P, Frischauf AM, Brown DA, Zhou J (2002) Constitutive activation of G-proteins by polycystin-1 is antagonized by polycystin-2. *J Biol Chem*, 277; 11276-11283.

Deval E, Baron A, Lingueglia E, Mazarguil H, Zajac JM, Lazdunski M (2003) Effects of neuropeptide SF and related peptides on acid sensing ion channel 3 and sensory neuron excitability. *Neuropharmacology*, 44; 662-671.

Dirajlal S, Pauers LE, Stucky CL (2003) Differential response properties of IB4-positive and -negative unmyelinated sensory neurons to protons and capsaicin. *J Neurophysiol*, 89; 513-524.

Djouhri L, Bleazard L, Lawson SN (1998) Association of somatic action potential shape with sensory receptive properties in guinea-pig dorsal root ganglion neurons. *J Physiol*, 513; 857-872.

Djouhri L, Fang X, Okuse K, Wood JN, Berry CM, Lawson SN (2003a) The TTX-resistant sodium channel $Na_v1.8$ (SNS/PN3): expression and correlation with membrane properties in rat nociceptive primary afferent neurons. *J Physiol*, 550; 739-752.

Djouhri L, Newton R, Levinson SR, Berry CM, Carruthers B, Lawson SN (2003b) Sensory and electrophysiological properties of guinea-pig sensory neurones expressing Na_v 1.7 (PN1) Na^+ channel alpha subunit protein. *J Physiol*, 546; 565-576.

Docherty RJ, Yeats JC, Piper AS (1997) Capsazepine block of voltage-activated calcium channels in adult rat dorsal root ganglion neurones in culture. *Br J Pharmacol*, 121; 1461-1467.

Dray A, Perkins M (1993) Bradykinin and inflammatory pain. *Trends Neurosci*, 16; 99-104.

Drummond HA, Price MP, Welsh MJ, Abboud, FM (1998) A molecular component of the arterial baro-receptor mechanotransducer. *Neuron*, 21; 1435-1441.

Drummond HA, Abboud FM, Welsh MJ (2000) Localization of beta and gamma subunits of ENaC in sensory nerve endings in the rat foot pad. *Brain Res*, 884; 1-12.

Du H, Gu G, William CM, Chalfie M (1996) Extracellular proteins needed for *C. elegans* mechano-sensation. *Neuron*, 16; 183-194.

Duggan A, García-Añoveros J, Corey DP (2002) The PDZ domain protein PICK1 and the sodium channel BNaC1 interact and localize at mechanosensory terminals of dorsal root ganglion neurons and dendrites of central neurons. *J Biol Chem*, 277; 5203-5208.

Eberl DF, Hardy RW, Kernan MJ (2000) Genetically similar transduction mechanisms for touch and hearing in *Drosophila*. *J Neurosci*, 20; 5981-5988.

Eilers A, Martinez-Salgado C, Lewin GR (2002). Molecular interactions between stomatin and ASIC/DEG family proteins. Program No. 449.7. *2002 Abstract Viewer/Itinerary Planner.* Washington, DC: Society for Neuroscience.

England S, Okuse K, Ogata N Wood JN (1998) Heterologous expression of the sensory neuron-specific sodium channel (SNS) α-subunit in rat sympathetic neurons. *J. Physiol*, 511; 124P.

Ernstrom GG, Chalfie M (2002) Genetics of sensory mechanotransduction. *Annu Rev Genet*, 36; 411-453.

Escoubas P, De Weille JR, Lecoq A, Diochot S, Waldmann R, Champigny G, Moinier D, Menez A, Lazdunski M (2000) Isolation of a tarantula toxin specific for a class of proton-gated Na^+ channels. *J Biol Chem*, 275; 25116-25121.

Fain GL (2003) *Sensory transduction*. Sinauer Associates.

Fainzilber M, Hasson A, Oren R, Burlingame AL, Gordon D, Spira ME, Zlotkin E (1994) New mollusc-specific alpha-conotoxins block *Aplysia* neuronal acetylcholine receptors. *Biochemistry*, 33; 9523-9529.

Fitzgerald M, Fulton, BP (1992) The physiological properties of developing sensory neurons. In: *Sensory Neurons. Diversity, Development, and Plasticity* (Ed. SA Scott), pp. 287-306, Oxford University Press, New York.

Fricke B, Lints R, Stewart G, Drummond H, Dodt G, Driscoll M, von During M (2000) Epithelial Na^+ channels and stomatin are expressed in rat trigeminal mechanosensory neurons. *Cell Tissue Res*, 299; 327-334.

Gale JE, Marcotti W, Kennedy HJ, Kros CJ, Richardson GP (2001) FM1-43 dye behaves as a permeant blocker of the hair-cell mechanotransducer channel. *J Neurosci*, 21; 7013-7025.

García-Añoveros J, Ma C, Chalfie M (1995) Regulation of *Caenorhabditis elegans* degenerin proteins by a putative extracellular domain. *Curr Biol*, 5; 441-448.

García-Añoveros J, Samad TA, Zuvela-Jelaska L, Woolf CJ, Corey DP (2001) Transport and localization of the DEG/ENaC ion channel BNaC1alpha to peripheral mechanosensory terminals of dorsal root ganglia neurons. *J Neurosci*, 21; 2678-2686.

Gardner EP, Martin JH, Jessell TM (2000) The bodily senses. In *Principles of neural science* (Eds. Kandel ER, Schwarz, JH, Jessell TM), pp. 430-450, McGraw-Hill.

Geiger B, Bershadsky A (2002) Exploring the neighborhood: adhesion-coupled cell mechanosensors. *Cell*, 110; 139-142.

Gerke MB, Plenderleith MB (2001) Binding sites for the plant lectin Bandeiraea simplicifolia I-isolectin B_4 are expressed by nociceptive primary sensory neurones. *Brain Res*, 911; 101-104.

Gilbert SF (1994) Early vertebrate development: Neuralation and the ectoderm. In *Developmental Biology* (pp.244-294). Sinauer Associates, Sunderland, Massachusetts.

Gillespie PG, Walker RG (2001) Molecular basis of mechanosensory transduction. *Nature*, 413; 194-202.

Goldin AL, Barchi RL, Caldwell JH, Hofmann F, Howe JR, Hunter JC, Kallen RG, Mandel G, Meisler MH, Netter YB, Noda M, Tamkun MM, Waxman SG, Wood JN, Catterall WA (2000) Nomenclature of voltage-gated sodium channels. *Neuron*, 28; 365-368.

Goldstein ME, House SB, Gainer H (1991) NF-L and peripherin immunoreactivities define distinct classes of rat sensory ganglion cells. *J Neurosci Res*, 30; 92-104.

Goodman MB, Hall DH, Avery L, Lockery SR (1998) Active currents regulate sensitivity and dynamic range in *C. elegans* neurons. *Neuron*, 20; 763-772.

Goodman MB, Schwarz EM (2002) Transducing touch in *Caenorhabditis elegans*. *Annu Rev Physiol*, 65; 429-452.

Goodman MB, Ernstrom GG, Chelur DS, O'Hagan R, Yao CA, Chalfie M (2002) MEC-2 regulates *C. elegans* DEG/ENaC channels needed for mechanosensation. *Nature*, 415; 1039-1042.

Gotoh H, Takahashi A (1999) Mechanical stimuli induce intracellular calcium response in a subpopulation of cultured rat sensory neurons. *Neuroscience*, 92; 1323-1329.

Gover TD, Kao JPY, Weinreich D (2003) Calcium signaling in single peripheral sensory nerve terminals. *J Neurosci*, 23; 4793-4797.

Gschossmann JM, Chaban VV, McRoberts JA, Raybould HE, Young SH, Ennes HS, Lembo T, Mayer EA (2000) Mechanical activation of dorsal root ganglion cells *in vitro*: comparison with capsaicin and modulation by kappa-opioids. *Brain Res*, 856; 101-110.

Gu G, Caldwell GA, Chalfie M (1996) Genetic interactions affecting touch sensitivity in *Caenorhabditis elegans*. *Proc Natl Acad Sci U S A*, 93; 6577-6582.

Gu JG, MacDermott AB (1997) Activation of ATP P2X receptors elicits glutamate release from sensory neuron synapses. *Nature*, 389; 749-753.

Gu CX, Juranka PF, Morris CE (2001) Stretch-activation and stretch-inactivation of Shaker-IR, a voltage-gated K^+ channel. *Biophys J*, 80; 2678-2693.

Guler AD, Lee H, Iida T, Shimizu I, Tominaga M, Caterina M (2002) Heat-evoked activation of the ion channel, TRPV4. *J Neurosci*, 22; 6408-6414.

Gunthorpe MJ, Benham CD, Randall A, Davis JB (2002) The diversity in the vanilloid (TRPV) receptor family of ion channels. *Trends Pharmacol Sci*, 23; 183-191.

Guo A, Simone DA, Stone LS, Fairbanks CA, Wang J, Elde R (2001) Developmental shift of vanilloid receptor 1 (VR1) terminals into deeper regions of the superficial dorsal horn: correlation with a shift from TrkA to Ret expression by dorsal root ganglion neurons. *Eur J Neurosci*, 14; 293-304.

Guo A, Vulchanova L, Wang J, Li X, Elde R (1998) Immunocytochemical localization of the vanilloid receptor 1 (VR1): relationship to neuropeptides, the P2X3 purinoceptor and IB4 binding sites. *Eur J Neurosci.*, 11; 946-958.

Hackney CM, Furness DN, Benos DJ, Woodley JF, Barratt J (1992) Putative immunolocalization of the mechanoelectrical transduction channels in mammalian cochlear hair cells. *Proc R Soc Lond B Biol Sci*, 248; 215-221.

Hamill OP, Marty A, Neher E, Sakmann B, Sigworth FJ (1981) Improved patch-clamp techniques for high-resolution current recording from cells and cell-free membrane patches. *Pflugers Arch*, 391; 85-100.

Hamill OP, McBride DW Jr (1996) The pharmacology of mechanogated membrane ion channels. *Pharmacol Rev*, 48; 231-252.

Hamill OP, McBride DW Jr (1997) Induced membrane hypo/hyper-mechanosensitivity: a limitation of patch-clamp recording. *Annu Rev Physiol*, 59; 621-631.

Hamill OP, Martinac B (2001) Molecular basis of mechanotransduction in living cells. *Physiol Rev*, 81; 685-740.

Hamilton SG, Wade A, McMahon SB (1999) The effects of inflammation and inflammatory mediators on nociceptive behaviour induced by ATP analogues in the rat. *Br J Pharmacol*, 126; 326-332.

Hamilton SG, McMahon SB, Lewin GR (2001) Selective activation of nociceptors by P2X receptor agonists in normal and inflamed rat skin. *J Physiol*, 534; 437-445.

Harper AA, Lawson SN (1985a) Conduction velocity is related to morphological cell type in rat dorsal root ganglion neurons. *J Physiol (Lond)*, 359; 31-46.

Harper AA, Lawson SN (1985b) Electrical properties of rat dorsal root ganglion neurons with different peripheral nerve conduction velocities. *J Physiol (Lond)*, 359; 47-63.

Hart AC, Kass J, Shapiro JE, Kaplan JM (1999) Distinct signaling pathways mediate touch and osmosensory responses in a polymodal sensory neuron. *J Neurosci*, 19; 1952-1958.

Harteneck C, Plant TD, Schultz G (2000) From worm to man: three subfamilies of TRP channels. *Trends Neurosci*, 23; 159-166.

Harvey AL (2002) Toxins 'R' Us: more pharmacological tools from nature's superstore. *Trends Pharmacol Sci*, 23; 201-203.

Heidmann T, Changeux JP (1978) Structural and functional properties of the acetylcholine receptor protein in its purified and membrane-bound states. *Annu Rev Biochem*, 47; 317-357.

Hensel H, Iggo, A (1971) Analysis of cutaneous warm and cold fibres in primates. *Pflugers Arch*, 329; 1-8.

Hensel H, Zotterman Y (1951) The effect of menthol on the thermoreceptors. *Acta Physiol. Scand.* 24; 27-34.

Hille B (2001) *Ion channels of excitable membranes*. Sinauer Associates, Inc, Sunderland Massachusetts.

Hong K, Driscoll M (1994) A transmembrane domain of the putative channel subunit MEC-4 influences mechanotransduction and neurodegeneration in *C. elegans*. *Nature*, 367; 470-473.

Hong K, Mano I, Driscoll M (2000) *In vivo* structure-function analyses of *Caenorhabditis elegans* MEC-4, a candidate mechanosensory ion channel subunit. *J Neurosci*, 20; 2575-2588.

Hruska-Hageman AM, Wemmie JA, Price MP, Welsh MJ (2002) Interaction of the synaptic protein PICK1

(protein interacting with C kinase 1) with the non-voltage gated sodium channels BNC1 (brain Na^+ channel 1) and ASIC (acid-sensing ion channel). *Biochem J*, 361; 443-450.

Huang M, Chalfie M (1994) Gene interactions affecting mechanosensory transduction in *Caenorhabditis elegans*. *Nature*, 367; 467-470.

Huang M, Gu G, Ferguson EL, Chalfie M (1995) A stomatin-like protein necessary for mechanosensation in *C. elegans*. *Nature*, 378; 292-295.

Hummler E, Barker P, Gatzy J, Beermann F, Verdumo C, Schmidt A, Boucher R, Rossier BC (1996) Early death due to defective neonatal lung liquid clearance in alpha-ENaC-deficient mice. *Nat Genet*, 12; 325-328.

Immke DC, McCleskey EW (2001) Lactate enhances the acid-sensing Na^+ channel on ischemia-sensing neurons. *Nat Neurosci*, 4; 869-870.

Immke DC, McCleskey EW (2003) Protons open acid-sensing ion channels by catalyzing relief of Ca^{2+} blockade. *Neuron*, 37; 75-84.

Ismailov II, Berdiev BK, Shlyonsky VG, Benos DJ (1997) Mechanosensitivity of an epithelial Na^+ channel in planar lipid bilayers: release from Ca^{2+} block. *Biophys J*, 72; 1182-1192.

Jahr CE, Jessell TM (1983) ATP excites a subpopulation of rat dorsal horn neurons. *Nature*, 304; 730-733.

Johnson KO, Yoshioka T, Vega-Bermudez F (2000) Tactile functions of mechanoreceptive afferents innervating the hand. *J Clin Neurophysiol*, 17; 539-558.

Jordt SE, Tominaga M, Julius D (2000) Acid potentiation of the capsaicin receptor determined by a key extracellular site. *Proc Natl Acad Sci U S A*, 97; 8134-8139.

Jordt SE, Julius D (2002) Molecular basis for species-specific sensitivity to "hot" chili peppers. *Cell*, 108; 421-430.

Jordt SE, McKemy DD, Julius, D (2003) Lessons from peppers and peppermint: the molecular logic of thermosensation. *Curr Opin Neurobiol*,13; 487-492.

Julius D, Basbaum AI (2001) Molecular mechanisms of nociception. *Nature*, 413; 203-210.

Katz E, Verbitsky M, Rothlin CV, Vetter DE, Heinemann SF, Elgoyhen AB (2000) High calcium permeability and calcium block of the alpha9 nicotinic acetylcholine receptor. *Hear Res*, 141; 117-128.

Kellenberger S, Schild L (2002) Epithelial sodium channel/degenerin family of ion channels: a variety of functions for a shared structure. *Physiol Rev*, 82; 735-767.

Kenins P (1982) Responses of single nerve fibres to capsaicin applied to the skin. *Neurosci Lett*, 29; 83-88.

Kenshalo DR, Duclaux R (1977) Response characteristics of cutaneous cold receptors in the monkey. *J Neurophysiol*, 40; 319-332

Kernan M, Cowan D, Zuker C (1994) Genetic dissection of mechanosensory transduction: mechanoreception-defective mutations of *Drosophila. Neuron*, 12; 1195-1206.

Kernan M, Zuker C (1995) Genetic approaches to mechanosensory transduction. *Curr Opin Neurobiol*, 5; 443-448.

Kieffer BL, Befort K, Gaveriaux-Ruff C, Hirth CG (1992) The delta-opioid receptor: isolation of a cDNA by expression cloning and pharmacological characterization. *Proc Natl Acad Sci U S A*, 89; 12048-12052.

Kim J, Chung YD, Park DY, Choi S, Shin DW, Soh H, Lee HW, Son W, Yim J, Park CS, Kernan MJ, Kim C (2003) A TRPV family ion channel required for hearing in *Drosophila. Nature*, 424; 81-84.

Kinkelin I, Stucky CL, Koltzenburg M (1999) Postnatal loss of Merkel cells, but not of slowly adapting mechanoreceptors in mice lacking the neurotrophin receptor p75. *Eur J Neurosci*, 11; 3963-3969.

Kirschstein T, Greffrath W, Busselberg D, Treede RD (1999) Inhibition of rapid heat responses in nociceptive primary sensory neurons of rats by vanilloid receptor antagonists. *J Neurophysiol*, 82; 2853-2860.

Kizer N, Guo XL, Hruska K (1997) Reconstitution of stretch-activated cation channels by expression of the alpha-subunit of the epithelial sodium channel cloned from osteoblasts. *Proc Natl Acad Sci U S A*, 94; 1013-1018.

Koerber HR, Druzinsky RE, Mendell, LM (1988) Properties of somata of spinal dorsal root ganglion cells differ according to peripheral receptor innervated. *J Neurophysiol*, 60; 1584-1596.

Koerber HR, Mendell LM (1992) Functional heterogeneity of dorsal root ganglia cells. In *Sensory Neurons: Diversity, development and plasticity* (Ed. SA Scott), pp. 77-96, Oxford University Press.

Koltzenburg M, Stucky CL Lewin GR (1997) Receptive properties of mouse sensory neurons innervating hairy skin. *J Neurophysiol*, 78;1841-1850.

Koulen P, Thrower EC (2001) Pharmacological modulation of intracellular Ca^{2+} channels at the single-channel level. *Mol Neurobiol*, 24; 65-86.

Krishtal OA, Pidoplichko VI (1980) A receptor for protons in the nerve cell membrane. *Neuroscience*, 5; 2325-2327.

Krishtal OA, Pidoplichko VI (1981) A receptor for protons in the membrane of sensory neurons may participate in nociception. *Neuroscience*, 6; 2599-2601.

Lai CC, Hong K, Kinnell M, Chalfie M, Driscoll M (1996) Sequence and transmembrane topology of MEC-4, an ion channel subunit required for mechanotransduction in *Caenorhabditis elegans*. *J Cell Biol*, 133; 1071-1081.

Lawson SN (1979) The postnatal development of large light and small dark neurons in mouse dorsal root ganglia: a statistical analysis of cell numbers and size. *J Neurocytol*, 8; 275-294.

Lawson SN, Harper AA, Harper EI, Garson JA, Anderton BH (1984) A monoclonal antibody against neurofilament protein specifically labels a subpopulation of rat sensory neurones. *J Comp Neurol*, 228; 263-272.

Lawson SN, Waddell PJ (1991) Soma neurofilament immunoreactivity is related to cell size and fibre conduction velocity in rat primary sensory neurons. *J Physiol*, 435; 41-63.

Lawson SN (1992) Morphological and biochemical cell types of sensory neurons. . In *Sensory Neurons: Diversity, development and plasticity* (Ed. SA Scott), pp. 27-59, Oxford University Press.

Lawson SN (2002) Phenotype and function of somatic primary afferent nociceptive neurons with C-, Adelta- or Aalpha/beta-fibres. *Exp Physiol*, 87; 239-244.

Lee KH, Chung K, Chung JM, Coggeshall RE (1986) Correlation of cell body size, axon size, and signal conduction velocity for individually labelled dorsal root ganglion cells in the cat. *J Comp Neurol*, 243; 335-346.

Lee N, Chen J, Sun L, Wu S, Gray KR, Rich A, Huang M, Lin JH, Feder JN, Janovitz EB, Levesque PC, Blanar MA (2003) Expression and characterization of human transient receptor potential melastatin 3 (hTRPM3). *J Biol Chem*, 278; 20890-20897.

Lewin GR, Stucky CL (2000) Sensory neuron mechanotransduction: Regulation and underlying molecular mechanisms. In *Molecular Basis of Pain Transduction* (Ed. JN Wood), pp. 129-148, Wiley-Liss.

Liedtke W, Choe Y, Martí-Renom MA, Bell AM, Denis CS, Šali A, Hudspeth AJ, Friedman JM (2000) Vanilloid receptor-related osmotically activated channel (VR-OAC), a candidate vertebrate osmoreceptor. *Cell*, 103; 525–535.

Liedtke W, Friedman JM (2003) Abnormal osmotic regulation in *trpv4-/-* mice. *Proc Natl Acad Sci USA*, 100; 13698-13703.

Liedtke W, Tobin DM, Bargmann CI, Friedman JM (2003) Mammalian TRPV4 (VR-OAC) directs behavioral responses to osmotic and mechanical stimuli in *Caenorhabditis elegans*. *Proc Natl Acad Sci U S A*, 100 (Suppl 2); 14531-14536.

Lingueglia E, de Weille JR, Bassilana F, Heurteaux C, Sakai H, Waldmann R, Lazdunski M (1997) A modulatory subunit of acid sensing ion channels in brain and dorsal root ganglion cells. *J Biol Chem*, 272; 29778-29783.

Liu J, Schrank B, Waterston RH (1996) Interaction between a putative mechanosensory membrane channel and a collagen. *Science*, 273; 361-364.

Loewenstein WR, Skalak R (1966) Mechanical transmission in a Pacinian corpuscle. An analysis and a theory. *J Physiol (Lond)*, 182;346-378.

Ma HP, Li L, Zhou ZH, Eaton DC, Warnock DG (2002) ATP masks stretch activation of epithelial sodium channels in A6 distal nephron cells. *Am J Physiol Renal Physiol*, 282; F501-5.

Maeda T, Sato O, Kannari K, Takagi H, Iwanaga T (1991) Immunohistochemical localization of laminin in

the periodontal Ruffini endings of rat incisors: a possible function of terminal Schwann cells. *Arch Histol Cytol*, 54; 339-348.

Maingret F, Fosset M, Lesage F, Lazdunski M, Honore E (1999) TRAAK is a mammalian neuronal mechano-gated K^+ channel. *J Biol Chem*, 274; 1381-1387.

Malik-Hall M, Poon WY, Baker MD, Wood JN, Okuse K (2003) Sensory neuron proteins interact with the intracellular domains of sodium channel $Na_V1.8$. *Brain Res Mol Brain Res*, 110; 298-304.

Mansour SL, Thomas KR, Capecchi MR (1988) Disruption of the proto-oncogene *int-2* in mouse embryo-derived stem cells: a general strategy for targeting mutations to non-selectable genes. *Nature*, 336; 348-352.

Marrion NV, Smart TG, Brown DA (1987) Membrane currents in adult rat superior cervical ganglia in dissociated tissue culture. *Neurosci Lett*, 77; 55-60.

Massilia GR, Schinina ME, Ascenzi P, Polticelli F (2001) Contryphan-Vn: a novel peptide from the venom of the Mediterranean snail *Conus ventricosus*. *Biochem Biophys Res Commun*, 288; 908-913.

Massilia GR, Eliseo T, Grolleau F, Lapied B, Barbier J, Bournaud R, Molgo J, Cicero DO, Paci M, Schinina ME, Ascenzi P, Polticelli F (2003) Contryphan-Vn: a modulator of Ca^{2+}-dependent K^+ channels. *Biochem Biophys Res Commun*, 303; 238-246.

Matthews BD, Overby DR, Alenghat FJ, Karavitis J, Numaguchi Y, Allen PG, Ingber DE (2004) Mechanical properties of individual focal adhesions probed with a magnetic microneedle. *Biochem Biophys Res Commun*, 313; 758-764.

McCarter GC, Reichling DB, Levine JD (1999) Mechanical transduction by rat dorsal root ganglion neurons *in vitro*. *Neurosci Lett*, 273; 179-182.

McDonald FJ, Yang B, Hrstka RF, Drummond HA, Tarr DE, McCray PB Jr, Stokes JB, Welsh MJ, Williamson RA (1999) Disruption of the beta subunit of the epithelial Na^+ channel in mice: hyperkalemia and neonatal death associated with a pseudohypoaldosteronism phenotype. *Proc Natl Acad Sci U S A*, 96; 1727-1731.

McKemy DD, Neuhausser WM, Julius, D (2002) Identification of a cold receptor reveals a general role for TRP channels in thermosensation. *Nature*, 416; 52-58.

Meves H (1994) Modulation of ion channels by arachidonic acid. *Prog Neurobiol*, 43; 175-186.

Meyers JR, MacDonald RB, Duggan A, Lenzi D, Standaert DG, Corwin JT, Corey DP (2003) Lighting up the senses: FM1-43 loading of sensory cells through nonselective ion channels. *J Neurosci*, 23; 4054-4065.

Michael GJ, Priestley JV (1999) Differential expression of the mRNA for the vanilloid receptor subtype 1 in cells of the adult rat dorsal root and nodose ganglia and its downregulation by axotomy. *J Neurosci*, 19; 1844-1854.

Mills LR, Diamond J (1995) Merkel cells are not the mechanosensory transducers in the touch dome of the rat. *J Neurocytol*, 24; 117-134.

Molliver DC, Wright DE, Leitner ML, Parsadanian AS, Doster K, Wen D, Yan Q, Snider WD (1997) IB4-binding DRG neurons switch from NGF to GDNF dependence in early postnatal life. *Neuron*, 19; 849-861.

Molliver DC, Cook SP, Carlsten JA, Wright DE, McCleskey EW (2002) ATP and UTP excite sensory neurons and induce CREB phosphorylation through the metabotropic receptor, $P2Y_2$. *Eur J Neurosci*, 16; 1850-1860.

Montell C, Birnbaumer L, Flockerzi V, Bindels RJ, Bruford EA, Caterina MJ, Clapham DE, Harteneck C, Heller S, Julius D, Kojima I, Mori Y, Penner R, Prawitt D, Scharenberg AM, Schultz G, Shimizu N, Zhu MX (2002) A unified nomenclature for the superfamily of TRP cation channels. *Mol Cell*, 9; 229-231.

Morris CE, Horn R (1991) Failure to elicit neuronal macroscopic mechanosensitive currents anticipated by single-channel studies. *Science*, 251; 1246-1249.

Nagy A, Rossant J, Nagy R, Abramow-Newerly W, Roder JC (1993) Derivation of completely cell culture-derived mice from early-passage embryonic stem cells. *Proc Natl Acad Sci U S A.*, 90; 8424-8428.

Nagy I, Rang HP (1999) Similarities and differences between the responses of rat sensory neurons to noxious heat and capsaicin. *J Neurosci*, 19; 10647-10655.

Nakamura F, Strittmatter SM (1996) $P2Y_1$ purinergic receptors in sensory neurons: contribution to touch-induced impulse generation. *Proc Natl Acad Sci U S A*, 93; 10465-10470.

Nauli SM, Alenghat FJ, Luo Y, Williams E, Vassilev P, Li X, Elia AE, Lu W, Brown EM, Quinn SJ,

Ingber DE, Zhou J (2003) Polycystins 1 and 2 mediate mechanosensation in the primary cilium of kidney cells. *Nat Genet*, 33; 129-137.

Norman RI, Schmid A, Lombet A, Barhanin J, Lazdunski M (1983) Purification of binding protein for Tityus gamma toxin identified with the gating component of the voltage-sensitive Na^+ channel. *Proc Natl Acad Sci USA*, 80; 4164-4168.

Olivera BM, Cruz, LJ (2001) Conotoxins, in retrospect. *Toxicon*, 39; 7-14.

Olson TH, Riedl MS, Vulchanova L, Ortiz-Gonzalez XR, Elde R (1998) An acid sensing ion channel (ASIC) localizes to small primary afferent neurons in rats. *Neuroreport*, 9; 1109-1113.

Palmer LG, Frindt G (1996) Gating of Na channels in the rat cortical collecting tubule: effects of voltage and membrane stretch. *J Gen Physiol*, 107; 35-45.

Paoletti P, Ascher P (1994) Mechanosensitivity of NMDA receptors in cultured mouse central neurons. *Neuron*, 13; 645-655.

Park EC, Horvitz HR (1986) *C. elegans unc-105* mutations affect muscle and are suppressed by other mutations that affect muscle. *Genetics*, 113; 853-867.

Patapoutian A, Peier AM, Story GM, Viswanath V (2003) ThermoTRP channels and beyond: mechanisms of temperature sensation. *Nat Rev Neurosci*, 4; 529-539.

Patel AJ, Honore E, Maingret F, Lesage F, Fink M, Duprat F, Lazdunski M (1998) A mammalian two pore domain mechano-gated S-like K^+ channel. *EMBO J*, 17; 4283-4290.

Paukert M, Sidi S, Russell C, Siba M, Wilson SW, Nicolson T, Grunder S (2004) A family of acid-sensing ion channels (ASICs) from the zebrafish: Widespread expression in the central nervous system suggests a conserved role in neuronal communication. *J Biol Chem*, 279; 18783-18791.

Peier AM, Reeve AJ, Andersson DA, Moqrich A, Earley TJ, Hergarden AC, Story GM, Colley S, Hogenesch JB, McIntyre P, Bevan S, Patapoutian A (2002a) A heat-sensitive TRP channel expressed in keratinocytes. *Science*, 296; 2046-2049.

Peier AM, Moqrich A, Hergarden AC, Reeve AJ, Andersson DA, Story GM, Earley TJ, Dragoni I, McIntyre P, Bevan S, Patapoutian A (2002b) A TRP channel that senses cold stimuli and menthol. *Cell*, 108; 705-715.

Perl ER (1992) Function of dorsal root ganglion neurons. In: *Sensory Neurons. Diversity, Development, and Plasticity* (Ed. SA Scott), pp. 3-27, Oxford University Press, New York.

Perry SJ, Straub VA, Schofield MG, Burke JF, Benjamin PR (2001) Neuronal expression of an FMRFamide-gated Na^+ channel and its modulation by acid pH. *J Neurosci*, 21; 5559-5567.

Petruska JC, Napaporn J, Johnson RD, Gu JG, Cooper BY (2000) Subclassified acutely dissociated cells of rat DRG: histochemistry and patterns of capsaicin-, proton-, and ATP-activated currents. *J Neurophysiol*, 84; 2365-2379.

Petruska JC, Napaporn J, Johnson RD, Cooper BY (2002) Chemical responsiveness and histochemical phenotype of electrophysiologically classified cells of the adult rat dorsal root ganglion. *Neuroscience*, 115; 15-30.

Plopper G, Ingber DE (1993) Rapid induction and isolation of focal adhesion complexes. *Biochem Biophys Res Commun*, 193; 571-578.

Price MP, Snyder PM, Welsh MJ (1996) Cloning and expression of a novel human brain Na^+ channel. *J Biol Chem*, 271; 7879-7882.

Price MP, Lewin GR, McIlwrath SL, Cheng C, Xie J, Heppenstall PA, Stucky CL, Mannsfeldt AG, Brennan TJ, Drummond HA, Qiao J, Benson CJ, Tarr DE, Hrstka RF, Yang B, Williamson RA, Welsh MJ (2000) The mammalian sodium channel BNC1 is required for normal touch sensation. *Nature*, 407; 1007-1011.

Price MP, McIlwrath SL, Xie J, Cheng C, Qiao J, Tarr DE, Sluka KA, Brennan TJ, Lewin GR, Welsh MJ (2001) The DRASIC cation channel contributes to the detection of cutaneous touch and acid stimuli in mice. *Neuron*, 32; 1071-1083.

Priestley JV, Michael GJ, Averill S, Liu M, Willmott N (2002) Regulation of nociceptive neurons by nerve growth factor and glial cell line derived neurotrophic factor. *Can J Physiol Pharmacol*, 80; 495-505.

Rae J, Cooper K, Gates P, Watsky M (1991) Low access resistance perforated patch recordings using amphotericin B. *J Neurosci Methods*, 37; 15-26.

Raja SN, Meyer RA, Ringkamp M Campbell JN (1999) Peripheral neural mechanisms of nociception. In *Textbook of Pain* (Eds. PD Wall and R Melzack), pp. 11-57, Churchill-Livingstone.

Rasband MN, Park EW, Vanderah TW, Lai J, Porreca F, Trimmer JS (2001) Distinct potassium channels on pain-sensing neurons. *Proc Natl Acad Sci U S A*, 98; 13373-13378.

Raybould HE, Gschossman JM, Ennes H, Lembo T, Mayer EA (1999) Involvement of stretch-sensitive calcium flux in mechanical transduction in visceral afferents. *J Auton Nerv Syst*, 75; 1-6.

Reeh PW (1988) Sensory receptors in a mammalian skin-nerve *in vitro* preparation. *Prog Brain Res*, 74; 271-276.

Reeh PW, Kress M (2001) Molecular physiology of proton transduction in nociceptors. *Curr Opin Pharmacol*, 1; 45-51.

Reid G, Flonta ML (2001) Physiology. Cold current in thermoreceptive neurons. *Nature*, 413; 480.

Reid G, Babes A, Pluteanu F (2002) A cold- and menthol-activated current in rat dorsal root ganglion neurons: properties and role in cold transduction. *J Physiol*, 545; 595-614.

Reid G, Flonta ML (2002) Ion channels activated by cold and menthol in cultured rat dorsal root ganglion neurons. *Neurosci Lett*, 324; 164-168.

Ricci AJ, Fettiplace R (1998) Calcium permeation of the turtle hair cell mechanotransducer channel and its relation to the composition of endolymph. *J Physiol*, 506; 159-173.

Ritter AM, Mendell LM (1992) Somal membrane properties of physiologically identified sensory neurons in the rat: effects of nerve growth factor. *J Neurophysiol*, 68; 2033-2041.

Roayaie K, Crump JG, Sagasti A, Bargmann CI (1998) The G alpha protein ODR-3 mediates olfactory and nociceptive function and controls cilium morphogenesis in *C. elegans* olfactory neurons. *Neuron*, 20; 55-67.

Rose RD, Koerber HR, Sedivec MJ, Mendell LM (1986) Somal action potential duration differs in identified primary afferents. *Neurosci Lett*, 63; 259-264.

Rusch A, Hummler E (1999) Mechano-electrical transduction in mice lacking the alpha-subunit of the epithelial sodium channel. *Hear Res*, 131; 170-176.

Ryan TA (2001) Presynaptic imaging techniques. *Curr Opin Neurobiol*, 11; 544-549.

Sackin H (1995) Mechanosensitive channels. *Annu Rev Physiol*, 57; 333-353.

Saitou T, Ishikawa T, Obara K, Nakayama K (2000) Characterization of whole-cell currents elicited by mechanical stimulation of *Xenopus* oocytes. *Pflugers Arch*, 440; 858-865.

Schmidt CE, Dai J, Lauffenburger DA, Sheetz MP, Horwitz AF (1995) Integrin-cytoskeletal interactions in neuronal growth cones. *J Neurosci*, 15; 3400-3407.

Scott BS, Edwards BA (1980) Electric membrane properties of adult mouse DRG neurons and the effect of culture duration. *J Neurobiol*, 11; 291-301.

Sharma RV, Chapleau MW, Hajduczok G, Wachtel RE, Waite LJ, Bhalla RC, Abboud FM (1995) Mechanical stimulation increases intracellular calcium concentration in nodose sensory neurons. *Neuroscience*, 66; 433-441.

Sharpe IA, Gehrmann J, Loughnan ML, Thomas L, Adams DA, Atkins A, Palant E, Craik DJ, Adams DJ, Alewood PF, Lewis RJ (2001) Two new classes of conopeptides inhibit the alpha1-adrenoceptor and noradrenaline transporter. *Nat Neurosci*, 4; 902-907.

Shiga H, Tojima T, Ito E (2001) Ca^{2+} signaling regulated by an ATP-dependent autocrine mechanism in astrocytes. *Neuroreport*, 12; 2619-2622.

Shin JB, Martinez-Salgado C, Heppenstall PA, Lewin GR (2003) A T-type calcium channel required for normal function of a mammalian mechanoreceptor. *Nat Neurosci*, 6; 724-730.

Sidi S, Friedrich RW, Nicolson T (2003) NompC TRP channel required for vertebrate sensory hair cell mechanotransduction. *Science*, 301; 96-99.

Silos-Santiago I (2000) Neurotrophic signalling and sensory neuron survival and function. In *Molecular basis of pain induction* (Ed. Wood, JN), pp. 43-64, Wiley-Liss, New York.

Silverman JD, Kruger L (1990) Selective neuronal glycoconjugate expression in sensory and autonomic ganglia: relation of lectin reactivity to peptide and enzyme markers. *J Neurocytol*, 19; 789-801.

Sinclair D (1981) *Mechanisms of cutaneous sensation*. Oxford University Press.

Smith GD, Gunthorpe MJ, Kelsell RE, Hayes PD, Reilly P, Facer P, Wright JE, Jerman JC, Walhin JP, Ooi L, Egerton J, Charles KJ, Smart D, Randall AD, Anand P, Davis JB (2002) TRPV3 is a temperature-sensitive vanilloid receptor-like protein. *Nature*, 418; 186-190.

Steen KH, Reeh PW, Anton F, Handwerker HO (1992) Protons selectively induce lasting excitation and sensitization to mechanical stimulation of nociceptors in rat skin, *in vitro*. *J Neurosci*, 12; 86-95.

Steen KH, Steen AE, Reeh PW (1995) A dominant role of acid pH in inflammatory excitation and sensitization of nociceptors in rat skin, *in vitro*. *J Neurosci*, 15; 3982-3989.

Story GM, Peier AM, Reeve AJ, Eid SR, Mosbacher J, Hricik TR, Earley TJ, Hergarden AC, Andersson DA, Hwang SW, McIntyre P, Jegla T, Bevan S, Patapoutian A (2003) ANKTM1, a TRP-like channel expressed in nociceptive neurons, is activated by cold temperatures. *Cell*, 112; 819-829.

Strassmaier M, Gillespie PG (2002) The hair cell's transduction channel. *Curr Opin Neurobiol*, 12; 380-386.

Strotmann R, Harteneck C, Nunnenmacher K, Schultz G, Plant TD (2000) OTRPC4, a nonselective cation channel that confers sensitivity to extracellular osmolarity. *Nat Cell Biol*, 2; 695–702.

Stucky CL, Lewin GR (1999) Isolectin B4-positive and -negative nociceptors are functionally distinct. *J Neurosci*, 19; 6497-6505.

Suchyna TM, Johnson JH, Hamer K, Leykam JF, Gage DA, Clemo HF, Baumgarten CM, Sachs F (2000) Identification of a peptide toxin from *Grammostola spatulata* spider venom that blocks cation-selective stretch-activated channels. *J Gen Physiol*, 115; 583-598.

Sukharev S, Corey DP (2004) Mechanosensitive channels: multiplicity of families and gating paradigms. *Sci STKE*, 2004(219):re4.

Sullivan MJ, Sharma RV, Wachtel RE, Chapleau MW, Waite LJ, Bhalla RC, Abboud FM (1997) Non-voltage-gated Ca^{2+} influx through mechanosensitive ion channels in aortic baroreceptor neurons. *Circ Res*, 80; 861-867.

Sutherland SP, Benson CJ, Adelman JP, McCleskey EW (2001) Acid-sensing ion channel 3 matches the acid-gated current in cardiac ischemia-sensing neurons. *Proc Natl Acad Sci U S A*, 98; 711-716.

Suzuki H, Kerr R, Bianchi L, Frokjaer-Jensen C, Slone D, Xue J, Gerstbrein B, Driscoll M, Schafer WR (2003a) In vivo imaging of *C. elegans* mechanosensory neurons demonstrates a specific role for the MEC-4 channel in the process of gentle touch sensation. *Neuron*, 39; 1005-1017.

Suzuki M, Mizuno A, Kodaira K, Imai M (2003b) Impaired pressure sensation in mice lacking TRPV4. *J Biol Chem*, 278; 22664-22668.

Szolcsanyi J, Anton F, Reeh PW, Handwerker HO (1988) Selective excitation by capsaicin of mechano-heat sensitive nociceptors in rat skin. *Brain Res*, 446; 262-268.

Szolcsanyi J (1993) Actions of capsaicin on sensory receptors. In *Capsaicin in the Study of Pain* (Ed. JN, Wood), pp1-26, Academic Press.

Takahashi A, Gotoh H (2000) Mechanosensitive whole-cell currents in cultured rat somatosensory neurons. *Brain Res*, 869; 225-230.

Tavernarakis N, Shreffler W, Wang S, Driscoll M (1997) *unc-8*, a DEG/ENaC family member, encodes a subunit of a candidate mechanically gated channel that modulates *C. elegans* locomotion. *Neuron*, 18; 107-119.

Tavernarakis N, Driscoll M (1997) Molecular modeling of mechanotransduction in the nematode *Caenorhabditis elegans*. *Annu Rev Physiol*, 59; 659-689.

Terlau H, Olivera BM (2004) *Conus* venoms: a rich source of novel ion channel-targeted peptides. *Physiol Rev*, 84; 41-68.

Tobin D, Madsen D, Kahn-Kirby A, Peckol E, Moulder G, Barstead R, Maricq A, Bargmann C (2002) Combinatorial expression of TRPV channel proteins defines their sensory functions and subcellular localization in *C. elegans* neurons. *Neuron*, 35; 307-318.

Tomaselli KJ, Doherty P, Emmett CJ, Damsky CH, Walsh FS, Reichardt LF (1993) Expression of beta 1 integrins in sensory neurons of the dorsal root ganglion and their functions in neurite outgrowth on two laminin isoforms. *J Neurosci*, 13; 4880-4888.

Tominaga M, Caterina MJ, Malmberg AB, Rosen TA, Gilbert H, Skinner K, Raumann BE, Basbaum AI, Julius D (1998) The cloned capsaicin receptor integrates multiple pain-producing stimuli. *Neuron*, 21; 531-543.

Tracey WD Jr, Wilson RI, Laurent G, Benzer S (2003) *painless*, a *Drosophila* gene essential for nociception. *Cell*, 113; 261-273.

Trebak M, Bird GS, McKay RR, Putney JW Jr (2002) Comparison of human TRPC3 channels in receptor-activated and store-operated modes. Differential sensitivity to channel blockers suggests fundamental differences in channel composition. *J Biol Chem*, 277; 21617-21623.

Vassilev PM, Guo L, Chen XZ, Segal Y, Peng JB, Basora N, Babakhanlou H, Cruger G, Kanazirska M, Ye Cp, Brown EM, Hediger MA, Zhou J (2001) Polycystin-2 is a novel cation channel implicated in defective intracellular Ca^{2+} homeostasis in polycystic kidney disease. *Biochem Biophys Res Commun*, 282; 341-350.

Viana F, de la Pena E, Pecson B, Schmidt RF, Belmonte C (2001) Swelling-activated calcium signalling in cultured mouse primary sensory neurons. *Eur J Neurosci*, 13; 722-734.

Viana F, de la Pena E, Belmonte C (2002) Specificity of cold thermotransduction is determined by differential ionic channel expression. *Nat Neurosci*, 5; 254-260.

Vlaskovska M, Kasakov L, Rong W, Bodin P, Bardini M, Cockayne DA, Ford AP, Burnstock G (2001) $P2X_3$ knock-out mice reveal a major sensory role for urothelially released ATP. *J Neurosci*, 21; 5670-5677.

Voets T, Nilius B, Hoefs S, van der Kemp AW, Droogmans G, Bindels RJ, Hoenderop JG (2004) TRPM6 forms the Mg^{2+} influx channel involved in intestinal and renal Mg^{2+} absorption. *J Biol Chem*, 279; 19-25.

Waldmann R, Champigny G, Voilley N, Lauritzen I, Lazdunski M (1996) The mammalian degenerin MDEG, an amiloride-sensitive cation channel activated by mutations causing neurodegeneration in Caenorhabditis elegans. *J Biol Chem*, 271; 10433-10436.

Waldmann R, Champigny G, Bassilana F, Heurteaux C, Lazdunski M (1997a) A proton-gated cation channel involved in acid-sensing. *Nature*, 386; 173-177.

Waldmann R, Bassilana F, de Weille J, Champigny G, Heurteaux C, Lazdunski M (1997b) Molecular cloning of a non-inactivating proton-gated Na^+ channel specific for sensory neurons. *J Biol Chem*, 272; 20975-20978.

Waldmann R, Lazdunski M (1998) H^+-gated cation channels: neuronal acid sensors in the NaC/DEG family of ion channels. *Curr Opin Neurobiol*, 8; 418-424.

Walker RG, Willingham AT, Zuker CS (2000) A *Drosophila* mechanosensory transduction channel. *Science*, 287; 2229-2234.

Wan X, Juranka P, Morris CE (1999) Activation of mechanosensitive currents in traumatized membrane. *Am J Physiol*, 276; C318-27.

Watanabe H, Vriens J, Suh SH, Benham CD, Droogmans G, Nilius B (2002a) Heat-evoked activation of TRPV4 channels in a HEK293 cell expression system and in native mouse aorta endothelial cells. *J Biol Chem*, 277; 47044-47051.

Watanabe H, Davis JB, Smart D, Jerman JC, Smith GD, Hayes P, Vriens J, Cairns W, Wissenbach U, Prenen J, Flockerzi V, Droogmans G, Benham CD, Nilius B (2002b) Activation of TRPV4 channels (hVRL-2/mTRP12) by phorbol derivatives. *J Biol Chem*, 277; 13569-13577.

Welk E, Leah JD, Zimmermann M (1990) Characteristics of A- and C-fibers ending in a sensory nerve neuroma in the rat. *J Neurophysiol*, 63; 759-766.

Welsh MJ, Price MP, Xie J (2001) Biochemical basis of touch perception: Mechanosensory function of DEG/ENaC channels. *J Biol Chem*, 277; 2369-2372.

Wemmie JA, Askwith CC, Lamani E, Cassell MD, Freeman JH Jr, Welsh MJ (2003) Acid-sensing ion channel 1 is localized in brain regions with high synaptic density and contributes to fear conditioning. *J Neurosci*, 23; 5496-5502.

Wemmie JA, Chen J, Askwith CC, Hruska-Hageman AM, Price MP, Nolan BC, Yoder PG, Lamani E, Hoshi T, Freeman JH Jr, Welsh MJ (2002) The acid-activated ion channel ASIC contributes to synaptic plasticity, learning, and memory. *Neuron*, 34; 463-477.

Winter J (1987) Characterization of capsaicin-sensitive neurones in adult rat dorsal root ganglion cultures. *Neurosci Lett*, 80; 134-140.

Winter J, Forbes CA, Sternberg J, Lindsay RM (1988) Nerve growth factor (NGF) regulates adult rat cultured dorsal root ganglion neuron responses to the excitotoxin capsaicin. *Neuron*, 1; 973-981.

Wood JN, Winter J, James IF, Rang HP, Yeats J, Bevan S (1988) Capsaicin-induced ion fluxes in dorsal root ganglion cells in culture. *J Neurosci*, 8; 3208-3220.

Wood, JN (Ed.)(2000) *Molecular Basis of Pain Transduction*. Wiley-Liss.

Wood JN, Baker M (2001) Voltage-gated sodium channels. *Curr Opin Pharmacol*, 1; 17-21.

Woolf CJ, Ma QP, Allchorne A, Poole S (1996) Peripheral cell types contributing to the hyperalgesic action of nerve growth factor in inflammation. *J Neurosci*, 16; 2716-2723.

Woolf CJ, Costigan M (1999) Transcriptional and posttranslational plasticity and the generation of inflammatory pain. *Proc Natl Acad Sci U S A*, 96; 7723-7730.

Xie J, Price MP, Berger AL, Welsh MJ (2002) DRASIC contributes to pH-gated currents in large dorsal root ganglion sensory neurons by forming heteromultimeric channels. *J Neurophysiol*, 87; 2835-2843.

Xu H, Ramsey IS, Kotecha SA, Moran MM, Chong JA, Lawson D, Ge P, Lilly J, Silos-Santiago I, Xie Y, DiStefano PS, Curtis R, Clapham DE (2002) TRPV3 is a calcium-permeable temperature-sensitive cation channel. *Nature*, 418; 181-186.

Xu H, Zhao H, Tian W, Yoshida K, Roullet JB, Cohen DM (2003) Regulation of a transient receptor potential (TRP) channel by tyrosine phosphorylation. SRC family kinase-dependent tyrosine phosphorylation of TRPV4 on TYR-253 mediates its response to hypotonic stress. *J Biol Chem*, 278; 11520-11527.

Yoshida S, Matsuda Y (1979) Studies on sensory neurons of the mouse with intracellular-recording and horseradish peroxidase-injection techniques. *J Neurophysiol*, 42; 1134-1145.

Yusaf SP, Goodman J, Pinnock RD, Dixon AK, Lee K (2001) Expression of voltage-gated calcium channel subunits in rat dorsal root ganglion neurons. *Neurosci Lett*, 311; 137-141.

Zelena J (1994) *Nerves and mechanoreceptors*. Kluwer Academic Publishers.

Zhang Y, Hamill OP (2000) On the discrepancy between whole-cell and membrane patch mechano-sensitivity in *Xenopus* oocytes. *J Physiol*, 523; 101-115.

Zhang Y, Ma C, Delohery T, Nasipak B, Foat BC, Bounoutas A, Bussemaker HJ, Kim SK, Chalfie M (2002) Identification of genes expressed in *C. elegans* touch receptor neurons. *Nature*, 418; 331-335.

Zhang Z, Bourque CW (2003) Osmometry in osmosensory neurons. *Nat Neurosci*, 6; 1021-1022.